

G9001

Dynamic Characteristics of Atmospheric Boundary Layer during different Phases of Monsoon

Thesis submitted to the
Cochin University of Science and Technology
in partial fulfilment of the requirement for the Degree of

DOCTOR OF PHILOSOPHY

in

ATMOSPHERIC SCIENCES

Under the Faculty of Marine Sciences



By

Hamza Varikoden


Department of Atmospheric Sciences
Cochin University of Science and Technology
Lakeside Campus, Cochin 682016

May 2006

CERTIFICATE

This is to certify that the research work presented in this thesis entitled “**Dynamic Characteristics of Atmospheric Boundary Layer during different Phases of Monsoon**” has been carried out by **Mr. Hamza Varikoden** in the Department of Atmospheric Sciences, Cochin University of Science and Technology independently under my supervision and guidance for the award of the degree *Doctor of Philosophy*. I also certify that this is his original contribution and has not been submitted for the award of any degree or diploma in any other University or Institution.

Certified that **Mr. Hamza Varikoden** has passed the Ph.D qualifying examination conducted by the Cochin University of Science and Technology in February, 2005.



Dr. C A Babu, Reader
Department of Atmospheric Sciences
Cochin University of Science and Technology
Cochin – 682 016.

Cochin – 16,
30-05-2006.

PREFACE

Atmospheric Boundary Layer (ABL) is the layer just above the earth surface and is influenced by the surface forcing within a short period of an hour or less. In this thesis, characteristics of the boundary layer over ocean, coastal and inland areas of the atmosphere, especially over the monsoon regime are thoroughly studied. The thesis is divided into six chapters. The general characteristics of the ABL and some of the earlier studies are discussed in the Chapter-1, Introduction.

In the second chapter, the dynamics and turbulent properties of the coastal boundary layer in relation to sea breeze and land breeze circulations are included. Dynamical features of a coastal station, Cochin ($9^{\circ} 58'N$ $76^{\circ} 17'E$) are studied, since this station is not only a tropical coastal station but also an industrial city. The dispersion of effluents from the industries is mainly controlled by the sea breeze and land breeze circulation over the coastal stations, so it is imperative to study the onset and cessation times of this circulation. These are studied using a 20 m Automatic Weather Station (AWS) at Cochin with sensors of meteorological parameters at 5 m, 10 m and 20 m heights. The variation of the meteorological parameters and the surface turbulent fluxes are examined associated with these circulations in different seasons. The results after compilation are communicated to the Journal *Mausam*. The other parameters such as Monin-Obukhov length, drag coefficient, frictional velocity and temperature scale are also examined. The variations and differences are presented using the Monin-Obukhov similarity relations.

The Chapter-3, discusses the changes of the ABL during active and weak phases of southwest monsoon. The activity of the low level tropospheric winds is different at different heights and maximum is at 850 hPa (1.5 km), called Low Level Jetstream (LLJ). The influence of the LLJ is dominant even in the surface, so the boundary layer parameters are changed with different epochs of monsoon. In this chapter, the turbulent parameters such as the fluxes of momentum and sensible heat associated with different epochs of southwest monsoon using AWS data set are discussed. In addition to the above, Conserved Variable Analysis is also carried out to estimate the mixing height during these epochs of southwest monsoon. It is found that the mixing height of the CBL is confined to

1 km in most of the cases during the active phase over Trivandrum but in the Mangalore the mixing height is slightly different and found at higher altitude. During weak monsoon situations, the convective mixing height is found to be high in all the cases of Trivandrum and Mangalore due to the characteristics of the weak monsoon situation. To explore the thermodynamic structure of the boundary layer further, thermodynamic variables such as specific humidity, virtual potential temperature and equivalent potential temperature are also studied. These are related to the active and weak phases of southwest monsoon and they play significant role in the atmospheric boundary layer. The boundary layer oscillations are also incorporated in this chapter because these oscillations are physical manifestation of the active and weak phases of southwest monsoon. The oscillations in the ABL are important because the transport mechanism from the surface to the upper atmosphere is governed by the ABL characteristics. The study was carried out using wind and temperature data observed at surface, 925 hPa and 850 hPa levels. The different frequencies embedded in the boundary layer parameters are identified by employing wavelet technique. Surface boundary layer characteristics over the monsoon region are closely linked to the upper layer monsoon features. The various harmonics obtained at different levels are compiled to a paper and submitted to *Journal of Marine Sciences*.

Chapter-4 presents the dynamics of marine boundary layer and is studied using high resolution satellite derived QuikSCAT data with a spatial resolution of 0.25 X 0.25 latitude longitude grid. Marine atmospheric boundary layer plays a vital role in the transport of momentum and heat from the ocean surface to atmosphere. A detailed study is made on the marine boundary layer characteristics. Spatial variation of surface wind, frictional velocity, roughness parameter and drag coefficient for different seasons are studied and the results are highlighted. In addition to the above, various oscillations in the marine atmospheric boundary layer parameters are also evaluated employing wavelet technique and found that the intraseasonal and quasi biweekly mode of oscillations are different for Arabian Sea and Bay of Bengal. The major findings of this chapter is concluded and submitted to the *Journal Advances in Atmospheric Sciences* after presenting in the Int. Conference, IAMAS-2005.

Chapter-5 illustrates the inland boundary layer characteristics. High resolution wind data of clear sky days of the monsoon period from the L-band UHF radar (LAWP)

over Gadanki (13.47°N, 79.18°E), Andhra Pradesh, India and ~ 370 m above msl is used for the analysis. Diurnal variation of the zonal and meridional wind with height during May to September is analyzed to understand the evolution of LLJ with convective boundary layer. The vertical variation of wind shear using zonal and meridional wind and diurnal evolution of boundary layer depth using signal to noise ratio are discussed. Moreover, variation of LLJ with altitude during active and weak phases and their comparison with NCEP data are also discussed. The essence of this chapter is submitted as a paper to the *Journal of Marine Science*.

Chapter 6 comprises the summary of conclusion from the chapters 2 to 5, which also describes some future plans to carry out research work in the arena of ABL. The 6th chapter follows the references quoted for the all the chapters in this thesis.

CONTENTS

1	INTRODUCTION.....	1
1.1	GENERAL INTRODUCTION	1
1.2	ATMOSPHERIC BOUNDARY LAYER (ABL)	2
1.2.1	<i>Depth of ABL over land and ocean.....</i>	<i>2</i>
1.3	GENERAL STRUCTURE OF THE ABL.....	3
1.3.1	<i>Factors influencing the structure of the ABL.....</i>	<i>4</i>
1.3.2	<i>Diurnal evolution of the ABL.....</i>	<i>5</i>
1.3.2.1	Surface Layer (SL).....	6
1.3.2.2	Free Convection Layer.....	6
1.3.2.3	Mixed Layer (ML).....	6
1.3.2.4	Entrainment Zone (EZ).....	7
1.3.2.5	Residual Layer (RL).....	7
1.3.2.6	Stable Boundary Layer (SBL).....	7
1.4	MARINE BOUNDARY LAYER STRUCTURE	8
1.5	COSTAL ATMOSPHERIC BOUNDARY LAYER.....	8
1.6	MONSOON BOUNDARY LAYER.....	9
1.7	STABILITY OF THE ABL	10
1.8	TECHNIQUES FOR PROBING ABL.....	12
1.8.1	<i>In situ measurements.....</i>	<i>13</i>
1.8.2	<i>Remote sensing measurements.....</i>	<i>14</i>
1.9	NUMERICAL MODELING OF ABL.....	15
1.9.1	<i>Governing Equations.....</i>	<i>16</i>
1.9.2	<i>Closure Problem.....</i>	<i>16</i>
1.10	ABL – EARLIER STUDIES	17
1.11	PRESENT STUDY	23
2	SURFACE BOUNDARY LAYER CHARACTERISTICS OVER COCHIN	
	24	
2.1	INTRODUCTION.....	24
2.2	OUTLINE OF THE WORK	27
2.3	SCOPE OF THE STUDY	27
2.4	DATA AND METHODOLOGY	27
2.4.1	<i>Description of the tower site.....</i>	<i>27</i>
2.4.2	<i>Computation procedure.....</i>	<i>29</i>
2.5	DIURNAL VARIATION OF BOUNDARY LAYER PARAMETERS.....	31
2.5.1	<i>Air temperature.....</i>	<i>31</i>
2.5.2	<i>Soil temperature.....</i>	<i>32</i>
2.5.3	<i>Wind speed.....</i>	<i>33</i>
2.5.4	<i>Wind direction.....</i>	<i>34</i>
2.6	SEA BREEZE AND ASSOCIATED FEATURES.....	35
2.6.1	<i>Diurnal variation of averaged wind direction.....</i>	<i>35</i>
2.6.2	<i>Diurnal variation of sea breeze component.....</i>	<i>39</i>
2.6.3	<i>Diurnal variation during a rainy day.....</i>	<i>40</i>
2.6.4	<i>Diurnal variation of turbulent fluxes.....</i>	<i>41</i>
2.6.4.1	Momentum flux	41
2.6.4.2	Sensible heat flux.....	42
2.6.4.3	Momentum and Sensible heat fluxes for individual days.....	43
2.7	TURBULENT BOUNDARY LAYER FEATURES.....	46

2.7.1	<i>During land breeze</i>	46
2.7.2	<i>During sea breeze</i>	48
2.7.3	<i>Dependence of wind speed and temperature on boundary layer parameters</i>	50
3	ATMOSPHERIC BOUNDARY LAYER CHARACTERISTICS ASSOCIATED WITH ACTIVE AND WEAK PHASES OF MONSOON	53
3.1	INTRODUCTION	53
3.2	ACTIVE AND WEAK CYCLES OF SOUTHWEST MONSOON	53
3.3	SCOPE OF THE STUDY	56
3.4	DATA AND METHODS	56
3.4.1	<i>Vapour pressure (e)</i>	57
3.4.2	<i>Saturated vapour pressure (es)</i>	57
3.4.3	<i>Virtual potential temperature (θ_v)</i>	58
3.5	WIND STRUCTURE AT DIFFERENT LEVELS	58
3.6	VARIATION OF BOUNDARY LAYER FLUXES OVER COCHIN	60
3.7	CONSERVED VARIABLE ANALYSIS ($\theta_e - q$ PLOT)	61
3.8	VERTICAL VARIATION OF THERMODYNAMIC PARAMETERS	67
3.8.1	<i>Specific humidity (q)</i>	67
3.8.2	<i>Virtual potential temperature (θ_v)</i>	69
3.8.3	<i>Equivalent potential temperature (θ_e)</i>	70
3.8.4	<i>Relation of specific humidity with θ_v and θ_e</i>	72
3.9	MAJOR OSCILLATIONS IN THE ABL	73
3.9.1	<i>Oscillations in wind and temperature</i>	74
4	MARINE ATMOSPHERIC BOUNDARY LAYER CHARACTERISTICS OVER ARABIAN SEA AND BAY OF BENGAL	78
4.1	INTRODUCTION	78
4.1.1	<i>Arabian Sea</i>	78
4.1.2	<i>Bay of Bengal</i>	79
4.2	OBJECTIVE OF THE STUDY	80
4.3	DATA AND METHODS	81
4.3.1	<i>Data description</i>	81
4.3.1.1	SeaWinds sensor overview	81
4.3.1.2	Introduction to QuikSCAT	82
4.3.2	<i>Product description</i>	82
4.3.2.1	Spatial coverage	82
4.3.2.2	Spatial resolution	82
4.3.2.3	Temporal resolution	83
4.3.2.4	Main parameters	83
4.3.3	<i>Methodology description</i>	83
4.3.3.1	Retrieving wind vectors from scatterometer measurements	83
4.3.3.2	Wind stress estimation	84
4.4	SPATIAL VARIATION OF SURFACE LAYER PARAMETERS	85
4.4.1	<i>Surface wind</i>	85
4.4.2	<i>Frictional velocity</i>	86
4.4.3	<i>Roughness parameter</i>	88
4.4.4	<i>Wind stress curl</i>	89
4.5	DEPENDENCE OF WIND WITH SURFACE PARAMETERS	90

4.5.1	<i>Momentum flux (wind stress)</i>	90
4.5.2	<i>Roughness parameter</i>	91
4.5.3	<i>Frictional velocity</i>	96
4.5.4	<i>Wind against SST and Rainfall</i>	96
4.5.5	<i>Drag coefficient</i>	100
4.6	TEMPORAL VARIATION OF FRICTIONAL VELOCITY AND DRAG COEFFICIENT	101
4.6.1	<i>Frictional velocity over Arabian Sea and Bay of Bengal</i>	101
4.6.2	<i>Drag Coefficient over Arabian Sea and Bay of Bengal</i>	103
4.7	INTRASEASONAL VARIATIONS IN FRICTIONAL VELOCITY AND DRAG COEFFICIENT	103
5	INLAND BOUNDARY LAYER CHARACTERISTICS OVER A TROPICAL STATION USING UHF RADAR	106
5.1	INTRODUCTION.....	106
5.1.1	<i>ABL structure during clear sky day</i>	106
5.1.2	<i>Wind structure in the ABL during southwest monsoon</i>	107
5.2	LOWER ATMOSPHERIC WIND PROFILER (LAWP)	107
5.2.1	<i>Technical details</i>	109
5.3	GENERAL GEOGRAPHICAL AND METEOROLOGICAL CONDITIONS	111
5.4	SCOPE OF THE STUDY	112
5.5	DATA PROCESSING	113
5.6	COMPUTATION PROCEDURES.....	115
5.6.1	<i>Moments</i>	115
5.6.2	<i>Signal to noise ratio (SNR)</i>	115
5.6.3	<i>Height and wind components</i>	115
5.7	DIURNAL VARIATIONS.....	116
5.7.1	<i>Variation of the zonal wind</i>	118
5.7.2	<i>Variation of vertical wind shear</i>	122
5.7.3	<i>Atmospheric boundary layer depth</i>	125
5.8	VARIATION OF LLJ DURING ACTIVE AND WEAK PHASES	128
6	SUMMARY AND CONCLUSIONS	132
6.1	SCOPE FOR FUTURE STUDIES :.....	138
7	REFERENCES	139

LIST OF FIGURES

Fig.1.1 Schematic diagram of the Atmospheric boundary layer (From Arya, 1982).....	3
Fig.1.2 Diurnal evolution of the ABL with time (Based on Stull 1988). The X – axis is plotted with the time in hours and Y-axis represents the height in metre.....	4
Fig.1.3 Schematic diagram of the various stability categories based on virtual temperature (After Arya, 1988).....	12
Fig.2.1 Location map of Cochin (Tower location is marked by T).....	28
Fig.2.2 Micrometeorological Tower of 20 m height with three levels of sensors installed at Cochin University Campus for atmospheric boundary layer studies.....	28
Fig.2.3 Diurnal variation of air temperature during four different seasons.....	32
Fig.2.4 Diurnal variation of soil temperature in different seasons at four depths.....	33
Fig.2.5 Diurnal variation of wind speed during four different seasons at three levels.....	34
Fig.2.6 Diurnal variation of wind direction in different seasons at three levels.....	35
Fig.2.7 Diurnal variation of averaged wind direction in different seasons considering all non rainy days.....	36
Fig.2.8 Diurnal variation of air temperature, wind direction and wind speed for 12 th January, representative of winter, 15 th April for pre-monsoon, 23 rd July for southwest monsoon and 27 th November for post monsoon. Dotted solid line indicates 20 m level and solid line 10 m level.....	38
Fig.2.9 Diurnal variation of sea breeze component for representative days of the seasons...	39
Fig.2.10. Diurnal variation of air temperature, wind direction and wind speed during a rainy day (24 th June).....	40
Fig.2.11. Diurnal variation of averaged momentum flux during the four seasons.....	41
Fig.2.12. Diurnal variation of averaged sensible heat flux during the four seasons.....	42

Fig.2.13. Diurnal variation of momentum flux during individual day of the seasons.....	44
Fig.2.14. Diurnal variation of sensible heat flux during individual day of the seasons.....	44
Fig.2.15 Variation of drag coefficient with wind during sea breeze period.....	45
Fig.2.16 Variation of drag coefficient with wind during land breeze period.....	45
Fig.2.17 Day to day variation of (a) surface wind, (b) temperature, (c) frictional velocity and (d) temperature scale during land breeze period.....	47
Fig.2.18. Day to day variation of (a) Momentum Flux, (b) Sensible Heat Flux, (c) Stability Parameter and (d) Drag coefficient during land breeze period.....	47
Fig.2.19. Day to day variation of (a) surface wind, (b) temperature, (c) frictional velocity and (d) temperature scale during sea breeze period.....	49
Fig.2.20. Day to day variation of (a) Momentum Flux, (b) Sensible Heat Flux, (c) Stability Parameter and (d) Drag Coefficient during sea breeze period.....	49
Fig.2.21a. Dependence of boundary layer parameters with wind.....	51
Fig.2.21b. Dependence of boundary layer parameters with temperature.....	51
Fig.3.1. Spatial structure of a) NOAA OLR composite representing organized convective clouds and b) wind at 850 hPa composite during Active monsoon condition.....	55
Fig.3.2. Spatial structure of a) NOAA OLR composite representing organized convective clouds and b) wind at 850 hPa composite during weak monsoon situation.....	55
Fig.3.3. Spatial structure of wind at 850 hPa with magnitude and direction during active and weak phases of monsoon at different levels a) 1000 hPa, b) 925 hPa, c) 850 hPa, d) 700 hPa and e) 500 hPa.....	59
Fig.3.4. Variations of surface fluxes of momentum and sensible heat during active and weak phases of monsoon.....	60
Fig. 3.5 Conserved variable analysis for Trivandrum during the active period of southwest monsoon.....	63

Fig. 3.6 Conserved variable analysis for Mangalore during the active period of southwest monsoon.....	64
Fig. 3.7 Conserved variable analysis for Trivandrum during the weak period of southwest monsoon.....	65
Fig. 3.8 Conserved variable analysis for Mangalore during the weak period of southwest monsoon.....	66
Fig.3.9. Variation of the specific humidity during June and July of a) 2001 and b) 2002 in different standard levels.....	68
Fig.3.10. Variation of the virtual potential temperature during June and July of a) 2001 and b) 2002 in different standard levels.....	70
Fig.3.11. Variation of the virtual equivalent potential temperature during June and July of a) 2001 and b) 2002 in different standard levels.....	71
Fig.3.12. Cross relation of specific humidity with virtual potential temperature for the standard levels during the monsoon period.....	72
Fig.3.13. Cross relation of specific humidity with equivalent potential temperature for the standard levels during the monsoon season.....	73
Fig 3.14 Wavelet analysis of the wind at 850 hPa, 925 hPa and surface during southwest monsoon. The first row represents the original signal, the second row gives the harmonics of wind in the QBM band and the next is same for ISO band.....	75
Fig 3.15 Wavelet analysis of the temperature at 850 hPa, 925 hPa and surface during southwest monsoon. The first row represents the original signal, the second row gives the harmonics of wind in the QBM band and the next is same for ISO band.....	76
Fig.4.1 Averaged surface wind in ms^{-1} for the years from 1999 to 2003 during January, April, July and November representing different seasons.....	86
Fig.4.2 Averaged frictional velocity in ms^{-1} for the years from 1999 to 2003 during January, April, July and November representing different seasons.....	87

Fig.4.3 Averaged roughness parameter in mm for the years from 1999 to 2003 during January, April, July and November representing different seasons.....	88
Fig.4.4 Averaged wind stress curl (Nm^{-3}) parameter for the years from 1999 to 2003 during January, April, July and November representing different seasons.....	90
Fig.4.5 Relation of wind stress with wind speed for different seasons for Arabian Sea.....	92
Fig.4.6 Relation of wind stress with wind speed for different seasons for Bay of Bengal....	93
Fig.4.7 Relation of roughness parameter to wind speed during different seasons over Arabian Sea.....	94
Fig. 4.8 Relation of roughness parameter to wind speed during different season over Bay of Bengal.....	95
Fig.4.9 Relation of frictional velocity with wind speed during different seasons over Arabian Sea.....	97
Fig.4.10 Relation of frictional velocity with wind speed during different seasons over Bay of Bengal.....	98
Fig.4.11 Depending relations of sea surface parameters over Arabian Sea and Bay of Bengal.....	99
Fig.4.12 Relation of drag coefficient with wind for different season over Arabian Sea.....	100
Fig.4.13 Relation of drag coefficient with wind for different season over Bay of Bengal...100	
Fig.4.14 Day to day variation of frictional for Arabian Sea (solid line) and for Bay of Bengal (dotted line) averaged of four years from 2000 to 2003.....	102
Fig.4.15 Day to day variation of drag coefficient for Arabian Sea (solid line) and for Bay of Bengal (dotted line) averaged of four years from 2000 to 2003.....	102
Fig.4.16 Wavelet analysis of frictional velocity over Arabian Sea and Bay of Bengal.....	104
Fig.4.17 Wavelet analysis of Drag Coefficient over Arabian Sea and Bay of Bengal.....	105

Fig.5.1 The location of the LAWP (Gadanki) with map of India.....	108
Fig.5.2 Antenna and transmitter assembly unit of the LAWP.....	108
Fig. 5.3 Three dimension picture of Nallmala Hills over which Gadanki is located.....	112
Fig. 5.4 Schematic diagram for data processing in LAWP.....	114
Fig.5.5 Comparison of wind speed measured by LAWP, MST radar and radiosonde on 26 July 1999 (1030 IST) and 28 July 1999 (1615 IST).....	117
Fig.5.6 Diurnal variation of zonal wind component (ms^{-1}) from LAWP for the representative days (a) 6 th May, (b) 23 rd June, (c) 25 th July, (d) 8 th August and (e) 14 th September of 1999.....	120
Fig.5.7 Diurnal variation of vector wind from LAWP for the representative days (a) 6 th May, (b) 23 rd June, (c) 25 th July, (d) 8 th August and (e) 14 th September of 1999.....	121
Fig.5.8 Diurnal variation of vertical wind shear (s^{-1}) for the representative days (a) 6 th May, (b) 23 rd June, (c) 25 th July, (d) 8 th August and (e) 14 th September of 1999.....	124
Fig.5.9 Diurnal variation of signal to noise ratio (reflectivity) the representative days (a) 6 th May, (b) 23 rd June, (c) 25 th July, (d) 8 th August and (e) 14 th September of 1999.....	125
Fig.5.10 Diurnal variation of vertical wind (ms^{-1}) from LAWP for the representative days (a) 6 th May, (b) 23 rd June, (c) 25 th July, (d) 8 th August and (e) 14 th September of 1999.....	127
Fig.5.11 Time series of the area averaged (10° N - 20° N & 70° E – 80° E) zonal wind at 850 hPa during 1999.....	128
Fig.5.12 Height time intensity plot of the zonal wind (ms^{-1}) during active and weak phase of southwest monsoon 1999 taken from LAWP.....	129
Fig.5.13 Height - time plot of the zonal wind (ms^{-1}) during active and weak phase of southwest monsoon from NCEP/NCAR reanalysis data set.....	130

LIST OF PUBLICATIONS

- Hamza V** and C A Babu 'Boundary layer characteristics associated with sea breeze circulation over a tropical station', *Mausam* (communicated)
- Hamza V**, Babu C A and T P Sabin, 'Marine Atmospheric Boundary Layer Characteristics over Arabian Sea and Bay of Bengal', *Advances in Atmospheric Sciences* (submitted)
- Babu C A, **V Hamza** and T P Sabin, 'Characteristics of oscillation in surface layer and above over Kochi', *Journal of Marine Sciences*, (submitted).
- Hamza V**, C A Babu and T P Sabin, 'Diurnal variation of ABL structure during monsoon using UHF radar', *Journal of Marine Sciences*, (submitted).
- Hamza V**, C A Babu and P V Joseph, 'The Second Onset of Indian Summer Monsoon: A Diagnostic Study', IUGG-2003 held (30 June–11 July 2003) at Sapporo, Japan.
- Hamza V** and C A Babu 'Global Tele -connection of ITCZ heat source and circulation of Indian summer monsoon', IUGG-2003 held (30 June–11 July 2003) at Sapporo, Japan.
- Babu C A and **V Hamza** 'Features of Sea Breeze circulation over a tropical Station', IUGG-2003 held (30 June–11 July 2003) at Sapporo, Japan.
- Babu C.A.**V Hamza** and Joseph P.V "A thunderstorm of long duration over Kerala in February', INTROMET-2004 held (24 – 27 February 2004) at Hyderabad, India.
- Hamza V.**and C.A.Babu 'Moisture transport during active and weak phases of monsoon' METOC-2004 held (5 – 6 February 2004) at Cochin, India.

Joseph P V Babu C A and **V Hamza**, 'Monsoon Low Level Jetstream and surface wind gustiness', METOC-2004 held (5 – 6 February 2004) at Cochin, India.

Hamza V, C A Babu and T P Sabin, 'Surface turbulence features associated with the sea breeze circulation over Kochi' KEC-2005 held (6-7 May 2005) at Cochin, India

Hamza V Babu C A and T P Sabin, 'Characteristic Study of The Boundary Layer Parameters over Arabian Sea and Bay of Bengal using Quikscat data set' IAMAS-2005 held (2-11 August 2005) at Beijing, China.

Sabin T P, **Hamza V** and C A Babu, ' Features of tropical easterly jetstream during active and weak phases of boreal summer monsoon and its relation with low level jetstream' IAMAS-2005 held (2-11 August 2005) at Beijing, China.

Hamza V, C A Babu and T P Sabin, 'Diurnal Variation of ABL Structure during Monsoon using UHF Radar', ATMOCIN-2006 held at (11-13 January 2006) Cochin, India.

Hamza V and C A Babu, 'Atmospheric boundary layer structure during southwest monsoon period using L-band UHF radar', COSPAR-2006 to be held (16-23 July, 2006) Beijing, China.

Babu C A and **Hamza V**, 'Monsoon Boundary Layer characteristics using LAWP' VIII User Scientists Workshop to be held (20-21 June 2006) Gadanki, India.

CHAPTER – 1

INTRODUCTION

CHAPTER - 1

INTRODUCTION

1.1 General Introduction

Atmospheric Boundary layer is widely referred area by researchers working in the field of aerodynamics, hydraulics, fluid mechanics and heat transfer, as well as by the meteorologists and physical oceanographers. In a broad sense, the boundary layer can be defined as the layer of a fluid flow in the immediate vicinity of a material surface in which significant transfers of momentum, heat and mass between the boundary surface and the fluid occurs. The Atmospheric Boundary Layer (ABL) is also referred to as the Planetary Boundary Layer (PBL), can be identified as the lowest layer of the air directly above the earth surface that forms as a consequence of the interactions between the atmosphere and the underlying surface (land or water) over time scale of a few hours to about one day (Arya 1988, Garret 1992, Stull 1988). Within the ABL, the influence of the surface roughness, heating and other properties are quickly and efficiently transmitted through the mechanism of turbulent mixing. The turbulent nature of the ABL is one of its most conspicuous and important features. Almost the entire biosphere is either contained in, or depends on, the ABL. The ABL transfers heat and moisture from the surface and disperses them both horizontally and vertically, effectively air-conditioning the biosphere and providing a conduit for energy to power weather system on all scales. In many aspects, the ABL can be considered as the circulatory system of the biosphere.

Most of the oceanographic field experiments in the last four to five decade were confined to the tropical Atlantic and Pacific Ocean. Due to lack of coordinated field experiments, historical observations over the tropical Indian Ocean are a few. In this context, the meteorological data collected over the data-sparse region of the western tropical Indian Ocean during the various phases of the Indian Ocean Experiments (INDOEX) attains prime significance (Mitra, 2001, 1999; Mitra et al., 2001; Ramanathan et al., 2001; 1996). INDOEX, being a multi-disciplinary international field experiments, had several objectives focused towards developing a comprehensive analysis of the interactive role of radiation, clouds, and anthropogenic and continental aerosols transports for a better understanding of the role of aerosols

on natural and climatic forcing and its feedback on regional and global climate from experimental observations over the western tropical Indian Ocean (Ramanathan et al., 2001). Though the field experiment was aimed mainly towards aerosols and radiation studies, it essentially included a meteorological component for assessment of the magnitude of solar absorption at the surface and in the troposphere including Inter Tropical Convergence Zone (ITCZ) cloud system. The campaign also had an objective to assess the role of ITCZ in the transport of trace gases and pollutants and their radiative forcing.

1.2 Atmospheric Boundary Layer (ABL)

The ABL can be considered as the region in the lower troposphere, which is directly influenced by the earth surface. The winds in the ABL are influenced by the frictional forces at the earth surface and hence transport of properties from the earth surface to the atmosphere. Top of ABL is marked by a limit on vertical mixing from the surface.

1.2.1 Depth of ABL over land and ocean

In the atmospheric context, it has been quite difficult to mark the top of the ABL. In a wind tunnel, the thickness or depth of the boundary layer is defined as the distance from the surface where mean velocity reaches 99% of its ambient free stream velocity. However, such definitions are of no use in the case of the ABL, because the measurement of the mean wind profile is not that precise and also because such profile vary rarely monotonically with height. The most direct measurement of the ABL depth are provided by upward looking SODAR and LIDAR, which measure the height to which turbulent fluctuations in temperature and refractive index extends. Turbulent sensors mounted on a research aircraft, high tower or tethered balloon also provide alternate means of measuring the boundary layer depth. More often, the ABL depth is also estimated from the temperature and humidity profiles obtained from the standard radiosonde release (Arya, 1988; Garret, 1992; Stull, 1997). In day time unstable and convective condition, it has been found that the ABL usually extends all the way up to the base of the lowest inversion, which can be easily inferred from the radiosonde observation of temperature and humidity profiles. Above the inversion base potential temperature increases and specific humidity decreases fairly rapidly

with height, while these quantities remain very nearly uniform throughout the mixed layer below the inversion base. Thus the height of the lowest inversion base is, for all practical purposes, considered equal to the height of the unstable or convective ABL (Arya, 1988; Garratt, 1992; Stull, 1988). During night time stable conditions, the ABL is generally identified with the surface inversion layer. Based on the time and location of the observation, the ABL height at a given location varies over a wide range (several tens of metre to several kilometre) and also depends on the rate of heating or cooling of the surface, strength of the winds, the roughness and topographical characteristics of the surface, large scale vertical motion, horizontal advections of heat and moisture and many other factors.

1.3 General structure of the ABL

Following sunrise on clear sky day, the continuous heating of the earth surface by the sun and resulting thermal mixing in the ABL cause steady increase of ABL depth throughout the day and attain a maximum value in the late afternoon. Later in the evening and throughout the night, on the other hand, the radiative cooling of the

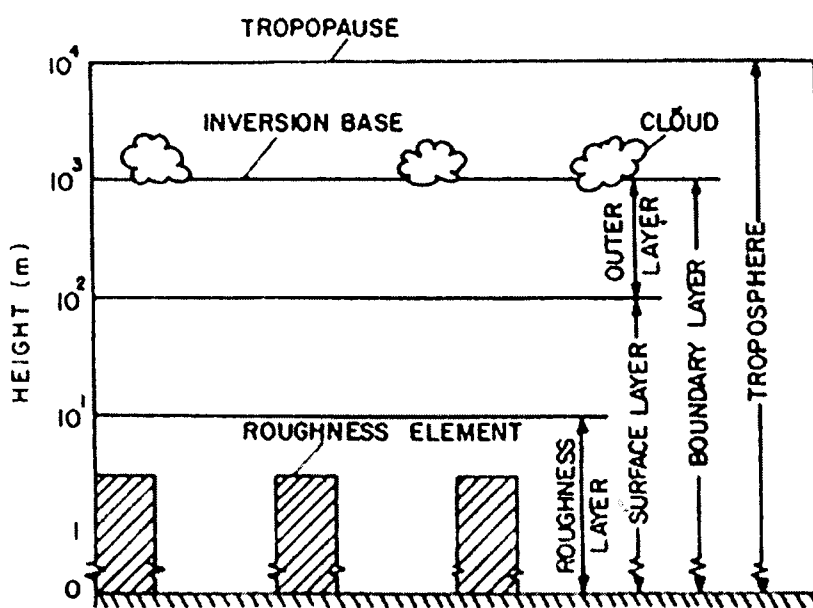


Fig.1.1 Schematic diagram of the Atmospheric boundary layer (From Arya, 1982)

ground surface results in the suppression or weakening of turbulent mixing and consequently shrinking of the ABL depth. Thus the ABL structure and its depth waxes and wanes in response to the diurnal heating and cooling cycle. Over land surface in high pressure regions the ABL has a well defined structure that evolves

with the diurnal cycle. A schematic of the ABL, as the lower part of the troposphere, over an underlying rough surface is given in Fig.1.1. Various sub layers of the ABL are also depicted on the figure. The ABL structure shown in the above figure occurs in neutral stability. The ABL thickness over land surface varies over a wide range (several tens of metre to several kilometre).

1.3.1 Factors influencing the structure of the ABL

The ABL is essentially driven by the large scale atmospheric flows such as geostrophic, thermal and gradient winds. Above the top of the boundary layer the flow is generally assumed to be geostrophic. The boundary layer height h is one of the importance parameters to determine the ABL structure. Generally, the dimension of largest eddies are fixed by the h and it depends on wind shear, turbulent intensities and fluxes. Due to these properties many investigators used h as one of the basic scales of length in describing ABL structure. The other important factor influencing the ABL is the drag coefficient. Surface drag essentially depends on the roughness characteristics of the underlying surface and primarily responsible for the characteristic wind profile with monotonic increase of wind speed with height in the lower part of the ABL. Thus the surface roughness exerts strong influence in the mean profile and turbulent structure in the surface layer and also in the upper part of the ABL. Besides, friction the underlying surface is also influence the ABL structure. On a clear day the surface absorbs a part of the solar radiation and warms up relative to the air above. This temperature difference usually gives rise to a variety of convective circulations, which transfer heat and other properties from the surface to the atmosphere. The radiative warming of the surface relative to air results in an unstably stratified ABL in which buoyancy forces generate turbulence in addition to that generated by the wind shear. On a clear night, on the other hand, the surface cools down relative to the air above, resulting in a stably stratified or surface inversion layer. It can be seen that buoyancy inhibits vertical motions in such a layer. Consequently in stable ABL, the vertical turbulent transfers are generally reduced.

Thus the diurnal cycle of the heating and cooling in the surface is one of the important factors in determining the thermal stability of the ABL and hence turbulent structure. Other factors influencing the vertical structure of the ABL are the presence of fog, stratus layers within the ABL and advection of heat and moisture. The

entrainment of the air from the free atmosphere into the turbulent boundary layer can also influence the structure of the ABL. Due to entrainment at the top of the unstable ABL, significant amount of heat and momentum flux transport takes place.

1.3.2 Diurnal evolution of the ABL

The structure of the ABL over land surface is strongly influenced by the diurnal cycle of surface heating and cooling and also by the presence of clouds. Generally, the ABL structure over the land surface in high pressure regions can be classified into three broad categories (Stull, 1988): 1. Convective boundary layer; 2. Residual layer and 3. Stable boundary layer and it is given in Fig. 1.2. The unstably

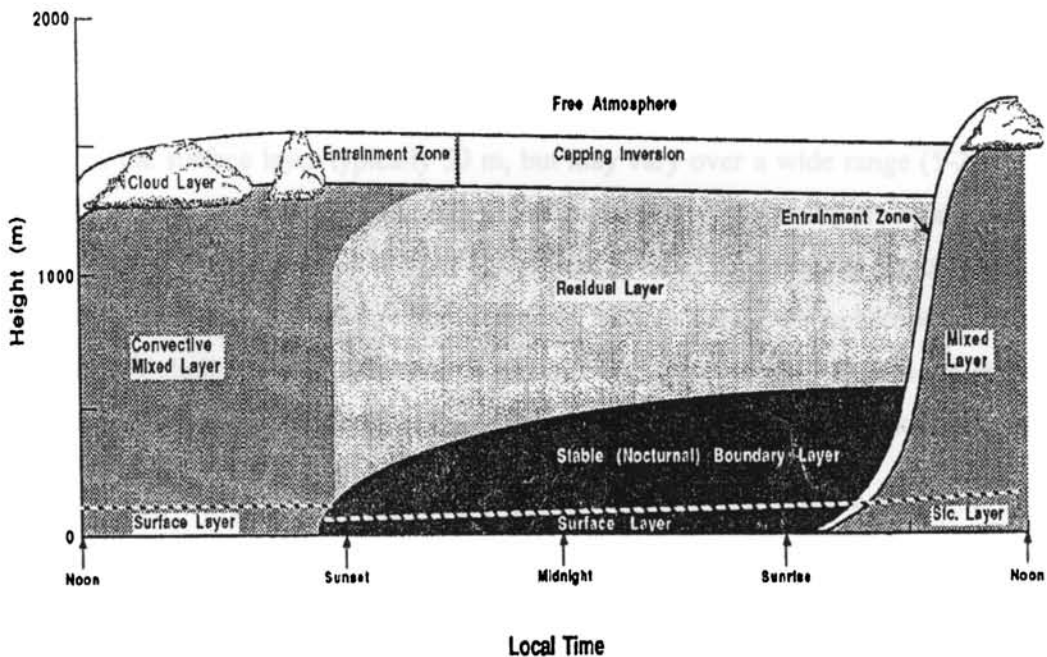


Fig. 1.2 Diurnal evolution of the ABL with time (Based on Stull 1988). The X – axis is plotted with the time in hours and Y-axis represents the height in metre.

stratified ABL or convective boundary layer (CBL), occurs when strong surface heating produces permanent instability or convection in the form of thermals and plumes and upside-down convection is generated by cloud top radiative cooling. In strong unstable condition driven by surface heating, the outer layer in particular is dominated by convective motions and is often referred to as mixed layer. In contrast, the stably stratified ABL or stable boundary layer (SBL) occurs mostly during night. The residual layer (RL) is often observed after the sunset hours during the transition from CBL to SBL.

1.3.2.1 Surface Layer (SL)

The lowest one tenth of the ABL, which is very close to the earth surface and in which earth's rotational or coriolis effects can be ignored is termed as the SL. It is characterised by the sharp variation of wind speed, temperature and other meteorological parameters with height. It is also characterised by intense small scale turbulence generated by surface roughness or friction and also by the thermal convection, in the case of a heated surface. The turbulence in this layer is mainly due to wind shear, which is generated by surface frictional force generally known as mechanical turbulence. The small scale turbulence is largely responsible for the vertical exchanges of momentum, heat and mass to and from the surface. Within the surface layer, the vertical fluxes of these quantities are found to remain nearly constant with height and vertical variations are observed to be within 10 % of their surface values. This layer, therefore, is also referred to as a constant flux layer. The height of the surface layer typically 50 m, but may vary over a wide range (5-200 m) as do the ABL height. The ability of the surface layer to transport momentum, sensible heat, water vapour and other constituencies is of fundamental importance in all studies related to land surface/atmosphere as well as ocean/atmosphere interaction processes, including parameterisation in global circulation models. Due to the above mentioned properties of the surface layer, it has received far greater attention from the researchers than the outer part of the ABL.

1.3.2.2 Free Convection Layer

Free convection layer is the layer in which buoyant convection dominates. This layer formed under conditions of large heat flux and calm wind and forced convection, gradient of wind speed and potential temperature is almost negligible. The properties of turbulence are influenced mainly by the surface characteristics than that of the capping inversion.

1.3.2.3 Mixed Layer (ML)

It is a part of CBL characterised by intense mixing in a statically unstable situation or condition where thermals of warm air rise from the ground. The turbulence in the ML is usually driven by convective sources such as heat transfer

from warm ground and radiative cooling from the top of the cloud layer. Turbulence in the mixed layer tends to mix turbulent parameters uniformly with height. Even when convection is dominant mechanism, there is usually wind shear across the top of the ML that contribute turbulence generation. The ML reaches its maximum depth in the afternoon.

1.3.2.4 Entrainment Zone (EZ)

The EZ is the region of statically stable air at the top of the ML, where is entrainment of air from free atmosphere downwards and overshooting of thermals upward. EZ is characterised by increased vertical wind shear, potential temperature and humidity and negative heat flux, large momentum flux and positive moisture flux are seen in this layer. When the ML is shallow during morning hours EZ is proportionally shallow. Thin EZ are expected for large temperature changes across the ML top, because thermals will not penetrate as far and entrainment will be slow. Thick EZ are expected with more intense ML turbulence when convection is vigorous.

1.3.2.5 Residual Layer (RL)

After the sunset, the thermal cease to form allowing turbulence to decay and the resulting layer of air is called residual layer. The RL is neutrally stratified and hence the smoke plumes emitted into the RL tend to disperse equally in all directions. The cooling rate is more or less uniform throughout the depth, thus allowing the RL theta-v profile to remain nearly adiabatic. The RL does not have any direct contact with the ground. The RL often exists for a while in the mornings before being entrained into the new ML.

1.3.2.6 Stable Boundary Layer (SBL)

The ABL can become stably stratified when the air above is warmer than the earth surface and this type of layer can be formed during night hours so this layer is called Stable Boundary Layer (SBL) or Nocturnal Boundary Layer (NBL). Such layer can also be formed during day time when warm air advects over cold surface. The SBL is characterised by statically stable air with weak and sporadic turbulence. This

statically stable air tends to suppress turbulence, while the enhanced wind shear due to the development of nocturnal jet tends to generate turbulence. Pollutants emitted into the stable layer is dispersed little in the vertical, however horizontal dispersion of pollutants is more rapidly.

1.4 Marine boundary layer structure

The boundary layers are traditionally divided into sublayers as explained. Over the marine atmosphere during calm condition, in the lowest layer up to a few millimetre from the surface vertical transports are mainly due to viscosity and molecular diffusion. The atmospheric surface layer is about 10 % of the ABL depth where the height dependence of the turbulent fluxes is small. Mixed layer exists above the surface layer and it extends up to about 80 % of the ABL. In the mixed layer turbulent mixing takes place resulting small vertical gradients of mean properties. The inversion layer is the interface between the mixed layer and free atmosphere, typically it is upper 10 % of the ABL. Stable ABL is generally formed over the region where warm air is advected over cool water. Gill (1982); Panofsky and Dotton (1984) and Kagan (1995) were described the structure and dynamics of the ABL.

1.5 Costal atmospheric boundary layer

The structure of the coastal boundary layer is of great importance in air pollution problem, because the coastal areas are often heavily industrialised areas and densely populated. In addition there is a basic scientific interest in understanding the meteorological state that frequently prevails in coastal zone.

Sea/land breeze circulations are local mesoscale atmospheric phenomena frequently observed over coastal regions. These circulations are formed due to the temperature gradient between land and sea. The temperature contrast causes a horizontal pressure gradient, which drives the surface wind from sea to land called as sea breeze. The land breeze occurs when the surface wind blows from land to sea during evening and night hours due to relatively quick cooling of the land. It is because of the less specific heat capacity of land. These circulations are eventually transformed into kinetic energy of the flow. The closed circulation begins near the shoreline and extends both offshore and onshore. It is known that the prevailing wind,

land sea thermal contrast, frictional retardation, surface heating, coastal shape, terrain and sea surface temperature are factors influencing the time of onset, intensity and nature of the sea breeze circulation (Raghukumar *et al*, 1986; Prakash *et al.*, 1992). Sea breeze as it penetrates inland affects the climatology and meteorology of the coastal zones. The general features of the sea/land breeze circulations were investigated numerically as well as field observations (Estoque, 1961,1962; McPherson, 1970; Pielke, 1974; Keen and Lyons, 1978; Mitsumoto *et al.*, 1983).

1.6 Monsoon boundary layer

Atmospheric boundary layers observed during southwest monsoon are different from those of the trade wind boundary layers. The monsoon boundary layer is influenced by the large scale monsoon features such as monsoon trough, depressions etc. Holt and Sethuraman (1987) made a detailed analysis of mean boundary layer structure over Arabian Sea and Bay of Bengal during active and break periods using MONEX-77 and MONEX-99 data. During weak and active phases the boundary layer showed different characteristics (Parasnis and Morwal, 1991; Parasnis, 1991 and Kusuma *et al* 1991). Study by Parasnis *et al* (1991) over the monsoon trough region reported that boundary layer height varies significantly. Monsoon experiments such as IIOE, ISMEX-73, Monsoon -77, Monsoon-88 and MONEX-79 focused on the study of Arabian Sea marine atmospheric boundary layer. The monsoon boundary layer over Arabian Sea was critically reviewed by Young (1987) and extensively studied using the data from the field experiments by Colon (1964), Sikka and Mathur (1965), Pant (1978) etc. These studies revealed the existence of low level atmospheric inversions over the west and central Arabian Sea, which disappeared near the West Coast of India. Ramanathan (1978) found that the buoyancy effects are permanent in May compared to June when the mechanical processes are significant over Arabian Sea from the analysis using ISMEX data. During active rainfall period the inversion disappears and exists saturated mixed layers, positive sea-air virtual temperature difference and large specific humidity. MONTBLEX-90 was the first large-scale field experiment conducted over the Indian land area to study the boundary layer characteristics during monsoon with special reference to the monsoon trough region. The Indian summer monsoon trough region is characterised by organised moist convection for about four months from June to September. The western end of the trough is associated with a heat low of small

vertical extent and convergence up to lowest half kilometre whereas eastern end is characterised by a convergence up to mid troposphere. The circulation associated with the convergence extends throughout the troposphere with intense convection. The eastern end lies on the warm waters of Bay of Bengal, which is a heat and moisture source (Sikka and Narasimha 1995). Therefore, the atmospheric boundary layer over the region requires special study and MONTBLEX-90 was designed to cater the requirement. Extensive literature is available on the monsoon trough boundary layer as a result of the field experiment. Sivaramakrishnan et al (1992) studied the characteristics of turbulent fluxes of sensible heat and momentum in the surface boundary layer using sonic anemometer. Heat fluxes show a diurnal trend whereas the momentum flux shows variability without any diurnal trend.

The large scale monsoon is characterised by the Intraseasonal oscillations (Sikka and Gadgil, 1980) and associated features in the ABL also show the similar oscillations (Kusuma *et al*, 1991). The strong Low Level Jetstream with peak wind speed at 850 hPa exists with large variability to bring the active and weak cycles. The oscillation of the cloud band associated with this LLJ begins with the onset of southwest monsoon from the southern region of south Kerala and hence the oscillations of different harmonics persist over the surface boundary layer of this region.

1.7 Stability of the ABL

Atmospheric stability is based on the equilibrium conditions of the air parcels under considerations. To explore the behaviour of rising and sinking air, a small volume of air is to be considered and is referred to as the air parcel. At the earth surface, the parcel has the same temperature and pressure as the surrounding air. Suppose the air parcel is lifted. Since the pressure decreases with increasing altitude, the air pressure surrounding the air parcel lowers, allowing the air molecules inside to push the parcel walls outward leading expansion of the parcel. The temperature of the air parcel decreases due to expansion. On the other hand, if an air parcel is moved downwards, the compression of air parcel takes place leading to increase in temperature. Hence, a rising parcel of air expands and cools, while a sinking parcel gets compressed and warmed. The variations in temperature and humidity with height in the ABL lead to density stratification with the consequence that an upward

or downward moving parcel of the air will find itself in an environment whose density will, in general, differ from that of the parcel, after accounting for the adiabatic cooling or warming of the parcel. In the presence of gravity, this density difference act as buoyancy force on the parcel, which would accelerate or decelerate its vertical movement. If the vertical motion of the parcel is enhanced, i.e, the buoyancy force accelerates the parcel: the environment is called statically unstable. On the other hand, if the parcel is decelerated, the atmosphere is called stably stratified. When the atmosphere exerts no buoyancy force on the parcel at all, it is considered as neutral. In particular the static stability parameter of the atmosphere s is defined as (Arya, 1988):

$$s = (g / T_v) \left(\frac{\partial \theta_v}{\partial z} \right) \quad 1.1$$

where g is the acceleration due to gravity; T_v is the virtual temperature. Based on equation 1.1 the atmospheric stability can be divided in to three categories.

1. Unstable, when $s < 0$, $\frac{\partial \theta_v}{\partial z} < 0$, $\frac{\partial T_v}{\partial z} < -\Gamma$.
2. Neutral, when $s = 0$, $\frac{\partial \theta_v}{\partial z} = 0$, $\frac{\partial T_v}{\partial z} = -\Gamma$.
3. Stable, when $s > 0$, $\frac{\partial \theta_v}{\partial z} > 0$, $\frac{\partial T_v}{\partial z} > -\Gamma$.

from equation 1.1 another important feature can be noted that vertical motions are generally enhanced in an unstable atmosphere, while they are suppressed in a stably stratified environment. The stability condition can also be expressed on the basis of θ_v gradient or lapse rate, relative to adiabatic lapse rate Γ , atmospheric layers are variously categorised a follows:

1. Superadiabatic, when $\frac{\partial T_v}{\partial z} > -\Gamma$.
2. Adiabatic, when $\frac{\partial T_v}{\partial z} = -\Gamma$.
3. Subadiabatic, when $0 < \frac{\partial T_v}{\partial z} < -\Gamma$.
4. Isothermal, when $\frac{\partial T_v}{\partial z} = 0$.
5. Inversion, when $\frac{\partial T_v}{\partial z} > 0$.

Fig 1.3 gives a schematic of the above static stability categories in the lower part of the ABL. In the figure the surface temperature is assumed to be the same and the virtual temperature profiles are assumed to be linear for convenience only; actual profiles are usually curvilinear.

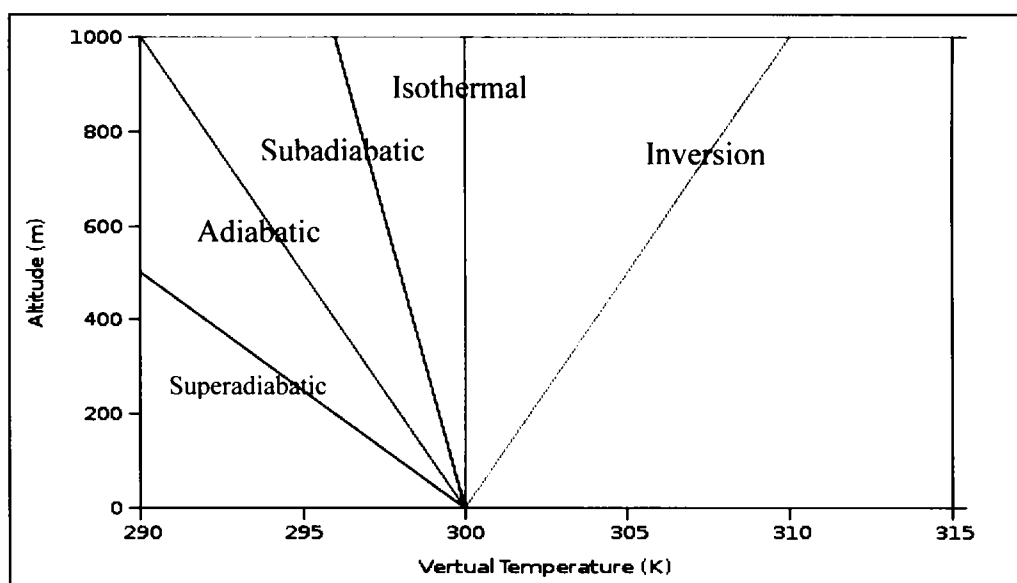


Fig. 1. 3 Schematic diagram of the various stability categories based on virtual temperature (After Arya, 1988).

1.8 Techniques for probing ABL

A better understanding of the structure and dynamics of the ABL and its interactions with earth surface and the overlying free atmosphere evolve as a result of synergistic combination of theoretical, observational, numerical and laboratory simulation studies and dimensional analysis. Observational studies are particularly important because they can provide direct means for checking of model results and visualization of the physical processes that govern the structure and dynamics of the ABL. During the past years, the study on the atmospheric structure and dynamics was triggered by the availability of fast computers and by the introduction of the various measurement techniques. Planning of observational studies requires complete understanding of instrument capabilities and limitations, techniques for data handling and analysis. In addition it requires the strategies for designing and implementation of field experiments. The experimental techniques for the probing the atmospheric boundary layer fall into two categories : *in situ* observations and remote sensing.

1.8.1 *In situ* measurements

The direct sensing technique includes surface measurements (instrumented shelters) and sensors mounted on various platforms, such as fixed platforms (mast, towers, booms) and moving platforms (aircraft, balloons). *In situ* sensors are traditional instruments for surface and lower boundary layer studies, being capable of providing accurate and high-resolution information required for a quantitative work, but are costlier and limited to lower heights. In this method the atmospheric flow field can be modified by the structure of the platform and require physical positioning and alignment of the sensor. Platforms such as towers and masts are convenient for carrying out surface layer studies. Multiple level (ranging from few metre to few hundred metre) installations of suitable combinations of mean and fast response sensors can be performed on these platforms to measure different variables such as wind speed, temperature, humidity, fluxes and radiant energy. Various sensors usually employed in the ABL experiments include anemometers, thermometers, hygrometers etc.

Balloon systems play an important role in studies concerning the structure of the ABL. Various types of balloon systems that are often used in the ABL studies include constant density balloons, Tethered balloons (Kytoon), Free balloons such as Radiosonde (provide measurement of temperature, pressure and humidity) or Rawinsonde (wind measurement is also possible with ground based tracking or by the receiving systems in the instrument package eg: OMEGA, LORAN-C). Recent technical developments made it possible to measure wind with the help of Global Positioning Satellites (GPS) and the system is commonly known as GPS Sonde. The balloons have the disadvantage that it provides an unrepresentative point measurement, that is neither a time nor space average.

Aircraft based instruments measure the spatial - temporal distribution of different ABL variables. Typically instruments are mounted on special booms projecting forward from the nose or wings of the aircraft in order to get the sensors out of the flow disturbed by the air craft itself. It can be used for either vertical profiling or horizontal traverse and can obtain statistically significant measurements much faster than that provided by direct fixed-point measurements. It is possible to investigate large areas and quickly to explore the areas of difficult access such as ocean, forest, mountain etc. Aircraft flight legs are usually too short and have

potentially large sampling errors yielding large scatter in the data. If the flight legs are long, it is difficult to probe the unique boundary layer structure.

1.8.2 Remote sensing measurements

Passive remote sensing involves visual observations and radiometric techniques. The active remote sensing has gained much recognition as excellent tools for ABL studies since many kinds of observations are impossible by direct or *in situ* measurements alone. The obvious advantage of the remote sensors is its ability to sample large volumes of ABL with no perturbation of the flow as is common with immersion instruments (Wyngaard, 1986). The remote sensing methods can be classified into two : passive and active sensors, depending on the operation. Active remote sensing techniques involve Radar, Sodar, and Lidar, whereas remote sensors fall into three major categories depending on the type of signal used and are commonly referred to as Sodar, Radar and Lidar for sound, radio and light detection and ranging respectively. They provide instantaneous vertical coverage and almost continuous temporal coverage with increased range and spatial scanning capability, but have constraints such as minimum range and spatial resolution limit.

Sodar also referred to as acoustic sounder can be used for detecting the spatial and temporal distribution of velocity and thermal parameters characterizing the atmospheric turbulence. Many ABL structures like convective plumes, waves, fronts, capping layers, and ground based stable turbulent layers can be identified using sodar. But, sound attenuate very rapidly so that it is very difficult to detect layers above 1-1.5 km. This makes the detection of ABL height practically impossible, if it is greater than the above range. But it is an excellent tool for probing the night time boundary layer where it is able to detect turbulence, waves etc.

Pulsed Doppler Lidars are optical analog of the Doppler radars. These instruments use laser light and because of the shorter wavelength, it became sensitive to the aerosols and cloud particles that follow air motions and therefore serve as good targets for wind sensing. It can be used to measure the component of wind velocity, temperature, humidity, concentration and ABL height. The Lidar cannot be operated in the cloudy and foggy conditions because the laser beam will be attenuated very easily under these conditions. Because of the complexity and high operating cost, they are rarely used in the boundary layer studies.

Radar probes the atmosphere by directing the electromagnetic energy at the region of interest and receiving the relatively weak signal that is scattered back. The signal processing yields information about the required variable of interest. Doppler wind profiling radars operating at Ultra High Frequency (UHF) (300 MHz to 3 GHz) and Very High Frequency (VHF) (30-300MHz) currently used for monitoring wind in the atmosphere have a minimum range that is too high for boundary layer studies. Recent developments (Ecklund et al., 1988; Carter et al., 1995) in the Doppler radar techniques is able to provide wind profiles at one minute interval up to a height of 2 to 3 km with 100 m resolutions or even less. The wind profilers can operate reliably for long periods in nearly all weather conditions and can provide valuable information about the boundary layer evolution that is difficult to obtain from other measurement techniques. These systems offer a unique opportunity to study the boundary layer structure, wind and turbulence field.

Radio Acoustic sounding system (RASS) combines both radar and acoustic techniques to sense temperature profiles remotely. These radars are capable of tracking Doppler shifts in the weak signals scattered back from radar refractive index undulations induced by sound waves propagating upward from a source near the radar. Strong signals are obtained when the wavelength of the transmitted acoustic signal is matched to half radar wavelength and radar acoustic phase fronts are matched. The height resolutions are of the same order as the boundary layer radars. For the boundary layer studies combinations of both remote and direct sensing techniques are the better choice. In the present study observation from both *in situ* and remote sensing (radar and satellite) techniques are employed.

1.9 Numerical modeling of ABL

Modelling provides a theoretical basis for the interpretation of measured characteristics and allows their prediction. The numerical modelling of the boundary layer are useful because they enable us to examine the relative importance of the different external factors and internal processes in determining the behaviour of the ABL. The external factors or parameters, which must be considered, are the large-scale synoptic conditions and the properties of the underlying surface of the earth. The internal processes are the various transport processes, most important among these being the eddy transport along the vertical.

Basic problem in numerical modelling is the determination of the space-time variation of the various variables (wind, temperature, moisture), which describe the ABL as functions of different external parameters. Modelling basically consists of two stages: selection of an appropriate closure scheme and solution of the closed set of the averaged governing equations.

1.9.1 Governing Equations

To describe quantitatively the state of the Atmospheric Boundary Layer, the equations of the fluid mechanics, that describe the dynamics and thermodynamics of the gases in the atmosphere can be used. These basic equations are collectively called the equations of motion and they include equation of state, conservation of mass, momentum, heat and moisture. In addition to these equations for scalar quantities such as tracer concentration can also be added. The system of equations describe the x, y, z, t dependence of ABL variables such as wind components, temperature, pressure, specific humidity, air density etc.

1.9.2 Closure Problem

Closure problem is the fundamental problem in the mathematical modelling of the boundary layer processes. The closure problem arises from representing the total turbulent flow in terms of the mean flow. In this problem, the number of unknowns in the set of equations for turbulent flow is larger than the number of equations. When equations are included for these unknowns (changing them into known variables), one discovers even more unknowns. Thus for any finite set of these equations, the description of the turbulence is not closed and this is called the closure problem. In order to make the mathematical /statistical description of the turbulence tractable, one of the approaches is to use finite number of equations and approximate the remaining unknowns in terms of known quantities – closure approximation. The number of unknowns is more for higher orders of closure schemes. In the first order closure the higher order moments are replaced by the mean quantities at the particular level. The second order closure models employ equations for the second moment, which are closed on the third moment level. Generally an n -order closure employs equations for the n moments and all equations are closed on the level of $n+1$ moment.

Another method is combination of local and non-local closure schemes. In the local closure, an unknown quantity at any point in space is parameterized by gradients of known quantities at the same points in space, whereas in the non-local closure, the unknown quantity at one point is parameterized by values and/or gradients of known quantities at many points. Regardless of the order or method of closure schemes used the unknown quantities must be parameterized as a function of known quantities or parameters. The ABL parameterization basically deals with the approximation of the turbulent fluxes in terms of the mean quantities known. The ABL parameterization schemes are very important input to the weather prediction or to the global circulation models, because the numerical models of the atmospheric general circulation incorporate the statistical effect of boundary layer processes in terms of parameters computed by the model through the parameterization techniques.

1.10 ABL – Earlier studies

The research in the ABL gained considerable attention from the last few decades due to the increased emphasis on its role in the studies related to exchange processes between land and atmosphere and also between ocean and atmosphere. The theoretical and experimental investigation of atmospheric boundary layer showed advancement in the early 1960's even though a number of individual efforts led to the theoretical formulation of the theory of turbulence and boundary layer and its importance in the atmospheric boundary layer context (Hinze, 1959; Lumely and Panofsky, 1964; Haugen, 1973; Monin and Yaglom, 1971). The reasons for the slow progress in this area are due to the difficulties in measurement and handling mathematical equations. The root cause is the nature of turbulence, essentially unpredictable variations in the atmospheric properties. The advances in sensing technology and computing power have greatly enhanced our ability to tackle these problems.

The earliest ABL research was focused on the surface layer. Even though Monin-Obukhov surface similarity theory, which relates the vertical gradients of mean wind and temperature to the surface fluxes through universal stability functions, was developed in 1954. But stability functions were established from field measurements only in 1970's. Apart from the Great plains experiment in 1953 (Lettau and Davidson, 1957), Wangara experiment in 1967 (Clark *et al* 1971; Hicks,

1976,1981; Yamada 1976; Webb, 1970; Dyer and Hicks 1970; Wyngaard *et al.*, 1974) and Kansas -1968 experiment (Businger *et al.*, 1971; Izumi, 1971) led to the definitive description of the surface layer statistics (Wyngaard *et al.*, 1971; Kaimal *et al.* 1972) and profile forms including the determination of the von Karman constant (Businger *et al.*, 1971), which later led to considerable controversy (Wieringa, 1980; Högström, 1985). The Minnesota- 1973 experiment (Izumi and Caughey, 1976; Willis and Deardorff, 1974) paved the way for the understanding of the mixed layer (Kaimal *et al.*, 1976) and stable boundary layer turbulence statistics. The detailed investigation on the turbulent instrumentation performance with special emphasis on humidity sensors and the interpretation of the flux gradient relations was the focus of International Turbulence Comparison Experiment (ITCE-1976 & 1981). This experiment showed the need for reliable measurements of variances and covariances and the possible errors associated with the single point measurements over a finite averaging time (Dyer and Hicks, 1982; Dyer and Bradley, 1982; Francey and Garratt, 1981; Tsvang, *et al.*, 1985). Apart from these, the above experiments paved the way for understanding the spectral and cospectral behaviour in the surface layer (Kaimal *et al.*, 1972; Kaimal, 1973; Wyngaard and Coté, 1972) and also an idea about the contributing terms to the budget of turbulence kinetic energy (Wyngaard and Coté, 1971; Wyngaard *et al.*, 1971; Deardorff and Willis, 1985; Moeng and Wyngaard, 1989)

With additional observations of the unstable surface layer Kadar and Yaglom (1990) was able to provide a definite description of the stability dependence of a number of profiles and turbulence statistics over wide range of instabilities. However, the description of the stable boundary turbulence still remains unresolved due to the lower level of the turbulence and the need for the high-resolution data to probe into this problem. Nevertheless, some observations and theoretical attempts lead to the idea of the stable boundary layer profile forms (Webb, 1970; Hicks, 1976; Beljaars and Holtslag; 1991) and structure of the scaling of the boundary layer (Niewstadt, 1984). However, the studies of stably stratified flows including laboratory experiments (Yamada, 1976; Stillinger *et al.*, 1983; Lienhard and Van Atta, 1990), numerical simulations (Holt *et al.*, 1992; Kaltenbach *et al.*, 1994), and field observations (Webb, 1970; Hicks, 1976; Mahrt *et al.*, 1979; Hunt *et al.*, 1985; Coulter, 1990; Weber and Kurzeja, 1991; Dias *et al.*, 1995; Schumann and Gerz, 1995; Mahrt, 1999) indicate that even in the very stable boundary layer some turbulence and

vertical mixing persist. This also pointed to the need for new parameterization schemes that include physical processes not covered by Monin Obukhov similarity theory (Derbyshire, 1999; Mahrt, 1999). Even then, for the description of the turbulence structure in the atmospheric surface layer and for modelling the surface layer processes in the large-scale models, the Monin Obukhov similarity theory still finds wide usage. However, the empirical relations between the physical variables and stability parameter should ultimately be determined by experiments because most of the earlier field experiments were conducted in ideal and homogeneous conditions especially in the mid latitudes and the experiments taken together do give rather coherent picture of the fundamental issues of surface layer physics as reviewed in Högström (1996). The question on the validity of the similarity theory over terrains of varying complexities (Zang et al., 2001; Al-Jiboori et al., 2001) and also during low wind conditions still remains due to the paucity of the experiments especially over the tropical regions.

The surface layer experiments discussed above shown the advancement in the systematic implementation of tower-based instruments, sonic anemometry and computer controlled data acquisition in field experiments. However, the nature of the vertical heat flux profiles and the knowledge about the outer regions of the convective boundary layer began to emerge from the late 1970's advent from the laboratory models (Willis and Deardroff, 1974), large eddy simulations (Deardroff, 1974; Moeng, 1984), observations using aircraft and balloons (Lenschow, 1973; Kaimal et al., 1976; Nicholls, 1984) and also based on surface based remote sensors (Lenschow, 1986). The advancement in the remote sensing devices such as Radars, Lidars, Sodars, RASS has provided much insight into the structure of the ABL because of their ability to monitor important meteorological parameters continuously in space and time. The developments in this field in the past few decades are reviewed in Wilczak et al. (1996). With these developments attempts are now focused on the development of instruments such as Fourier Transform Infra Red Spectroscopy (FTIR) that can provide vertical profiles of temperature, moisture and trace gases, space antenna boundary layer Doppler radars (Holloway *et al*, 1995; Van Baelen, 1995) for wind and flux profiles, Frequency Modulated–Continuous Wave (FM-CW)/RASS for high resolution temperature profiles and also development of aircraft and satellite borne remote sensors.

The knowledge about the region above the surface layer, i.e., mixed layer, mainly emerged through various studies incorporating the experimental facilities. The laboratory and numerical studies not only gave us the first look at the mixed layer structure but also quantified the difference between convective and neutral ABL. They also revealed the effects of entrainment at the top of the ABL. So, understanding the convective boundary layer was mainly focusing on the problems of the role of entrainment at the top of the CBL, counter gradient heat flux and also on the inclusion of the contribution of large convective eddies in the flux measurements and turbulent closure schemes. The issues invoked the study on flux gradient relationship in the boundary layer, which in turn provided the framework of modelling of the convective boundary layer and turbulence (Deardorff, 1972; Goldfrey and Beljaars, 1991; Holtslag and Moeng, 1991). Various methods and parameterization for ABL height estimation and entrainment process was proposed (Deardorff, 1974; Troen and Mahrt, 1986; Beljaars and Betts, 1993; Driedonks and Tennekes, 1984; Betts et al., 1992; Batchvarova and Gryning, 1994; Vogelezang and Holtslag, 1996). At the same time field programs provided insights into the mesoscale organization of low clouds and their relationship to ABL structure. A number of studies of the cloud topped boundary layer has brought some of the most exciting theoretical controversies of the period such as cloud top entrainment instability and the role of radiative fluxes in the entrainment processes etc. (Lilly, 1968, Betts, 1973; Deardorff, 1976, 1980; Stage and Businger, 1981; Nicholls, 1984; Driedonks and Duynkerke, 1989; Moeng, 1986, 1987). Even now the theoretical formulation of the cloud topped boundary layer remains as an unresolved problem. The glimpses of the development in the theory and observation of the ABL can be found in the recent literature and reviews (Stull, 1988; Garratt, 1992; Moeng and LeMone, 1995; Brutsaert, 1999).

It should be noted that the understanding of atmospheric boundary layer evolved basically through the organized field experiments apart from the individual and small-scale experiments. The era of the international field experiments began in 1960's with emphasis on tropical oceanic regions. Some of them include Indian Ocean expedition (IIOE) in 1964 (Badgley et al., 1972), Barbados Oceanographic and Meteorological Experiment (BOMEX) in 1969 (Davidson, 1974), Atlantic Trade Wind Experiment (ATEX) (Augstein et al., 1973; Dunkel et al., 1974), GARP (Global Atmospheric Research Programme) Atlantic Experiment (GATE) (Kuettner and

Parker, 1976; Volkov et al., 1982), Air Mass Transformation Experiment (AMEX) near Japan in 1974-1975, Joint Air- Sea Interaction (JASIN) experiment over north east Atlantic and north sea (Nicholls, 1985; Shaw and Businger, 1985), Marine Remote Sensing (MARSEN) Experiment (Geernaert et al., 1986), Humidity Exchange over the Sea (HEXOS) programme (Smith et al., 1990, 1992, 1996b; Decosmo et al., 1996), Coastal Ocean Dynamics Experiment (CODE) in 1985 (Zemba and Frieche, 1987; Enriquez and Frieche, 1994), Frontal Air Sea interaction Experiment (FASINEX) near the gulf stream southwest of Bermuda in 1986 (Li et al., 1989), TOGA Tropical Ocean Global Atmospheric coupled ocean Atmospheric Experiment (COARE) over tropical Pacific Ocean (Webster and Lukas, 1992), Joint air Sea monsoon Interaction Experiment (JASMINE) (Webster et al., 2002). The details of the experiments conducted over the marine region are given in Stull (1988) and Garratt (1992). These experiments provided important information regarding the drag coefficient, fluxes and air sea interaction.

Over the land region, apart from Kansas, Minnesota and Wangara experiments sited above, some of major field experiments carried out include Venzulean International Meteorology and hydrology Experiment-VIHME (Betts and Miller, 1975), Boundary layer Experiment-1983 (Stull and Eloranta, 1984), Amazon and Arctic Boundary layer Experiment (ABLE) (Harris, *et. al* 1990), HAPEX (Hydrological and Atmospheric Boundary Layer Experiment)-MOBILHY (Andre et al., 1990; Mahrt and Ek, 1993), First ISLSCP (International Satellite Land surface Climatology Project) field Experiments (FIFE) (Sellers et al., 1988; Betts et al., 1992), European Filed Experiment over the Desertification and Threatened Areas (EFEDA) (Bolle et al., 1993), Boreal Ecosystem Atmospheric Study –BOREAS (Davis et al., 1997). It can be noted that most of these experiments focused on the land atmospheric coupling and associated processes. To study the atmospheric boundary layer entrainment process Flatland Experiments were conducted for the first time using the wind profiler network (Angevine et al., 1998; Angevine, 1999). Cooperative Atmospheric Surface Exchange Study (CASES 97) was conducted to understand the warming and moistening of the atmospheric boundary layer (LeMone et al., 2000, 2002). It can be noted that most of these experiments were conducted in the oceanic and mid latitude regions and also the experiment conducted over the tropical continental region is sparse compared with that over the oceanic regions.

The basic experiments conducted over the tropical Indian region were focused mainly on the exploration of the marine boundary layer over the adjacent oceanic regions such as Indian Ocean, Arabian Sea and Bay of Bengal. These experiments include International Indian Ocean Expedition (IIOE 1963-65), Indo-Soviet Monsoon Experiment (ISMEX-1973), the Monsoon Experiments (MONSOON-77 and MONEX-79), Monsoon Trough Boundary layer Experiment (MONTBLEX-1990), Indian Ocean Experiment (INDOEX- 1996-99), Bay of Bengal and the Monsoon Experiment (BOBMEX-1999) (Bhat et al., 2001). Detailed account on the studies conducted over the Indian region on the features of ABL is reviewed by Narasimha et al. (1997).

Over the land, apart from the individual and small scale experiments conducted (Narasimha et al., 1997), the major field experiment carried out was MONTBLEX-1990 over the monsoon trough region of the Gangetic plains during the southwest monsoon season to understand the ABL features during active and break monsoon period (Goel and Srivastava, 1990; Sivaramakrishnan et al., 1992; Kusuma et al., 1991, 1995, Parasnis, 1991). Land Surface Process experiment (LASPEX-1997) was conducted over the Sabarmati basin of Gujarat (Pillai et al., 1998; Satyanarayana et al., 2000; Nagar et al., 2001; Sadani and Kulkarni, 2001) covering different seasons. But continuous monitoring of the Atmospheric Boundary Layer was not available during this experiment, which basically relied upon tower and radiosonde based observations. More over the surface layer experiments were limited and information on the turbulence statistics of wind components, temperature, and humidity based on the Monin Obukhov similarity theory is still lacking. This indicates the need for further experiments, which can provide light on the turbulence characteristics in the atmospheric surface layer. The response of the structure and evolution of the boundary layer to the different synoptic patterns, which is characteristics of the tropical Indian region can also be probed from the experiments. This type of information is particularly useful in improving our knowledge of the boundary layer process, which can be incorporated in the ABL models in turn will lead to the proper representation of the ABL process in the large- scale models. The rapidly growing interest in the climate and climate change problems and the need to simulate regional climate more precisely on time scales of several decades are leading to a greater appreciation of the role of the ABL processes in the climatic system.

1.11 Present study

In this thesis an elaborate study on the structure, dynamics and thermodynamics of the atmospheric boundary layer over tropical coastal, inland and oceanic regions are presented. From the available literature, it is understood that the studies using in situ measurements and remote sensing are imperative. Also, the measurements over tropical regions are still rare. The knowledge of ABL under different seasons, which are characteristics of the Indian sub continent are also essential for understanding the ABL structure over the region. Understanding the ABL processes can improve the forecasting techniques of southwest monsoon. In this perspective the investigation of ABL is carried out using field experiment, which includes mainly tower based Automatic Weather Station (AWS), Lower Atmospheric Wind Profiler (LAWP), first one of its kind in India and QuikSCAT data products.

The main issues addressed in the thesis include, dynamic and turbulence parameters such as surface fluxes over a coastal station of the atmospheric surface layer, the characteristic features of the ABL during active and weak phases of southwest monsoon, marine boundary features during different seasons and associated variabilities. The diurnal evolution and vertical extent of atmospheric boundary layer, the evolution of the atmospheric boundary layer and vertical variations of winds under southwest monsoon season are characteristics of this region especially over inland stations. These features are studied and presented by using UHF L-band wind profiler.

CHAPTER - 2

***SURFACE BOUNDARY LAYER
CHARACTERISTICS OVER COCHIN***

CHAPTER - 2

SURFACE BOUNDARY LAYER CHARACTERISTICS OVER COCHIN

2.1 Introduction

The lowest part of the Atmospheric Boundary Layer (ABL) is called surface layer. Usually 10 per cent of the total height of the ABL is taken as the height of surface layer. The typical height of the surface layer is 100 m during daytime and less than that during night time (Oke, 1978). The variation of the surface fluxes in the surface boundary layer with height is less (not more than 10 %) so that this layer also called constant flux layer (Haugen *et al.*, 1971, Hogstorm, 1988). The variation of fluxes of momentum and heat in surface boundary layer and their distribution in the rest of the planetary boundary layer play a vital role in the energy transport mechanism of the ocean-land-atmosphere system. The primary mechanism for these processes is mainly affected by the turbulence. The turbulence in this layer caused mainly due to the wind shear, which is generated by the surface frictional force known as mechanical turbulence (Arya, 1988).

Thermal and dynamic interaction between the atmosphere and underlying surface occur through the turbulent exchange of momentum, heat and moisture at their interface. Over the Indian region the meteorological features exhibit a wide variability during different seasons. Several studies were carried out over the region with special emphasis to the monsoon trough region using the MONTBLEX-90 data set (MONTBLEX REF). All those studies bring out the variation in the surface layer parameters, structure of the boundary layer etc. during the southwest monsoon period. In the tropics, convection is important and the sensible heat flux shows high correlation with convection rainfall, hence deep convection may influence surface fluxes.

The most striking feature associated with the ABL is the land sea transition with flow perpendicular to the coast in the coastal stations. The characteristic features such as sea breeze and land breeze circulations in the coastal areas have considerable attention because the coastal areas are densely populated, dispersion of pollutants from various industries and other anthropogenic activities depend in the coastal

boundary layer. Pollutants emitted near the shore can remain confined in stagnant condition for a long time in a closed sea breeze cell (Keen and Lyons, 1978; Ozoe *et al*, 1983). The coastal ABL zone is a transition zone in which airflow constantly adjusts to the new boundary conditions when it crosses the shoreline.

The sea breeze is a mesoscale circulation and also a thermally direct circulation that arises from the differential heating along the land-sea interface and it is due to the difference in heat capacity and molecular conductivity of land and sea. The land and sea breezes are locally induced lower atmospheric mesoscale circulation and occur everywhere in the coastal belt. The other type of circulations formed due to the differential heating are lake breezes, land breezes and inland breezes (Bechtold, *et al* 1991), snow breezes (Segal *et al* 1991), fog breezes and breezes formed by difference in cloud cover. In tropical and subtropical areas the sea breeze are very regular, occurring almost daily (Simpson, 1994). It has been well established that as cool and stable air over water bodies crosses the shore line and advected over a heated land mass, a temperature inversion is formed over land which gradually slops up as function of distance (Kunhikrishnan *et al* 1993) from the shore line (fetch distance). In both coastal and inland areas sea breeze phenomena play an important role in the transport of air pollutants by forming characteristic meteorological situations (Kimura, 1983). Sea breeze has a very crucial role in dispersing pollutants from the source region and features of such local circulation is important for aviation safety, sailing and forest fire forecasting.

Sea breeze circulation has a vertical extent of about 2 km and horizontal extent of about 50 km. In order to satisfy the mass continuity, there is a return flow from land to sea in the upper level during the sea breeze and vice versa. The sea breeze study is important in view of onset and cessation time, maximum intensity, vertical and horizontal extension etc. Theoretical aspects of sea breeze circulation were studied extensively by Pearson (1973), Rutunno (1983) and Dalu and Pielke (1989). They introduced characteristic time scale for sea breeze circulation and identified the importance of friction in the intensity and horizontal extension of sea breeze. Aircraft measurements were used for studying sea breeze features by Fisher (1960). After analyzing data over Trivandrum for 392 days (spread over three years), Narayanan (1967) reported that sudden onset of sea breeze is usually accompanied by a rise in humidity, shift in wind direction and increase in wind speed. Nakane and Sasano

(1986) used high-resolution measurements with the help of a Lidar to study sea breeze events. Yoshikado (1990) used soundings for the observational studies on sea breeze. Other observational studies on horizontal structure of sea breeze circulation carried out by Wakimoto and Atkins (1994) and Atkins and Wakimoto (1997). They found that the gradient of temperature and moisture structure during sea breeze passage were strongest and weakest during offshore and onshore flow days respectively. Sha et al (1991) showed that inland penetration of sea breeze slows down in the after noon due to Kelvin-Helmholtz instabilities on the transition from the sea breeze layer to the return current layer. Kusaka et al (2000) established from the simulations that land-use alteration modified the wind system and the time required for the sea breeze to reach inland areas increased by two hours. Sea breeze characteristics over Kalpakam, a tropical site is studied using mesoscale model by Jamima and Lakshminarasimhan (2004) and they found that the sea breeze duration is about 6 hours and the model also agrees with observation. Ohashi and Kida (2001) observed that sea breeze circulation penetrating from Osaka Bay to the inland Kyoto basin, weak wind region (wind speed of less than 2 ms^{-1}) of greater than 1000 m in height was found just ahead of the inland moving a sea breeze front. Kitada (1987) studied to predict the dynamical behavior of eddy diffusivity, turbulent kinetic energy and its dissipation rate associated with moving sea breeze front.

A good amount of work has been carried out by different investigators to understand the climatological as well as the general studies on sea breeze (Arakawa and Utsugi, 1937; Hatcher and Sawyer, 1947; Leooped, 1949). Substantial work has been carried out on the climatological and observational aspects of sea breeze circulation on western and eastern coast of India (Ramadoss, 1931; Ramanathan, 1937; Roy, 1941; Ramakrishnan and Jambunathan, 1958; Ramanathan and Subbaramayya, 1965; Narayanan, 1967; Dekate, 1968; Sivaramakrishnan and Rao, 1989; Prakash *et al* 1993; Kunhikrishnan *et al* 1993; Prakash 1993; Radhika, 1994; Sunil, 1997; Sumabai, 1997; Ramana, 2001). The prevailing wind, land-sea thermal contrast, frictional retardation, surface heating are the factors that influence the time of onset, intensity and nature of sea breeze circulation (Prakash *et al* 1992). The sea breeze is one of the best known and well studied boundary layer mesoscale phenomena. Despite the long history of study of the sea breeze, there still remain many unanswered questions about its microscale structure and dynamics, especially in regions of complex or sloping topography (Wilczak *et al* 1996).

2.2 Outline of the work

In this chapter, the diurnal and seasonal variation of the boundary layer parameters such as air temperature, soil temperature, wind direction and speed are presented. The features of the sea breeze such as onset and cessation time and associated turbulent behaviours are discussed in the next section. The day to day variation of turbulent parameters associated with land breeze and sea breeze is discussed there after. Surface boundary layer height variations is derived from the spectral method is described in the next section.

2.3 Scope of the study

In this study, an attempt is made to bring out the various boundary layer features over Cochin during the land breeze and sea breeze period. Cochin is the one of the big industrial cities of Kerala state so that the study of the boundary layer features such as characteristics of wind, temperature, surface fluxes, drag coefficient, etc. are very important. The onset and cessation time and duration of sea breeze and associated turbulent fluxes are examined closely because these parameters are very important in the diffusion of pollutants in the atmospheric boundary layer.

2.4 Data and methodology

2.4.1 Description of the tower site

Micrometeorological tower observatory is established for boundary layer studies, at Cochin, in the western peninsular India ($9^{\circ} 58'N$ latitude and $76^{\circ} 17'E$ longitude). The terrain around the tower is complex in nature with laterite soil. The shoreline over Cochin is almost parallel to longitude as indicated in Fig.2.1, the location of micrometeorological tower observatory system marked by T (shoreline is inclined to longitude by about 20° with western side is Arabian Sea and eastern side is Indian land mass) and is about 8 km away from the tower site. Fig.2.2 shows the micrometeorological tower system with three levels of sensors. The tower observatory system was set up at Thrikkakara, near south Kalamassery, Cochin (in the main campus of Cochin University of Science and Technology) in November, 2001. The tower has a height of 20 m with sensors for temperature, wind speed and wind direction mounted at three levels: 5 m, 10 m and 20 m. Sunshine recorder and sensor

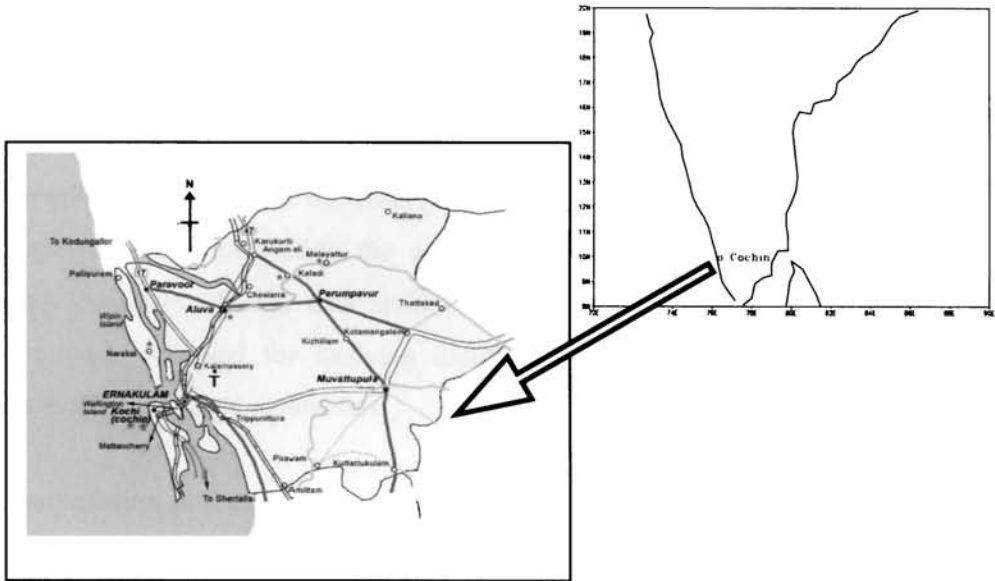


Fig. 2.1 Location map of Cochin (Tower location is marked by T).



Fig.2.2 Micrometeorological Tower of 20 m height with three levels of sensors installed at Cochin University Campus for atmospheric boundary layer studies

for net solar radiation were installed at 10 m level and automatic rain gauge at the ground. The data set was collected in a regular interval of 30 minutes to compute the surface fluxes and other boundary layer parameters and fast response (1 Hz) data was procured during selected periods at an interval of 1 second to understand the evolution of the surface boundary layer height by the Fast Fourier Transformation analysis. Calibration and quality check of the observations from the tower system were carried out thoroughly. After completing the quality check, data set from the memory module was transferred to the data archives for the further analysis. Wind and temperature were observed for studying diurnal variation of the boundary layer parameters and their derived parameters.

2.4.2 Computation procedure

The wind direction, wind speed and temperature at 10 m and 20 m levels observed at the micrometeorological tower were used for the analysis of sea breeze/land breeze and associated features. The non rainy days were selected for the study during winter, pre-monsoon, southwest monsoon and post-monsoon seasons. A few instantaneous observations individually analysed for selected days in each season to bring out the characteristic boundary layer features for the season. The days chosen are 12th January (winter), 15th April (pre-monsoon), 23rd July (southwest monsoon) and 27th November (post-monsoon). Similarly, the mean features for January, April, July and November representing winter, pre-monsoon, southwest monsoon and post-monsoon respectively were also made to understand the general characteristics in respective seasons. Further, to study the boundary layer features during sea breeze and land breeze, long continuous data series (180 data points) during land breeze (around 8 am) and during sea breeze (around 3 pm) were prepared. The prevailing surface wind over Cochin during the southwest monsoon season is northwesterly and that in the other season is northeasterly.

Sea Breeze Component (SBC) was obtained by using the equation (Narayanan, 1967) $SBC = U * \sin(340 - ddd)$. Where U is the wind speed and ddd is the wind direction in meteorological angle. Cochin station is oriented to the coastline by 160-340 azimuth. Thus SBC is positive for sea breeze and negative for land breeze.

The fluxes of momentum and sensible heat are calculated by profile method. It is an indirect method based on Monin-Obukhov similarity theory for estimating surface fluxes. The profiles of wind and temperature in the surface layer are defined in the forms (Dyer and Hicks 1970, Businger et al 1971):

$$\Delta \bar{u} = \frac{u_*}{k} \left(\ln \frac{z_1}{z_2} - \psi_m(\zeta_2) + \psi_m(\zeta_1) \right),$$

$$\Delta \bar{\theta} = R \frac{\theta_*}{k} \left(\ln \frac{z_1}{z_2} - \psi_h(\zeta_2) + \psi_h(\zeta_1) \right),$$

where $\Delta \bar{u} = u_1 - u_2$ and $\Delta \bar{\theta} = \theta_1 - \theta_2$ the subscripts denotes the level at 10m and 20m respectively u_* is the frictional velocity and θ_* is the temperature scale. ψ_m and ψ_h are the stability functions associated with wind and temperature respectively $\zeta = z/L$ where L is the Monin-Obukhov length and is given by $L = \frac{\bar{T} u_*^2}{gk\theta_*}$ and $R = 0.74$, a ratio of eddy diffusivities in neutral limit and k is the von Karman constant and the value is 0.4

The stability functions are given as follows (Paulsen 1970; Barker and Baxter 1975):

In unstable condition ($\zeta < 0$):

$$\psi_m(\zeta) = \ln \left(\left(\frac{1+x}{2} \right)^2 \frac{(1+x^2)}{2} \right) - 2 \arctan x + \frac{\pi}{2},$$

$$\psi_h(\zeta) = 2 \ln \left(\frac{1+y}{2} \right),$$

where $x = (1 - 15\zeta)^{\frac{1}{4}}$, and $y = (1 - 15\zeta)^{\frac{1}{2}}$,

in stable condition ($\zeta > 0$):

$$\psi_m(\zeta) = -4.7\zeta, \text{ and } \psi_h(\zeta) = \frac{-4.7}{R}\zeta,$$

the frictional velocity and temperature scale are computed iteratively.

The drag coefficient can be determined from the relation $C_d = \left(\frac{u_*}{U}\right)^2$.

where U is the wind at reference height.

The fluxes of momentum can be calculated using the equations

$$\tau = \rho u_*^2$$

And sensible heat flux is found by $SHF = -\rho C_p u_* \theta$.

where C_p is the specific heat capacity at constant pressure and value is $1004 \text{ Jkg}^{-1}\text{K}^{-1}$

2.5 Diurnal variation of boundary layer parameters

2.5.1 Air temperature

The atmospheric temperature is mainly governed by the incoming solar radiation, it mainly depends on latitude and time of the day. Furthermore, it is affected by the nature of the surface of the underlying surface, by the altitude and by the prevailing wind. Diurnal variation of air temperature at the three levels (5 m, 10 m and 20 m) for different months is examined on a seasonal basis. Fig.2.3 shows the diurnal variation of air temperature at the three levels for winter, pre-monsoon, southwest monsoon and post-monsoon seasons. The mean diurnal variation of temperature for the four seasons is presented using data chosen for non rainy days in the respective seasons. The maximum diurnal variation of air temperature is found during winter season with a range of 13°C . This can be due to relatively cloud free situation during the season causing high maximum temperature and low minimum temperature due to less sunshine duration during winter. The lowest minimum temperature recorded during the observation period is 20°C in the month of February and highest maximum temperature is found to be more than 35°C in the month of March and April. This is in agreement with the variation in insolation in the northern hemisphere, which receives more solar radiation during pre-monsoon and southwest monsoon seasons. In general the minimum temperature is found just before the

sunrise and maximum temperature in the day is found around 3 pm local time (IST). Oke, 1978 observed similar diurnal variation over land regimes.

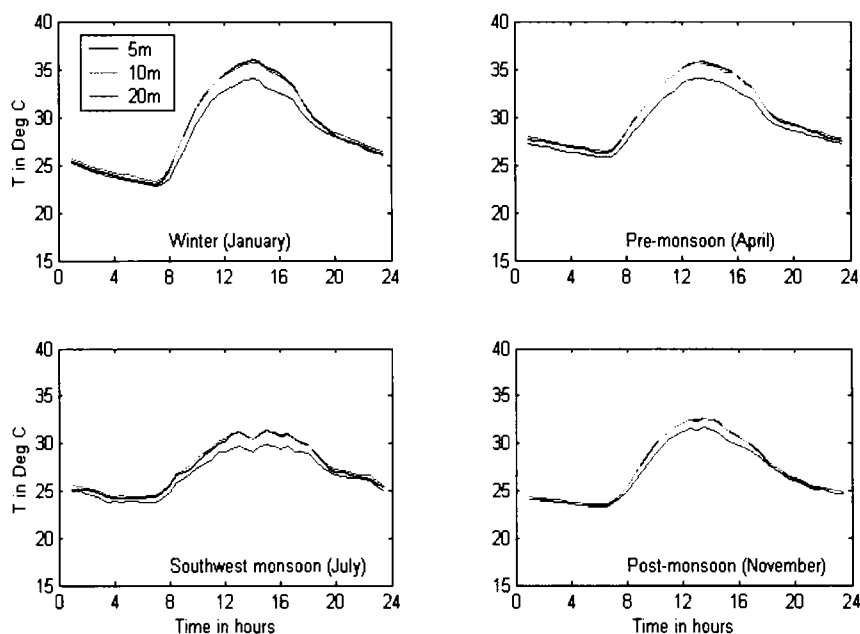


Fig.2.3 Diurnal variation of air temperature during four different seasons

2.5.2 Soil temperature

Soil temperature shows well-marked diurnal variation in upper part of the earth's surface. Temperature penetration to depth is mainly depends upon the nature and thermal conductivity of the soil. The maximum diurnal variation is found in the upper level of the soil. Fig.2.4 shows the diurnal variation of soil temperature during winter, pre-monsoon, southwest monsoon and post monsoon seasons for 5 cm, 10 cm, 20 cm and 40 cm. The diurnal variation of soil temperature at 5 cm depth is almost same as that of air temperature at 5 m. The diurnal variation is maximum at 5 cm and minimum at 40 cm because the thermal conductivity of soil is small (the soil type in the observation site is laterite). At 40 cm depth, diurnal and seasonal variations are comparatively small. The annual mean temperature is maximum at 5 cm depth and minimum is at 40 cm. The time delay for reaching the temperature from 5 cm to 10 cm is almost 30 minutes. Thus temperature change by external forcing affects mainly in the top layer. The maximum diurnal variation is found during the winter season as

in the case of air temperature and the least is found during southwest monsoon and post monsoon seasons.

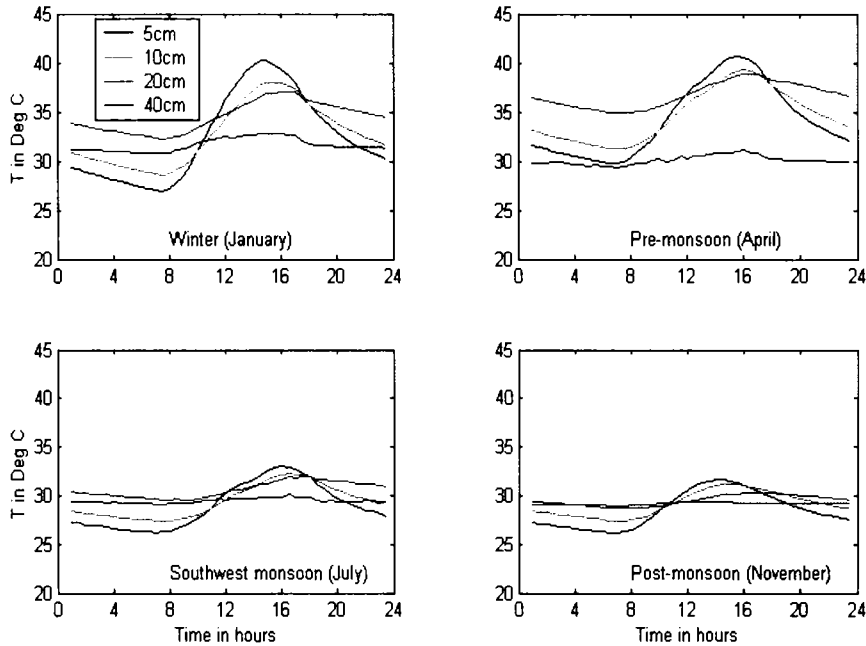


Fig.2.4 Diurnal variation of soil temperature in different seasons at four depths

2.5.3 Wind speed

Diurnal variation of wind over Cochin station at the three levels for the four seasons is presented in Fig.2.5. The wind speed is very small near the ground. At 5 m and 10 m levels, wind is almost calm during night hours in all the seasons owing to surface friction. The wind speed increases with height and the variation agrees with the general pattern of wind in the surface boundary layer i.e, the logarithmic profile as described in Stull, 1997. Generally, wind is calm during night time and increases due to the modulation of the local circulation by the sea breeze caused by differential heating as the day progresses. The wind strength is highest at 20 m among the 3 levels. Maximum wind speed of about 4 ms^{-1} is found at 20 m level on a few days of July, which is attributed by the strong Low Level Jet stream at 850 hPa associated with the active situation of southwest monsoon. In most of the cases, maximum wind speed is found around 16 hours. The winds not only determine the travel time of pollutants from the source region to a given receptor but also control the ground level concentration. The calm/weak winds deteriorate the air quality. Thus better dispersal of pollutants can be expected in pre-monsoon season and less during winter season.

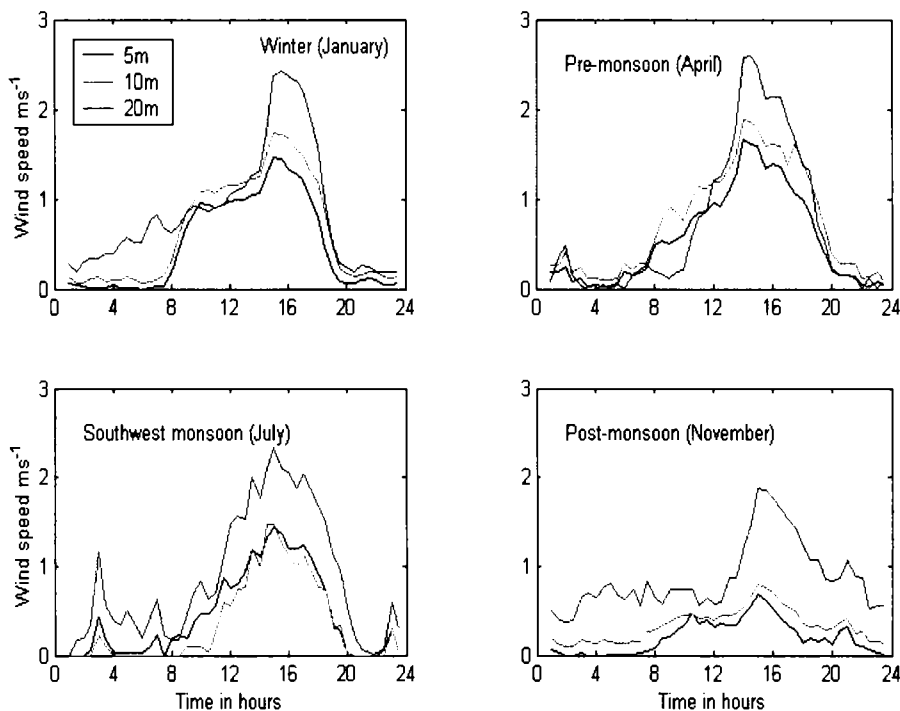


Fig.2.5 Diurnal variation of wind speed during four different seasons at three levels

2.5.4 Wind direction

Diurnal variation of the wind direction observed during winter, pre-monsoon, southwest monsoon and post monsoon seasons are given in Fig.2.6. The local circulation induced by differential heating of the coastal region viz sea breeze is seen in all the cases. The transition time of wind direction from land breeze (around 90 degree during night time and early morning hours) to sea breeze (around 270 degree) is changing from day to day and also from season to season. Earliest sea breeze onset is found during southwest monsoon season and the delayed one occurs during post-monsoon season. Generally wind direction turns clockwise with height due to decrease in surface friction with height. However, during the onset of sea breeze or just before the onset the turning of wind direction with height becomes counter clockwise (backing).

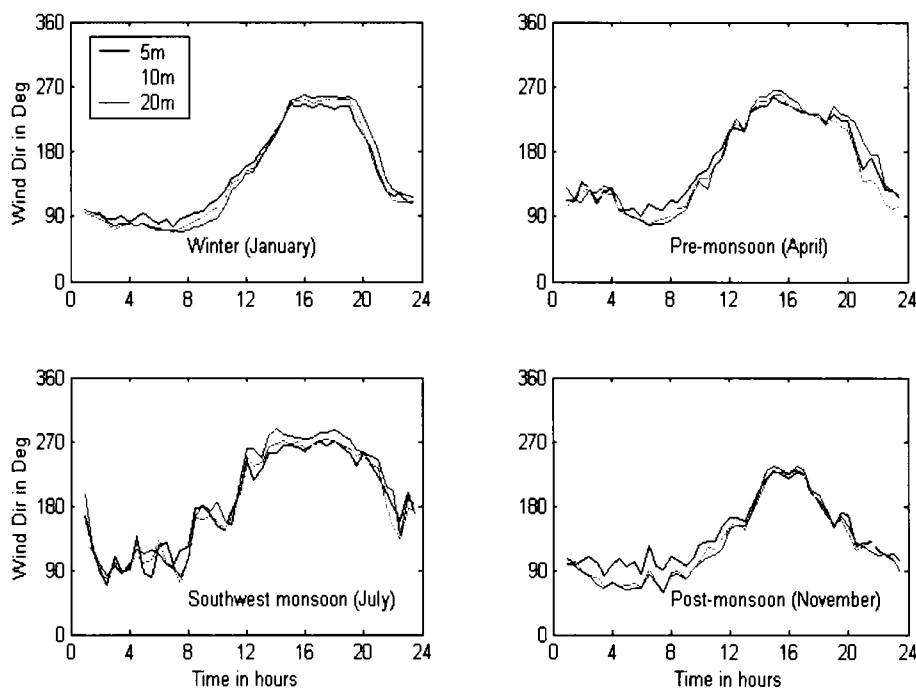


Fig.2.6 Diurnal variation of wind direction in different seasons at three levels

2.6 Sea breeze and associated features

2.6.1 Diurnal variation of averaged wind direction

The features of sea and land breeze circulations are discussed using air temperature, wind direction and wind speed observed at 10 m and 20 m levels. The analysis was carried out considering all non rainy days in the representative months of the seasons. The average diurnal variation of the wind direction for all the seasons is presented in Fig.2.7. Solid line indicates for 10 m level and solid-dotted line is for 20 m level. In the winter season, average sea breeze period during the season is from 1500 hours to 2000 hours. In general, the prevailing surface wind during the season is easterly and it becomes westerly by the afternoon due to sea breeze circulation. In pre-monsoon the duration of sea breeze is slightly larger than that in winter. In general, the transition time from land breeze to sea breeze is less for the averaged pre-monsoon season compared to that during winter season, due to less variation of onset time of individual cases. The strength of sea breeze during this season is slightly higher than that in the winter season. Intermittent cloud clusters formed on most of the days during the southwest monsoon season reduces the insolation and hence the air temperature. So, the time of onset of sea breeze and its intensity vary widely. In

this season, sea breeze lasts for a long period due to more sun shine duration. Even though the intensity is small, land breeze is formed during this period. In the post monsoon season, the duration of sea breeze is small due to less sun shine duration and intermittent cloud clusters formed in association with pressure system.

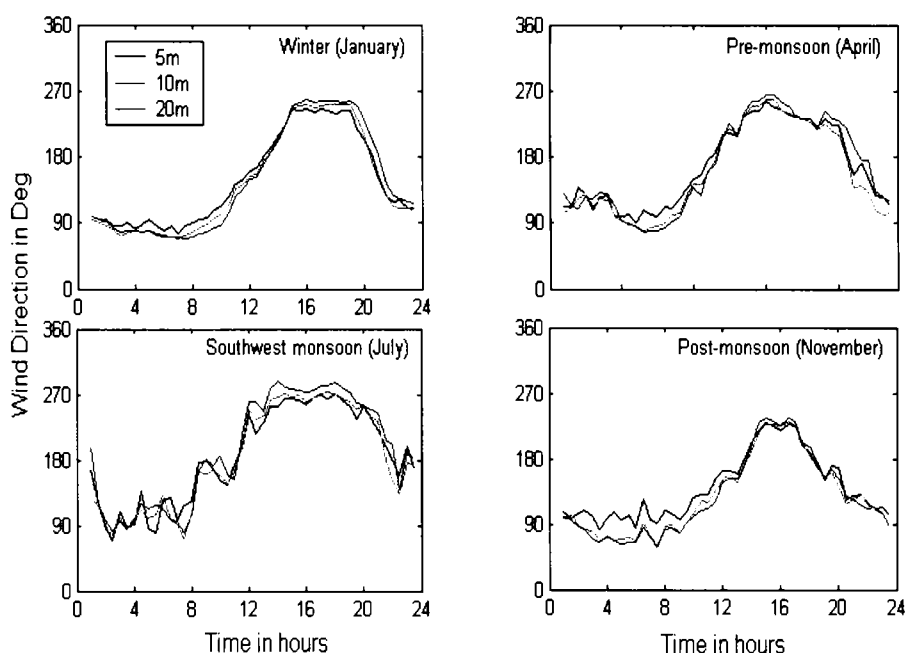


Fig.2.7 Same as Figure 2.6 but for the wind direction in different seasons. Contour interval is 10 degrees.

Among the sea breeze circulation patterns in different seasons, it is found that maximum strength is during pre-monsoon, followed by southwest monsoon. This is contributed by high differential heating in these seasons. The duration of sea breeze is highest in southwest monsoon season followed by pre-monsoon, due to high sunshine duration in these seasons. The strength of land breeze is relatively small during southwest monsoon season compared to other seasons due to the prevailing surface westerly zonal wind in the southwest monsoon season. By further analysis of the averaged features, it is found that the time of onset and cessation of sea breeze on individual days during the same season vary widely. So, the averaged features may not reflect on seasonal sea breeze circulation properly. This can result in lengthy transition time of onset of sea breeze, absence of sea breeze characteristics such as decrease of temperature and wind speed at the time of onset, backing and veering

features in association with the sea breeze. Thus the sea breeze circulation is studied further by considering the temperature and wind on individual non-rainy days in different seasons to bring out the detailed sea breeze characteristics. The differential heating is small during overcast or rainy days and hence the land and sea breeze circulations are feeble. One case of a rainy day during southwest monsoon season was also presented.

The features for 12th January, representative of winter, 15th April for pre-monsoon, 23rd July for southwest monsoon and 27th November for post monsoon are given in Fig.2.8. Diurnal features of the wind direction and corresponding wind speed and air temperature associated with the sea breeze circulation are studied for the above representative days. In the case of winter, it is observed that sea breeze occurs from 1200 hours to 1900 hours. During this period the strength of wind is around 2 ms⁻¹ at 20 m level. The transition from sea breeze to land breeze occurs from 1800 hours to 2100 hours. The mean wind direction of the land breeze on the day is around 76 degrees. The wind strength during this period is feeble at 20 m and is calm at 10 m. It is found that the wind direction turns anticlockwise with height (backs) just before/during the onset time of sea breeze. Air temperature decreases during the time of onset of sea breeze due to the cold air advection (Hsu, 1988). It is noticed that the wind speed decreases for a short period during the setting time of sea breeze due to the combined effect of land breeze and sea breeze in opposite directions. This behavior is evident when the transition from land breeze to sea breeze occurs rapidly. Similar features for 15th April, representing pre-monsoon, as in the case of winter, the strength of wind is more during the sea breeze and the wind is calm at 10 m level except during sea breeze. Since the transition from sea breeze to land breeze is slow, the decrease in temperature at the time of onset of sea breeze is not seen and backing is occurred just before the onset. On 23rd July representing southwest monsoon season, the duration of sea breeze circulation is highest in comparison with the other three seasons. This can be thought of attributed by the increase in insolation during summer. The sea breeze direction is between 270° and 280° and is steady whereas the land breeze direction is not steady (fluctuating about 90 degree) and the strength is feeble (less than 1ms⁻¹). Similar features are noticed for 27th November (post monsoon). Decrease of temperature (though it is small) and wind speed are found due to rapid transition of land breeze to sea breeze. Another notable feature is almost same magnitude of land and sea breezes during this season. The prevailing wind

during the northeast monsoon season is easterly, which is relatively strong and modulates land breeze.

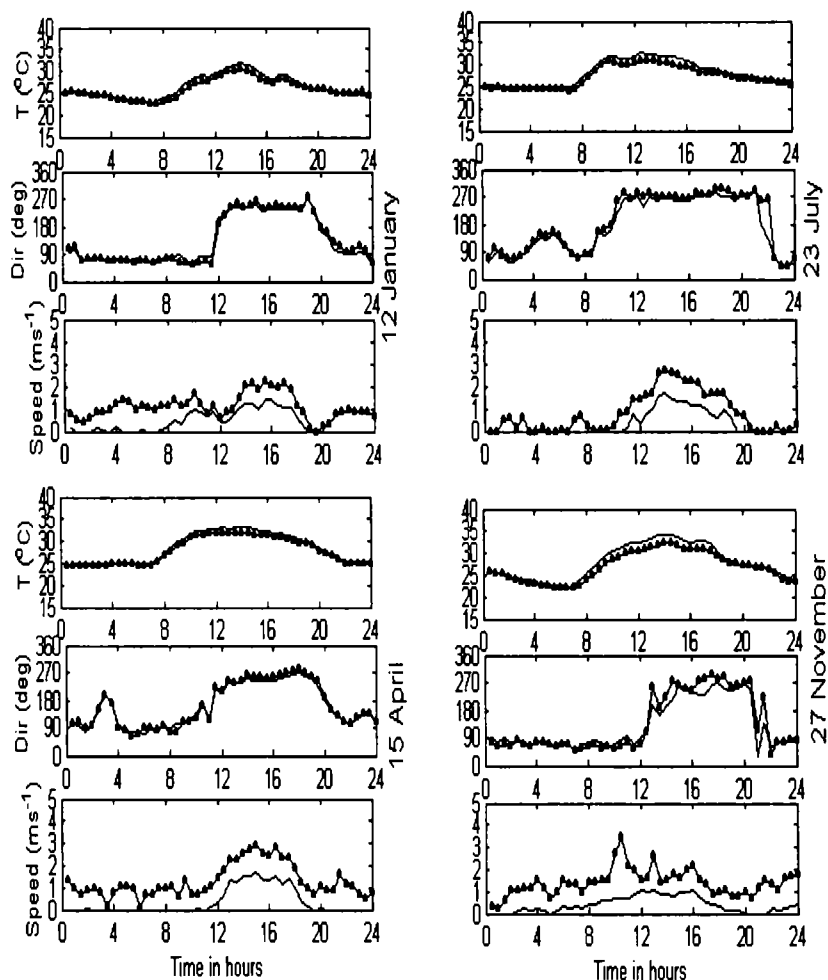


Fig.2.8 Diurnal variation of air temperature, wind direction and wind speed for 12th January, representative of winter, 15th April for pre-monsoon, 23rd July for southwest monsoon and 27th November for post monsoon. Dotted solid line indicates 20 m level and solid line 10 m level.

Though we presented a few samples (one each for January, April, July and November considered here as representative for winter, pre-monsoon, southwest monsoon and post monsoon seasons), analysis was carried out with many cases in all the seasons. It is found that the turning of wind direction with height is clockwise with height (veering by the effect of surface friction) except just before/during the transition from land breeze to sea breeze. Accordingly, there is a sudden decrease of temperature for a very short period at the time of onset of sea breeze accomplished by

the backing (associated with cold air advection). The wind speed decreases at the time of onset of sea breeze, if the transition is rapid. So, the wind observed may be interpreted as the combined effect of the land/sea breeze and the prevailing synoptic wind. The prevailing wind direction is modified by the presence of local mesoscale circulation due to differential heating. The sea and land breezes are predominant compared to the synoptic wind and hence local features determine the resultant wind direction.

It is found that the wind direction turns clockwise with height during the periods other than just before or during the onset of sea breeze contributed by surface friction. The evolution of sea breeze from the land breeze is a slow process and full establishment of sea breeze takes place from 15 minutes to half an hour (confirmed with observations taken at 5 minutes interval). The sea and land breeze circulations are more sensitive at 20 m compared to that 10 m, indicating the frictional dissipation of the circulation.

2.6.2 Diurnal variation of sea breeze component

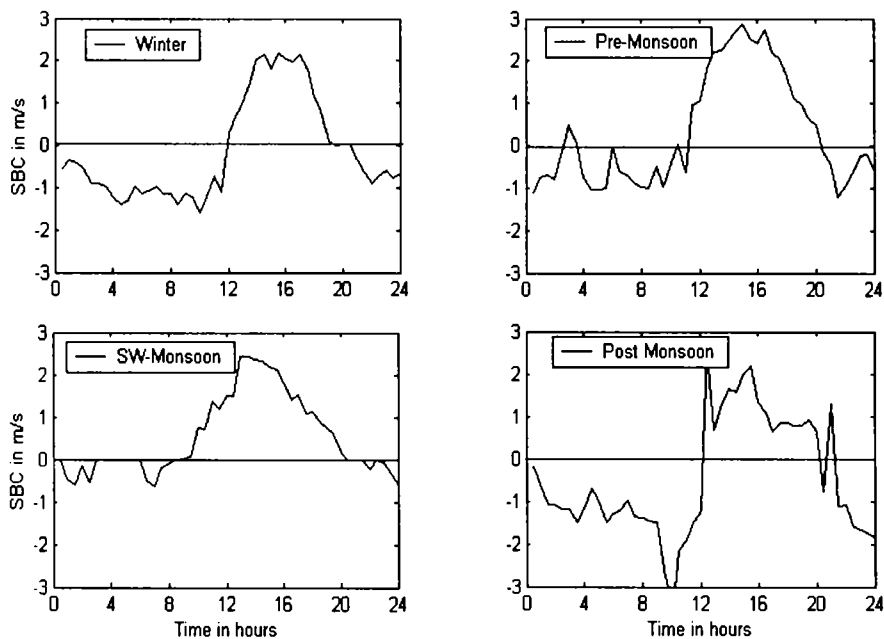


Fig.2.9 Diurnal variation of sea breeze component for representative days of the seasons

To understand the setting time of sea breeze and land breeze, the sea and land breeze components were obtained by using the above formula. The negative side of the graph represents the land breeze and the positive side indicates the sea breeze component. Fig.2.9 explains the sea and land breeze circulations, clearly indicating the onset and cessation time as well as the intensity of the sea breeze circulation for all seasons.

2.6.3 Diurnal variation during a rainy day

The land and sea breeze circulation during a rainy day is shown in Fig.2.10 (for 24th June). Since it was a rainy day, the land-sea temperature contrast is small and hence the local circulation induced by the differential heating is not occurred on this day. However, the wind direction is around 260 degree in both levels for the entire day. The prevailing synoptic wind over this region during southwest monsoon season is ~~westerly~~ ^{WNW} and it is strong since the monsoon is active. So, the wind direction

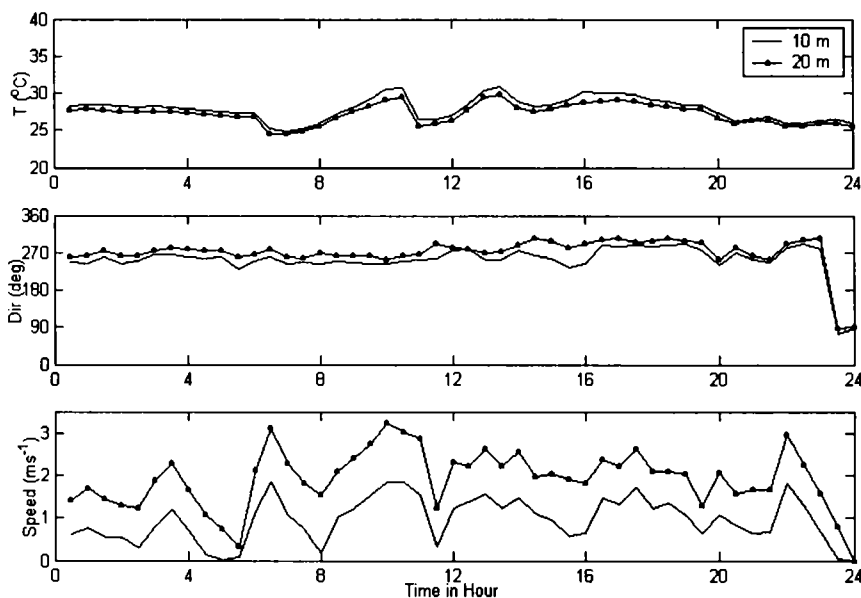


Fig.2.10. Diurnal variation of air temperature, wind direction and wind speed during a rainy day (24th June).

happened to be westerly, though there is no sea breeze or land breeze. The wind speed is relatively high during the entire period due to the influence of low level jet, which is strong in the active monsoon situation. It is seen that the wind direction turns clockwise with height throughout the day due to the effect of surface friction.

Since no transition and no backing of wind. Similar features are seen during all rainy days in the southwest monsoon season.

2.6.4 Diurnal variation of turbulent fluxes

2.6.4.1 Momentum flux

To understand the general dynamics of surface boundary layer during different seasons, diurnal variation of surface momentum flux during all non-rainy days together for the representative months of the seasons were studied. The averaged diurnal variation of momentum flux during winter, pre-monsoon, southwest monsoon and post monsoon seasons are given in Fig.2.11. The high values of momentum flux are found during pre-monsoon season attributed by high wind shear. The momentum flux values are found to be very high during the presence of sea breeze circulation, since the prevailing westerly surface wind as well as wind fluctuation is further modulated by the local heating during the afternoon hours of southwest monsoon season. In all these seasons, the mean surface momentum flux values are directed downward. Small momentum flux values are found during the presence of land breeze of southwest monsoon season, since the wind during this period is feeble.

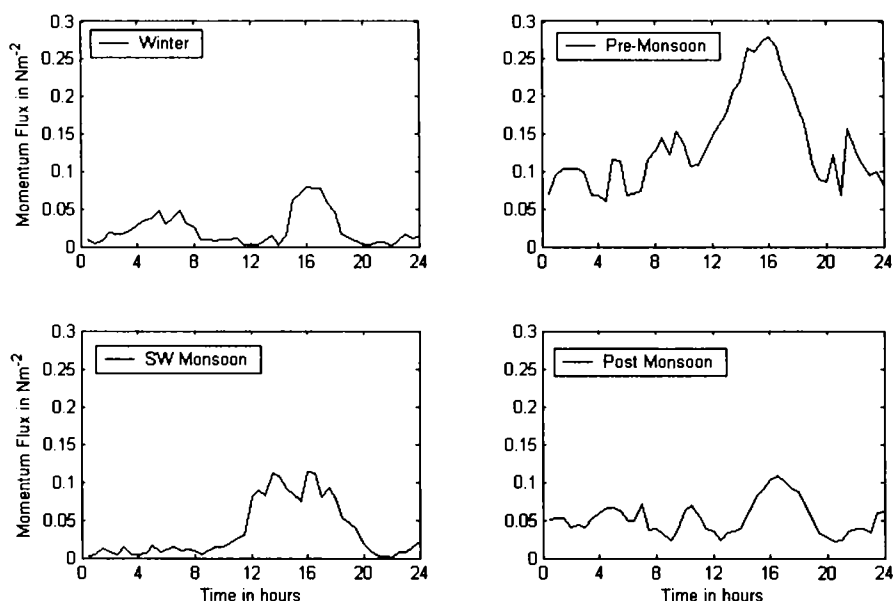


Fig.2.11. Diurnal variation of averaged momentum flux during the four seasons.

2.6.4.2 Sensible heat flux

Diurnal variation of averaged sensible heat flux during the above four seasons estimated by the wind and temperature data during the non-rainy days together for the respective month is given in Fig.2.12. As in the earlier case, the mean sensible heat flux values are high during the afternoon of pre-monsoon season and low values are found to be in the winter season. It may be noted that the averaged pattern of sensible heat flux is directed upward during the entire period. The occurrence of surface based inversion layer is rare over this near equatorial coastal station and hence the averaged sensible heat flux is directed upward even during early morning of winter. It is found that average sensible heat flux during night time is almost zero in the winter and southwest monsoon seasons and during day time it is less than 150 Wm^{-2} in the winter season and more than 200 Wm^{-2} in the southwest monsoon season.

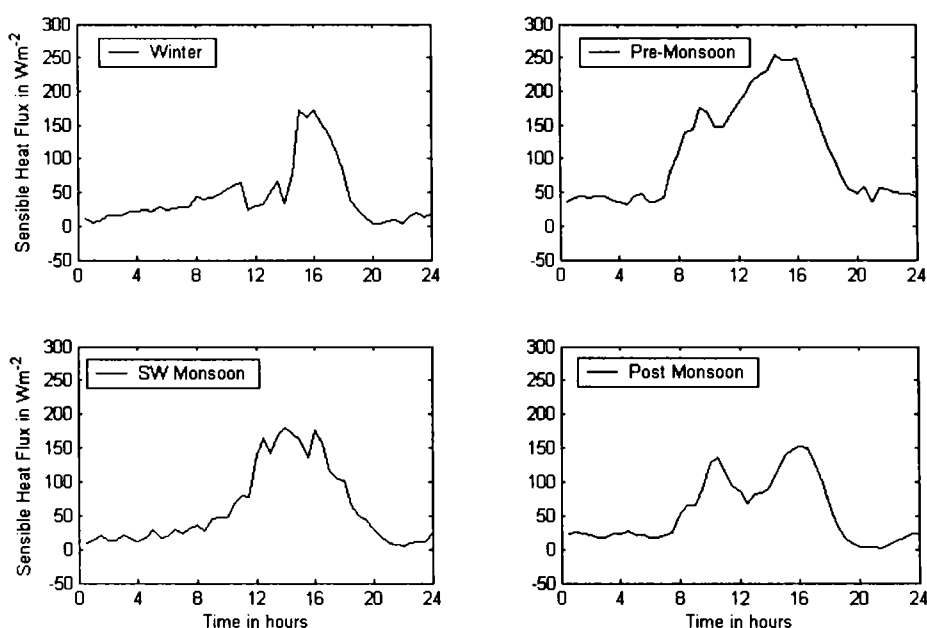


Fig.2.12. Diurnal variation of averaged sensible heat flux during the four seasons.

The averaged surface fluxes need not represent the actual situation due to smoothening of irregularities by the difference in time of onset of sea breeze etc. For a better understanding, the diurnal variation of surface momentum and sensible heat fluxes were studied by considering representative days in each season.

2.6.4.3 *Momentum and Sensible heat fluxes for individual days*

Diurnal variation of surface momentum flux for individual representative days for each season is presented in Fig.2.13. The range of values is slightly higher for individual case compared to mean for the season. During the southwest monsoon season, high values of momentum flux are seen during the presence of sea breeze. The intensity of momentum flux decreases during onset and cessation of sea breeze for all the cases. This is due to decrease of wind during the transition time as explained earlier. The momentum flux depends mainly on vertical wind shear and increases during after noon due to the influence of sea breeze. Fig.2.14 represents the diurnal variation of sensible heat flux for individual cases for different seasons. As expected, the sensible heat flux values are high during day time and small during night. Averaged surface momentum and sensible flux patterns resemble closely to the instantaneous pattern for all the seasons. Since the irregularities are smoothed in the average pattern, the range in the diurnal variation is less than that in the instantaneous for all the seasons. The land breeze over this station during the pre-monsoon season is prominent after 1900 hours, but this is not strong enough to record at 10 m level. So, the vertical wind shear is very high, causing the unusual behaviour of surface momentum flux for the representative case for pre-monsoon season. The sensible heat flux also decreases during the onset of sea breeze, similar to that of momentum flux. The cold air advection associated with the sea breeze results in the decrease of sensible heat flux at the time of onset of sea breeze. Among the four representative days considered here, sensible heat flux is found to be maximum during non rainy day in the southwest monsoon season, the maximum value is found to be 250 Wm^{-2} around 1600 hours, followed by pre-monsoon season. This is attributed by the variation of insolation over this station, which is maximum during clear sky days of monsoon season, followed by pre-monsoon season. It may be noted that there is a situation of downward sensible heat flux during winter season due to the temperature inversion, though the winter effect is feeble over this near equatorial coastal station.

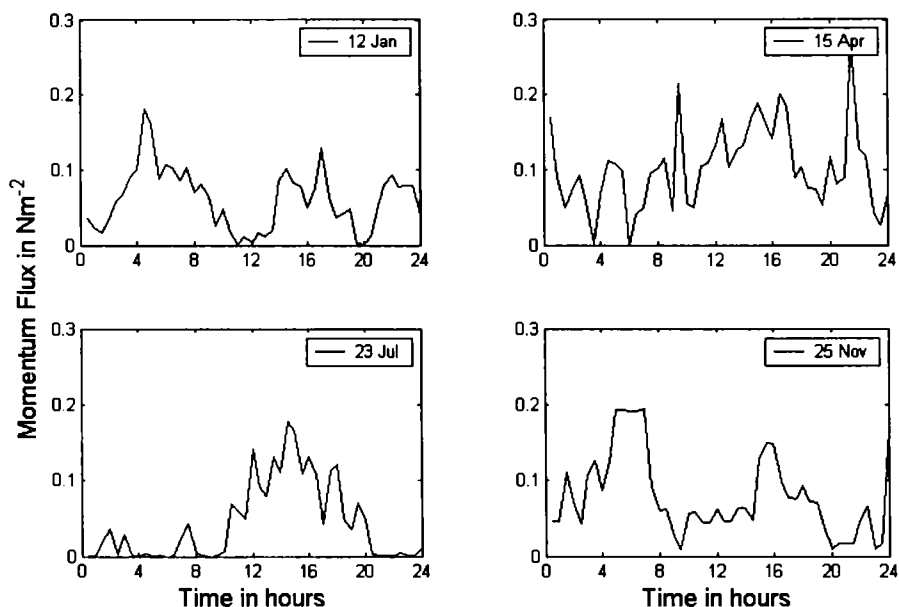


Fig.2.13. Diurnal variation of momentum flux during individual day of the seasons.

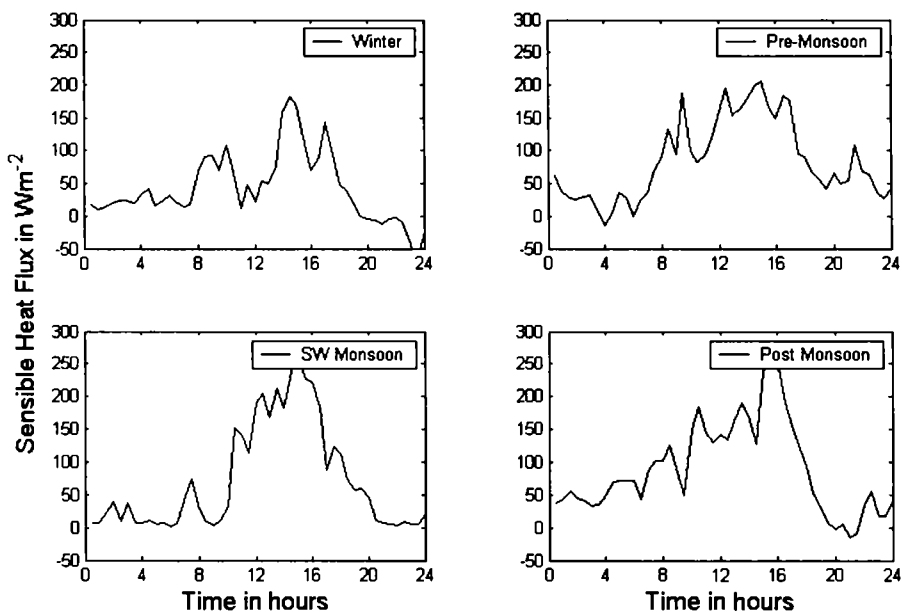


Fig.2.14. Diurnal variation of sensible heat flux during individual day of the seasons.

Variation of drag coefficient with wind speed during sea breeze and land breeze for the four seasons (representative days as in the earlier case) was presented in Fig.2.15 and Fig.2.16 respectively. Generally, sea breeze (westerly) is stronger than land breeze (easterly) in all the seasons. Accordingly, the drag coefficient power

relationship with wind is different for sea breeze and land breeze situations. The respective equations are presented in the corresponding figures. These equations can be employed for obtaining drag coefficient on a seasonal basis for sea breeze and land breeze.

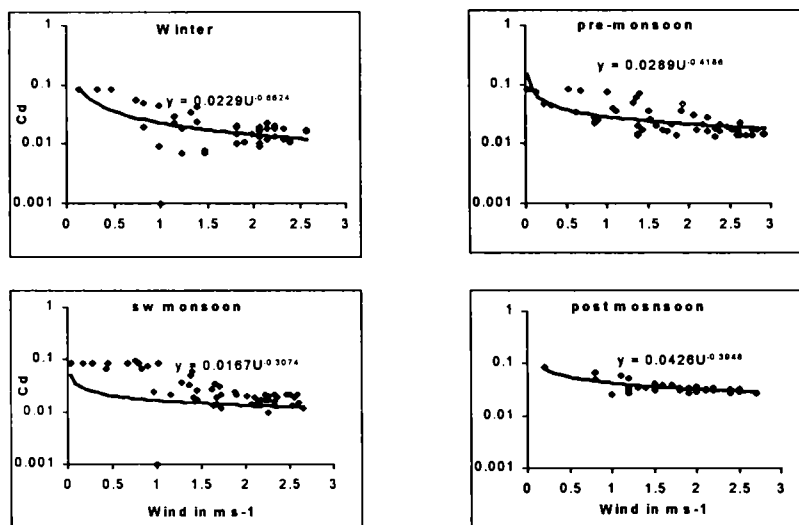


Fig.2.15 Variation of drag coefficient with wind during sea breeze period.

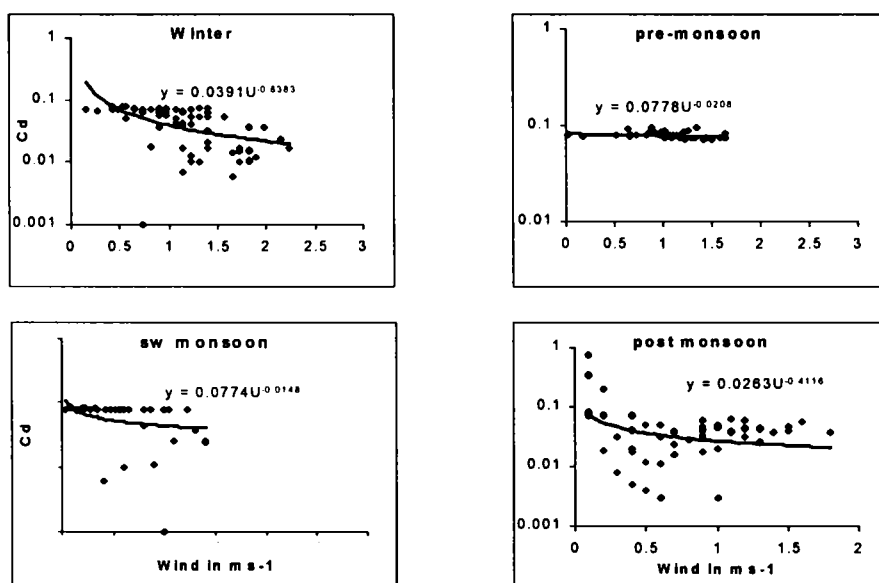


Fig.2.16 Variation of drag coefficient with wind during land breeze period.

In general the properties of the boundary layer parameters are different during sea breeze and land breeze periods. To investigate thoroughly, we made two data sets

one during the land breeze time (8 am IST) and another set during the sea breeze time (3 pm IST). The data set has a length of 180 days starting from 2nd November, 2001 to 30 April 2002. The continuous data set was subjected to quality check.

2.7 TURBULENT BOUNDARY LAYER FEATURES

2.7.1 During land breeze

In general, during land breeze period the intensity of the wind and temperature is less than that during the sea breeze period. Fig.2.17a, 2.17b, 2.17c and 2.17d represent the wind at 20 m level, temperature at 20 m level, frictional velocity and temperature scale respectively. It is found that the wind speed is generally less and average speed is around 1 ms^{-1} . The wind speed frequently crosses 2 ms^{-1} . The strength of the land breeze is almost same in all days under consideration. Temperature at 20 m level is presented in Fig.2.17b, temperature during morning hours is less due to the less insolation, but the temperature increases afterwards due to the intensity of the insolation. During the study period the temperature ranges from 20°C to 29.4° . The temperature shows an oscillation like feature around 30 day other than fluctuation. The average temperature over this period is around 24°C . Derived parameter such as frictional velocity and temperature scale are given in Fig.2.17c and Fig.2.17d respectively. The concept of frictional velocity in the boundary layer flow is first introduced by Prandtl (1949). The important scaling parameters in the similarity theory are that of wind and temperature (Monin and Obukhov, 1954). The frictional velocity is always independent of height but depends on the nature of the ground, magnitude of the wind and turbulent state of the atmosphere. The daily variation of frictional velocity (u_*) is highly fluctuating during the land breeze period and the values ranges from 0.001 ms^{-1} to 0.194 ms^{-1} . The frictional velocity depends upon the strength of the wind speed and hence momentum flux. The average frictional velocity during the period is 0.05 ms^{-1} . The day to day variation of temperature scale (t_*) is varied in a range -0.93 to -0.1 . The t_* depends mainly on the temperature compared to wind. The minimum value of t_* is found during the winter period due to the effect of temperature.

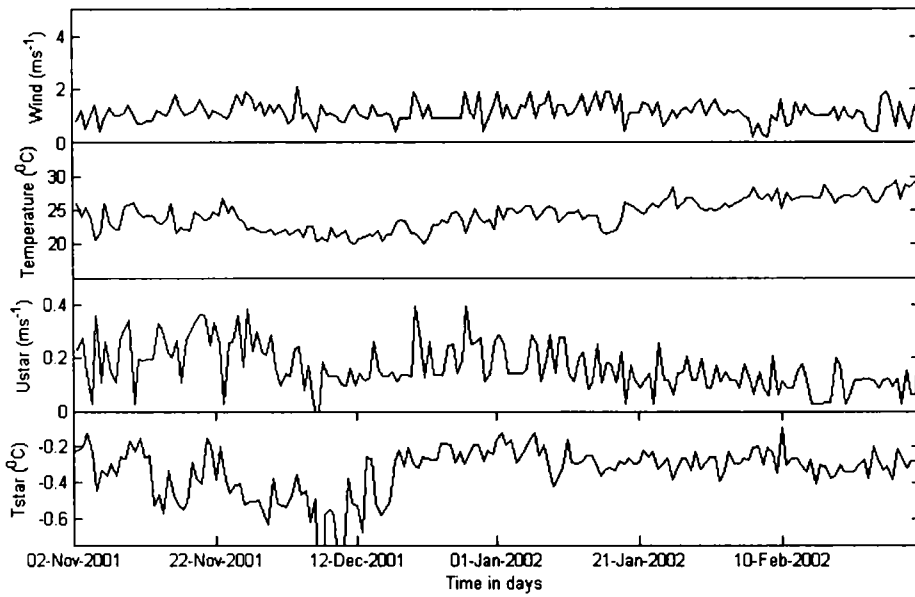


Fig.2.17 Day to day variation of (a) surface wind, (b) temperature, (c) frictional velocity and (d) temperature scale during land breeze period.

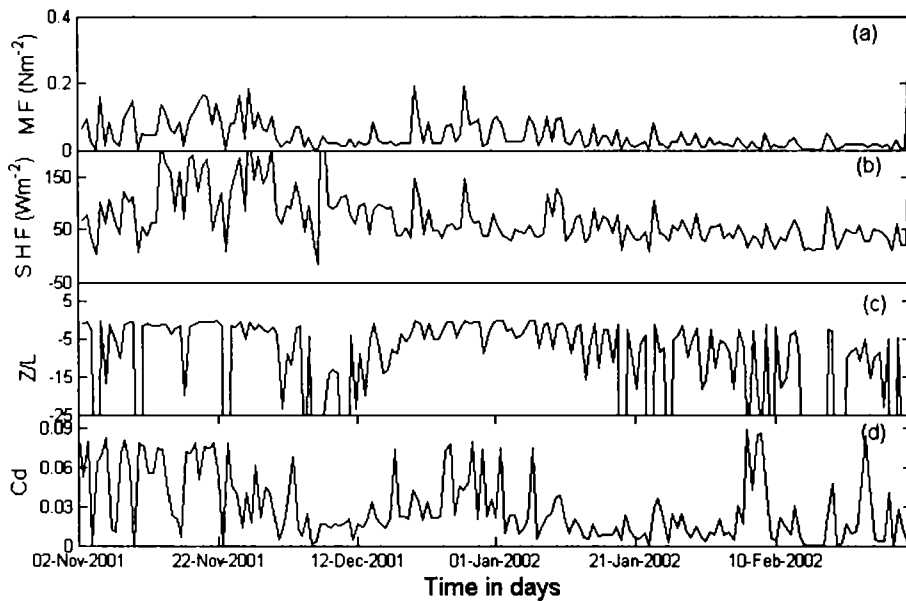


Fig.2.18. Day to day variation of (a) Momentum Flux, (b) Sensible Heat Flux, (c) Stability Parameter and (d) Drag coefficient during land breeze period.

Fig.2.18a to Fig.2.18d represent daily variations of momentum flux, sensible heat flux, drag coefficient and stability parameter respectively during land breeze period. All these parameters are computed using profile method described in

methodology section. The surface momentum flux during early morning hours around 8 pm IST are given in Fig.2.18a. The momentum flux shows high variability from day to day due to the effect of wind. The maximum momentum flux values are nearly 0.2 Nm^{-2} and at the time of high values of momentum flux the wind gradient between two levels (10 m and 20 m) are high. The sensible heat flux during the period of land breeze is presented in Fig.2.18b. Computation of sensible heat flux is essential for the energy budget estimation. A knowledge of the sensible heat flux is useful for description of the dynamics in the atmospheric boundary layer dynamics. During study period the high values of sensible heat flux are noticed during December month. The sensible flux also shows the variability as that of momentum flux. The maximum sensible heat flux values are varied from -15 Wm^{-2} to 250 Wm^{-2} . Sensible heat flux depends mainly on wind and temperature. Wind is a main contributing factor compared to temperature for sensible heat flux and it can be clear from the figure 2.21. The average value of the sensible heat flux during the hours of land breeze (early morning hours) is 70 Wm^{-2} . Variation of drag coefficient is given in Fig.2.18c; the drag coefficient is highly varying from day to day with an average value 0.03 over the region during early morning hours. Fig.2.18d describes the stability parameter (z/L) during land breeze obtained by profile method using iterative solutions. The z/L shows negative values throughout the period indicating unstable condition.

2.7.2 During sea breeze

All the described above are studied separately for the sea breeze case to differentiate the features of the surface boundary layer from land breeze. The Fig.2.19a, 2.19b, 2.19c and 2.19d are represented the wind at 20 m level, temperature at 20 m Level, frictional velocity and temperature scale respectively. In Fig.2.19a shows the daily variation of wind speed during the sea breeze time (3 pm IST). Sea breeze is fully established by this time. Generally wind speed increases with time in the day. From the figure, the wind speed is varying with an average value of 2.3 ms^{-1} . The wind speed in certain days exceeds 3.8 ms^{-1} . The strength of the sea breeze during this period is varied from month to month. The maximum wind is found during the pre-monsoon periods (April). Fig.2.19b shows the daily variation of air temperature during 3 pm. Here temperature varies from 26.6°C to 34.3°C and this variation is may due to the seasonal difference in insolation by the sun. The average temperature

is around 31°C. The maximum temperature is found during the month of April because April month receives more insolation due to relatively clear sky. The

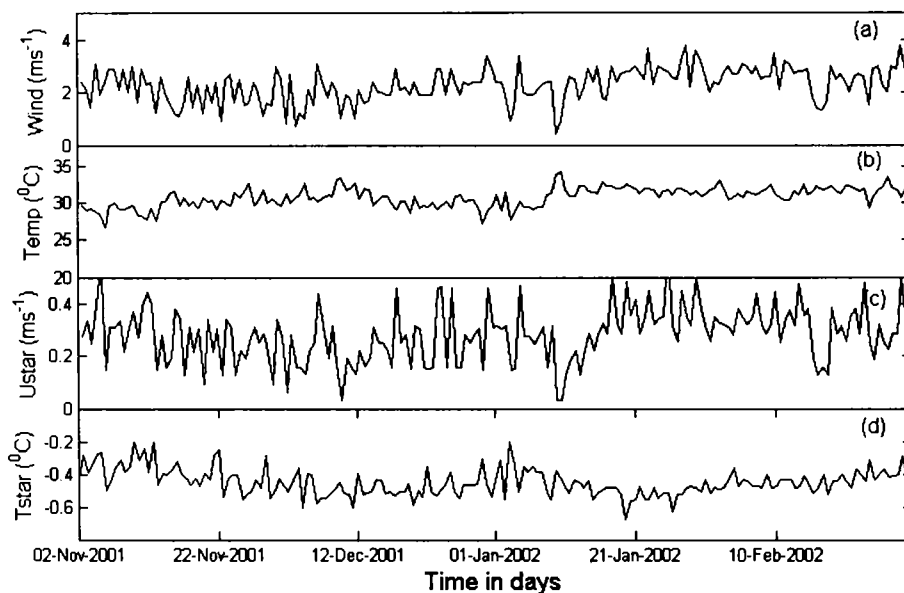


Fig.2.19. Day to day variation of (a) surface wind, (b) temperature, (c) frictional velocity and (d) temperature scale during sea breeze period.

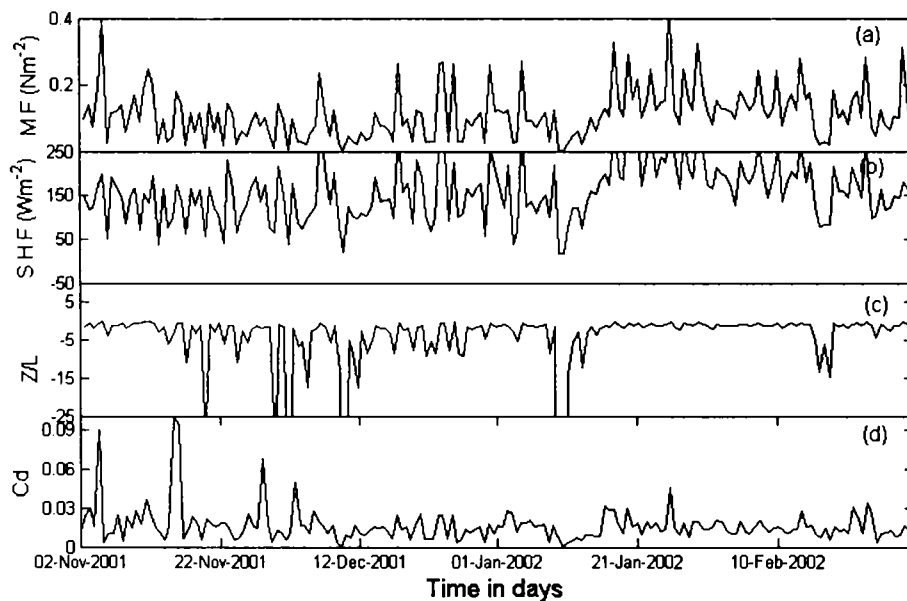


Fig.2.20. Day to day variation of (a) Momentum Flux, (b) Sensible Heat Flux, (c) Stability Parameter and (d) Drag Coefficient during sea breeze period.

derived parameter u^* during sea breeze time is presented in Fig 2.19c. The profile of the u^* is almost same as that of the profile of the wind. The frictional velocity during sea breeze period varies from 0.03 ms^{-1} to 0.6 ms^{-1} and average value is 0.28 ms^{-1} . The variation of t_* is varied from its average values -0.45°C to a minimum of -0.67°C and to the maximum of -0.2°C (Fig2.19d).

Momentum flux, sensible heat flux, drag coefficient and stability parameter during the sea breeze is presented in Fig.2.20a, 2.20b,2.20c and 2.20d respectively. The profile of the momentum flux is very similar to the profile of the u^* and hence to the wind. The average value of the momentum flux is 0.12 Nm^{-2} , the maximum value is found in the months of March/April. Sensible heat flux also shows its peak value during the period of March/April and it is due to the high insolation. The sensible heat flux shows its maximum in pre-monsoon season around 200 Wm^{-2} and least is during winter season and the value is about 100 Wm^{-2} . The average sensible heat flux is 160 Wm^{-2} . Daily variation of drag coefficient is given in Fig.2.20c, the drag coefficient shows some peaks during winter period and the value reaches about 0.9, the remaining periods the drag coefficient shows almost constant value. The average drag coefficient during the sea breeze period is 1.7×10^{-2} . Time series plot of stability parameter is given in Fig.2.20. Here, also the value is negative throughout indicating unstable condition.

Generally the values of the boundary layer parameters during sea breeze period is more than that during the land breeze time. The modulation of the parameters during the sea breeze period is due to the land-sea thermal contrast and hence the development of the sea breeze. But the values of drag coefficient is high during the period of land breeze. It may due to the reduced wind speed in land breeze time.

2.7.3 Dependence of wind speed and temperature on boundary layer parameters

Since it is very difficult to obtain the boundary layer parameters directly, an attempt is made to obtain the relations involving the wind and temperature so that boundary layer parameters can be obtained for the given values of wind and temperature. Fig.2.21a and 2.21b are variation of boundary layer parameters to the wind and to the temperature respectively. From the figure, it is clear that the u_* , momentum flux,

sensible heat flux are functions of wind, and these parameters are linearly related to wind speed. The drag coefficient decreases with the increase of wind speed up to a critical value and beyond which C_d increases with wind speed. From the figure it is clear that the stability parameter has not any relation to the wind

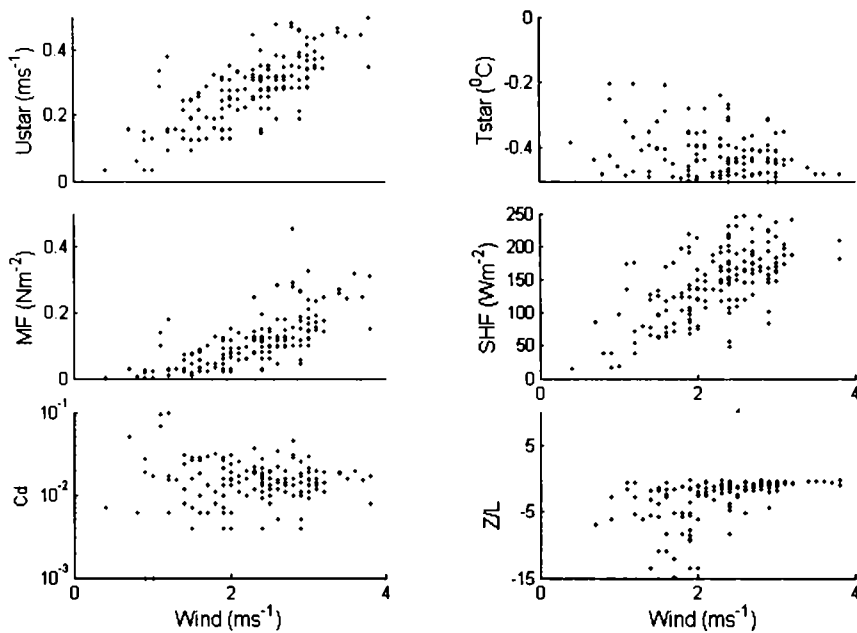


Fig.2.21a. Dependence of boundary layer parameters with wind

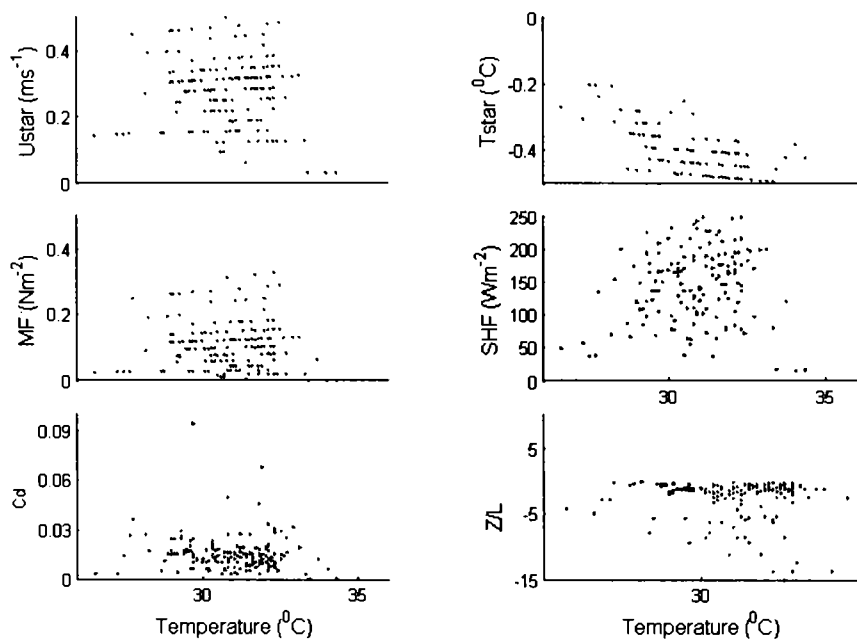


Fig.2.21b. Dependence of boundary layer parameters with temperature

speed but the relation with temperature is clearly seen and the functional fit is the polynomial equation. Temperature scale is more related to the temperature and least to the wind speed. The relation with temperature is treated as linear

An automatic weather station (AWS) of 20 m height was installed over Cochin, a tropical coastal station to study the micrometeorological properties on a diurnal and seasonal basis. This data set has a good reliability and no other data sets are available in this region. In this perspective this study using this data has attained its importance. The main feature studied using the above data set was the characteristics of the sea breeze and land breeze circulations. The setting and cessation time of sea breeze is very important over the station because Cochin is an industrial capital of Kerala state. The setting time of sea breeze is early in the southwest monsoon months followed by the pre-monsoon, winter and post monsoon periods during the clear sky days. These variations are occurs due to the difference in insolation during different months. Due to the orientation of the shoreline the direction of land breeze is 90° (*i.e* easterly) and the direction for sea breeze is 270° (*i.e* westerly). The fluxes of momentum and sensible heat and other parameters such as drag coefficient, frictional velocity, temperature scale, Monin-Obukhov length are computed using the Monin-Obukhov similarity relation on diurnal and seasonal time scales. The momentum and sensible heat flux show high diurnal variation during pre-monsoon period and the values are 0.28 Nm^{-2} and 250 Wm^{-2} respectively. The least variation of the fluxes is noticed during post monsoon period and the values are 0.1 Nm^{-2} for momentum flux and that for sensible heat flux is 150 Wm^{-2} . The day to day variation of the parameters such as frictional velocity, temperature scale, drag coefficient, Monin-Obukhov length are examined during land breeze (8 AM) and sea breeze (3 PM) periods and concluded that the turbulent parameters are less during land breeze period due to the less intensity of the land breeze time and high during sea breeze hours because of the high turbulence and convective activities.

CHAPTER – 3

***ATMOSPHERIC BOUNDARY LAYER
CHARACTERISTICS ASSOCIATED WITH
ACTIVE AND WEAK PHASES OF MONSOON***

CHAPTER - 3

ATMOSPHERIC BOUNDARY LAYER CHARACTERISTICS ASSOCIATED WITH ACTIVE AND WEAK PHASES OF MONSOON

3.1 Introduction

Indian summer monsoon is associated with a large convective heat source on the ITCZ in the northern hemispheric tropics extending from the Arabian Sea to the West Pacific Ocean. A strong cross-equatorial Low Level Jet-stream (LLJ) with core around 850 hPa exists over the south Asia during the boreal summer monsoon season June to September. Analysing the wind data of five years collected by the radiosonde / radio-wind network of India, Joseph and Raman (1966) established the existence of a westerly LLJ over peninsular India with strong vertical and horizontal wind shears. This LLJ is seen over peninsular India on many days in the month of July with core at about 1.5 km above mean sea level with a core speeds in the range of 40-60 knots. Findlater (1969) found that the Asian summer monsoon LLJ has its origin in the south Indian Ocean north of the Mascarene high as an easterly current and it crosses the equator in a narrow longitudinal belt close to the east African coast as a southerly current with the speed exceeds 100 knots occasionally. It turns into a westerly current over the Arabian Sea and passes through India to the western Pacific Ocean. Findlater's LLJ is a combination of the LLJs found by Bunker (1965) for the Arabian Sea and Joseph and Raman (1966) for peninsular India.

3.2 Active and weak cycles of southwest monsoon

A strong inter hemispheric Low Level Jetstream with peak wind speed at 850 hPa exists with large variability to bring the active and break cycles over Indian monsoon region during summer. This active and weak spells of monsoon are distinct events in the intraseasonal oscillation (Sikka and Gadgil, 1980) where eastwest oriented convective cloud band and the wind core at 850 hPa are found to move northwards/north-eastwards from the equatorial region at intervals of 30 to 50 days (Yasunari, 1979; 1981; Sikka and Gadgil, 1980; Krishnamurty and Subramanyam, 1982). The oscillation of the cloud band begins with the onset of southwest monsoon from the southern region of south Kerala and dissipates over the Himalayan region.

By the decay of this band, a fresh band is formed over the central Indian Ocean and repeats the same process. This formation and propagation of the cloud band and associated movement of the LLJ core are manifestations of the active and weak cycles of Indian Summer Monsoon Rainfall (ISMR). The normal date of onset of southwest monsoon is 1st June with a standard deviation of 8 days (Rao, 1976). Traditionally the term 'break' refer to very weak spells of rainfall over the Indian monsoon region, different scientist uses the same term to express the different features of the convection/circulation over different regions (Webster et al, 1998). Large intraseasonal fluctuations in the Indian monsoon rainfall between active and break spells have been known since over a century (Gadgil and Joseph, 2003). The number of active and break days in a monsoon season has significant influence on the annual rainfall and it make changes in the surface boundary layer parameters such as surface fluxes, momentum transfer, energy budget, etc. Joseph and Sijikumar, (2004) studied the features of the break and active spells for a 11 year period (1979-1990) in terms of wind at 850 hPa using NCEP/NCAR reanalysis data set and NOAA OLR data. Fig.3.1 and Fig.3.2 show the spatial structure of LLJ and OLR during the active phase and weak phase of monsoon. During active condition the LLJ passes through central India and shows high convection from OLR. During weak situation the LLJ bypasses over south Kerala and passes to the south China sea and OLR minimum values are found at the south of south India. By the onset of monsoon, the outgoing long wave radiation over the Kerala region is small (less than 180 Wm^{-2}), indicating high organized convection and the strength of the wind at 850 hPa is more than 15 ms^{-1} . Similar situations are repeated two or more times during the same season, indicating active phases of monsoon. The monsoon trough also shows a significant variation during active and weak cycles. In general the monsoon trough is located along the Gangetic plane dipping in to the Bay of Bengal for the period June to September during the active phase of the monsoon and shifts northward when there is break (Ramage, 1971). Thermodynamic structure and boundary layer parameters over the monsoon trough region indicate significant and consistent variation between active and weak phases of monsoon (Kusuma, et al, 1991).

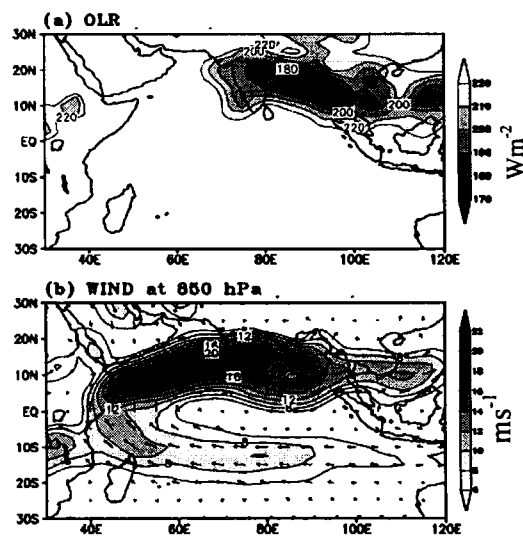


Fig.3.1. Spatial structure of a) NOAA OLR composite representing organized convective clouds and b) wind at 850 hPa composite during Active monsoon condition.

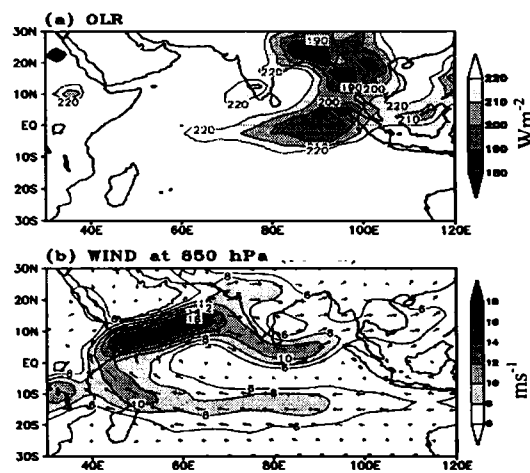


Fig.3.2. Spatial structure of a) NOAA OLR composite representing organized convective clouds and b) wind at 850 hPa composite during weak monsoon situation.

In south India, during the southwest monsoon season prominent wind in the surface layer of the atmosphere is northwesterly. Between March and May the prominent wind direction over the sea in this region changes gradually from northeasterly to northwesterly and then to westerly (Anonymous 1966). By the onset of monsoon the westerly wind over Kerala coast strengthens and prominent surface wind direction during the monsoon season over this region is northwesterly. On the other hand, during the weak monsoon situations, the wind direction turns southerly off

the Kerala coast and oriented with along shore component near Kerala coast although the intensity is small.

3.3 Scope of the study

Indian southwest monsoon has very dominant active and weak phases. This active and weak situations are very important in the human activity because more the number of active monsoon situation, more the quantity of the rainfall over the region. By the present study, the atmospheric boundary layer parameters during active and weak monsoon situations are studied using different datasets. The variation of surface fluxes, wind at 850 hPa, Outgoing Longwave Radiation (OLR) are studied during different phases of summer monsoon. Thermodynamic features show significant variations associated with the surge of monsoon. So, the study of these parameters helps to provide an indication of convection. In addition, the oscillations of the surface parameters are also examined using wavelet technique to identify its embedded harmonics.

3.4 Data and methods

The boundary layer features during active and weak phases of monsoon are studied using the data sets taken from the NCEP/NCAR reanalysis, it has a research quality data used for meteorological and oceanographical studies (Kalnay et al, 1996) having a spatial resolution of 2.5 x 2.5 latitude-longitude grid and from the All India Daily Monsoon Rainfall (AIDMR) available from the IMD. OLR data taken from NOAA satellite were also used (Gruber and Krueger, 1984) with a resolution of 2.5 x 2.5 latitude-longitude grid. The active and weak phases of the monsoon are estimated from the area average of zonal wind at 850 hPa over 10°N-20°N & 70°E-80°E suggested by Joseph and Sijikumar (2004) and AIDMR. The active days are the days in which the area averaged zonal wind over the area is 15 ms⁻¹ or more and weak days are when it 9 ms⁻¹ or less. Active days considered in June and July and weak days considered in July and August. The active and weak days estimated by wind and AIDMR were strongly correlated.

Dines Pressure Tube (DPT) anemograph are also used for Mangalore and Bangalore during the period of July for 12 years from 1987 to 1998. The active and weak days during the period are identified as explained earlier. Mangalore is a

windward side and Bangalore is the leeward side of the LLJ core. During active monsoon situation, the boundary layer exhibits its features differently over windward side and leeward side. DPT charts available from the India Meteorological Department (IMD) are used for the analysis.

Radiosonde data for 00Z are used to estimate the thermodynamics of boundary layer during different phases of monsoon. The radiosonde data is accessed from the web site of <http://weather.uwyo.edu/upperair/sounding.html>

The fluxes of momentum and sensible heat flux and other parameters are computed using the equations explained in the Chapter.2.

The virtual potential temperature and humidity were computed using the standard equations. The equations are given below

3.4.1 Vapour pressure (e)

$$e = 6.1078 \exp[(TD * A)/(TD + B)] \quad (3.1)$$

where TD is the dew point temperature in degree C.

3.4.2 Saturated vapour pressure (es)

$$es = 6.1078 \exp[(T * A)/(T + B)] \quad (3.2)$$

where T is the temperature in degree C.

the coefficients A and B for water and ice are different as given below

$$A = 7.5 \}$$

$$B = 237.3 \} \text{ with respect to WATER}$$

$$* A = 9.5 \}$$

$$B = 265.5 \} \text{ with respect to ICE}$$

specific humidity (q) is given by the equation

$$q = 0.623.e / (P - 0.377.e) \quad (3.3)$$

where e and P are in the same units (hPa) and q is dimensionless and can be expressed in kg.kg^{-1}

3.4.3 Virtual potential temperature (θ_v)

$$\theta_v = \theta(1 + 0.61.r) \quad (3.4)$$

where θ_v is virtual potential temperature, r is mixing ratio and θ is the potential temperature and

$$\theta = T \left(\frac{1000}{P} \right)^{0.286} \quad (3.5)$$

where P is the pressure and T is the temperature.

3.5 Wind structure at different levels

The active and weak phases of monsoon are identified from the time series plot of the area averaged (10°N - 20°N & 70°E - 80°E) zonal wind at 850 hPa and the dates were confirmed using All India daily monsoon rainfall (AIDMR). Fig.3.3 shows the spatial structure of the zonal wind at different levels (1000 hPa, 925 hPa, 850 hPa, 700 hPa and 500 hPa) for active and weak phases, considering all active and weak phases from 1999 to 2003. The spatial structure of the wind is varying according to the activity of the monsoon. The changes in the atmospheric variables are evident in the entire atmospheric column from the surface to the top of the atmosphere associated with the monsoon activity. It is found that the variations are high in the lower levels. The spatial surge is more in the surface levels such as 1000 hPa, 925 hPa and 850 hPa. The 850 hPa level has the maximum intensity of the Low Level Jetstream (LLJ) and is very critical by showing high response to the monsoon oscillations. From this level either to surface or to the top of the atmosphere, the response to the monsoon surge gets weakened. During active monsoon situation the core of the zonal wind passes from the central Arabian Sea through the central India and then to Bay of Bengal. The wind core speed at 850 hPa is $\sim 18 \text{ ms}^{-1}$ in the Arabian Sea but in the surface the core speed over the area is $\sim 14 \text{ ms}^{-1}$. This decrease is due to the frictional effect from the surface. The wind from the southern part of Indian Ocean carrying ample of moisture enters to the Arabian Sea by crossing the

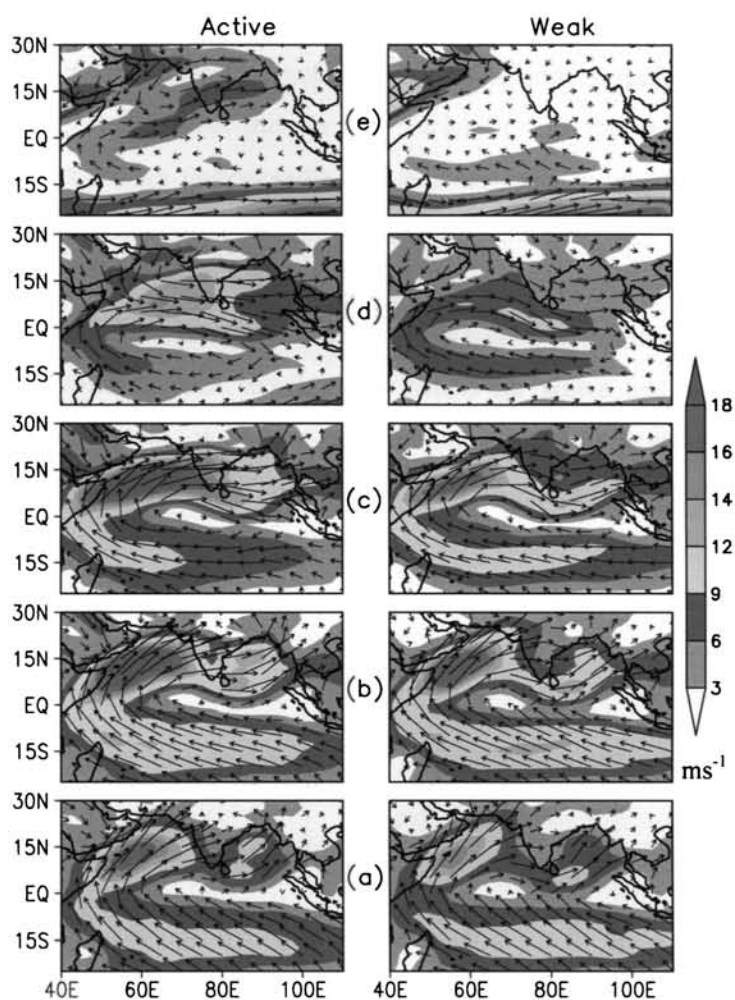


Fig.3.3. Spatial structure of wind at 850 hPa with magnitude and direction during active and weak phases of monsoon at different levels a) 1000 hPa, b) 925 hPa, c) 850 hPa, d) 700 hPa and e) 500 hPa.

equatorial Somali coast over a narrow belt and strengthens its speed from the Arabian Sea. During weak situation the core of the wind speed turns towards south and passes through the west coast of India and then to Bay of Bengal through the Sri Lanka region. It is clear that the wind during active and weak situation is different in the southern part of Indian peninsula, but the difference is comparatively feeble than over the central India. As the wind pattern changes from active to weak, all the boundary layer parameters undergo changes because the surface parameters mainly depend on the wind and temperature pattern of the surface.

3.6 Variation of boundary layer fluxes over Cochin

Surface boundary layer parameters show significant variation during active and weak phases of monsoon due to the variability in the surface wind and temperature. The thorough understanding of this variation is very important in the many studies related to Indian monsoon. Variation in the boundary layer parameters are studied with available data from the micrometeorological tower system and the data set is very crucial for this region because no such data is available before for this kind of study. Momentum and sensible heat fluxes for active and weak monsoon situations are examined very closely. Active monsoon situation is taken from 8th to 14th of August and the weak situation from 30th July to 2nd August in 2002. Fig.3.4 explains the variation in momentum and sensible heat fluxes during active and weak epochs of monsoon. The surface fluxes were calculated using the Monin Obukhov similarity theory and was explained in Chapter-2.

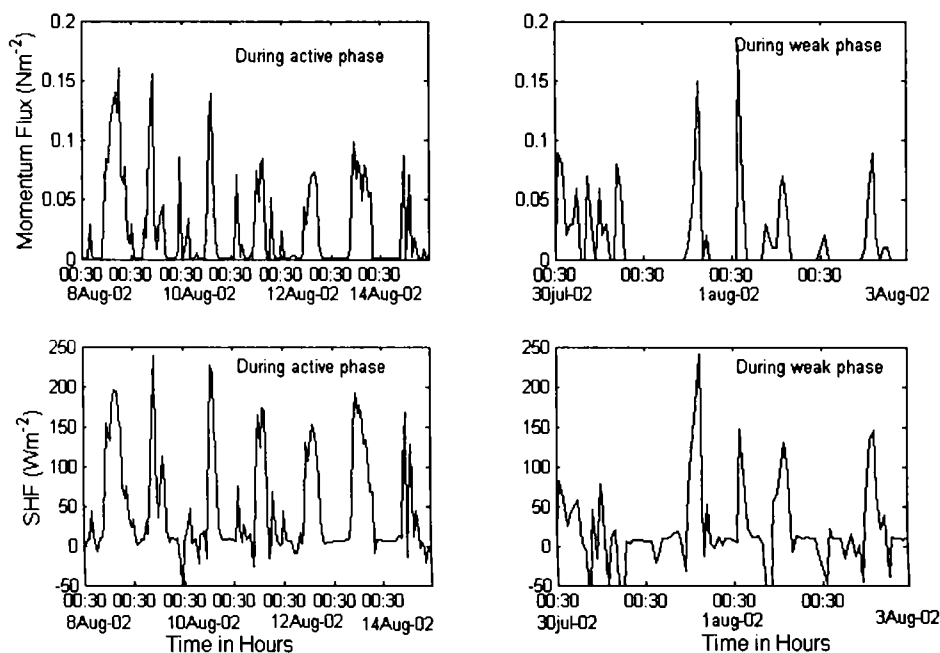


Fig.3.4. Variations of surface fluxes of momentum and sensible heat during active and weak phases of monsoon

The flux values vary considerably during active and weak phases. During active phase, momentum flux values are high in the daytime compared to the flux

values during the weak situation. This can be due to the high surface wind shear caused by the strong surface wind associated with the LLJ during active monsoon situation. Similarly, the sensible heat flux values are also high in the active case compared to that in the weak monsoon situation. However, a few high upward directed sensible heat flux situations are noticed during the daytime of weak monsoon situation. Weak monsoon situation is characterised by weak surface wind and clear sky or intermittent cloudy condition without or very little rain. This helps the insolation to reach more at the surface creating high upward surface sensible heat flux. The similar type of variation is noticed in frictional velocity, temperature scale and drag coefficient.

3.7 Conserved variable analysis (θ_e - q plot)

Conserved Variable Analysis (CVA) is carried out during the active and weak spells of southwest monsoon situations. This CVA is made for selected stations in the west coast namely Trivandrum and Mangalore using radiosonde observations taken at 12 UTC. The west coastal stations show significant variations during monsoon season according to the movement of LLJ and subsequent convective clouds. The convective clouds can influence radiative process and hence the thermodynamic structure of the atmosphere (Betts and Albrecht, 1987). The thermodynamic structure of the east coastal stations and marine atmosphere of Bay of Bengal was studied using BOBMEX-99 data set employing conserved variable analysis (Maorwal and Seetharamayya, 2003). Bala subramanyam and Radhika Ramachandran (2003) made similar analysis using the IDOEX-90 cruise data set over the central Arabian Sea. Prasnis and Morwal (1991) carried out the CVA of convective boundary layer for the southwest monsoon over Deccan Plateau. Kusuma *et al* 1991 reported that the boundary layer height is high during weak monsoon and it is low during active monsoon phase. An attempt is made to understand the variation of thermodynamic structure during active and weak phases of monsoon using CVA over west peninsular region. This helps for diagnostic studies on boundary layer processes and the thermodynamic structure of ABL. During a radiative process the magnitudes of q will not change, but radiative cooling moves points to lower θ_e at constant q . The CBL mixing line shows intense mixing of the lower atmospheric constituents within the mixed layer. Fig. 3.5 and Fig.3.6 show the CVA plots depicting θ_e versus q for six

consecutive days (from 8th July to 13th July) during active monsoon phase for the evening radiosonde observation (5.30 pm IST) for Trivandrum and Mangalore respectively. In the figure, q -axis is reversed so that a sounding plotted superficially resembles a more familiar $(\theta_e - P)$ plot. From the figure, it is found that the mixing height is confined within 1 km except in the last day of the active phase. It may be noted that the mixing height can be treated as the top of the Convective Boundary Layer (CBL). The mixing height over Trivandrum for the active situation is 302 m, 569 m, 464 m, 569 m and 1180 m for the days 8th, 9th, 10th, 12th and 13th July respectively. The CVA plot for 11th July is peculiar and it is very difficult to estimate the mixing height. In the case of Mangalore, the mixing height values are more than that of Trivandrum. This may be due to the effect of orographic clouds formed over the windward side of the Western Ghats during active monsoon phase. During active monsoon situation, the surface westerly wind over the station increases due to the influence of strong LLJ associated with active monsoon. The values of mixing height are 915 m, 730 m, 1399 m, 1498 m, 1539 m and 2071 m respectively for the six days during the active monsoon. The values obtained are realistic even though the vertical resolution of the radiosonde observations is small. During the case of weak monsoon situations the convective mixing height is found to be high in all the cases of Trivandrum and Mangalore. Fig. 3.7 and Fig.3.8 show the $\theta_e - q$ plot for the weak monsoon days in the year 2001. Over Trivandrum, the CBL mixing height is higher than that of active monsoon. This increase is attributed to the characteristics of the weak monsoon situation. During weak phase the convective cloud band and LLJ core prevail over the equatorial region. Accordingly, convective cloud band and associated rainfall over Indian continent is less except Himalayan regions. The rest of the place is more or less cloud free and transparent to the insolation. Thus the local heating triggers convective activity and hence increase in the mixing height. The mixing height values over Trivandrum during weak situation are 1056 m, 764 m, 1473 m, 1477 m and 400 m for the respective six weak days 18th, 19th, 20th, 22nd and 23rd respectively. There is no reversal of q in the 21st July, so it is difficult to estimate the mixing height based on the CVA. In the case of Mangalore the CBL mixing heights are 3129 m, 763 m, 1852 m, 2618 m and 2792 m for the 18th, 19th, 21st, 22nd and 23rd respectively.

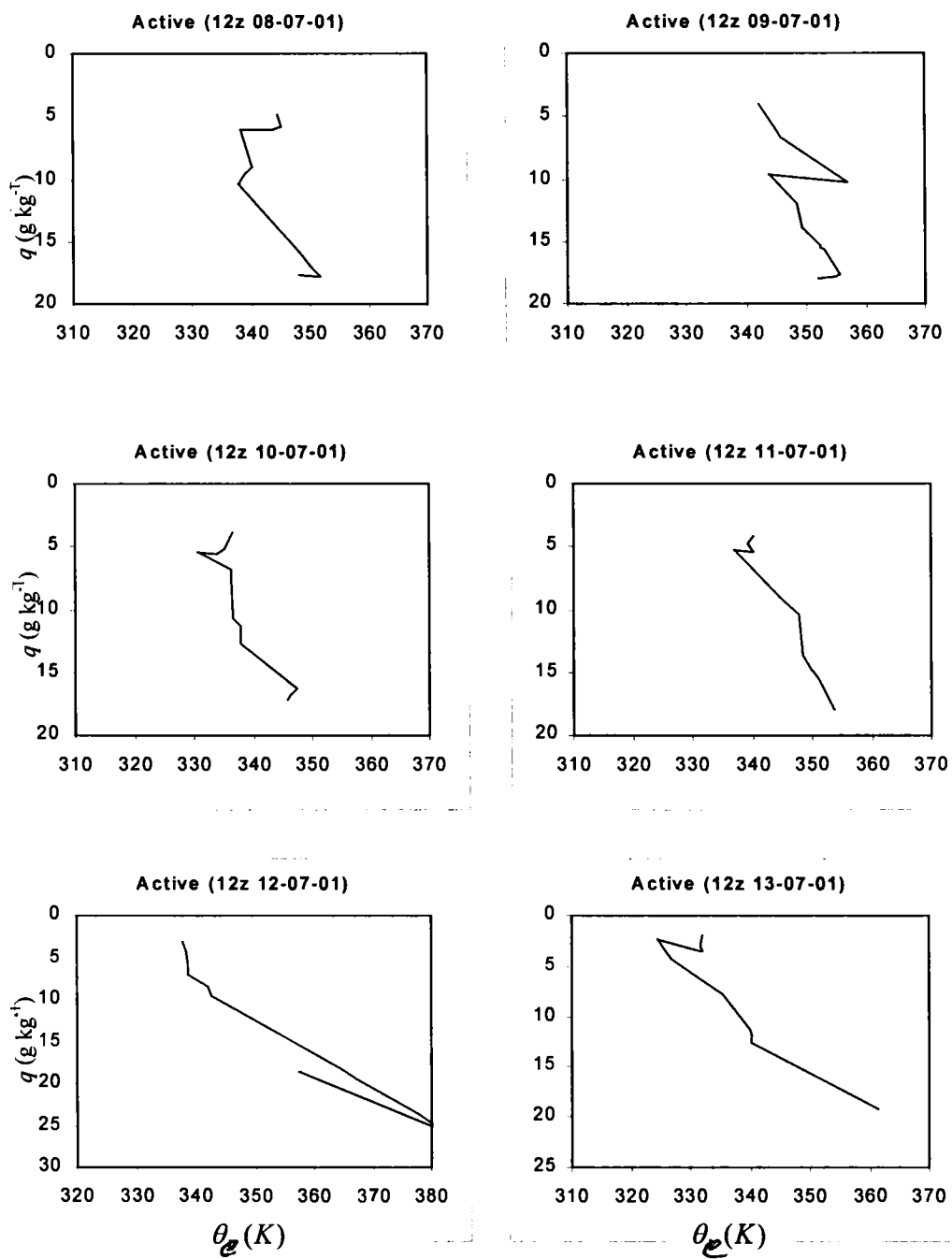


Fig. 3.5 Conserved variable analysis for Trivandrum during the active period of southwest monsoon

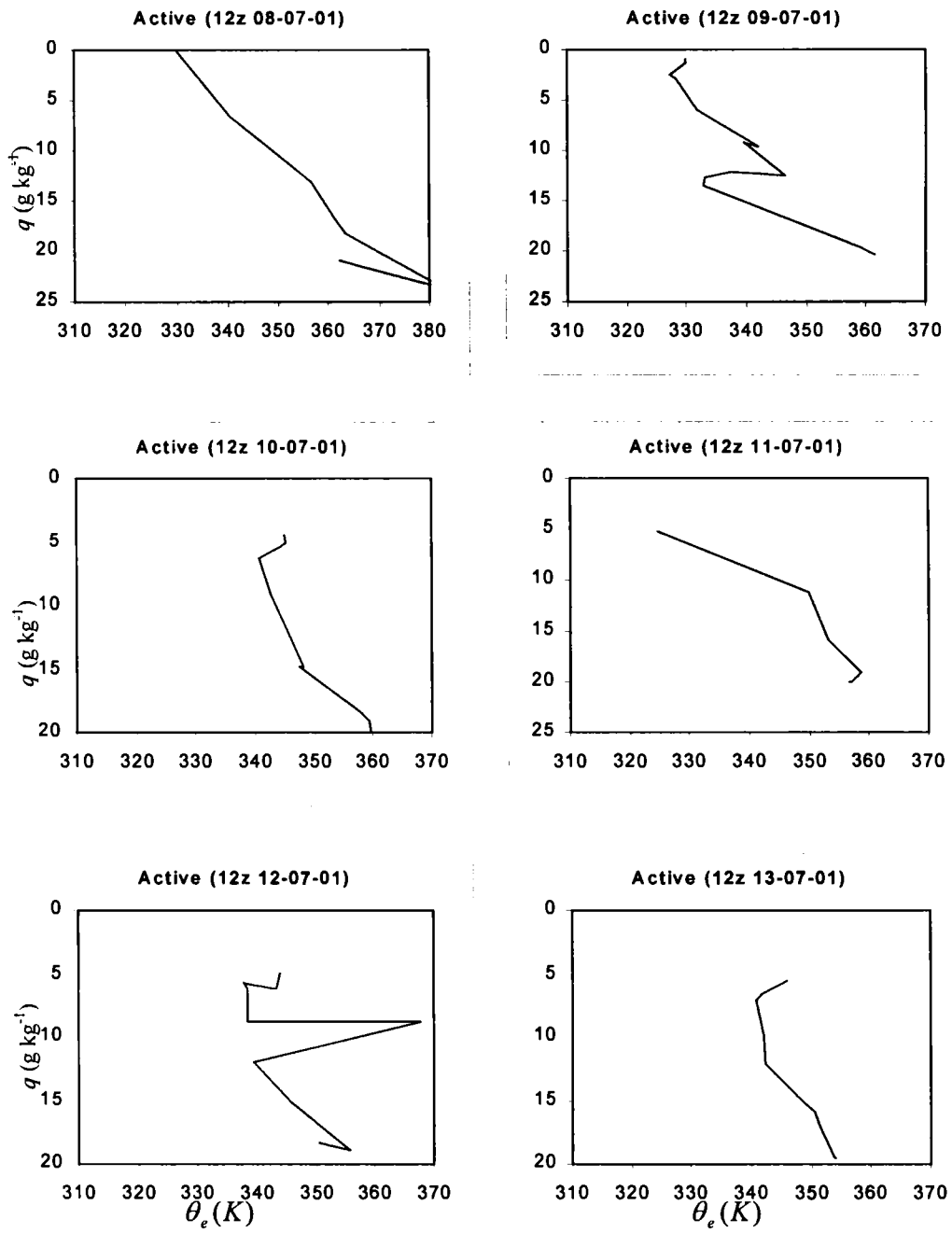


Fig. 3.6 Conserved variable analysis for Mangalore during the active period of southwest monsoon

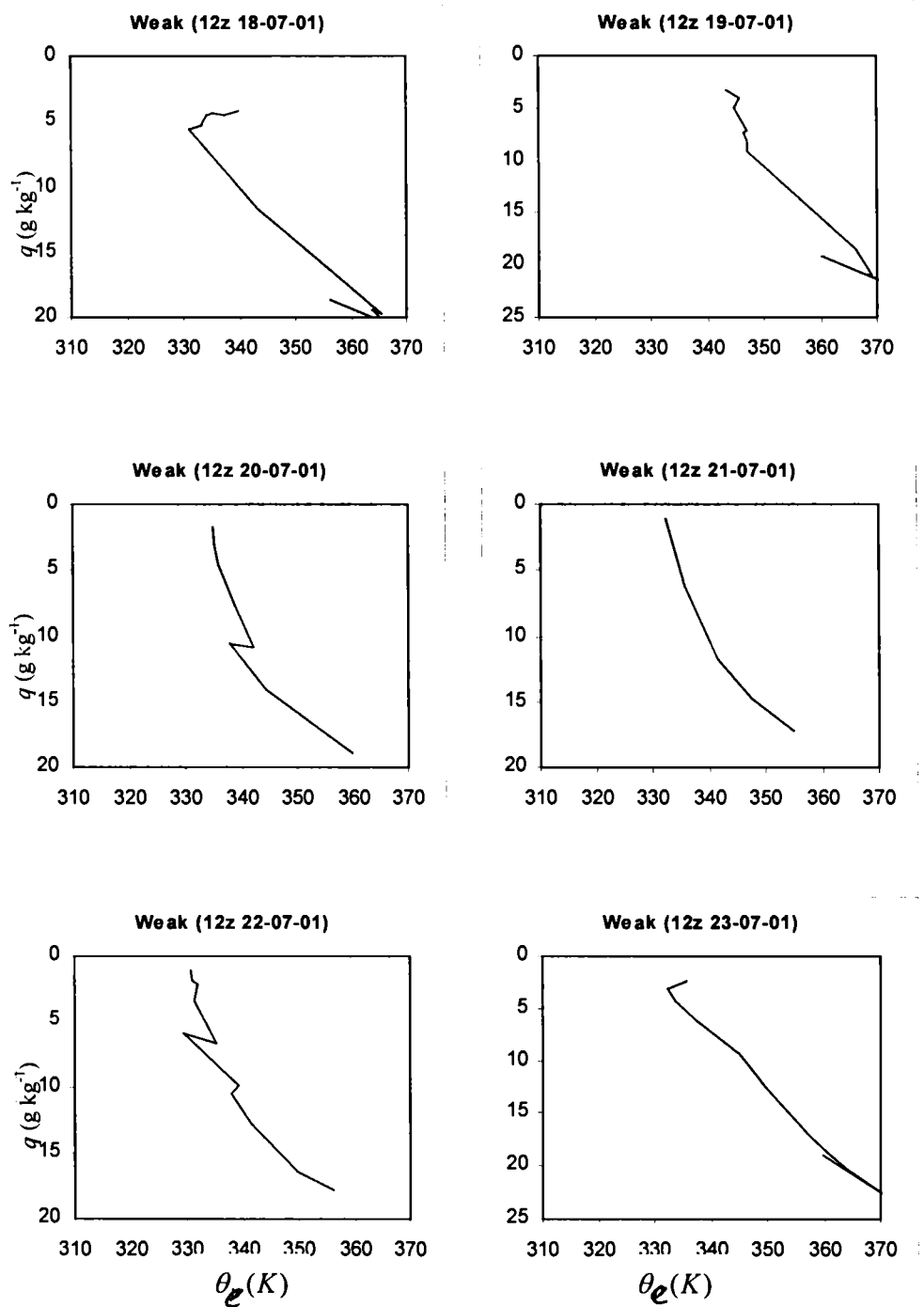


Fig. 3.7 Conserved variable analysis for Trivandrum during the weak period of southwest monsoon

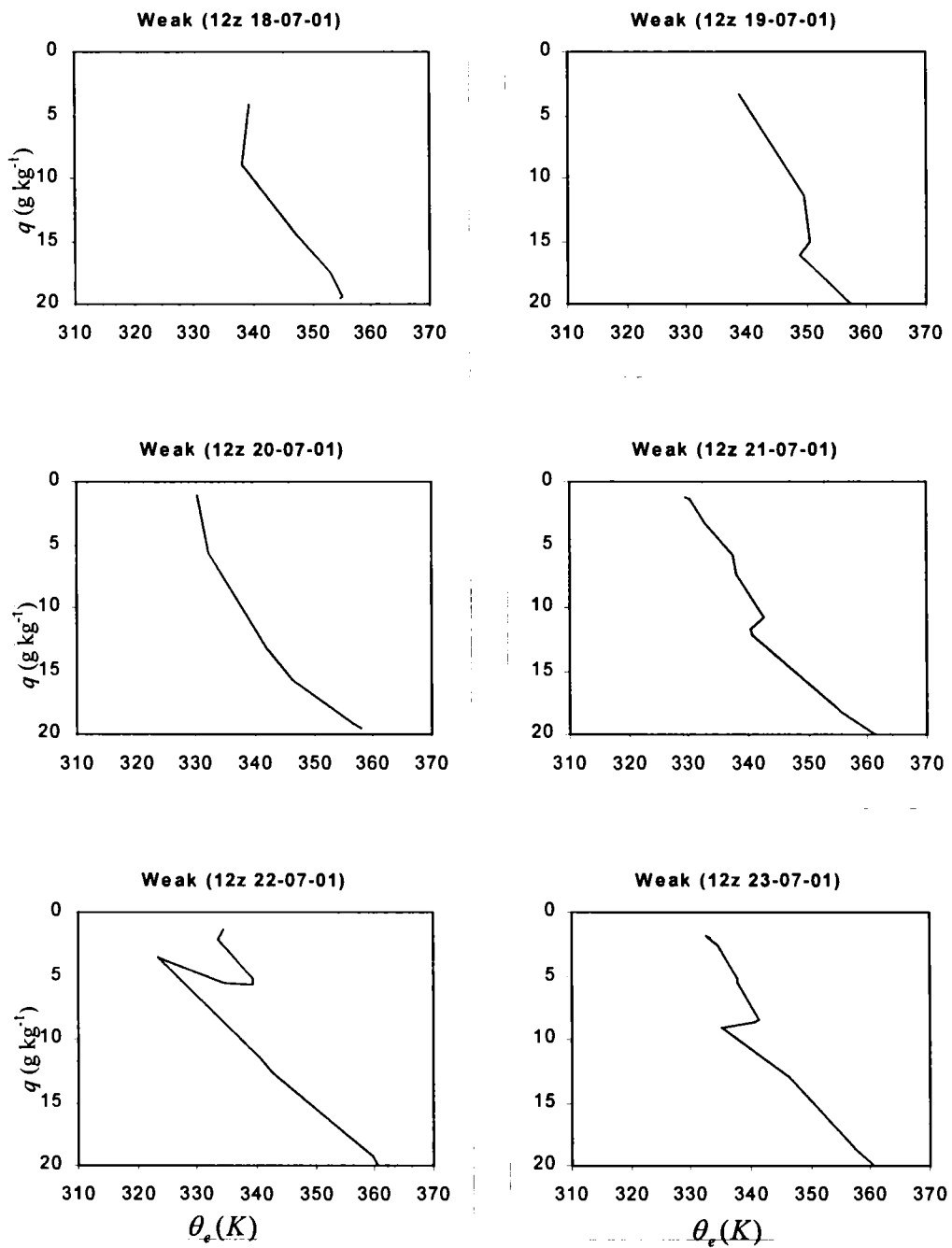


Fig. 3.8 Conserved variable analysis for Mangalore during the weak period of southwest monsoon.

Generally, the mixing height is more during weak phase of monsoon due to less cloudiness. The mean mixing height values over Trivandrum and Mangalore for the active phase of southwest monsoon are 617 m and 1359 m respectively. And that

for the weak monsoon situations are 1034 m and 2230 m for Trivandrum and Mangalore respectively.

3.8 Vertical variation of thermodynamic parameters

In this section we describe some moisture variables, which are related to the active and weak phases of southwest monsoon and contribute a good role in the atmospheric boundary layer. Here we describe the moisture variables such as specific humidity (q), virtual potential temperature (θ_v) and equivalent potential temperature (θ_e).

3.8.1 Specific humidity (q)

Specific humidity is the ratio of mass of water vapour to the mass of moist air and is represented by ' q ', which is expressed as gram of water vapour per kilogram of air (g/kg). The equation of specific humidity is described in data and methodology section of the current chapter. Fig.3.9 shows the vertical slices of the q at six standard levels during July and August of the southwest monsoon as representative years for the stations Mumbai, Mangalore and Trivandrum. The selected stations are all west coastal stations and oriented from North to South. The standard levels presented here are 1000 hPa, 925 hPa, 850 hPa, 700 hPa, 500 hPa and 300 hPa levels. In the figure the blue coloured star represent the values at the station Mumbai, the red coloured plus represent the values at the station Mangalore and the black coloured cross represent the values at the station Trivandrum. As expected the magnitude of the q decreases with height during the entire period of study. The values of q are almost constant in the surface level (1000 hPa) and the value ranges from 16 g.kg⁻¹ to 21 g.kg⁻¹, maximum value of specific humidity is found in Mumbai and it decreases towards the southern stations. It may be due to the variation of wind strength. In the 925 hPa, 850 hPa and 700 hPa the values of q vary widely as the propagation of the monsoon surge, but the maximum and minimum values of the q do not have direct link with the dates of active and weak monsoon phases. In the higher levels (500 hPa and 300 hPa) the variation is negligible. In 300 hPa the value of q is less than 1 g.kg⁻¹. The high fluctuations in the upper levels below 500 hPa is directly related to the variability in degree of convection. The convection process is high in the mixed layer and the mixing process is maximum at 850 hPa level (Bala Subramanyan,2003). In

the high convection time the values of q is found to be high in higher levels due to the moisture pumping and it is almost true in the case of active monsoon situation in all the cases.

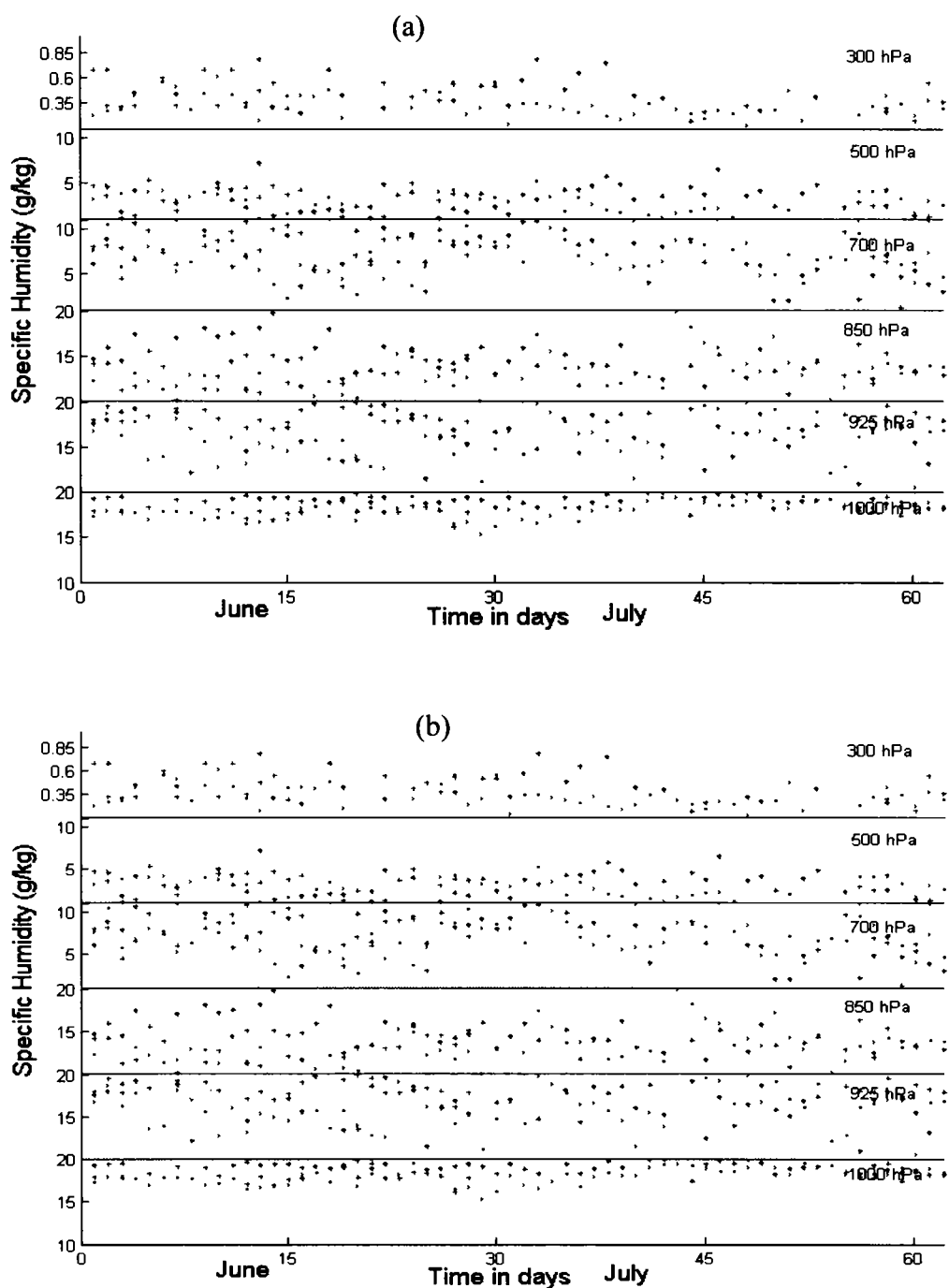
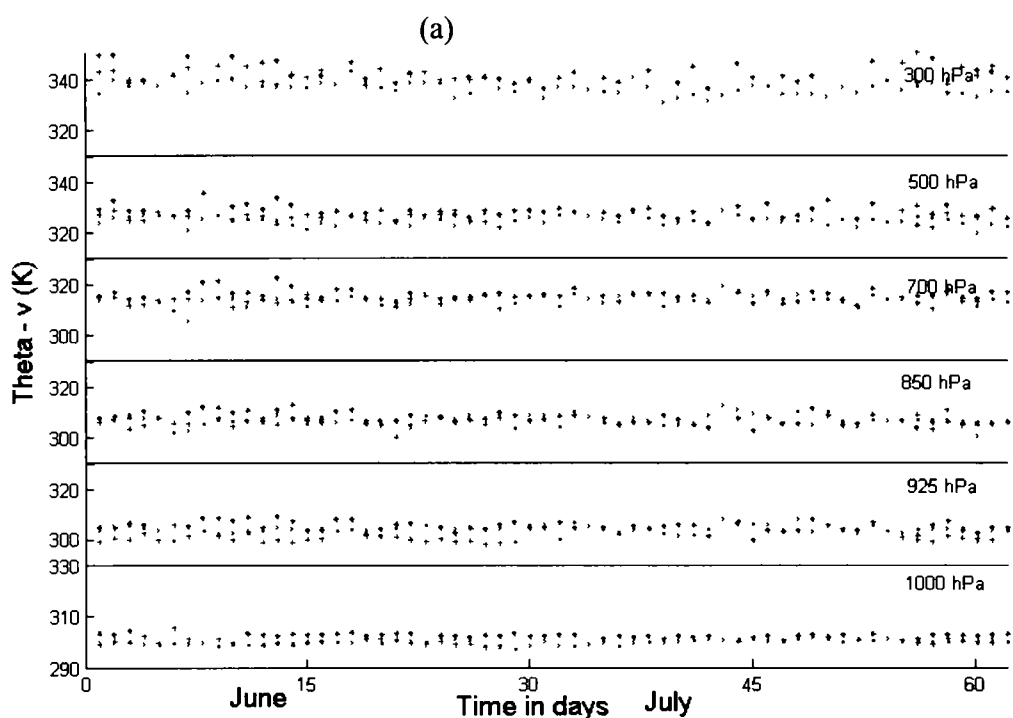


Fig.3.9. Variation of the specific humidity during June and July of a) 2001 and b) 2002 in different standard levels.

3.8.2 Virtual potential temperature (θ_v)

Virtual potential temperature is analogous to potential temperature in that it removes the temperature variations caused by changes in pressure altitude of an air parcel. For the boundary layer, where turbulence includes vertical movement of the air, θ_v is very important parameter for defining various processes. The detailed description of θ_v is given in Stull (1988). The θ_v profile is used to identify the top of the atmospheric boundary layer in which a sharp increase of the value is seen. Here, analysis of vertical slices of θ_v at six standard levels for the three stations of the west coast is carried out and presented in Fig.3.10. It is found that the mixed layer is confined below 850 hPa because above 850 hPa the values show sudden increase with height. The values of θ_v are constant in the surface layer (1000 hPa) and the value is around 300 K for the stations Mangalore and Trivandrum but for Mumbai it is slightly higher and the values is about 302 K, this small variation is noticed in all the levels. A small variation in the value with time is noticed in all levels except surface. Because surface is always with high humidity and it may not respond to the variations in the monsoon activity. During the monsoon season the core of the LLJ height and the ABL heights are closely linked as reported by Madhu (2004). In this study, the constant value of θ_v is found up to the core of LLJ and it is about 850 hPa and afterwards it varies sharply.



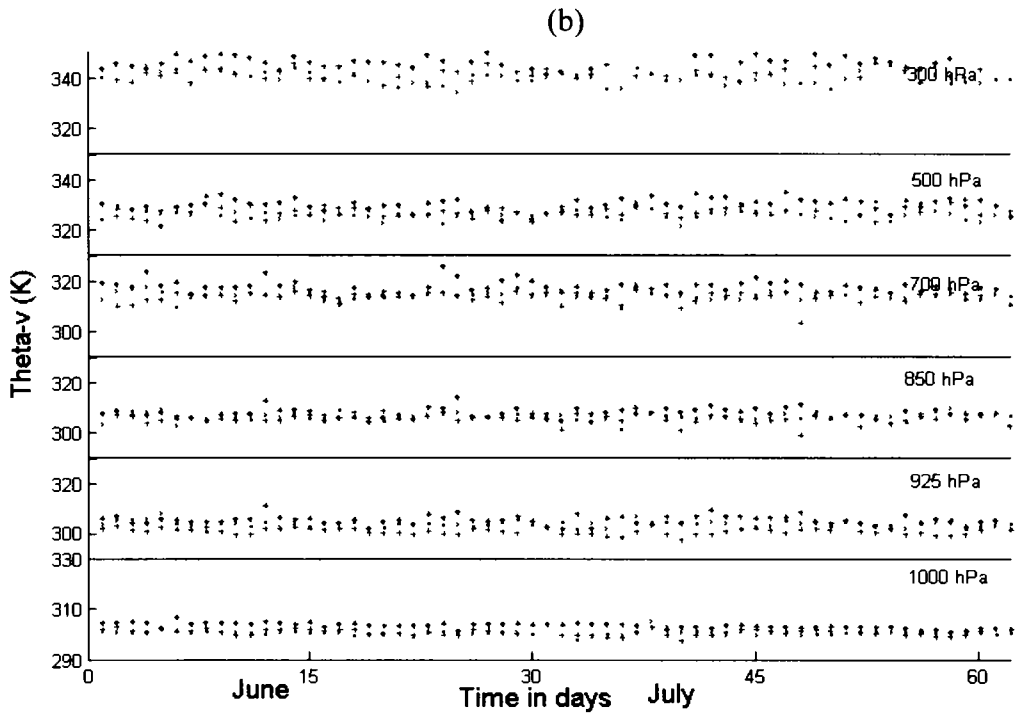


Fig.3.10. Variation of the virtual potential temperature during June and July of a) 2001 and b) 2002 in different standard levels.

3.8.3 Equivalent potential temperature (θ_e)

The equivalent potential temperature (θ_e) is defined as the final temperature which a parcel of air attains when it is lifted dry adiabatically to its LCL, then pseudo-wet adiabatically (with respect to water saturation) to a great height (dropping out all condensed water in the air parcel) then finally dropping down dry adiabatically to 1000 hPa (Bolton, 1980). In another words, it is the temperature at which an air parcel would have if the latent heat is set free and supplied to the air. In this analysis θ_e is calculated using the formula

$$\theta_e = \vartheta \cdot \exp(2.67 \cdot r / T_{LCL}) \quad (3.6)$$

where r is the mixing ratio, θ is the potential temperature (in K) and T_{LCL} is the temperature at LCL in $^{\circ}\text{C}$

Similar to the above figure, Fig.3.11 gives the vertical variation of the θ_e in six standard levels for the three stations. As discussed in the specific humidity section, the values of θ_e is also decreased with height and found to be almost constant in the surface levels and fluctuating in the higher levels as the propagation of the monsoon surge. θ_e is also a good indicator of the convection and the convective

clouds are associated with active monsoon. Hence during active monsoon the values of θ_e is generally high as in the case of the specific humidity.

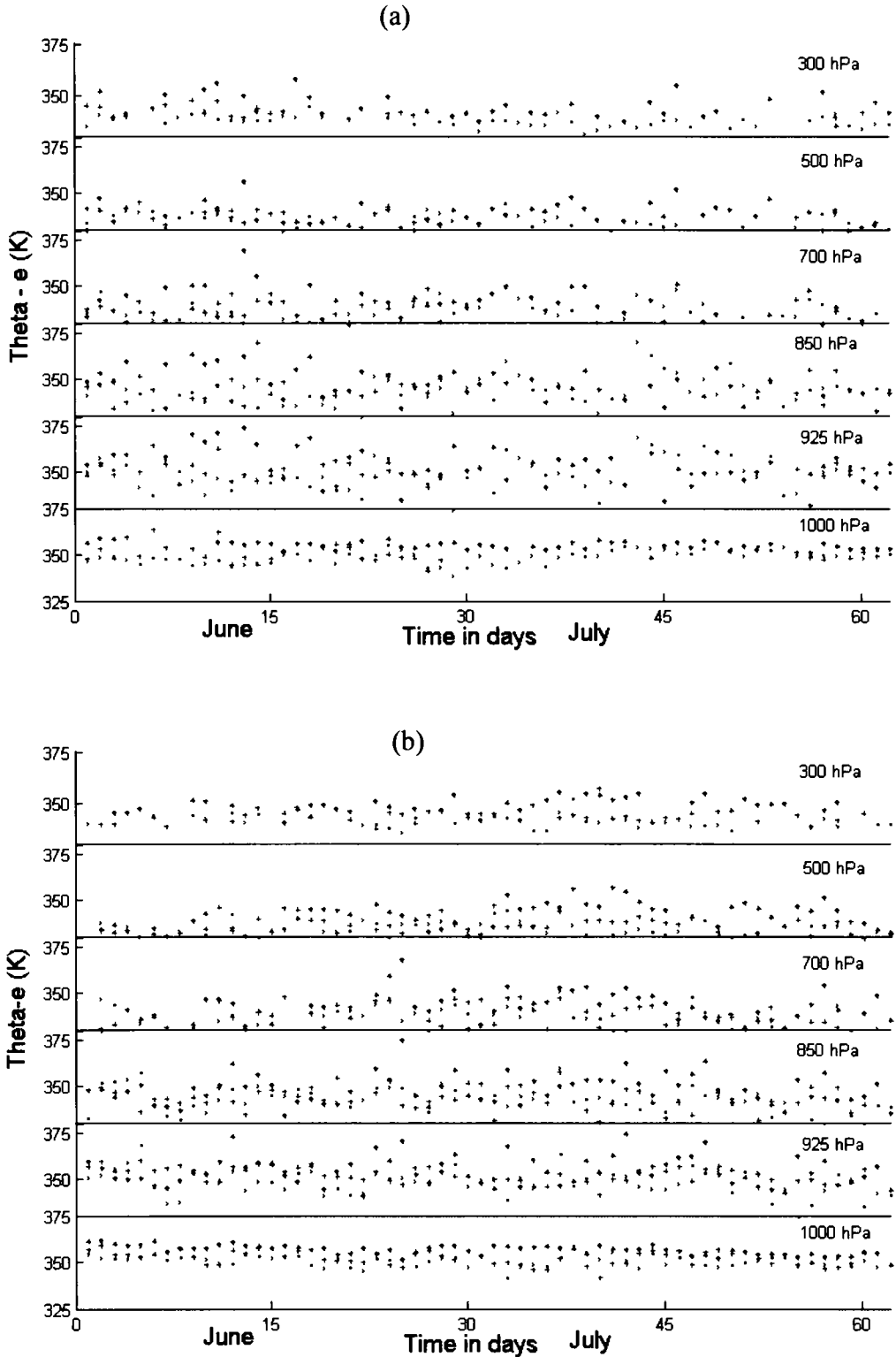


Fig.3.11. Variation of the virtual equivalent potential temperature during June and July of a) 2001 and b) 2002 in different standard levels.

3.8.4 Relation of specific humidity with θ_v and θ_e

The virtual potential temperature and equivalent potential are related to the specific humidity. θ_v is related to the q linearly in the lower levels of the atmosphere. It is inferred that θ_v is linearly related in the mixed layer of the ABL and the relation is given in Fig.3.12 as a scatter plot in which the black 'x' mark represents the station Trivandrum, the red coloured '+' mark represents the station Mangalore and '*' marked blue colour represents the station Mumbai. In the lower level q does not vary much so that θ_v also does not vary. But in the levels 925 hPa and 850 hPa θ_v increases linearly with the increase of the specific humidity. Above mixed layer the relation does not hold good. In the case of θ_e , it is related to the q in a linear way in all the levels as indicated in Fig.3.13. The variation of θ_e is noticed in the mixed layer except in the surface. In higher altitudes the values of θ_e and θ_v increase with a small increase of specific humidity.

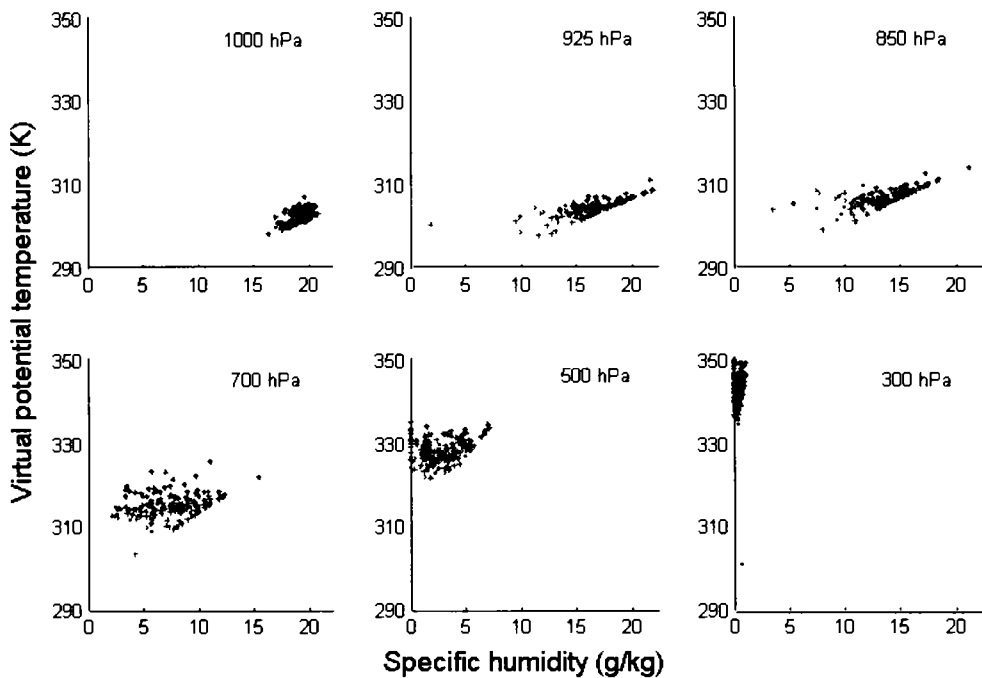


Fig.3.12. Cross relation of specific humidity with virtual potential temperature for the standard levels during the monsoon period.

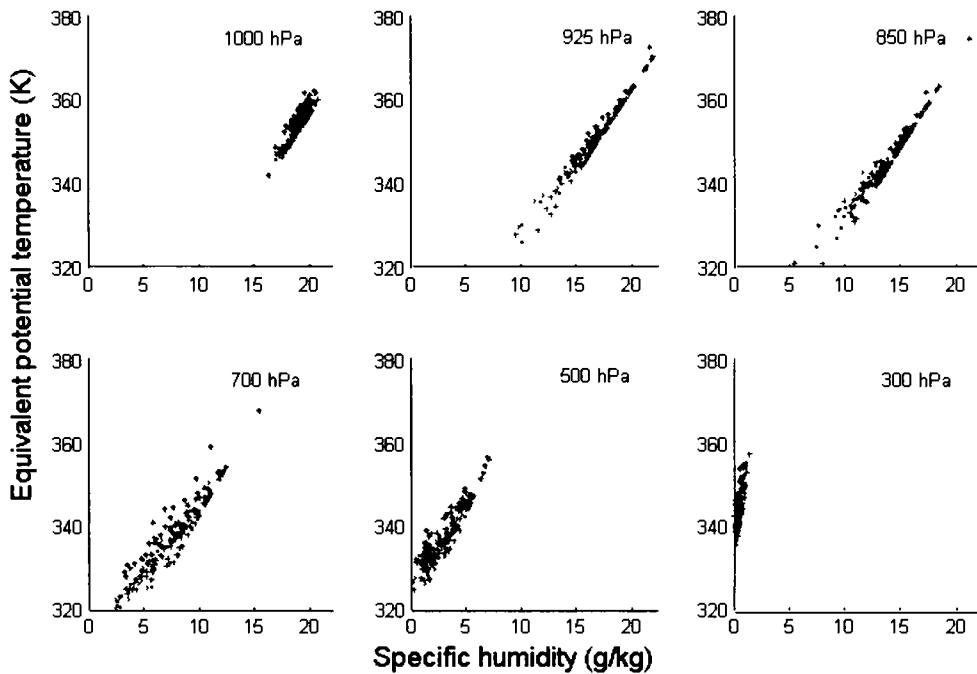


Fig.3.13. Cross relation of specific humidity with equivalent potential temperature for the standard levels during the monsoon season.

3.9 Major oscillations in the ABL

Intraseasonal oscillations (ISO) is one of the major oscillation in the equatorial region and the 30 – 60 day mode is manifestation in the form of northward propagating intraseasonal oscillation during the boreal summer over the Asian monsoon region (Yasunari, 1979, 1981; Sikka and Gadgil, 1980; Krishnamurthy and Subramanyam, 1982). The Quasi biweekly mode (QBM) is also known as 10 – 20 day oscillation and it can be seen in spectral analysis of precipitation, convection and in many circulation parameters (Chen and Chen, 1993; Numaguti, 1995; Kiladis and Wheeler, 1995). The QBM is an important component of the monsoon ISO as its amplitude is comparable to the northward propagating 30-60 day mode (Goswami *et al*, 1998; Goswami and Ajayamohan, 2001) and its phase is relative to that of the 30-60 day mode that determines the active and weak spells of the Indian summer monsoon (Krishnamurthy and Ardhunuy, 1980; Yasunari, 1981; Goswami *et al* 2003). It has been recently shown by Sengupta *et al* (2001) that the observed biweekly fluctuations of the upper ocean zonal transport in the equatorial Indian Ocean is driven by the biweekly fluctuations of the surface stress. The oscillations in boundary layer parameters are show different types of oscillations such as ISO and QBM. Here

an attempt is made to study the QBM and ISO mode of oscillation found in the surface, 925hPa and 850hPa and how they connected each other.

Wavelet decomposition is a method of time-frequency localization that is scale independent. This method of decomposition can be employed where a predetermined scaling may not be appropriate because of a wide range of dominant frequencies. Wavelet analysis attempts to solve by decomposing the time series signals into time / frequency space domains simultaneously. This method of signal decomposition provides information on both the amplitude of any periodic signals within the series, and how this amplitude varies with time. In this study, dmey wavelet is utilized to obtain the predominant signals embedded in the time series of vector wind and temperature. Analysis was carried out in MATLAB computing package. The wave decomposition is performed using $[C,L] = \text{wavedec}(X,N,'wname')$ which, returns the wavelet decomposition of the signal X at level N, using 'wname'. N is a positive integer. The output decomposition structure contains the wavelet decomposition vector C and bookkeeping vector L. wrecoef reconstructs the coefficients of a one-dimensional signal, given a wavelet decomposition structure (C and L) and either a specified wavelet. $X = \text{wrecoef}('type',C,L,'wname',N)$ computes the vector of reconstructed coefficients, based on the wavelet decomposition structure [C,L], at level N. From the reconstructed coefficients the harmonics can be computed (Torrence and Compo, 1998).

3.9.1 Oscillations in wind and temperature

Indian subcontinent has characterised by the seasonal reversal of wind from northeasterly during winter to southwesterly during summer. In major part of the country the rain giving season is southwest monsoon season in which the prominent wind direction is southwesterly. In addition to this intra annual variability, there are low and high frequency variabilities embedded in the meteorological parameters during the southwest monsoon. Atmospheric surface layer characteristics over this season are closely linked with the upper monsoon features and under this perception it is imperative to study the variabilities in the lower troposphere with different altitudes. Praveena *et al* (2005) studied such variability using UHF radar over an equatorial station. The features of the variability at different time scales over southern part of India are studied at different heights (surface, 925 hPa and 850 hPa) by

subjecting temperature and wind to wavelet analysis for the decomposition of all the harmonics in the original data. From the different harmonics obtained, it is noted that the major harmonics are 30 to 60 day mode and 10 to 20 day mode. Fig 3.14 shows the wind during the southwest monsoon of 2002 at different heights (surface, 925 hPa and 850 hPa) and its major harmonics. In the figure the first, second and third columns show the original signal and its harmonics at 850 hPa, 925 hPa and surface respectively. The zonal wind at 850 hPa shows the clear indication of active (wind speed is more than 15 ms^{-1}) and weak (wind speed is less than 9 ms^{-1})

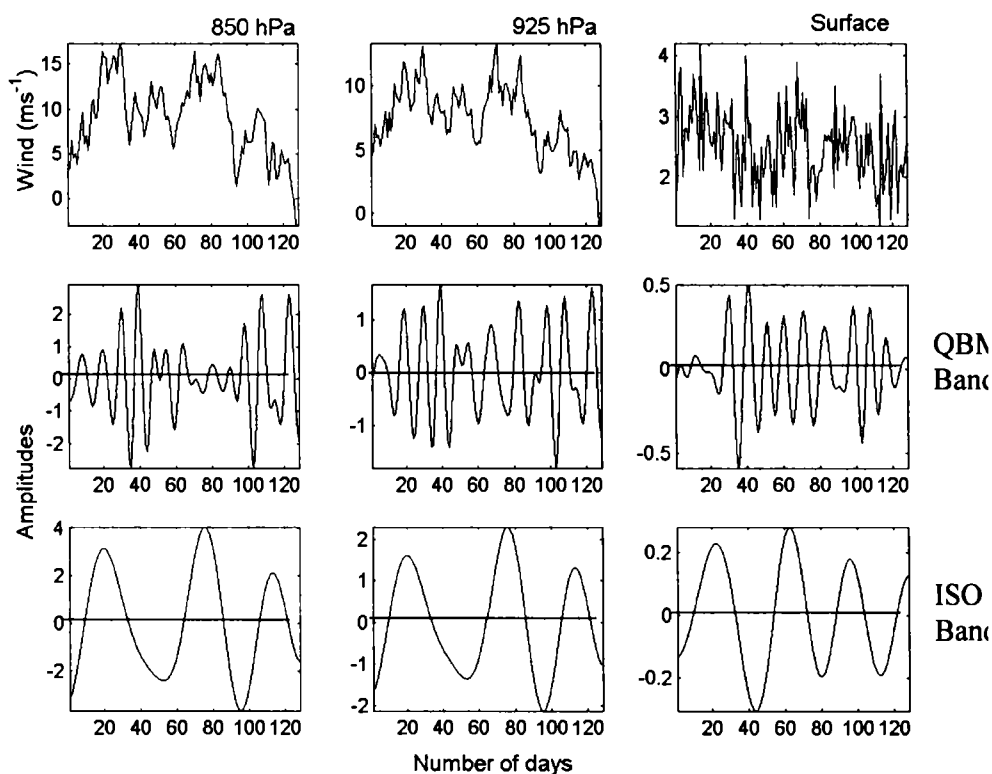


Fig 3.14 Wavelet analysis of the wind at 850 hPa, 925 hPa and surface during southwest monsoon. The first row represents the original signal, the second row gives the harmonics of wind in the QBM band and the next is same for ISO band.

spells. The major oscillations are found to be 10 to 20 day mode (QBM) and 30 to 60 day mode (ISO). The QBM has a periodicity of about 11 days and the ISO is around 47 days. The amplitude of the harmonics is higher in the ISO band, so at 850 hPa the major oscillation is ISO band. In the case of 925 hPa, the zonal wind shows the same type of variation as that of the 850 hPa but the magnitude is comparatively less. The QBM periodicity is around 13 days and ISO periodicity is around 43 days. Here, the

important oscillation is ISO band because the amplitude of the harmonics is higher in the ISO band than that of the QBM band. In the case of surface layer, the wind pattern shows almost similar behavior to the layer above. It is obvious that surface friction plays vital role on the surface wind. The important oscillations in this layer is QBM with a periodicity of about 12 days because the amplitude of this harmonics are higher to this mode of oscillation than that of the ISO band. The ISO band has less influence in the surface layer so that its harmonics is far less than that of the QBM and the periodicity (~ 39 days) is also less compared to the upper levels.

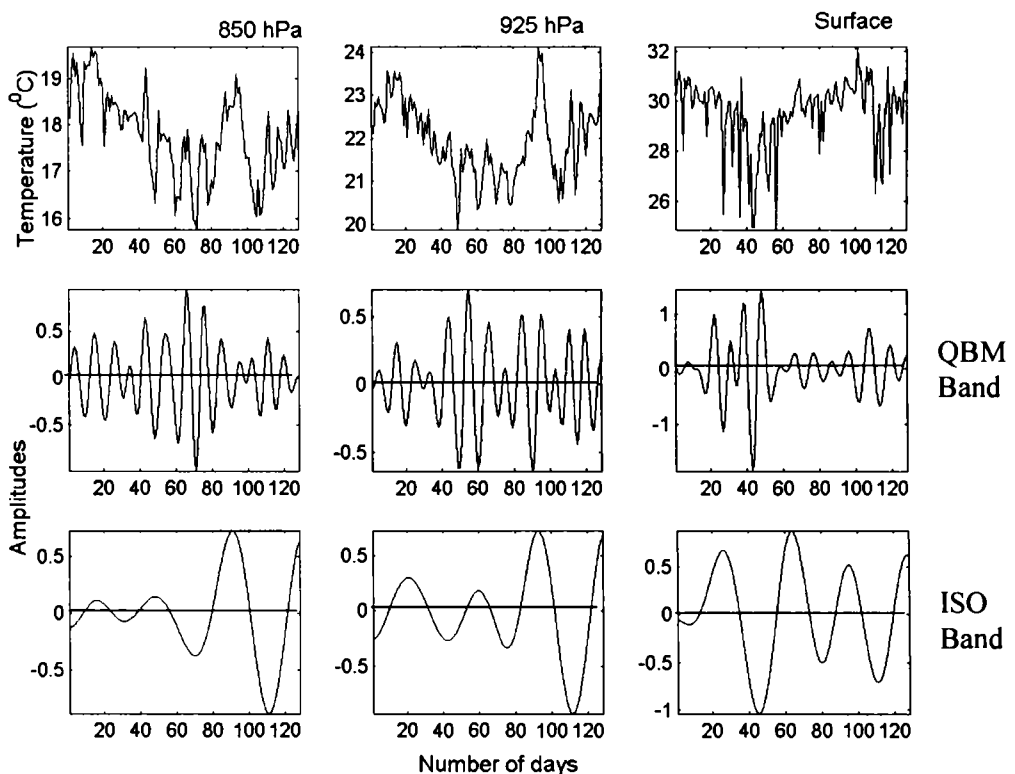


Fig 3.15 Wavelet analysis of the temperature at 850 hPa, 925 hPa and surface during southwest monsoon. The first row represents the original signal, the second row gives the harmonics of wind in the QBM band and the next is same for ISO band.

The temperature at the above levels were also studied in the same way as that of the wind and presented in Fig.3.15. But there are some differences in the variability to temperature from the wind. The 850 hPa and 925 hPa levels have the ISO and QBM periodicities are around 37 and ~ 10 days respectively and they are almost equal importance because of their harmonics are almost same amplitude. In the surface layer, the most contributed periodicity is QBM band than that of the ISO

mode. The QBM is around 11 days and ISO has around 34 days periodicities. The periodicity of the oscillation in temperature at 850 hPa and 925 hPa levels are comparatively less than that of the wind and the amplitudes are also less to temperature. But in the case of surface layer, the maximum amplitude of the harmonics are seen to the temperature in both QBM and ISO periodicities.

Influence of surface friction and associated turbulent eddies can be attributed as the mechanism responsible for the intense QBM in the surface layer. It is found that the amplitude of ISO band increases towards 850 hPa. This is because the intra seasonal oscillation of the monsoon regime governs oscillations at this level. In other words once can infer that the surface layer controls the QBM periodicity and the upper levels control the ISO periodicity.

From the analysis of ABL characteristics associated with the different epochs of monsoon, it is found that the turbulent parameters are high due to the presence of organized convective clouds in the active monsoon situation and less during weak monsoon situation. It is found that the thermodynamic parameters show variability during active and weak phases of monsoon. From the conserved variable analysis, it is found that the mixing height of the boundary layer over the west coastal stations are high during weak phase of monsoon and low during active monsoon situations. The prominent oscillations in the meteorological parameters in the surface layer are in the QBM and ISO bands. The amplitude of QBM dominates in the surface layer while ISO mode dominates in the 925 hPa and above. It is important to understand the characteristics of the ABL structure over ocean during different seasons and hence next chapter is devoted for the ABL features over marine atmosphere.

CHAPTER – 4

***MARINE ATMOSPHERIC BOUNDARY LAYER
CHARACTERISTICS OVER ARABIAN SEA
AND BAY OF BENGAL***

CHAPTER - 4

MARINE ATMOSPHERIC BOUNDARY LAYER CHARACTERISTICS OVER ARABIAN SEA AND BAY OF BENGAL

4.1 INTRODUCTION

The prime focus of this study is to examine the dynamics of marine atmospheric boundary layer (MABL) over Arabian Sea and Bay of Bengal during the different seasons using data from satellite derived QuikSCAT sea wind sensor. MABL is the layer just above the sea surface, influenced by the presence of the ocean surface and plays an important role in the exchange of momentum, mass and energy across the surface and influences to a large extent the atmospheric and oceanic circulations. The planetary boundary layer (PBL) process over land and ocean constitute important physical inputs in the numerical simulation of the monsoon (Rao, 1988, Krishnamurti *et al.* 1973, Manabe *et al.* 1974, Shukla *et al.* 1981) and PBL physics are usually incorporated in models by adopting suitable parameterisation schemes (Kusuma, *et al.*, 1991).

4.1.1 Arabian Sea

Arabian sea is one of the important play grounds of the South Asian monsoon especially in wind and SST regimes. Seasonal variation of wind is well documented in literature, northeasterly during winter and during summer it is southwesterly. Many field studies were carried out to bring out the characteristics of Arabian Sea. The IIOE (International Indian Ocean Expedition, 1963-1965) paved the way to study thermal and kinetic features of the monsoon flow over the Arabian Sea and adjoining West Indian Ocean. In this expedition, the experimental arrangement consists of a six leveled logarithmically scaled vertical sensors mounted on a floating mast, measurements were made between 1.6 m and 8 m above mean sea level under a variety of stability and wind speed conditions (Badgley, *et al* 1972). The radiosonde and dropsonde data were first used in this experiment and they provide valuable information about the marine atmosphere over Indian Ocean region and the results were discussed in Bunker (1965). After the IIOE Indo-Soviet Monsoon Experiment

(ISMEX) in 1973 and monsoon Experiment in 1979 were carried out. Using ISMEX data set Jambunathan and Ramamurty (1975) studied the air sea temperature distribution over West Indian Ocean and Pant (1978) studied the MABL structure over West Indian Ocean. INDOEX (Indian Ocean Experiment) were carried out in 1998 to bring out characteristics of aerosol, radiation and solar absorption at the surface and in the troposphere including the ITCZ cloud systems (Ramanathan *et al*, 1995).

4.1.2 Bay of Bengal

Most of the rainfall occurs in association with synoptic systems such as lows and depressions, which are generated over the warm oceans and subsequently propagate to Indian land mass. Many of them are formed and intensified over Bay of Bengal and then moved to land mass. The Bay of Bengal is exceptionally fertile to these systems and play an important role in the monsoon variability (Gadgil and Mohanty, 2000). Many observational studies based on satellite data suggest that tropical SST and deep convection are strongly related (Graham and Barnett, 1987). It is due to the sensible and latent heat fed deep convection formed in the atmosphere at the ocean surface. The sensible and latent heat transfer in the ABL over the region plays vital role in the generation of deep convection. Hence the process in the ocean and atmosphere are strongly interrelated each other and their coupling mechanism is important in identifying features of deep convection. It has been known that the more pronounced variabilities in SST and other meteorological parameters are in the Bay of Bengal than the Arabian Sea (Krishnamurty, *et al* 1988). Studies carried out over Pacific Ocean showed that MABL plays a vital role in the growth and maintenance of the tropical disturbances (Neelin *et al* 1987; Yano and Emanuel, 1991). They reported further that the boundary layer itself gets modified by the disturbance and their interaction can lead in the variability of deep convection on subseasonal and seasonal time scales.

Several studies were carried out in the Bay of Bengal to explore the ABL features since the last two decades. The first two major field experiments were MONSOON-77 and MONEX-79 and they involved several Indian and Soviet ships. The third experiment conducted were MONTBLEX-90 (Monsoon trough boundary layer experiment) during the period 18-31 August, 1990 and 9-19 September 1990 in

the head Bay. From the above field experiments, dynamic and thermodynamic characteristics of the MABL over Bay of Bengal were found (Mohanty and Das, 1986; Mohanty and Mohankumar, 1990). Another field cruise named BOBMEX (Bay of Bengal monsoon experiment) was carried out in the Bay of Bengal during the months of July and August, 1999, a BOBMEX-Pilot experiment was also conducted during the period October to November, 1998 to study the features of MABL associated with convection and to study the coupling between atmosphere and ocean (Sikka and Sanjeevarao, 2000).

Holt and Raman (1987) studied the structure of boundary layer over the Arabian Sea and Bay of Bengal during active and break phases of monsoon using ISMEX-77 & MONEX-79 data set. They found that the height of the boundary layer decreases during active phase and increases during weak phases of monsoon. Sam *et al.*, 2003 examined the temporal evolution of turbulent kinetic energy, sensible and latent heat fluxes and drag coefficient using radiosonde data taken at the BOBMEX-99 during the different epochs of Indian summer monsoon. They reported that simulation results using 1-D model agree with the observational analysis. TOGA COARE (Tropical Ocean Global Atmosphere Coupled Ocean Atmosphere Response Experiment), which was aimed to describe the coupling of the west Pacific warm pool to the atmosphere (Webster and Lukas, 1992), gave an insight to the atmosphere ocean coupling on time scales of intra seasonal (Godfrey and Lindstorm, 1989; Shinoda *et al.* 1998). The energy supplied by the atmosphere is mostly trapped in the MBL, except in the region of deep convection. Mahrt and Ek (1993) studied the spatial variability of the turbulent fluxes and roughness lengths over a heterogeneous surface using the flight data during clear sky days and found that the effective roughness length is about 1 m. So, it is very important to understand the various characteristics such as drag coefficient, roughness length and other parameters of the MABL.

4.2 Objective of the study

The study is focused on the dynamical characteristics of the marine atmosphere over Arabia Sea and Bay of Bengal with QuikSCAT wind products and TMI SST derived from satellites. This high-resolution data set can be used to derive a better understanding of the MABL and provides valuable information over the

Arabian Sea and the Bay of Bengal since it is very difficult to get the data in the region. Many studies were made to calibrate the reliability of the data set and it can be found in Bentamy *et al* (2002) and also available in the website <http://www.ifremer.fr/cersat/english>. Goswami and Rajagopal, (2004) also made comparison of the QuikSCAT wind *in situ* observations taken from satellite data and buoys located over Arabian Sea and Bay of Bengal and found that this dataset agrees well with observations. So, the surface information on wind vector and its products are reliable to study the characteristics of wind stress, frictional velocity, roughness length and wind stress curl on seasonal basis.

4.3 Data and Methods

4.3.1 Data description

The data sets used for the present study are the zonal and meridional components of the surface wind, wind stress and wind stress curl from 20th June 1999 to 30th December, 2003 taken from the two dimensional surface wind fields measured by the SeaWinds scatterometer on board of QuikSCAT satellite of National Aeronautics and Space Agency, the description can be found in the *QuikSCat Mean Wind Field User Manual*. In addition to ERS-2 scatterometer launched by European Space Agency (ESA) in April 1995, a new scatterometer, SeaWinds was launched onboard QuikSCAT satellite by NASA/JPL in June 1999 (<http://podaac.jpl.nasa.gov/quikscat/>).

4.3.1.1 SeaWinds sensor overview

The SeaWinds instrument uses a rotating dish antenna with two spot beams that sweep in a circular pattern. The antenna radiates microwave pulses at a frequency of 13.4 GHz across broad regions on Earth's surface. The instrument collects data over ocean, land, and ice in a continuous, 1,800-wide-wide band centred on the spacecraft's nadir sub track, making approximately 1.1 million ocean surface wind measurements and covering 90% of Earth's surface each day. The SeaWinds instrument on QuikSCAT is an active microwave radar designed to measure electromagnetic backscatter from wind roughened ocean surface. QuikSCAT/SeaWinds is a conically scanning pencil-beam scatterometer. A pencil-

beam scatterometer has several key advantages over a fan-beam scatterometer; it has a higher signal-to-noise ratio, is smaller in size and it provides superior coverage.

4.3.1.2 Introduction to QuikSCAT

QuikSCAT has two major systems, the space borne observatory system and the ground data processing system. The SeaWinds observatory instrument is specialised microwave radar designed to measure winds over the oceans. The ground system computers produces wind measurements within 3 days of receiving raw QuikSCAT data from the spacecraft, with no backlog, throughout the mission. QuikSCAT data products currently include global backscatter data and 25 km resolution ocean wind vectors in the measurement swaths. There are also plans to provide spatially and temporally averaged, gridded, wind field maps and other special products.

4.3.2 Product description

This section describes the main characteristics of the QuikSCAT mean wind fields produced at CERSAT, and provides detailed specifications of the format of the data files.

4.3.2.1 Spatial coverage

The QuikSCAT mean wind fields cover global oceans from 80° North to 80° South in latitude and 180° West to 180° East in longitude.

4.3.2.2 Spatial resolution

The QuikSCAT mean wind fields are provided on a rectangular 0.5°x0.5° resolution grid. The data are projected on a 0.5° rectangular grid of 720 columns and 320 lines. A grid cell spans 0.5° in longitude and 0.5° in latitude. Latitude and longitude of each grid cell refers to its centre. The origin of each data grid is the grid cell defined by 179.75° West in longitude and 79.75° North in latitude. The last grid cell is centered at 79.75° South and 179.75° East.

4.3.2.3 Temporal resolution

Mean winds fields are available from 20 July 1999 to present. Three different temporal resolutions are provided and they are daily mean, which covers the time period from 0h to 24h in the current day, weekly mean, which covers the time period from Monday 0h to Sunday 24h in the current week and monthly mean, which covers the time period from the first day at 0h to the last day at 24h in the current month

4.3.2.4 Main parameters

The main parameters derived from the QuikSCAT wind field are (1) Wind speed modulus ($0 - 60 \text{ ms}^{-1}$), (2) Zonal wind component ($-60 - 60 \text{ ms}^{-1}$), (3) Meridional wind component ($-30 - 30 \text{ ms}^{-1}$), (4) Wind stress modulus ($0 - 2.5 \text{ Pa}$), (5) Zonal wind stress component ($- 2.5 - 2.5 \text{ Pa}$), (6) Meridional wind stress component ($- 2.5 - 2.5 \text{ Pa}$), (7) Wind vector divergence ($- 10^{-3} - 10^{-3} \text{ s}^{-1}$), (8) Wind stress curl ($- 2.5 - 2.10^{-5}$) and (9) Estimated error of each of the above parameters is provided with the same unit.

4.3.3 Methodology description

4.3.3.1 Retrieving wind vectors from scatterometer measurements

Scatterometer instruments on board satellites can routinely provide an estimation of the surface wind vector with high spatial and temporal resolution over all ocean basins. Although the exact mechanisms responsible for the measured backscatter power under realistic oceanic conditions are not fully understood, theoretical analysis, controlled laboratory and field experiment, and measurements from space borne radars all confirm that backscatter over the oceans power at moderate incidence angles is substantially dependent on near-surface wind characteristics (speed and direction with respect to the radar viewing geometry). At the present time, the microwave scatterometer is the only satellite sensor that observes wind in terms of wind speed and wind direction. To date, the most successful inversions of scatterometer measurements rely on empirically derived algorithms. An empirical relationship is typically given by the following harmonic formula:

$$\sigma^0 = \sum_{j=0}^k A_j(\lambda, P, \theta, U) \cos(j\chi) \quad (4.1)$$

Where k is the degree of σ^0 representation that uses cosines as orthogonal basis (number of harmonics), λ , the scatterometer wavelength, P , the polarization, θ , the radar incidence angle, U the wind speed for neutral stability and χ is the angle between wind direction and radar azimuth. A_j are the model coefficients to be determined through regression analysis. Surface wind speed and direction at a given height are retrieved through the minimization, in U and χ space, of the Maximum Likelihood Estimator (MLE) function defined by

$$F = -\sum_{i=1}^N \frac{(\sigma_i^0 - \sigma_{im}^0)}{\text{Var}(\sigma_{im}^0)} \quad (4.2)$$

Where σ^0 and σ_m^0 are the measured and estimated, from (1), backscatter coefficients, respectively. Variance (σ_m^0) stands for σ^0 variance estimation. N is the number of measured σ^0 used in the wind vector estimation. This approach yields up to four solutions and an ambiguity removal procedure is needed in order to estimate the most probable wind vector (Quilfen *et al*, 2001). A main task for a scatterometer investigator is the calibration of the sensor data. The calibration involves both the determination of the empirical model (1) and the development of the surface wind retrieval algorithm. A second task consists in validating the accuracy of backscatter coefficients and wind estimates and their comparison with other sources of data. Since July 1999, two scatterometers are available and provide surface wind estimates with different instrumental configurations. The first one is on board the European Remote Sensing satellite 2 (ERS-2) and the second is the NASA scatterometer SeaWinds on board QuikSCAT. The use of both wind estimates should potentially lead to a more refined wind field analysis calculated from satellite data.

4.3.3.2 Wind stress estimation

To estimate surface wind stress, τ for each scatterometer wind vector, the bulk formulation is used:

$$\tau = (\tau_x, \tau_y) = \rho C_D W(u, v) \quad (4.3)$$

Where W , u and v are the scatterometer wind speed, zonal component (eastward) and meridional component (northward), respectively. The surface wind is assumed to be

parallel to the stress vector. ρ is the density of surface air equal to 1.225 kg/m^3 . C_D is the drag coefficient. The magnitude of the stress is:

$$|\tau| = C_D W^2 \rho \quad (4.4)$$

There have been many estimates of C_D . We have selected the one published and recommended by Smith (1988), which was chosen by the WOCE community.

Frictional velocity, u_* is obtained from the formula

$$u_* = \sqrt{\tau / \rho} \quad (4.5)$$

where τ is the wind stress and ρ is the density of air. The roughness length, z_0 is calculated using

$$\bar{U} = \frac{u_*}{k} \ln \frac{z}{z_0} \quad (4.6)$$

where \bar{U} is the mean wind, k is Von Karaman constant and the value is taken as 0.4 and z is the reference height and is taken as 10 m.

4.4 Spatial variation of surface layer parameters

4.4.1 Surface wind

The climatology of the surface wind pattern derived from QuikSCAT SeaWinds scatterometer for different seasons are presented in Fig.4.1. Here, the figures are presented over the region 50°E - 100°E to 25°S - 25°N to bring out the features over the entire monsoon domain. In the figure, the left top panel shows wind pattern for winter (January), which represents northeasterly over the Arabian Sea and Bay of Bengal since January belongs to northeast monsoon season. In the south of 10°S , the prominent wind direction is southeasterly. The winds from equatorial region and 20°S converge around 11°S and blow towards east. The top right panel of the figure shows similar features during pre-monsoon season (April). During April, the surface winds are in transition stage from northeasterly to southwesterly and hence winds are feeble both in the Arabian Sea and Bay of Bengal. The wind over the west peninsular coastal belt is relatively stronger and the direction is northwesterly. In Indian Ocean (south of the equator) the speed and direction of the wind are same but the convergent zone is shifted to the north and now occupies over the equator, but the wind is feeble in comparison with that in winter. The wind pattern during southwest

monsoon (July) is presented in the left bottom panel of the Fig.4.1. In this, the surface wind is stronger compared to all other seasons and is due to the intensification of the surface wind by the Low Level Jetstream (LLJ). The LLJ core occurs at 850 hPa over the Indian subcontinent during the southwest monsoon period only (Joseph and Raman, 1966; Findlater, 1966). This strengthening of the surface wind results in the abundant transfer of moisture from the sea surface to the atmosphere over this region for the maintenance of the southwest monsoon. The bottom right panel of the figure shows the wind pattern during the post monsoon season (November). During this period, the prominent surface wind direction is northeasterly due to the influence of post monsoon and the strength is relatively low.

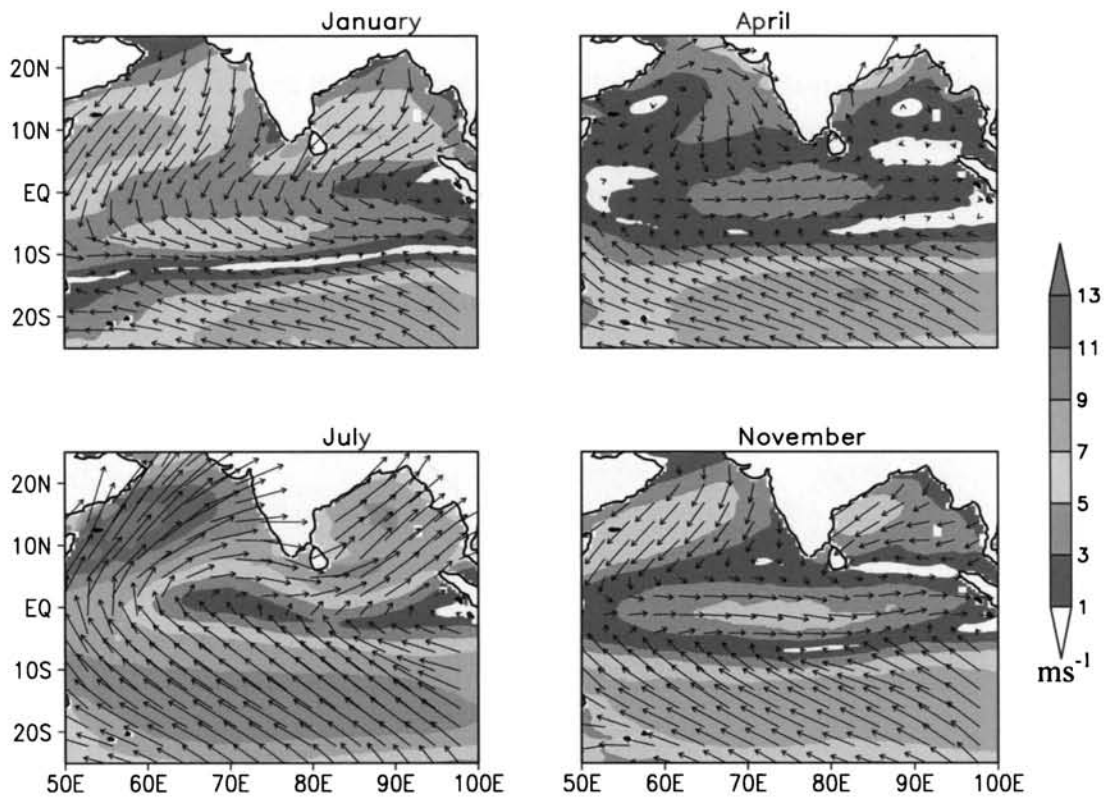


Fig.4.1 Averaged surface wind in ms^{-1} for the years from 1999 to 2003 during January, April, July and November representing different seasons.

4.4.2 Frictional velocity

Frictional velocity is the scaling parameter of wind speed (Stull, 1997). As described in the previous section, it can be evaluated from the wind stress available from QuikSCAT data set. Fig.4.2 gives frictional velocity (u_*) over the Arabian Sea

and Bay of Bengal during the four seasons. During winter, spatial variation of u_* is small both in the Arabian Sea and Bay of Bengal. The isolines of u_* are oriented with values increasing towards north with slightly high values in the Bay of Bengal. During pre-monsoon period, the value of u_* over Arabian Sea is around 0.15 ms^{-1} and that over Bay of Bengal is between 0.1 and 0.25 centered near the central Bay of Bengal region surrounded by contours of increasing values. The frictional velocity values are high during southwest monsoon season compared to all other seasons. The highest values (more than 0.55 ms^{-1}) are found near Somali coast in the Arabian Sea. In the Bay of Bengal, the highest value is more than 0.375 ms^{-1} in the central Bay. During the southwest monsoon season surface winds as well as the vertical wind shear are strong resulting high u_* . The horizontal variation of frictional velocity over both the Arabian Sea and Bay of Bengal is small during the post-monsoon season and the value is around 0.2 ms^{-1} . Maximum spatial variation of frictional velocity among the four seasons is during the southwest season in the south Arabian Sea, varying from 0.3 ms^{-1} to 0.5 ms^{-1} followed by the variation during the pre-monsoon season over the Bay of Bengal, varying from 0.1 ms^{-1} to 0.25 ms^{-1} .

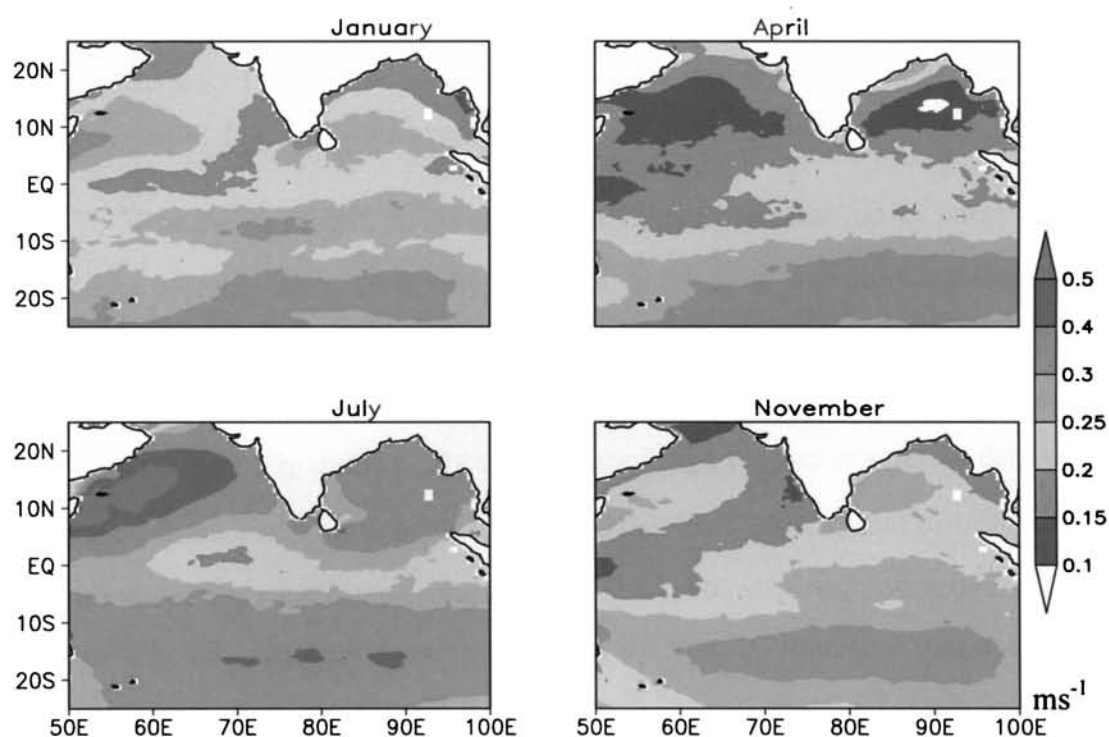


Fig.4.2 Averaged frictional velocity in ms^{-1} for the years from 1999 to 2003 during January, April, July and November representing different seasons.

4.4.3 Roughness parameter

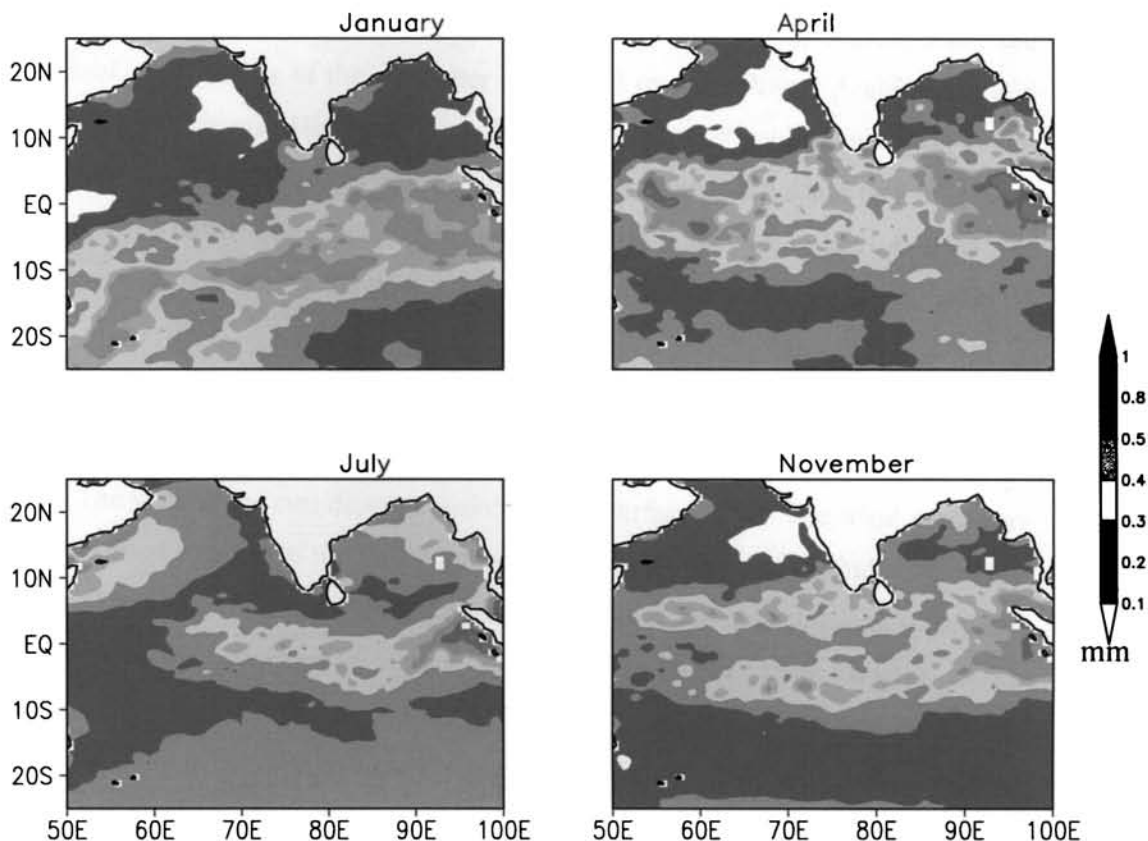


Fig.4.3 Averaged roughness parameter in mm for the years from 1999 to 2003 during January, April, July and November representing different seasons.

Roughness length, z_0 is the length from the surface up to which the wind velocity becomes zero. Generally, information on z_0 is derived using data observed in connection with field experiments over land or ocean. Since it is difficult to take such observations during all seasons over entire region, the characteristic features of z_0 are not properly studied. By the advent of high resolution satellite derived wind data, this parameter can be evaluated with reliability. Here, spatial distribution of z_0 is presented for winter, pre-monsoon, southwest monsoon and post monsoon seasons in the Fig.4.3. During winter, z_0 values vary from 0.2 mm to 1 mm and are more than 0.5 mm over the entire coastal belt except over the Sri Lankan region. The values are high (more than 1 mm) over the north AS and Somali coast. During the pre-monsoon season, the roughness length is more than 9 mm over the entire south Bay of Bengal and coastal regions of Somali due to feeble wind over these regions in

the transition period. During the southwest monsoon season, the values are extremely low (in range of 10^{-4} mm) both over Arabian Sea and Bay of Bengal due to the high wind speed associated with the monsoon. In the post-monsoon season, there are regions of small values of the parameter ($< 1 \times 10^{-4}$) over southwest Arabian Sea and central Bay of Bengal. High values are found over the west peninsular region (more than 1 mm), over the head Bay of Bengal (more than 9 mm) and south Bay of Bengal (more than 10 mm). The range of roughness length is maximum in both Arabian Sea and Bay of Bengal during the post monsoon season due to large spatial variation of wind.

4.4.4 Wind stress curl

The wind stress curl depends mainly on the surface wind. The wind stress curl is a measure of rotation of the force applied by the wind. The zonal wind stress in the equatorial region is westerly during pre-monsoon season and largest during spring and fall that drive the equatorial spring and fall jets in the Indian Ocean (Wyrski, 1973). The atlas by Hastenrath and Lamb (1979) gave a complete reference to the atmospheric fields over the equatorial region. The climatological wind stress and curl of the wind stress showed maximum amplitude off the coast of Somalia (Hellerman and Rosenstein, 1983). However, the curl changes its sign during northeast and southwest monsoon seasons. Here, we made an attempt to study the wind stress curl over different parts of the AS and BOB during the four seasons and influence of monsoon activity on wind stress curl. The mean distribution of wind stress curl is presented in Fig.4.4. Winter season is characterized by cyclonic stress (positive values) over the equatorial region (10°N to 10°S) with a maximum value of $1.5 \times 10^{-7} \text{ Nm}^{-3}$ but on either side of the equatorial belt anticyclonic stress is seen. Maximum value is found around $-1.5 \times 10^{-7} \text{ Nm}^{-3}$, but on the northern side, the value of negative stress is less ($-0.5 \times 10^{-7} \text{ Nm}^{-3}$). During pre-monsoon period the area and intensity of the cyclonic stress is decreased. Over the southern part, the anticyclonic stress increases and shifts towards north. During the southwest monsoon season, the cyclonic stress is extended to both AS and BOB, the value (more than $-3.5 \times 10^{-7} \text{ Nm}^{-3}$) of stress curl is more over the east central AS (near Somali coast). But near Sri Lanka, anticyclonic wind stress curl is noticed. During the post-monsoon season positive values are found over the equatorial region and negative values are seen on either side of the equatorial belt.

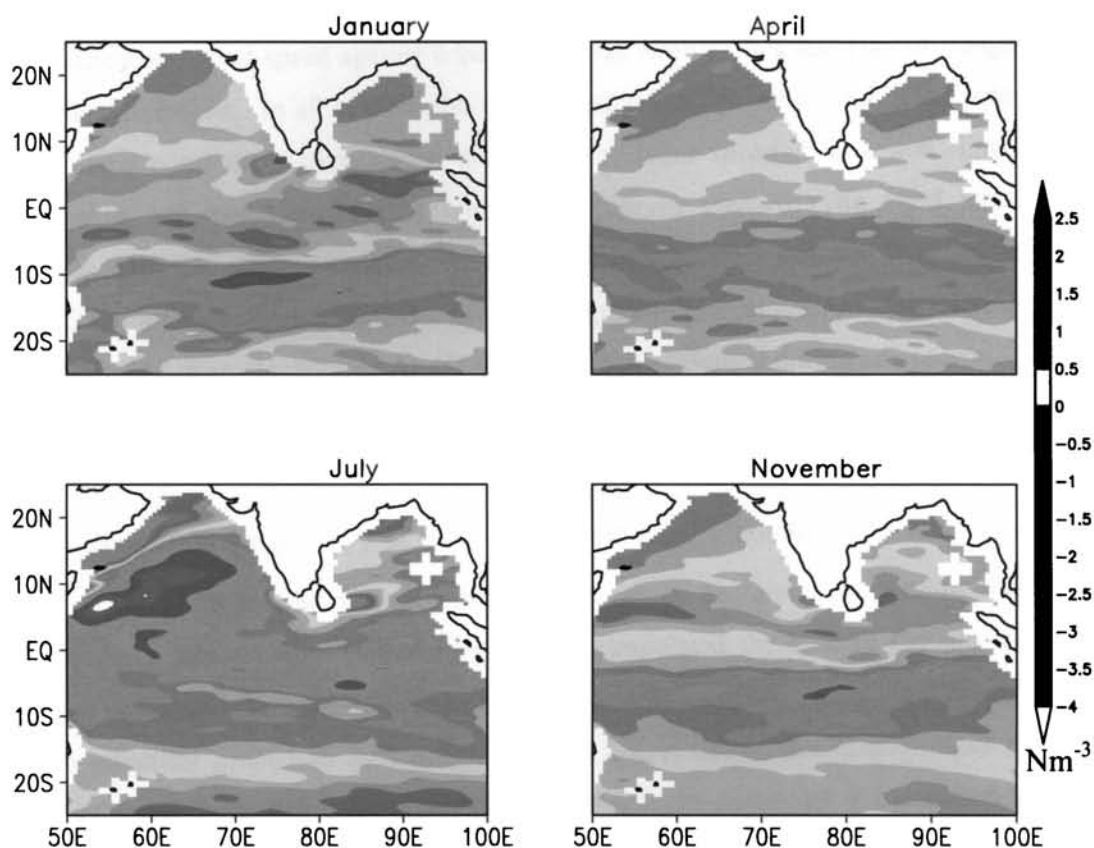


Fig.4.4 Averaged wind stress curl (Nm^{-3}) parameter for the years from 1999 to 2003 during January, April, July and November representing different seasons.

4.5 Dependence of wind with surface parameters

4.5.1 Momentum flux (wind stress)

The surface flux of momentum or wind stress influences all aspects of air-sea interactions. For example, it drives the growth of capillary and surface gravity waves, the development of the mixed layer and even the large-scale circulation of the oceans. An improved understanding of the wind stress vector is of interest to meteorologists, oceanographers, and climatologists alike (Dobson and Toulany, 1991). Wind stress is the pressure exerted on the surface of the ocean by wind and here it is expressed in the unit Pascal (Pa). The relation of surface wind speed at surface with wind stress, roughness length are studied over Arabian Sea and Bay of Bengal for January, April, July and November representing winter, pre-monsoon, southwest monsoon and post monsoon seasons respectively. The surface wind stress estimated by using bulk aerodynamic formulae stated in equation (4). The relation of the wind stress with surface wind over Arabian Sea (15°N - 20°N & 60°E - 70°E) and Bay of Bengal (15°N -

20°N & 85°E-90°E) shows a good relation in an exponential way. The Fig.4.5 and Fig.4.6 show the wind speed against wind stress over Arabian Sea and Bay of Bengal for different seasons. In all seasons the wind stress related to wind field in the same way. Since wind stress depends on the square of wind speed, it is a non-linear relationship. *viz*, the stress versus wind speed curves upward. The wind stress increases with the wind in an exponential way resulting the power law fit. On the basis of the interrelationship, one can obtain an equation to evaluate wind stress from the wind speed at any location in Arabian Sea and Bay of Bengal during any season.

4.5.2 Roughness parameter

Roughness length (z_0) of wind can be physically interpreted as the virtual origin of the wind profile. The roughness length can be calculated by plotting $\ln(z)$ against the measured wind at that height and extrapolated the best fit straight line down to the level where the winds are zero. Generally roughness length is estimated by the graphical procedure with different levels but in ocean, the measurement for different levels quite difficult. Therefore, the roughness parameter is calculated by using equation (4). Fig.4.7 defines the wind speed dependence of roughness length over Arabian Sea for different seasons. In all the season the dependence of z_0 is as defined by Charnock, (1955). The values of the roughness parameter in the figure have a multiplying factor of 10^{-3} . The z_0 increases as the wind speed decreases and after a critical value of z_0 the z_0 increase with wind speed. The critical value for Arabian Sea under the study region is 4.68 ms^{-1} and the value of z_0 is $0.06 \times 10^{-3} \text{ m}$. The average values of z_0 for winter, pre-monsoon, southwest monsoon and post monsoon seasons are 0.15×10^{-3} , 0.33×10^{-3} , 0.24×10^{-3} and 0.15×10^{-3} respectively for the corresponding wind speed are 6.39 ms^{-1} , 4.76 ms^{-1} , 11.04 ms^{-1} and 5.89 ms^{-1} .

In the case of Bay of Bengal also the Charnock's relation holds good, but it has many uncertainties and is clear from Fig.4.8. The wind speed is relatively low in the Bay of Bengal while comparing with the Arabian Sea. Generally the increase of z_0 with decrease of wind speed and increase of z_0 with increase of wind speed after the critical value of wind speed are noticed with many irregularities. The average values of z_0 for winter, pre-monsoon, southwest monsoon and post monsoon seasons

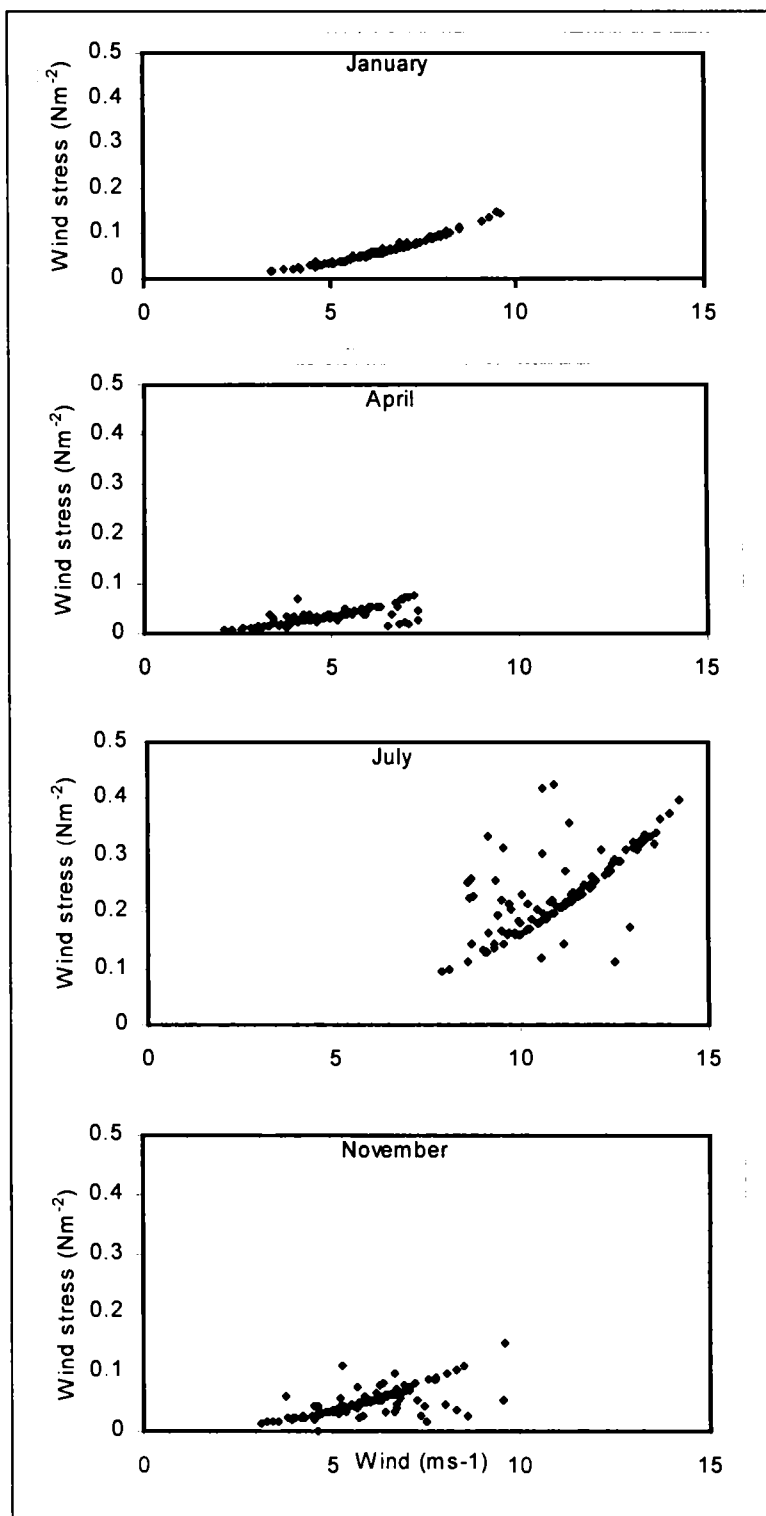


Fig.4.5 Relation of wind stress with wind speed for different seasons for Arabian Sea.

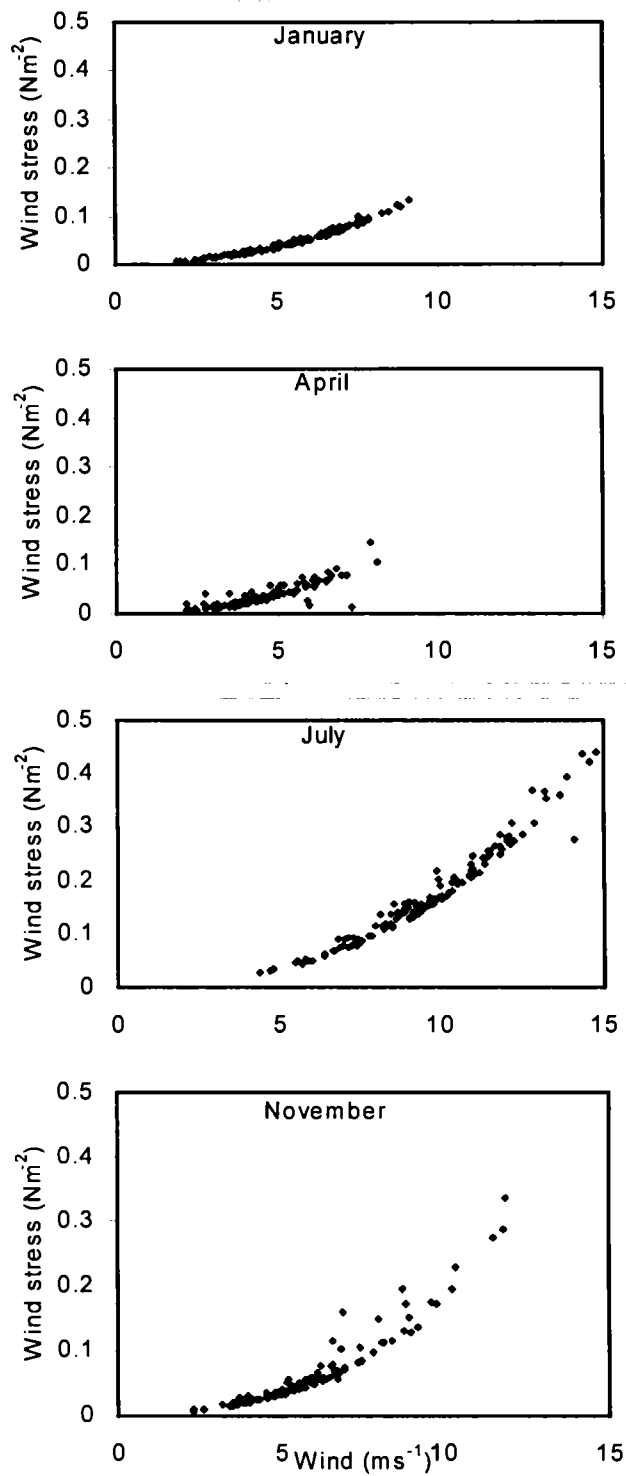


Fig.4.6 Relation of wind stress with wind speed for different seasons for Bay of Bengal.

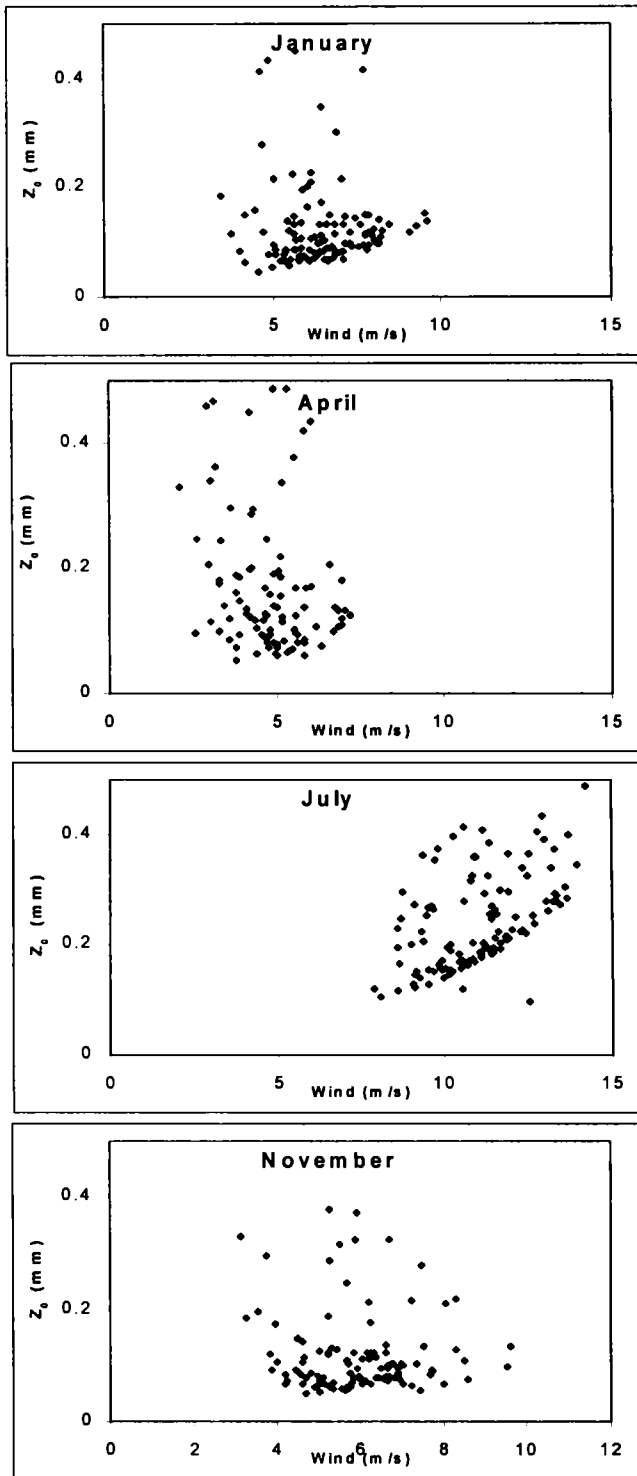


Fig.4.7 Relation of roughness parameter to wind speed during different seasons over Arabian

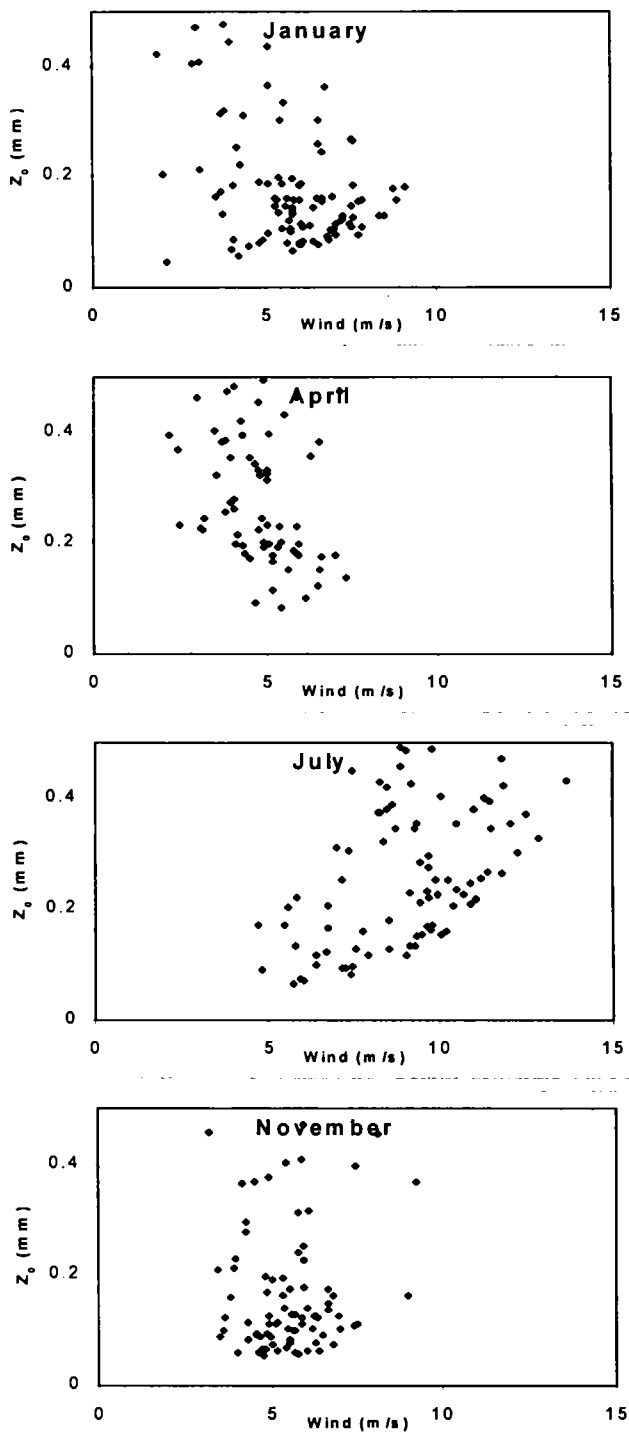


Fig. 4.8 Relation of roughness parameter to wind speed during different season over Bay of Bengal

are 0.51×10^{-3} m, 1.19×10^{-3} m, 0.80×10^{-3} m and 0.50×10^{-3} m respectively for the corresponding wind speed are 5.32 ms^{-1} , 4.6 ms^{-1} , 9.52 ms^{-1} and 5.90 ms^{-1} .

4.5.3 Frictional velocity

The frictional velocity u_* is one of the important scaling variables in the surface boundary layer or MABL (Monin and Obukhov, 1954) and is computed from wind stress and density of the air. The equation to evaluate u_* is given in (5). u_* is drawn against the surface wind for different seasons for Arabian Sea and Bay of Bengal (Fig.4.9 and fig.4.10). From the observation, we can delineate that u_* varies with wind in linear way. For both Arabian Sea and Bay of Bengal, u_* increases as the wind increases. For winter (January) and southwest monsoon (July) the variation can be represented properly by a linear fit, but for pre-monsoon and post monsoon u_* values very little randomly distributed to either side of the least square fit line. This uneven distribution of the u_* from the fit line may be due to the influence of wind direction because the April and November are months of transition in which reversal of wind direction from northeast to southwest and southwest to northeast take place respectively. So, during these periods the wind direction varies widely. This may influence the frictional velocity.

4.5.4 Wind against SST and Rainfall

An attempt is made to relate QuikSCAT wind and TMI SST over Arabian Sea and Bay of Bengal for southwest monsoon season is given in Fig.4.11. In both cases the SST shows a decreasing trend with wind speed. In Arabian Sea the slope of decrease is comparatively less than that of the Bay of Bengal. The linear equation of the decreasing trend is $U = -0.233xSST + 17.527$ where U is the wind speed and SST is the Sea Surface temperature. The relation in the Bay of Bengal is same but the decreasing trend is higher with respect to wind speed and the equation obtained is $U = -1.334xSST + 48.026$. The range of SST in Arabian Sea is from 26.81°C to 29.41°C with wind ranges from 7.89 ms⁻¹ to 14.24 ms⁻¹ during July representing southwest monsoon season and the range of SST in Bay of Bengal is from 27.72°C to 29.86°C with a wind range from 4.41 ms⁻¹ to 14.77 ms⁻¹, but the average value is high for Arabian Sea. Fig.4.11c and fig.4.11d show the dependence of precipitation (downloaded from the web site <ftp.ncep.noaa.gov>) with wind at surface and SST over

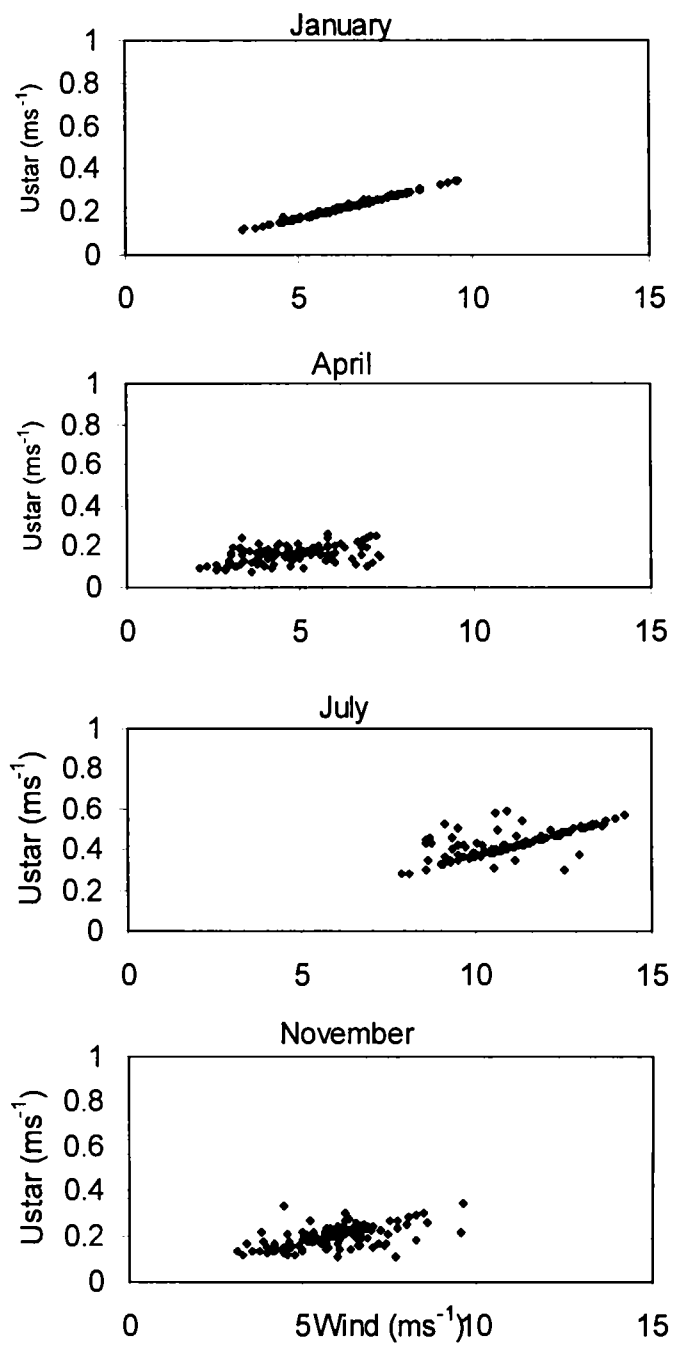


Fig.4.9 Relation of frictional velocity with wind speed during different seasons over Arabian Sea

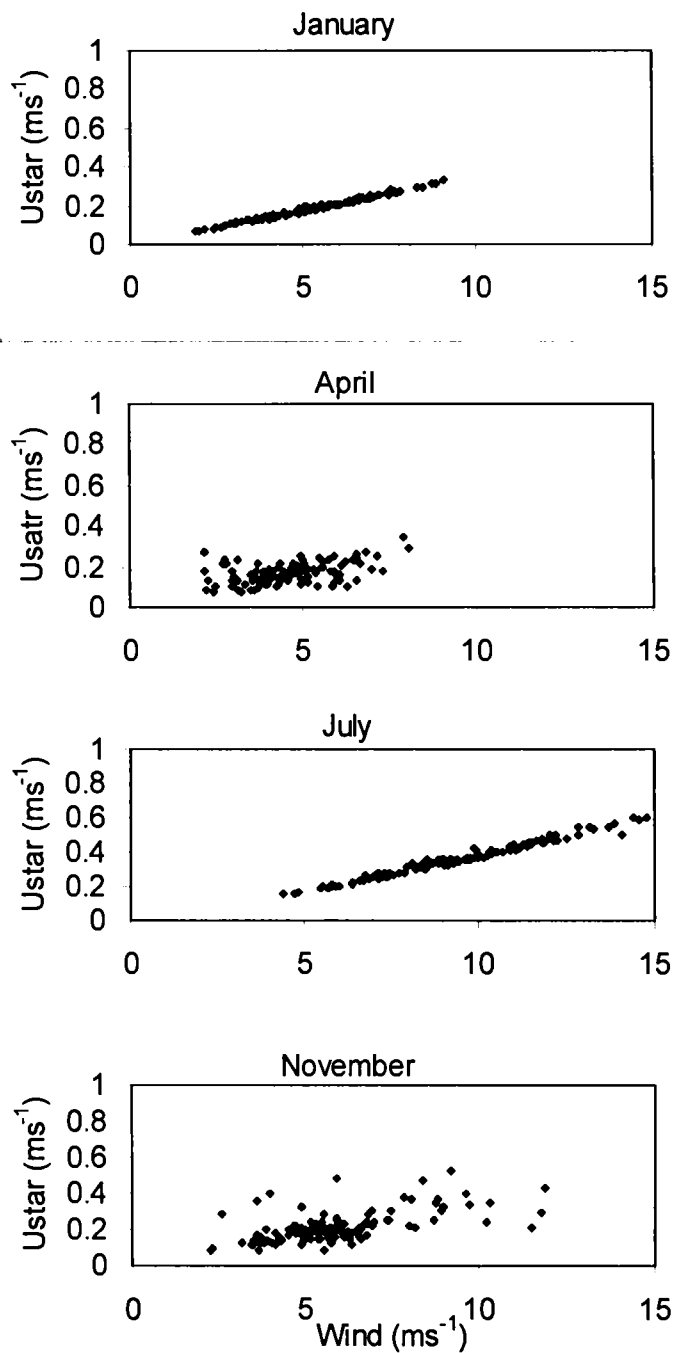


Fig.4.10 Relation of frictional velocity with wind speed during different seasons over Bay of Bengal.

Arabian Sea and Bay of Bengal. The relation of rainfall over Arabian Sea with temperature and wind is not encouraging. In the Bay of Bengal for July (aggregate of July from 2000 to 2003) the rainfall against wind and temperature shows linear fit and the corresponding equations are given in respective figures. The rainfall increases in

G9001

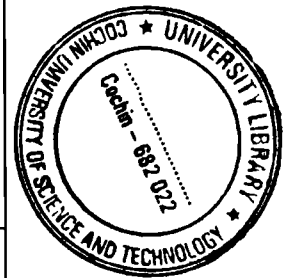
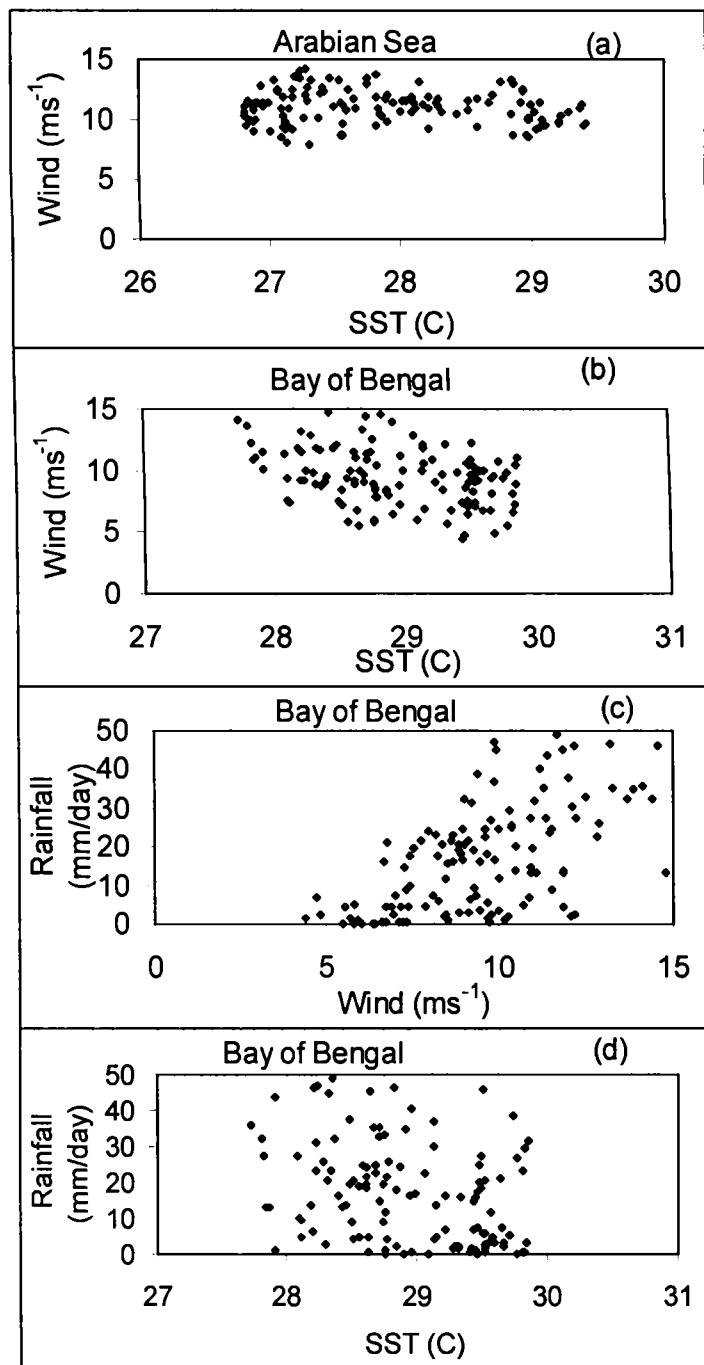


Fig.4.11 Depending relations of sea surface parameters over Arabian Sea and Bay of Bengal.

trend with wind i.e., as the wind increases rainfall increases indicating organized convection. Due to the convergence of wind organized cloud band formed (Joseph and Sijkumar, 2004) and this cloud band feeds moisture by the LLJ to enhance the rainfall activity. As in the case of SST (Fig.4.11d) the rainfall shows a decrease in

trend with increase of SST. The sea surface cools with the rainfall. The SST shows a decreasing linear trend with rainfall.

4.5.5 Drag coefficient

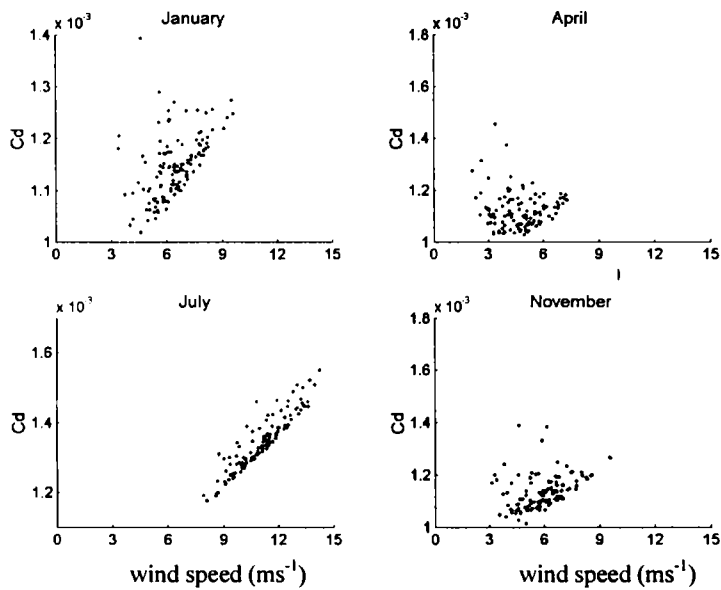


Fig.4.12 Relation of drag coefficient with wind for different season over Arabian Sea.

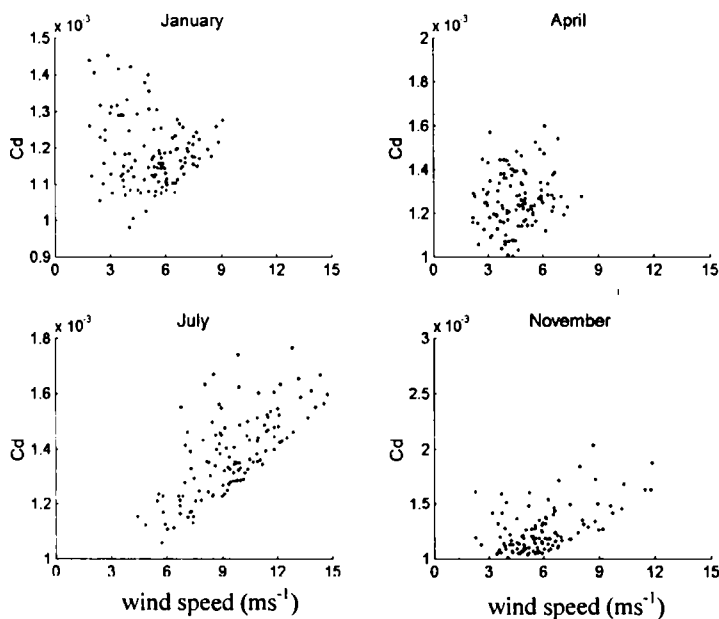


Fig.4.13 Relation of drag coefficient with wind for different season over Bay of Bengal.

The variation of drag coefficient is also drawn for different years for both Arabian Sea and Bay of Bengal. Fig.4.12 and Fig.4.13 shows the variation of drag coefficient in Arabian Sea over the considered region. The Bay of Bengal shows the

same trend as that of the Arabian Sea. From the figure it is clear that the drag coefficient varies with wind speed not in a linear way, it tends to increase from a critical value wind speed 4 ms^{-1} .

4.6 Temporal variation of frictional velocity and drag coefficient

4.6.1 Frictional velocity over Arabian Sea and Bay of Bengal

Frictional velocity (u_*) is very important parameter as the scaling parameter of the velocity, information of values of u_* is important in various atmospheric boundary layer studies. To examine the general variation of u_* in different season, time series graph of frictional velocity is plotted for the entire year from 1st January to 31st December (averaged for 1st Jan, 2nd Jan and so on up to 31st Dec for 2000 to 2003) for both Arabian Sea and Bay of Bengal. The 5 day moving average values of the frictional velocity is represented in Fig.4.14 in which solid line indicates the values for Arabian Sea and dotted line indicates that for the Bay of Bengal. It is observed that the values of u_* in both Arabian Sea and Bay of Bengal are found to be around 0.18 ms^{-1} (for Arabian Sea the value is 0.19 ms^{-1} and for Bay of Bengal, 0.17 ms^{-1}) from January to end of May. During monsoon period the value of u_* is increased and it remains almost constant with a little fluctuation around 0.35 ms^{-1} in Arabian Sea and around 0.33 ms^{-1} in Bay of Bengal. After the monsoon season the u_* comes back to its pre-monsoon value. During monsoon season the value of u_* in both Arabian Sea and Bay of Bengal are different. The increased u_* during southwest monsoon season is due to the monsoon surge associated with low level Jetstream and associated modulation in the surface wind. During monsoon period the u_* exhibits variability similar to intra seasonal oscillation (ISO) found over Indian monsoon region (Sikka and Gadgil, 1980). This pattern of u_* is maintained till the end of the monsoon period. The variability of u_* is attributed to the active and weak cycles in the Indian monsoon. The activity of these epochs, especially in the wind pattern is greater in the Bay of Bengal than that in the Arabian Sea so that the variability in u_* is also high in the Bay of Bengal. As monsoon is recedes, the values return to the earlier status. The situation is same over the Arabian Sea and Bay of Bengal.

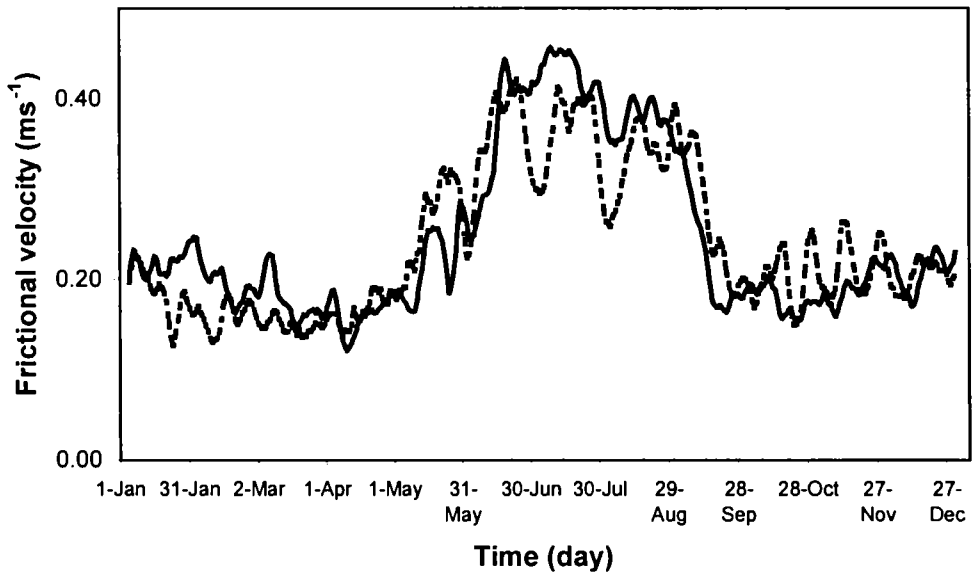


Fig.4.14 Day to day variation of frictional for Arabian Sea (solid line) and for Bay of Bengal (dotted line) averaged of four years from 2000 to 2003.

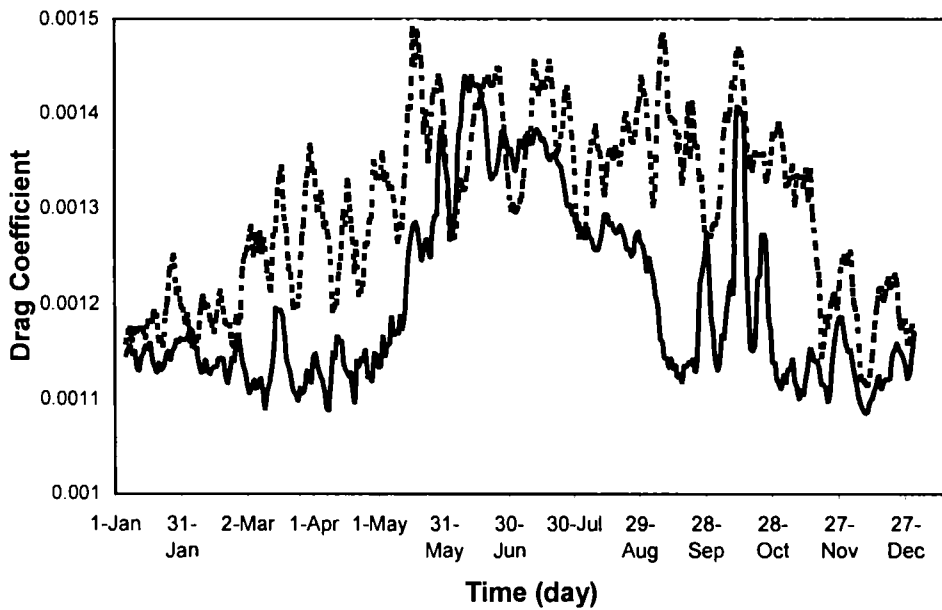


Fig.4.15 Day to day variation of drag coefficient for Arabian Sea (solid line) and for Bay of Bengal (dotted line) averaged of four years from 2000 to 2003.

4.6.2 Drag Coefficient over Arabian Sea and Bay of Bengal

The features of drag coefficient over the area in Arabian Sea and Bay of Bengal are studied using the 5-day moving average values are presented in Fig.4.15. It is found that the values of C_d in both the Seas are found to be different and the higher values found over the Bay of Bengal during the entire period. The general pattern varies with season. Over the Arabian Sea, the value is almost constant (1.14×10^{-3}) during the period from November to May. During southwest monsoon period values of C_d are more compared to other seasons. From first week of May, the value increases and reaches a maximum by June first week (1.42×10^{-3}) and decreases thereafter. The slope of increase is much more than that of the decrease in the Arabian Sea. Generally the values C_d in the Bay of Bengal are higher than that of the Arabian Sea in all the periods. The C_d over Bay of Bengal starts to increase from 1st week of March and reaches maximum during the monsoon season (1.35×10^{-3}). The variability in C_d over the Bay of Bengal is more than that over the Arabian Sea especially in the monsoon season. The variability in C_d is found throughout the year in the Bay of Bengal, but it is very small in the Arabian Sea except in the post monsoon season. The values of C_d are found to decrease after withdrawal of monsoon, in middle of November.

4.7 Intraseasonal variations in frictional velocity and drag coefficient

Intraseasonal oscillation (ISO) is one of the major oscillations in the equatorial region as a northward/northeastward propagating surge during the southwest monsoon (Yasunari, 1979, 1981; Sikka and Gadgil, 1980; Krishnamurthy and Subramanyam, 1982). This ISO has two major components and they are 30-60 day and 10–20 day mode can be seen in spectral analysis of precipitation, convection and in many circulation parameters (Chen and Chen, 1993; Numaguti, 1995; Kiladis and Wheeler, 1995).

Using wavelet technique suggested by Torrence and Compo (1998), we unraveled the different time frequency domains, which embedded in the marine boundary layer parameters such as frictional velocity and drag coefficient. Fig.4.16

represents the wavelet analysis of the frictional velocity in Arabian Sea and Bay of Bengal. The daily frictional velocity values from 1 January 2000 to 31st December 2003 were used for the analysis. From the figure it is evident that the variability of frictional velocity is different in both the Arabian Sea and Bay of Bengal. In the Arabian Sea the variability around 60 day is prominent with 95% confidence level. This oscillation is found to vary with a periodicity of 35-64 day but in the Bay of Bengal the periodicity is from 25 day to 65 day.

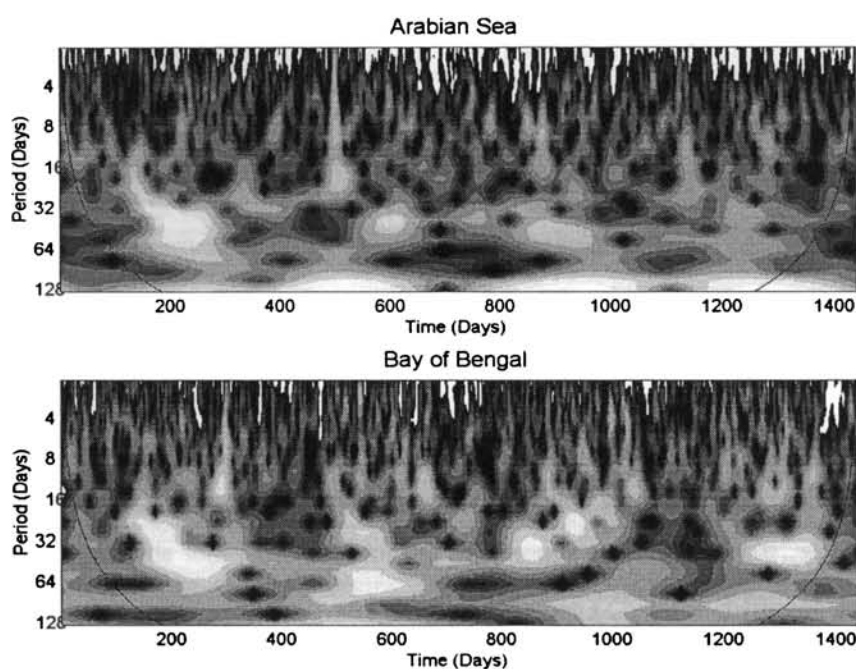


Fig.4.16 Wavelet analysis of frictional velocity over Arabian Sea and Bay of Bengal

The confidence level varies from year to year. The variability under 10-20 day mode is also exists, but this variation is found in all the seasons with 99% confidence. Fig.4.17 shows wavelet analysis for drag coefficient. The variability of drag coefficient is different for Arabian Sea and Bay of Bengal as that of the frictional velocity. The variability with 40-55 day mode in the Bay of Bengal is seen in all the years during monsoon months with 95% confidence level. But in the Arabian Sea it is evident only during the monsoon months of the years 2000 and 2002. During 2001 and 2003, it is difficult to understand the prominent mode of oscillations. The 10-20 day mode (QBM) is also significant in the Bay of Bengal in all the period irrespective of the monsoon months.

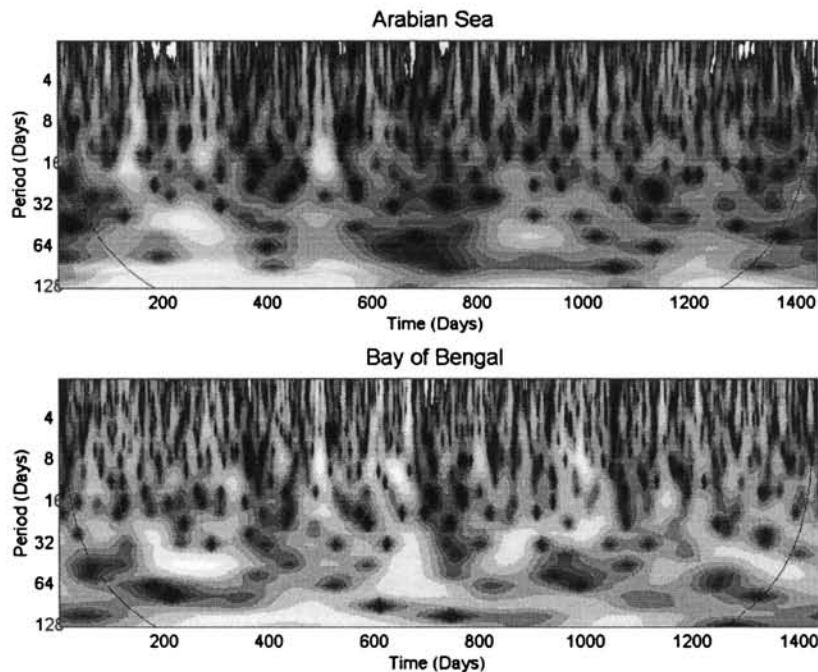


Fig.4.17 Wavelet analysis of Drag Coefficient over Arabian Sea and Bay of Bengal

Dynamic characteristics of the marine atmospheric boundary layer (MABL) using high resolution satellite derived QuikSCAT data set with a spatial resolution of 0.25×0.25 latitude longitude grid for the parameters surface wind, frictional velocity (u_*), roughness parameter (z_0) and drag coefficient (C_D) for different seasons are studied. Surface wind pattern shows more strength during the southwest monsoon season due to modulation by the Low Level Jetstream. C_D is more during southwest monsoon season due to the strong wind and less during winter. The spatial variation of u_* over the seas is small during the post-monsoon season (0.2 ms^{-1}) and maximum is during southwest season followed by the pre-monsoon season over the Bay of Bengal. The mean characteristic features of the wind stress curl during winter season is positive over the equatorial region with a maximum value of $1.5 \times 10^{-7} \text{ Nm}^{-3}$ but on either side of the equatorial belt anticyclonic wind stress is dominated. The interrelationship between u_* and surface wind speed in both Arabian Sea and Bay of Bengal are found to be exponential. From a critical value of wind (around 4 ms^{-1}), C_D increases to either side. The variabilities of the frictional velocity and drag coefficient are also examined over Arabian Sea and Bay of Bengal using the wavelet technique and found that the variabilities in 30 to 60 day mode are prominent over the entire period over the Bay of Bengal.

CHAPTER – 5

***INLAND BOUNDARY LAYER
CHARACTERISTICS OVER A TROPICAL
STATION USING UHF RADAR***

CHAPTER - 5

INLAND BOUNDARY LAYER CHARACTERISTICS OVER A TROPICAL STATION USING UHF RADAR

5.1 Introduction

The local features of the atmosphere mainly control the Atmospheric Boundary Layer (ABL) characteristics over an inland station. A knowledge of the ABL characteristics is important as it plays a vital role in various atmospheric processes such as convection triggering, turbulent transport (e.g., latent heat, pollutants, momentum etc.) and the development of Low Level Jetstream (LLJ) during monsoon periods. Understanding the turbulence and other boundary layer parameters is necessary for several applications in numerical weather prediction, chemical modeling and also the dynamics of the lower atmosphere. Turbulent dissipation and diffusion are the processes through which transport of heat energy, momentum and mass take place in the atmosphere close to the surface of the earth and it can affect the energy budget. Turbulence also influences the diffusion of pollutants from near earth surface to higher heights (Ramana, *et al*, 2004; Praveena and Kunhikrishnan, 2004). So, the knowledge of turbulence parameters is essential for understanding of the dynamics of ABL . One of the important features of the ABL is its diurnal variation since it controls the transport process of the ABL parameters.

5.1.1 ABL structure during clear sky day

The ABL structure during clear air conditions over land can be classified as daytime Convective Boundary Layer (CBL) and is also called Mixed Layer (ML), Nocturnal Boundary Layer (NBL) and Residual Layer (RL). The CBL exists from sunrise to sunset and boundary layer reaches its maximum depth around afternoon hours. Since convection is dominant mechanism, there is usually wind shear across the top of the CBL that contributes to the turbulence generation. The tropical regions export momentum to extra-tropical regions through the turbulent activities of the CBL. The tropical regions warm up continuously due to combined effect of insolation and heat exchange at earth-air interface. Diurnal variation of meteorological parameters in the tropical ABL is much stronger than in the extra-tropical ABL particularly over land, causing significant diurnal oscillations in wind

speed and convective activity. The properties of the tropical ABL are substantially different from the conditions of the subtropical ABL. Tropical regions are characterized as the hottest region of the globe and form large fields of convective clouds of all sizes. Strong solar fluxes, land-sea contrasts and Hadley cell circulation causes tropical ABL region more dynamic and due to this reason, the tropical convective clouds have unique characteristics such as maximum vertical extent and diurnal and seasonal variations.

5.1.2 Wind structure in the ABL during southwest monsoon

Wind plays a vital role in atmospheric transports of heat, mass, moisture and pollutants from one place to another. These transport processes play an important role in changing local weather. The winds and their variability in ABL are important in various fields like meteorology, atmospheric physics, environmental protection, agriculture, wind energy utilization, and air traffic control etc. Accordingly, the characterization of wind and its variability are extremely important and hence detailed observations of winds are necessary with high temporal and spatial resolution.

One of the important features that occur regularly in an irregular way over the Indian peninsula is the presence of the southwest monsoon with a strong southwesterly wind in the lower layers of the troposphere. The core of this strong southwesterly wind is around 850 hPa and this strong low level wind called low level jet stream (LLJ) (Joseph and Raman, 1966; Findlater, 1966, 1967; Desai *et al.*, 1976), carries ample of moisture from South Indian Ocean and Arabian Sea sufficient to precipitate over continental areas, as they account for the majority of the annual total rainfall. Monsoon is a synoptic phenomenon and strongly coupled with warm oceans around, which needs proper exploration for predicting the variability of the Indian monsoon rainfall, the LLJ is one of the factors and needs a full understanding on the basis diurnally, daily and monthly.

5.2 Lower Atmospheric Wind Profiler (LAWP)

The lower atmospheric wind profiler (LAWP) is an L-band Ultra High Frequency (UHF) wind profiler was installed at Gadanki (13.5°N, 79.2°E), Andhra Pradesh, India. The location map of the LAWP is given in Fig.5.1. The LAWP was established over Gadanki in collaboration with the Ministry of Posts and

Telecommunications/Communication Laboratory, Japan for investigating ABL dynamics and precipitation cloud systems. The LAWP is coherent, phased array, Doppler radar operating at 1357.5 MHz with a peak power aperture product of 10^4 Wm^2 (Reddy *et al.*, 2001) capable of providing continuous high-resolution wind measurements in the first few kilometres of the atmosphere. Fig.5.2 shows the antenna and transmitter assembly unit of the LAWP.

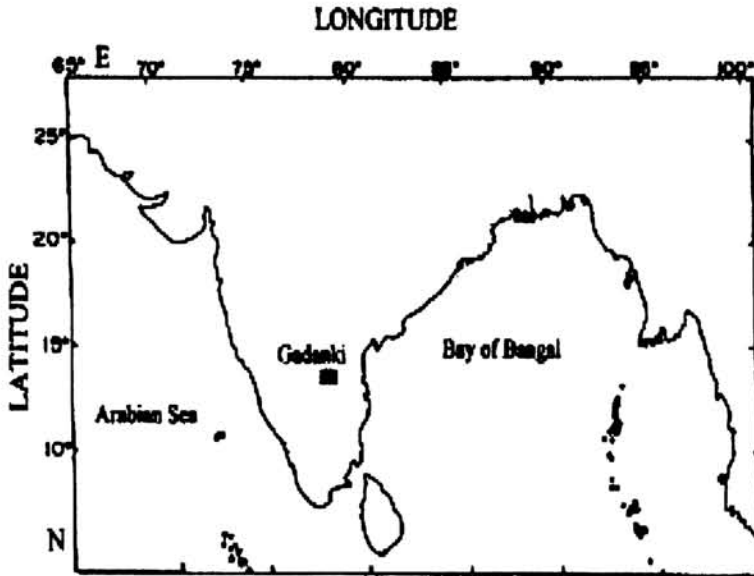


Fig.5.1 The location of the LAWP (Gadanki) with map of India

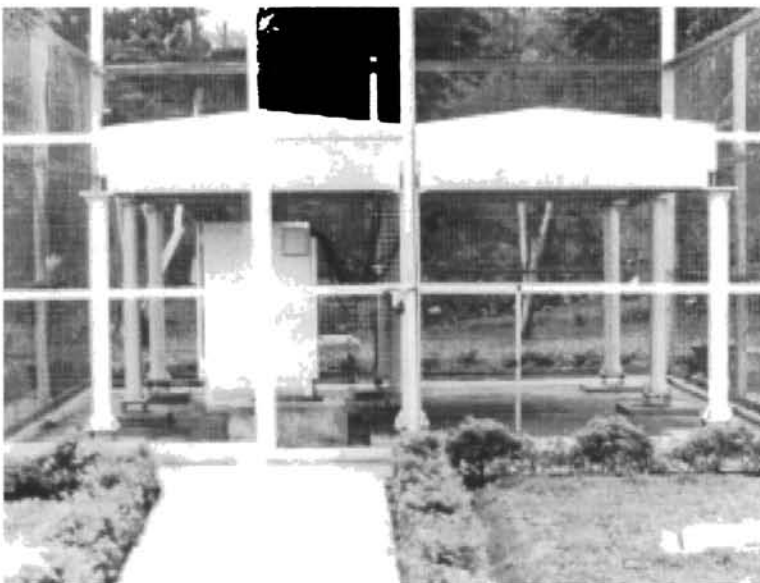


Fig.5.2 Antenna and transmitter assembly unit of the LAWP

However, the development of wind profilers has revolutionized the boundary layer studies with their excellent height and temporal resolutions (Gage and Balsley 1978; Balsley and Gage, 1982). The UHF wind profilers are better suited for boundary layer observations (Ecklund *et al.*, 1988; Rogers *et al.*, 1993a; Gage *et al.*, 1994; Gossard *et al.*, 1998). One such, UHF radar, known as Lower Atmospheric Wind Profiler (LAWP), is located at Gadanki to carry out studies on atmospheric boundary layer.

5.2.1 Technical details

The phased antenna array consists of 576 circular microstrip patch antenna elements arranged in a 24 x 24 matrix over an area of 3.8 m x 3.8 m. The LAWP technical and processing details are given in Table No.1. The total array is organized into four quadrants. A total peak power of 1000 W is delivered to the antenna array by a parallel array of four outputs from Power Amplifier (PA), each feeding 250 W to one quadrant (12 x 12 elements) of the array. The Transmitter (Tx) unit, preceded by PA, generates an output power of 175 W, which is sufficient to drive the PA. The PA generates the required final output power by a division-amplification-combining technique. The output power is fed via the beam changer switch and hybrid circulator. The power distribution across the array is tapered to obtain better side lobe suppression. The array produces a pattern having a beam width of 4° and directive gain of 33 dB. However, due to the ohmic loss of 4 dB, the effective gain of the array is only 29 dB. The beam can be tilted by 15° (fixed) towards north and east (two principal planes) from the zenith by electrical steering, that is by injecting a progressive phase difference between the successive elements. Phase shifters are used to steer the beam in the north plane. For the east beam, required phases are injected through the appropriate lengths of the feeder lines. The same antenna array is used for all the three beams.

The echo signal received by the antenna array from the atmosphere is delivered to the receiver via circulators. The receiver is a phase coherent heterodyne type having a quadrature detector at the final output and delivers the video outputs to the signal processor. The receiver has an overall gain of 50-120 dB depending upon the gain setting of automatic gain controller amplifier (AGC). The dynamic range of the receiver is about 66 dB. The quadrature (I & Q) outputs of the receiver are limited

to a peak-to-peak voltage of 10 volts and given to the Signal Processor Unit (SPU). The SPU consists of an Analog to Digital Converter (ADC) and a coherent accumulator.

5.2.1.1.1.1 PARAMETER SPECIFICATIONS (LAWP)	
Location	Gadanki (13.5°N, 79.2°E)
Antenna (Phased Array)	3.8m X 3.8m
Operating Frequency (f)	1357.5 MHz
Radar wave length (λ_R)	0.22 m
Transmitted peak power (P_t)	1000 Watts
Effective aperture (A_e)	10 m ²
Beam width	4°
No. of beams*	3(E15, Zenith and N15)
Gain (G)	33 dB
Receiver band width (B_N)	1.58 x 10 ⁶
Receiver path loss α_r)	4 dB
Transmitter path loss α_t)	0.5 dB
Cosmic temperature (T_c)	10 K
Receiver temperature (T_r)	107 K
Maximum duty ratio	5%
Pulse width	1 – 2 μ sec
Inter Pulse Period (IPP)	programmable
Range resolution (Δr)	150/300 m
Coherent Integration (N_C)	100
No. of FFT points	64 – 1024 (programmable)
<i>Observational window:</i>	
Lowest range bin (km)	0.3
Highest range bin (km)	9.25
Incoherent integration	100
Beam Dwell time (sec.)	93

* The number after letter E and N is in degrees indicates the oblique angle from zenith.

Table. 5.1 System specification for LAWP unit

The ADC has 12-bit resolution and samples the analog input at the interval set at the Data Processing Unit (DPU). The SPU performs the coherent accumulation on the ADC output data. The constituted coherent data is then transferred to the DPU for further processing. The DPU performs Fast Fourier Transform (FFT) on the received coherent data. The on-line computer displays the frequency spectra (North, East and Zenith beams), signal strength, wind speed and direction. The data is further processed to compute moments before being transferred to the off-line computer via Ethernet for archival. Finally the data of incoherent, spectral moments and velocity field is archived on magneto-optical disks and eventually transferred to compact disks (CD-ROM). The LAWP spectral data is processed on-line. It can also be processed in off-line. The on-line data processing algorithm makes use of single peak detection for producing the moments and three-wind vector (u , v and w) by simply picking the strongest peak outside the clutter bounds. Quality control procedures are used to obtain the hourly horizontal winds. This data processing method works well for most of the time, however, there are the occasions when there are unrealistic wind data or when the consensus averaging method fails.

5.3 General geographical and meteorological conditions

The experimental site, LAWP is located at the National MST Radar Facility (NMRF), now it is renamed as National Atmospheric Research Laboratory (NARL), Gadanki (13.5°N , 79.2°E), about 370 m above the mean sea level. The terrain around Gadanki is complex, with many hills (average height of hills is about 750 m) within 10 km radius and a mixture of agricultural and population centers, the topography of this site can also influence the ABL features and it is about 120 km to North-West of Chennai on the east coast of Indian peninsula. Three-dimensional view of the main topography around Gadanki is shown in Fig.5.3.

According to India Meteorological Department (IMD), the onset of the southwest monsoon occurs at Gadanki around one week after the onset over Kerala. India experiences two monsoons namely southwest and northeast monsoons.

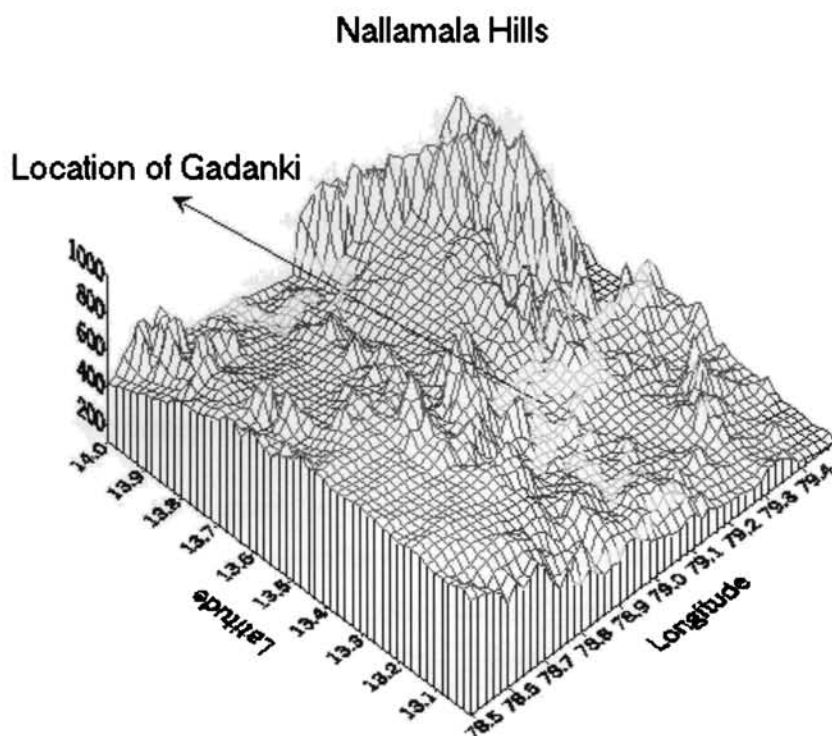


Fig. 5.3 Three dimension picture of Nallmala Hills over which Gadanki is located

They account for the majority of the annual rainfall. The two monsoons are different in the sense that in summer, warm equatorial maritime air predominates over a major portion of the country. In winter, the air masses recede south and are replaced by cool tropical continental air. The normal mean surface day temperatures over Gadanki during January, April, July, and October are around 23°C, 30°C, 30°C, and 28°C, respectively.

5.4 Scope of the study

The ABL over the tropical regions are more complex due to the intense convective activity associated with tropical convergence zone called ITCZ. This region is regarded as the source region for several weather activities. The ABL structure changes spatially and temporally and hence knowledge of the variation on different time scales is most essential. A knowledge of ABL in different seasons, which are characteristics of the Indian sub-continent, is still lacking, especially in the southwest monsoon season. In the above perception, an investigation of ABL is carried out using high resolution data obtained from the LAWP during the southwest

monsoon period. The data has a better quality in height and time to bring out the research results. The LAWP is an L-band UHF radar to observe the atmospheric boundary layer continuously and this high-resolution radar is first of its kind in India. The key objective of the present study is to understand the diurnal evolution of the ABL during monsoon season and variation of LLJ since this feature is important during monsoon. The other characteristics and dynamical processes associated with boundary layer during the southwest monsoon such as variation of the vertical wind shear, ABL height using the signal to noise ratio method etc. are also studied.

5.5 Data processing

The schematic diagram for processing LAWP data is given in Fig.5.4 and the details of the processing are given herewith. Usually the data is processed using the software called ADP (Atmospheric Data Processor) and the details of the ADP are given in Anandan *et al* (1996; 2004). The complex time series of the samples are subjected to the process of FFT for on-line computation of the Doppler power spectrum for each range bin of the selected range window. The Doppler spectra are recorded and transferred for off-line processing. The ADP involves the following steps : the dc contribution, which arises either from non- fading clutter or un-cancelled dc system biases or both, is eliminated by replacing the spectral point at zero frequency value with the average of two adjacent points (3 point dc removal) or with the four adjacent points (5 points dc removal). The data sets are further edited to remove interference band, if any, which might run through the entire range window and are subtracted out by estimating them in a range bin where they dominate the real signal. The spectrum contains background noise and it needs to be removed as a first step to compute the moments. The average noise value for each range bin is estimated by following the objective method of Hildebrand and Sekhon (1974). The mean noise level thus calculated is subtracted from all the range bins of the spectral frame. For each range bin, the signal peak is identified using ADP. The spectral window is determined by noting all the contiguous points that are above dc level. The three low order moments (0^{th} , 1^{st} and 2^{nd}) are computed using numerical integration by using the expressions adopted by Woodman (1985).

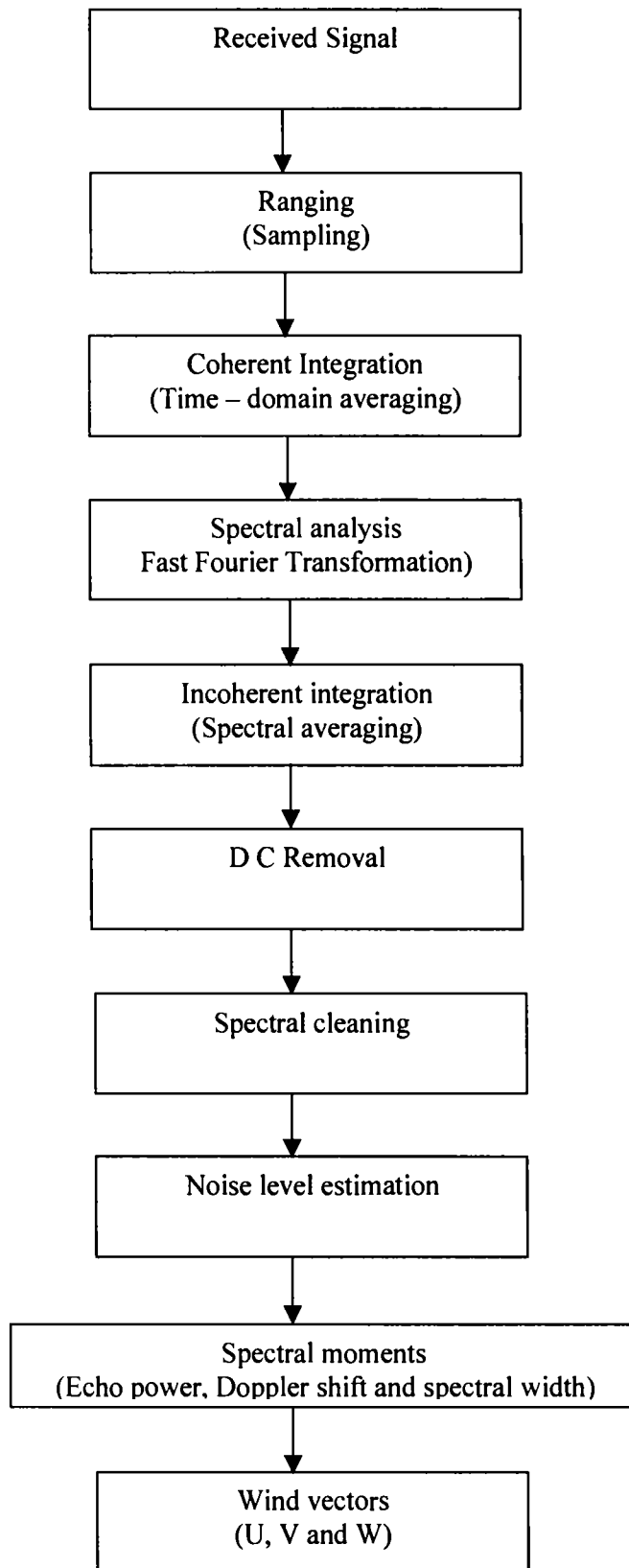


Fig. 5.4 Schematic diagram for data processing in LAWP

5.6 Computation procedures

5.6.1 Moments

The 0th moment represents the total signal power in the Doppler spectrum or total signal strength.

$$M_0 = \sum_{i=m}^n \bar{P}_i \quad (5.1)$$

The 1st moment represents the weighted mean Doppler shift.

$$M_1 = \frac{1}{M_0} \sum_{i=m}^n \bar{P}_i f_i \quad \text{where } f_i = \frac{(i - N/2)}{(IPP * n * N)} \quad (5.2)$$

The 2nd moment represents the variance, a measure of dispersion from central frequency.

$$M_2 = \frac{1}{M_0} \sum_{i=m}^n \bar{P}_i (f_i - M_1)^2 \quad (5.3)$$

where IPP is the inter pulse period, m and n are the lower and upper limits of the Doppler bin of the spectral window and \bar{P}_i and f_i are the power and frequency corresponding to the Doppler bin within the spectral window.

5.6.2 Signal to noise ratio (SNR)

Signal to noise ratio (SNR) can be calculated as,

$$SNR = 10 \log \left[\frac{M_0}{N * L} \right] \quad (5.4)$$

where N and L are the total number of Doppler bins and average noise level respectively. The product N and L give the total noise power over the whole signal spectral window.

5.6.3 Height and wind components

For representing the observation in physical parameters, the Doppler frequency and range bin have to be expressed in terms of corresponding radial velocity and height

$$\text{Height} \quad H = \frac{(c * t_R * \cos \theta)}{2} \quad (5.5)$$

$$\text{Velocity } V = \frac{(c * f_D)}{(2 * f_C)} \text{ in ms}^{-1} \quad (5.6)$$

where c is the velocity of light in free space ($2.98 \times 10^8 \text{ ms}^{-1}$), f_D is Doppler frequency in Hz and f_C is the carrier frequency and t_R is time delay of the pulse return.

After computing the radial velocity for different beam positions, the absolute velocity (u , v and w) can be calculated. To compute u , v , and w at least three non-coplanar beam radial velocity data are required. If higher number of different beam data is available, then the computation will give an optimum result in the least square method. Then the light of sight component of wind vector V (V_x, V_y, V_z) is

$$V_{Di} = V \cdot i = V_x \cos \theta_x + V_y \cos \theta_y + V_z \cos \theta_z \quad (5.7)$$

where i is the unit vector along the radar beam and X , Y and Z directions are aligned to East-West, North-South and Zenith respectively. Applying least square method (Sato, 1989)

$$\varepsilon^2 = (V_x \cos \theta_x + V_y \cos \theta_y + V_z \cos \theta_z - V_{Di})^2 \quad (5.8)$$

where $V_{Di} = f_{Di} * \lambda/2$. To satisfy the minimum residual $\partial \varepsilon / \partial V_k = 0$ where k corresponds to X , Y and Z .

$$\begin{bmatrix} V_x \\ V_y \\ V_z \end{bmatrix} = \begin{bmatrix} \sum_i \cos^2 \theta_{xi} & \sum_i \cos \theta_{xi} \cos \theta_{yi} & \sum_i \cos \theta_{xi} \cos \theta_{zi} \\ \sum_i \cos \theta_{xi} \cos \theta_{yi} & \sum_i \cos^2 \theta_{yi} & \sum_i \cos \theta_{yi} \cos \theta_{zi} \\ \sum_i \cos \theta_{xi} \cos \theta_{zi} & \sum_i \cos \theta_{yi} \cos \theta_{zi} & \sum_i \cos^2 \theta_{zi} \end{bmatrix} * \begin{bmatrix} V_{Di} \cos \theta_{xi} \\ V_{Di} \cos \theta_{yi} \\ V_{Di} \cos \theta_{zi} \end{bmatrix} \quad (5.9)$$

Thus on solving this equation we can derive V_x , V_y and V_z which corresponds to u , v and w components of velocity.

5.7 Diurnal variations

The data taken from the LAWP during non rainy days of the southwest monsoon is a good quality data set. The measured wind values were found to be in general agreement with those of the measured values of radiosonde and MST radar (Mesosphere, Stratosphere, Troposphere) during the period of 26th and 29th July 1999 (Praveena, *et al* 2003) and LAWP and MST were compared by Reddy *et al*,

2001. A typical example of simultaneous measurements of wind speed with LAWP, MST radar and radiosonde observations are given in Fig.5.5. The present study is based on the above data during the southwest monsoon period. We considered all non rainy days of the months of May, June, July, August and September for the years 1999 and 2000. The non rainy days in the above years during the months are given Table 5.2 and the days are collected from NARL. We generalise the characteristics of the ABL dynamics by considering a few days from each month of the year 1999 during southwest monsoon period. The representative days selected for the study are 6th May, 23rd June, 25th July, 14th September and 8th August of the year 1999. In addition the above, the dynamic behaviour of the ABL is studied in the case of active and weak phases of the southwest monsoon using the LAWP data and NCEP/NCAR reanalysis data set (Kalnay *et al*, 1996). The active days are selected from the daily rainfall and 850 hPa zonal wind following the procedure of Joseph and Sijikumar, 2004. The days selected are good agreement in both the methods and the active phase is from 15th July to 20th July and weak phase is from 12th August to 15th August in the year 1999.

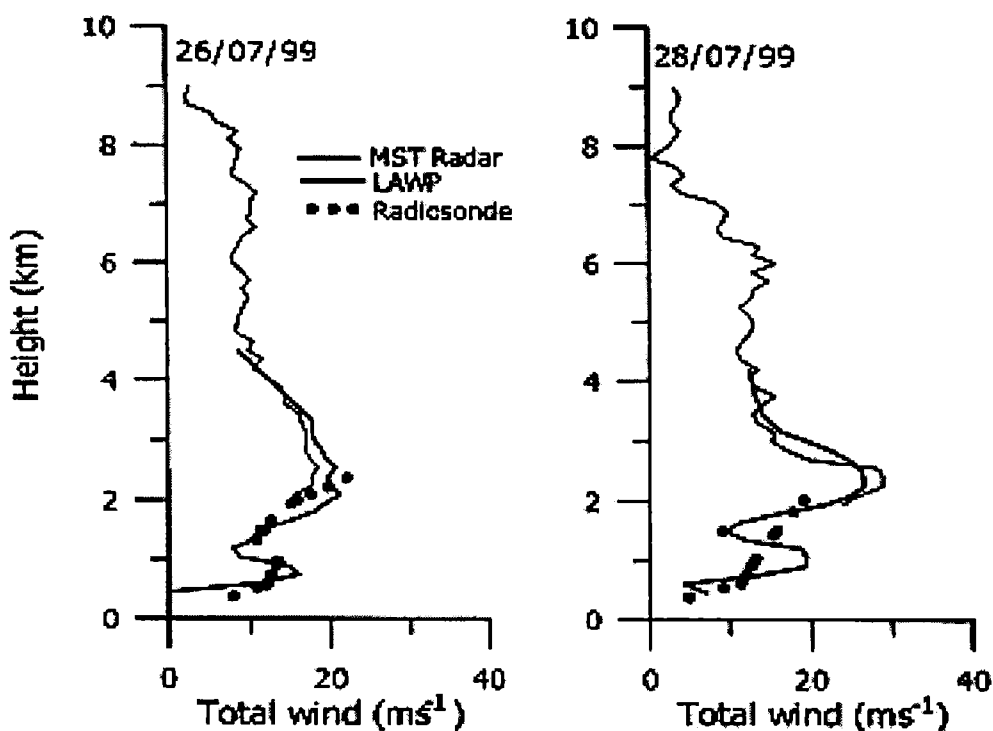


Fig.5.5 Comparison of wind speed measured by LAWP, MST radar and radiosonde on 26 July 1999 (1030 IST) and 28 July 1999 (1615 IST)

Year	Month	Days
1999	May	1, 4, 5, 6, 15, 16, 19, 20, 24, 25, 26, 29, 30
	June	3, 5, 7, 8, 9, 11, 12, 14, 20, 21, 22, 23, 24, 25, 26, 27, 28
	July	2, 3, 4, 11, 16, 18, 19, 20, 23, 24, 25, 26, 27, 28, 29, 30
	August	3, 4, 7, 8, 12, 13, 14, 15, 16, 17, 22, 23, 30, 31
	September	1, 2, 3, 4, 5, 10, 12, 13, 14, 15, 16, 18, 19, 20, 21, 22, 23, 24, 26
2000	May	1, 2, 5, 9, 10, 11, 13, 14, 18, 21, 22, 23, 30, 31
	June	1, 6, 9, 12, 14, 15, 16, 17, 18, 24, 25, 26
	July	7, 13, 14, 15, 16, 17, 23, 25, 26, 27
	August	12, 13, 14, 19, 21, 22, 23, 24, 25, 26, 27, 28, 29
	September	3, 4, 5, 8, 10, 11, 12, 14, 15, 19, 26, 27, 28, 29, 30

Table 5.2 Non rainy days considered for the analysis

5.7.1 Variation of the zonal wind

The day to day variation of the zonal wind is prominent during the southwest monsoon season other than diurnal variation and can observe from the time series of area averaged zonal wind from NCEP/NCAR reanalysis data (Fig.5.11). As the encroachment of southwest monsoon, the variability of the wind is found to be high in both vertical and temporal domains. The height time intensity contour of the hourly averaged zonal wind is plotted and presented in Fig.5.6 from a to e. The Fig.5.6a, top panel of the figure represents the diurnal variation of the wind for 6th May representing month of May. This date is not included in the southwest monsoon season because the long term climatological mean of the monsoon onset over India is 1st June with a standard deviation of 8 days (Rao, 1976) and the date of onset during the year is 25th May. This date is considered to study the evolution of the monsoon onset and propagation of the monsoon surge. During early May, the westerlies with a speed of more than 5 ms^{-1} are seen in early morning hours (~6 am) at an altitude of 1 km and as the day progresses the wind structure in the lower levels weakens (and occasionally wind becomes easterly). Around 2 km and above the wind is easterly because prevailing wind direction during May is easterly. After the onset of monsoon influence of LLJ increases due to the advancement of monsoon surge. The structure of the boundary layer also gets modified with the activity of the monsoon. To get a

detailed structure of the monsoon boundary layer, we present diurnal variation of zonal wind structure on representative days from each month of the southwest monsoon (Fig.5.6 from b to e). During the month of June (23rd June) the zonal wind strength is high and the wind speed is more than 15 ms^{-1} . This maximum speed is found in the early morning hours of the day over a long duration around 1.3 km. As the day progresses the strength of the LLJ weakens due to the convective activity and this shifts the westerly wind to a higher altitude about 2.8 km in the after noon hours. This is due to the development of the convective boundary layer due to the enormous supply of solar radiation. This convective activity made the ABL to become unstable. Generally, the LLJ can be treated as the geostrophic wind because it blows just above the ABL. During night time, thermals are absent and hence frictional effect in the ABL is small. So, the ABL depth during night is small. As the day progresses, convective activity increases and ABL depth increases. Accordingly, LLJ shifts to the higher level.

From Fig.5.6b it is obvious that the deepening of the LLJ core as the development of the CBL. Fig.5.6c & Fig.5.6d represent the contours of wind speed to show the diurnal variation of the LLJ during July and August respectively. The diurnal variation of the wind pattern during July and August is similar to that of the June, but the intensity is higher than that of the June. The maximum core strength of the LLJ is found to be in the early morning hours and the speed is more than 22 ms^{-1} . It is found that the CBL development pushes the LLJ core upward from its morning position and hence one feels that CBL causes the deepening of LLJ. This feature is noticed in all the cases. Further, when the CBL develops the LLJ wind speed exceeds 15 ms^{-1} , indicates the active monsoon situation. The decrease of the wind speed of LLJ from early morning hours to evening hours may be due to the interaction of the upper air circulations. This mode of variations is noticed in all the days considered. The maximum wind speed is $\sim 25 \text{ ms}^{-1}$ at 8 am about 1.4 km in the month of July and August, but maximum wind strength during June is around 6 am and the value is around 18 ms^{-1} . The LLJ core height during daytime exceeds 3 km in certain occasions.

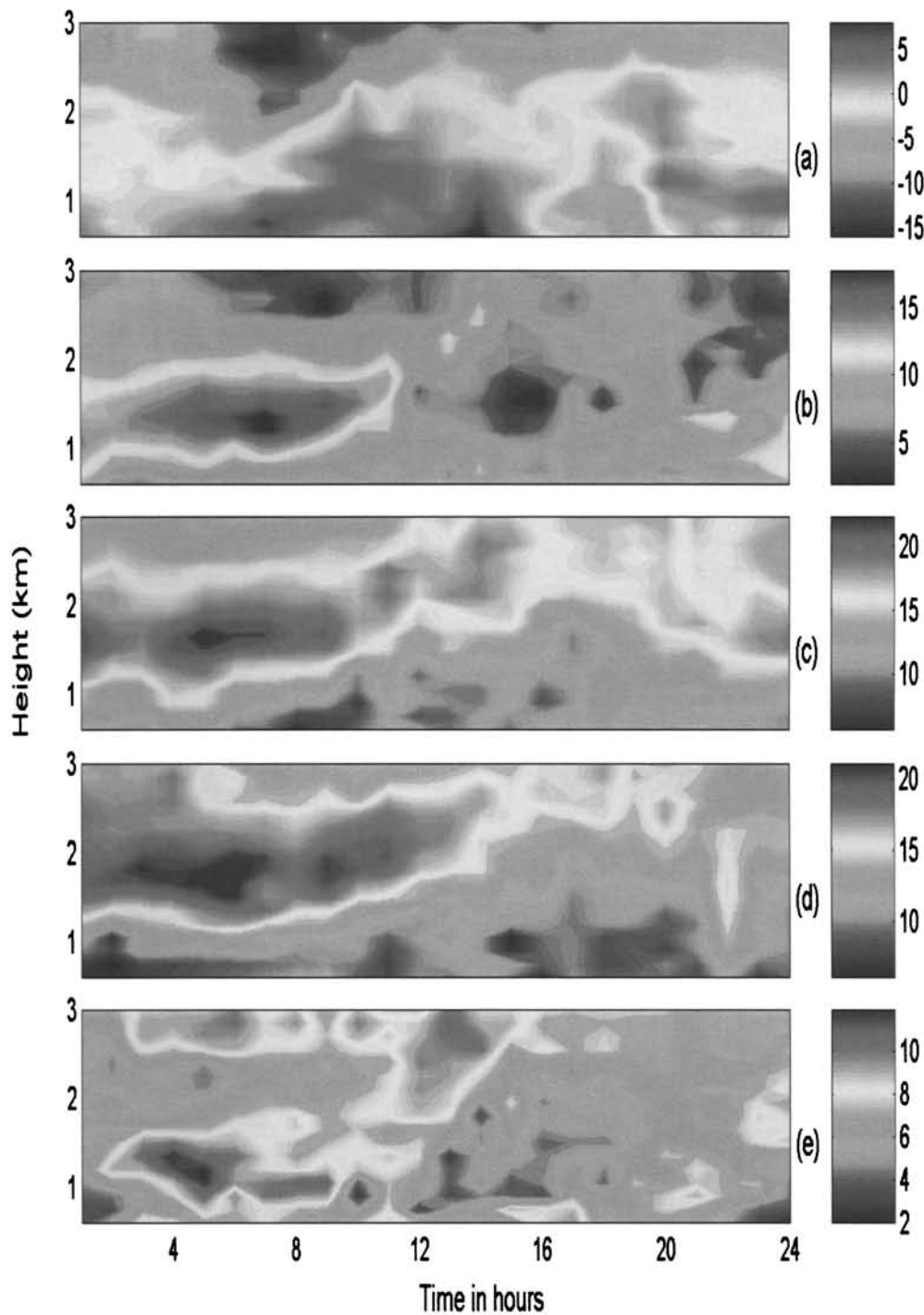


Fig.5.6 Diurnal variation of zonal wind component (ms^{-1}) from LAWP for the representative days (a) 6th May, (b) 23rd June, (c) 25th July, (d) 8th August and (e) 14th September of 1999.

The diurnal variation of the vector wind for each month along with its magnitude is given in Fig.5.7 (a - e), which is similar to figure 5.6. Generally, onset of monsoon over this station (Gadanki) is around one week after the onset of monsoon over Kerala. LLJ forms over the region along with onset of monsoon. Due

to this reason, one can expect easterly or feeble westerly winds at the surface during May, since the onset of monsoon over the station is in the early June. It is seen that in May near the surface during daytime, wind is generally westerly may be due to the local influence and the wind turns easterlies with altitude. The winds above ABL are

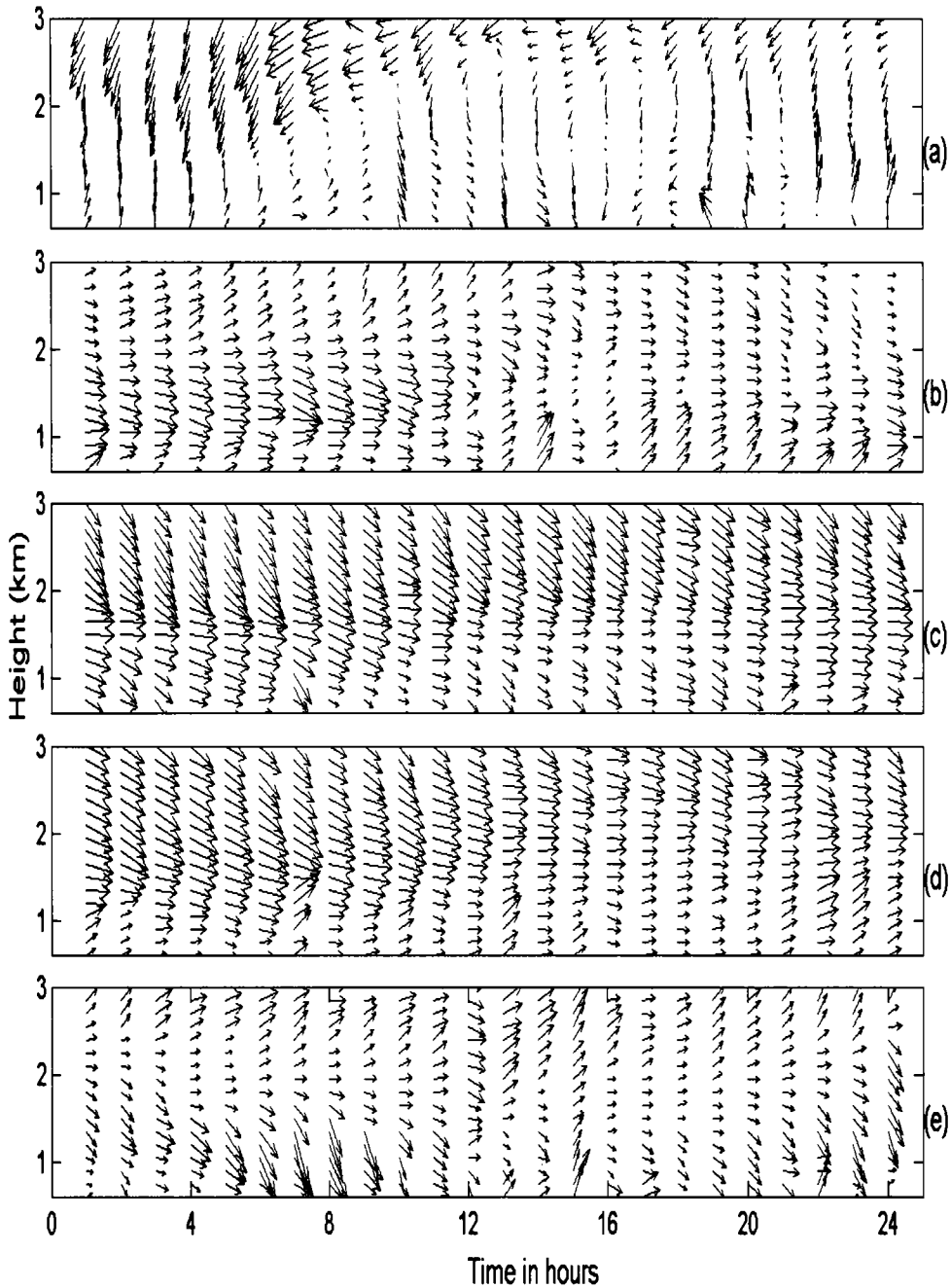


Fig.5.7 Diurnal variation of vector wind from LAWP for the representative days (a) 6th May, (b) 23rd June, (c) 25th July, (d) 8th August and (e) 14th September of 1999.

easterly generated by the influence of trade winds prevailing over the region before the onset of monsoon. The westerly winds in the ABL are feeble. During the month of June the entire atmosphere become under the influence of LLJ and it has a

noticeable change as the day progress. To study the diurnal variation of the wind during different months in the summer monsoon, vector wind in the lowest 3 km for a representative day in June, July, August and September are considered. Fig. 5.6 from b to e represent diurnal variation on these days. In monsoon months other than September, the wind pattern is more or less similar in nature but the difference is only in magnitude. It is found that the diurnal variation in wind strength is seen in all non rainy days, irrespective of the monsoon epochs, viz : active or weak phases of southwest monsoon. The wind direction in the ABL is almost westerly but the direction turns clockwise slightly with height indicating veering. In the month of September the wind is feeble indicating weakening of the southwest monsoon and the direction is also fluctuating with time. Even though the LLJ is weakened, the diurnal variation is prominent in the zonal wind component.

5.7.2 Variation of vertical wind shear

Wind shear is the sudden tearing or shearing effect encountered along the edge of a zone in which there is a violent change in wind speed or direction. It can exist in a horizontal or vertical direction and produces churning motions and consequently turbulence. Wind shear, encountered near the ground, is more serious and potentially very dangerous. One of the important reasons for generation of the low level wind shear is temperature inversion. Vertical shear is most common near the ground and can pose a serious hazard to aircrafts during take off and landing. In particular, observations suggest that a stable layer of air is unstable when the Richardson's number (the ratio of the stability over the wind shear) is less than 0.25. That is the mechanical wave production exceeds the buoyancy damping by a factor of 4. Also, the Clear Air Turbulence (CAT) is often observed in the vicinity of jet streaks, where the vertical wind shear is large. Clear Air Turbulence (CAT) is a zone of strong wind shear. Depending on wind shear, the intensity of CAT is divided into three main categories : light (L), medium (M), strong and severe (S) following Stull (1993). They are sub classified as follows

N	$0 < s < 0.0118$
L	$0.0118 < s < 0.0169$
L-M	$0.0169 < s < 0.0336$
M	$0.0336 < s < 0.0506$
M-S	$0.0506 < s < 0.0844$
S	$s > 0.0844$

The wind shear, s (s^{-1}) is computed from the u-component (u) and v-component (v) of the wind field obtained from the LAWP and the vertical distance, dz is taken as the vertical interval of the observations in metre (150 m). The wind shear computed using the following relation

$$s = \sqrt{\left(\frac{du}{dz}\right)^2 + \left(\frac{dv}{dz}\right)^2} \quad (5.10)$$

The diurnal variation of the wind shear for representative days during the southwest monsoon period are presented in the Fig.5.8 (a - e). The vertical wind shear values range from 0 to $0.048 s^{-1}$. Even though the vertical interval ($dz = 150$ m) is some what large for the computation of vertical wind shear, the shear values obtained are reasonably well and hence the probability of CAT. Certainly, we can obtain better results if the vertical interval is less than that of the present one. The intensity of CAT is less during May and September than that during June, July and August. The wind as well as wind shear during June to August is more than the other months. Although September belongs to monsoon season, the wind strength weakens rapidly by the withdrawal of monsoon. During May and September the variation of wind direction with height is not in a regular pattern compared to the other months. During monsoon period, due to the influence of LLJ the wind direction is almost constant throughout the day. Even the intensity of the shear is low, a layer of high wind shear is found in the Entrainment Zone (EZ). The maximum shear zone is found in ABL during morning hours and it is due to the development of the convective boundary layer. The high values of shear zone in the EZ is found in almost all the

cases. During evening around 1900 hours the vertical wind shear values are almost zero, indicating that a sudden breakup of the boundary layer turbulence due to the dissipation of the CBL. On certain days, the high intensity of CAT is seen during mid night hours and it may due to the increase of the wind strength. This increasing of wind strength may attribute to the nocturnal LLJ.

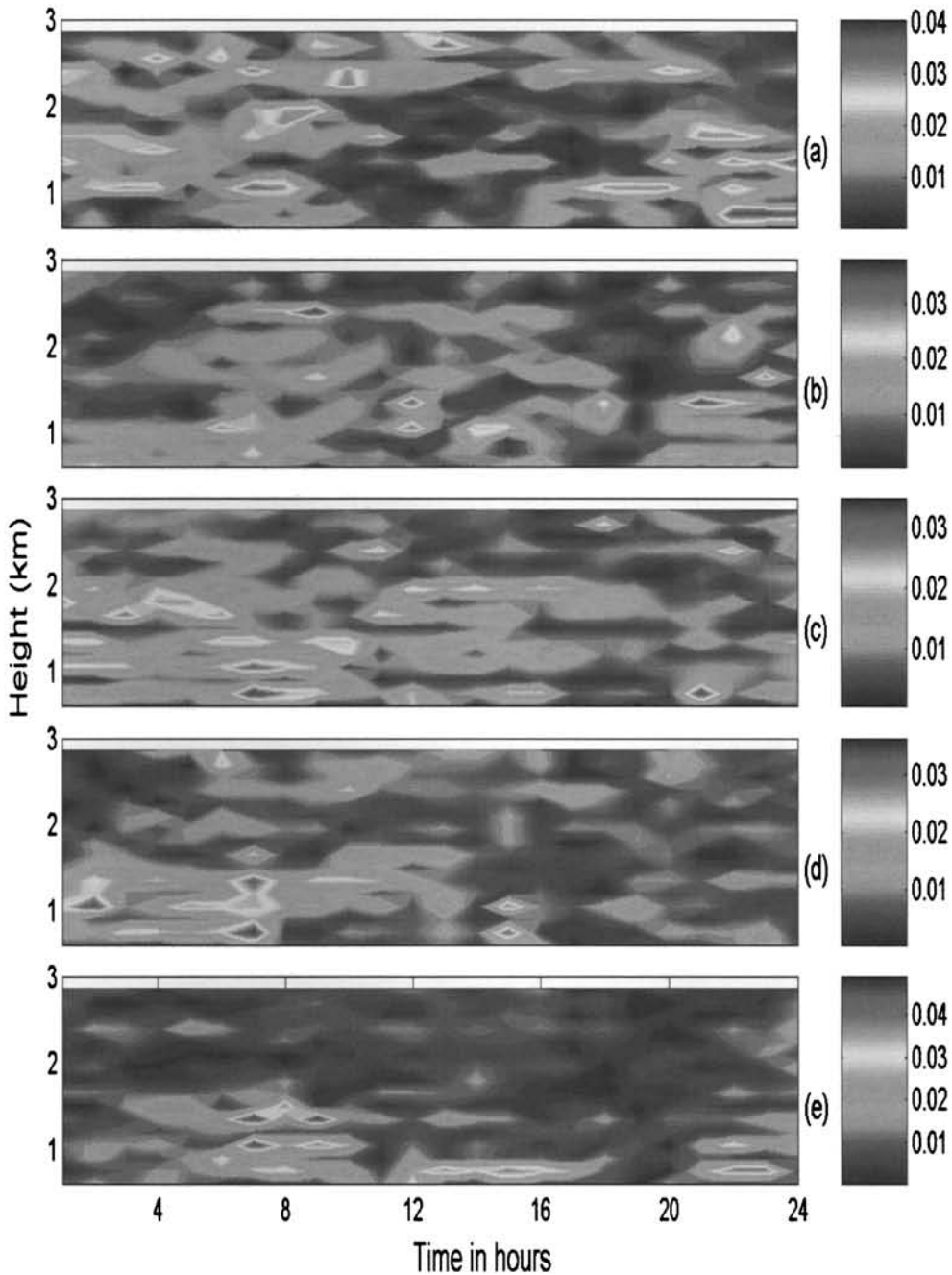


Fig.5.8 Diurnal variation of vertical wind shear (s^{-1}) for the representative days (a) 6th May, (b) 23rd June, (c) 25th July, (d) 8th August and (e) 14th September of 1999.

Generally, the intense CAT is found just below the LLJ core and it can be noticed from the figures of zonal wind and vertical wind shear. During the period of study the CAT ranges from 0 to 0.041 s^{-1} , 0.039 s^{-1} , 0.036 s^{-1} , 0.037 s^{-1} and 0.05 s^{-1} on 6th May, 23rd June, 25th July, 8th August and 14th September respectively. The maximum intensity of CAT is in a range of medium level, so it is not much hazardous to aircrafts but is capable of generating turbulence for triggering various convective activities.

5.7.3 Atmospheric boundary layer depth

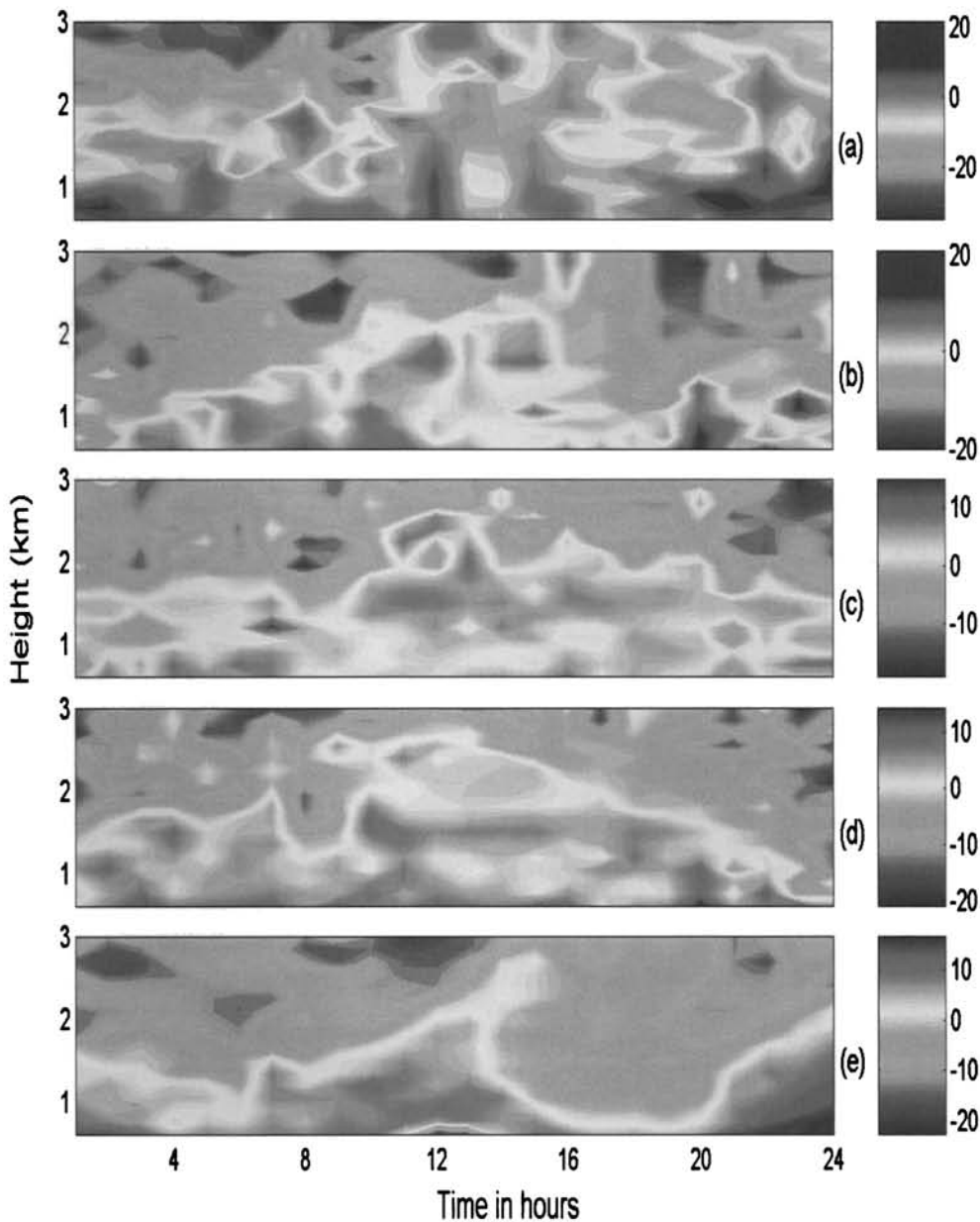


Fig.5.9 Diurnal variation of signal to noise ratio (reflectivity) the representative days (a) 6th May, (b) 23rd June, (c) 25th July, (d) 8th August and (e) 14th September of 1999.

ABL depth varies from 0.6 to 3.5 km at a particular location due to many meteorological factors prevailing over the station. One can see diurnal variation of ABL height. During day time CBL top can be treated as ABL depth. CBL height is one of the fundamental parameters in many meteorological applications. It is also very important for modeling and interpreting the dynamics and chemistry of the ABL. Unfortunately, simple parameterization of CBL height in terms of surface meteorological data is often insufficient, especially in tropical region (Reddy *et al* 2001). Our knowledge of the tropical ABL is to be updated with more reliable observations. Ground based remote sensing instrument such as LAWP can be used for ABL dynamics. Therefore, the observations using this instrument are useful to delineate the diurnal evolution of the ABL structure. The vertical extent of the ABL can be defined in different ways: the height where the vertical gradient of virtual potential temperature has a maximum; the cross over point of the buoyancy flux profiles (Wyngaard and Lemone, 1980); the region of enhanced radar reflectivity due to the sharp variation of the temperature and humidity (White and Fairall 1991).

The diurnal variation of the height time intensity plot of signal to noise ratio (SNR) is presented in Fig.5.9. The SNR is determined by the reflectivity turbulence seen by the LAWP, which depends on the strength of the mechanical turbulence and the background refractive index gradient (Gage .1990). The convective boundary layer top can be identified on the figure as the level at which sign of SNR change. During southwest monsoon season, the signal is almost captured by the LAWP to identify the ABL height. The diurnal evolution of the ABL is depicted in figure 5.9 from a to e. On a diurnal basis, the boundary layer height starts to grow from around 0800 hours in the morning and dissipate after sun set. The height of the ABL during daytime in May is almost 3 km. But during the southwest monsoon season the ABL height is small compared to that in May. The maximum reflectivity is seen just below LLJ core in the months of June, July and August. During early morning hours the reflectivity maximum is found around 1.5 km and CBL gets deepened as the day progresses. Due to the activity of the CBL, thermals are intensified and they transport surface properties upward and upper air properties to surface. Fig.5.10 shows the time-height plot of the vertical wind from the LAWP

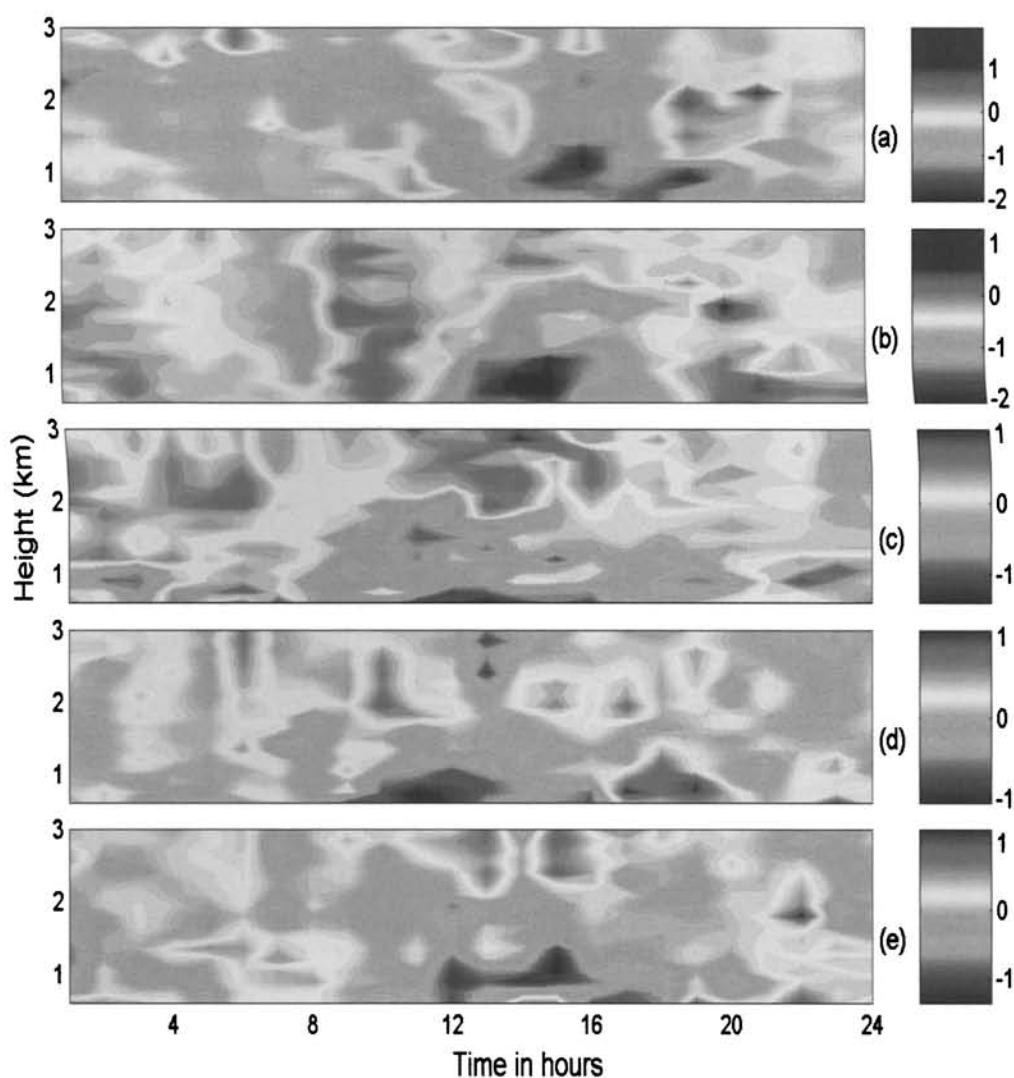


Fig.5.10 Diurnal variation of vertical wind (ms^{-1}) from LAWP for the representative days (a) 6th May, (b) 23rd June, (c) 25th July, (d) 8th August and (e) 14th September of 1999.

during the above periods. The vertical wind shows sinking motion during most of the daytime, indicating transport of momentum from LLJ to surface. In the entire CBL the vertical wind shows sinking motion during most of the days, indicating transport of momentum from upper level to surface. The intensity of the down ward component is high in the lower layers between noon to around 1600 hours. The structure is different from day to day. In most of the cases, the vertical wind in the upper levels show upward movement from the core of the LLJ.

5.8 Variation of LLJ during active and weak phases

The active and weak phases of southwest monsoon is a northward propagating component of Intra Seasonal Oscillation (Yasunari, 1979, 1981; Sikka and Gadgil, 1980; Krishnamurthy and Subramanyam, 1982). The wind strength during active and

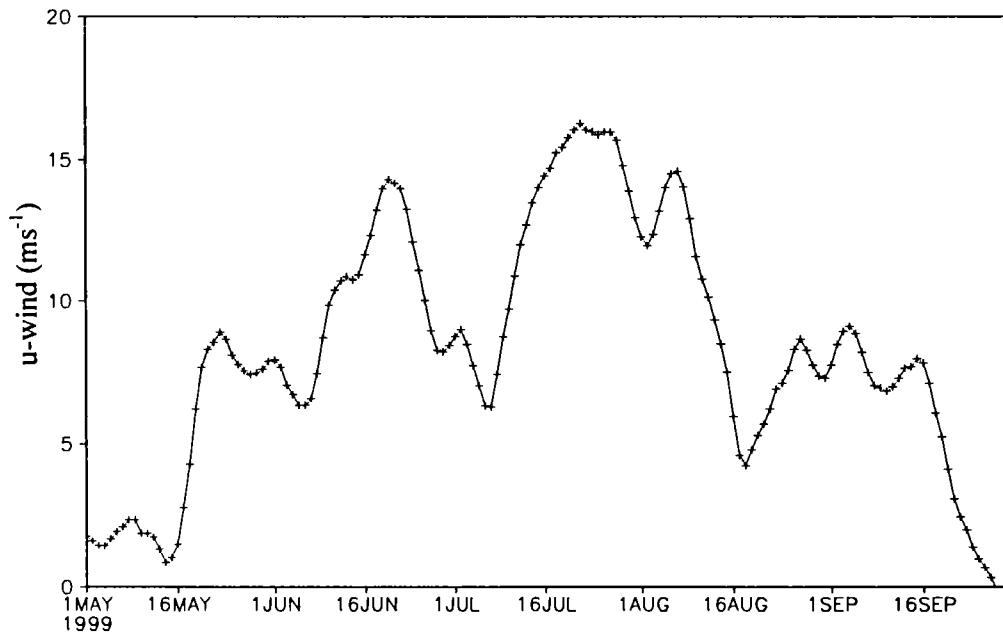


Fig.5.11 Time series of the area averaged (10° N - 20° N & 70° E - 80° E) zonal wind at 850 hPa during 1999.

weak phases has shown significant changes. The diurnal evolution of LLJ is studied using LAWP and NCEP/NCAR reanalysis data set. The time series plot of area averaged (10° N - 20° N & 70° E - 80° E) zonal wind at 850 hPa during monsoon season is given in Fig.5.11 to identify the variation in wind speed and to identify the days of active and weak phases. Zonal wind structure during active days (16th July to 20th July, 5 days) and weak days (12th August to 15th August, 4 days) of the year 1999 are seen in the Fig.5.12a and Fig.5.12b respectively. From the graph we can see that the LLJ wind strength during active monsoon period is more than 22 ms^{-1} and while during weak phases the maximum value is only about 18 ms^{-1} . Other than this variation, both of these phases have significant diurnal variation. During active phase of southwest monsoon the wind strength maximum found after mid night to early morning hours and this significant high value may be due to the modulation with the nocturnal LLJ. During the daytime the wind core strength is found to decrease and

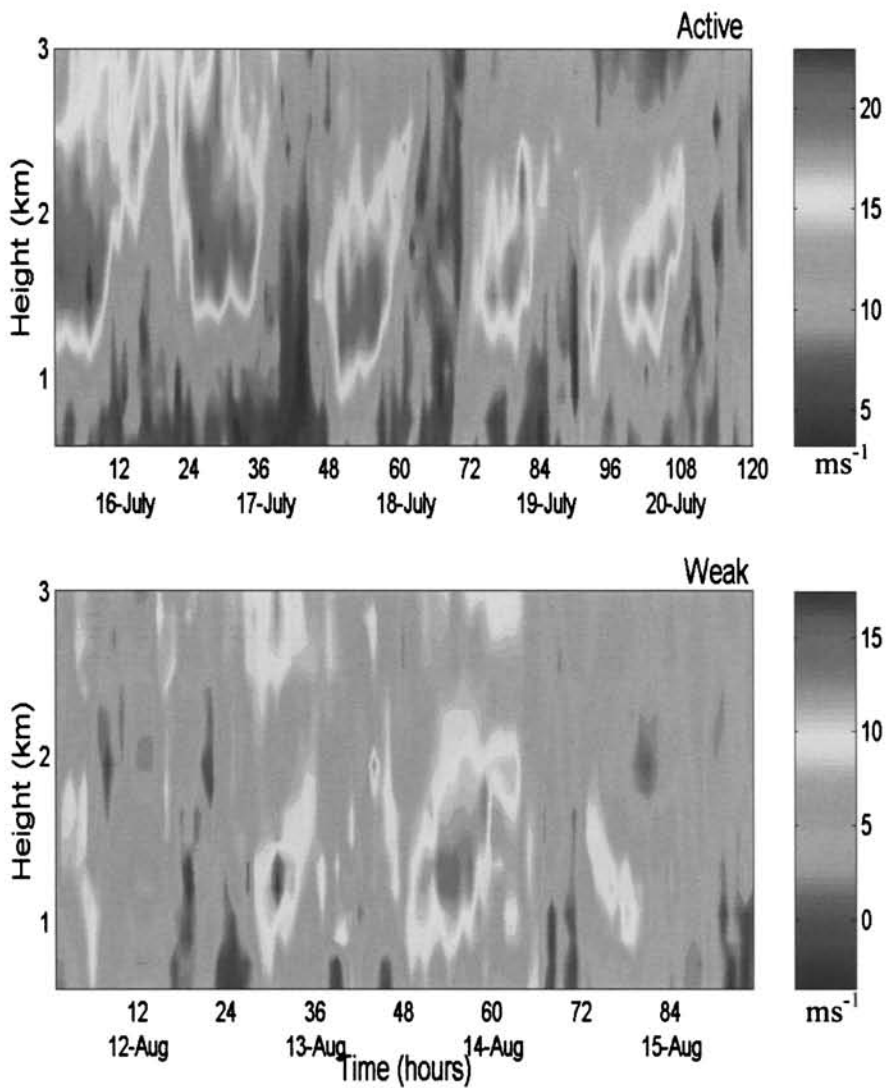


Fig.5.12 Height time intensity plot of the zonal wind (ms^{-1}) during active and weak phase of southwest monsoon 1999 taken from LAWP.

the depth of the LLJ core is found in a higher level due to the development of the CBL. In the surface layers during active phases the wind strength is almost 5 ms^{-1} but during weak phases in certain occasions the wind strength is less and perhaps the direction is found to be easterly. The core of LLJ during active phases is around 1.8 km in early morning hours and during weak it is about 1.2 km height.

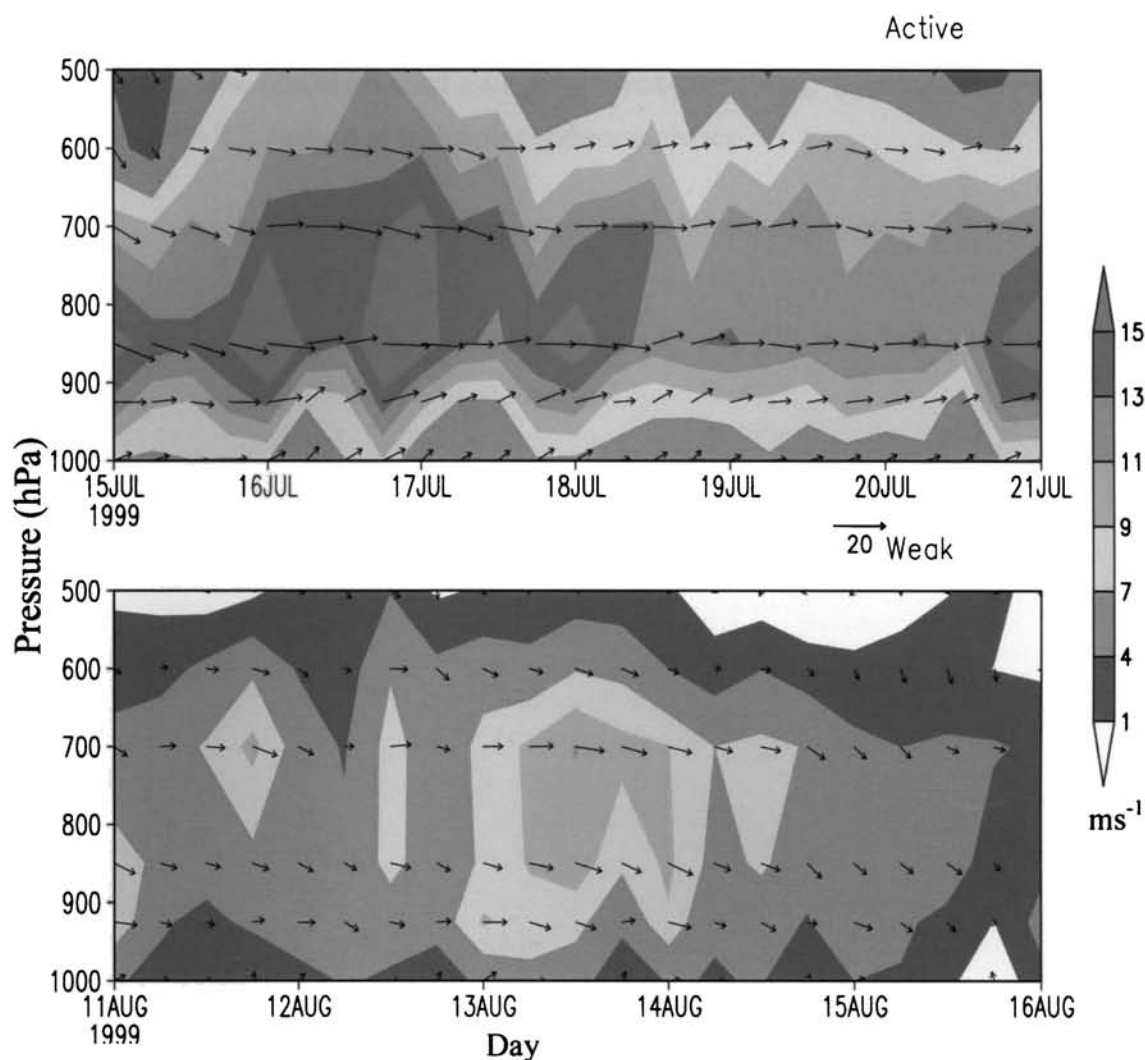


Fig.5.13 Height - time plot of the zonal wind (ms^{-1}) during active and weak phase of southwest monsoon from NCEP/NCAR reanalysis data set.

Similar features are further studied using NCEP/NCAR reanalysis : 4 times instantaneous observation of daily data set during the same period (Fig.5.11a and Fig.5.11b). The figure closely resembles that of the LAWPs results, confirming the earlier results. The NCEP data set has a spatial resolution of $2.5^\circ \times 2.5^\circ$ latitude-longitude grid. To capture the signal at the site, we selected an area over a small region ($12.5^\circ \text{ N} - 15^\circ \text{ N} \ \& \ 77.5^\circ \text{ E} - 80^\circ \text{ E}$) to take average wind with height during active and weak phases. From the figure, clear diurnal variation is noticed during both the phases. The wind strength during active days is more than that of the weak phases but the strength of wind is lower in the case of NCEP analysis during both active and weak phases. The reduced magnitude of the LLJ core in the NCEP

analysis can be attributed to the averaging effect. The maximum wind strength during active period is more than 15 ms^{-1} and the maximum wind speed during weak phase is around 9 ms^{-1} . The maximum wind strength is found during early morning hours as in the case of LAWP analysis in both active and weak phases.

CHAPTER – 6

SUMMARY AND CONCLUSIONS

CHAPTER - 6

SUMMARY AND CONCLUSIONS

Atmospheric boundary layer is the layer of fluids in the immediate vicinity of a material surface in which significant exchange of momentum, heat or mass takes place between the surface and the fluid and this interaction occurs over time scales of a few hours to 1 day. In the thesis, an attempt is made to study the dynamic and thermodynamic characteristics of boundary layer over marine, coastal and inland areas of the atmosphere. The ABL studies are sparse in the tropical region due to the non availability of reliable data set, especially over the Indian region where monsoon plays a vital role. As mentioned in the preface, special emphasis is given to analyse boundary layer characteristics during different epochs of monsoon. Thus major scientific problems addressed in this thesis are diurnal and seasonal variation of coastal meteorological properties, the characteristic difference in the ABL during active and weak monsoons, features of ABL over marine environment and the variation of the boundary layer structure over an inland station. In the following paragraphs summary of results are presented followed by the future research plan.

The study of the coastal zone is important due to its high vulnerability mainly due to sea breeze circulation and associated changes in the atmospheric boundary layer. Using the automatic weather station (AWS) over Cochin, characteristics of the sea breeze and land breeze circulations are carried out. The setting and cessation time of sea breeze is important over the station because Cochin is an industrial capital of Kerala state. The setting time of sea breeze is early in the southwest monsoon months because the sun's position is in the northern hemisphere so that Cochin receives comparatively high insolation. This is followed by the pre-monsoon, winter and post monsoon periods during the clear sky days. Due to the orientation of the shoreline, the direction of land breeze is 90° (*i.e* easterly) and the direction for sea breeze is 270° (*i.e* westerly). The onset time of the sea breeze is varying from season to season. *i.e* during winter, pre-monsoon, southwest monsoon and post monsoon seasons are 1200, 1100, 0900 and 1230 IST respectively. These variations are mainly due to the difference in insolation during different months. The fluxes of momentum and sensible heat and other parameters such as drag coefficient, frictional velocity,

temperature scale, Monin-Obukhov length are computed using the Monin-Obukhov similarity relation on diurnal and seasonal time scales. The momentum and sensible heat fluxes show high diurnal variation during pre-monsoon period and the values are 0.28 Nm^{-2} and 250 Wm^{-2} respectively. The least variation of the fluxes is noticed during post monsoon period and the values are 0.1 Nm^{-2} for momentum flux and sensible heat flux is 150 Wm^{-2} . It is found that the Momentum flux is exponentially related to the surface wind and sensible heat flux is related to wind and temperature but more to the wind. The day to day variation of the parameters such as frictional velocity, temperature scale, drag coefficient, Monin-Obukhov length are examined during land breeze (8 AM) and sea breeze (3 PM) periods. It is found that the turbulent parameters are less during land breeze period due to the less intensity of the land breeze time and high during sea breeze hours because of the high turbulence and convective activities.

In the perspective of southwest monsoon, the studies of ABL characteristics are important since the active and weak phases of monsoon are triggered by the surface layer properties or they can be controlled by the upper air features associated with the monsoon system. This thesis describes the various features in the ABL associated with the active and weak monsoons. On an average, LLJ maximum wind core is at 850 hPa (1.5 km) and decreases both upward and downward. During active monsoon situation, the influence of LLJ can be felt even in the surface, hence the boundary layer parameters change with these epochs of monsoon. The fluxes of momentum and sensible heat are estimated from the tower data using profile method during the active and weak monsoon phases. It is found that the turbulent activities are high during the active monsoon condition and less during weak. The high vertical wind shear during active monsoon by the influence of LLJ is responsible for high values of fluxes.

In addition to the surface fluxes, the thesis discusses the surface boundary layer properties associated with the active and weak epochs. Conserved Variable Analysis for estimated parameters θ_e and q for both Trivandrum and Mangalore during the active and weak monsoon situation is employed to diagnose the boundary layer processes and the thermodynamic structure. It is found that the mixing height of the CBL is confined in 1 km in most cases of the active phase over Trivandrum. In the case of Mangalore the mixing height is slightly different and found in higher

altitude. It can be attributed to the influence of the location of the station in the windward side of the Western Ghats which helps the development of the orographic clouds. During weak monsoon situations, the convective mixing height is found to be high in all the cases of Trivandrum and Mangalore. This is attributed to the characteristics of the weak monsoon situation. During this phase, even though convective cloud band prevails over the equatorial region (Indian Ocean), Trivandrum and Mangalore are more or less cloud free. In the cloud free atmosphere due to the availability of insolation, thermals are formed. Hence the mixing height is elevated. The mean mixing heights over Trivandrum and Mangalore for the active phase of southwest monsoon are 617 m and 1359 m respectively. The average heights for the weak monsoon situations are 1034 m and 2230 m for Trivandrum and Mangalore respectively. Moreover, the thermodynamic parameters such as specific humidity, virtual potential temperature and equivalent potential temperature in association with the monsoon epochs are studied using radiosonde observations over west coastal stations. These west coastal stations are oriented almost perpendicular to westerly flow of LLJ so that variability in LLJ and hence the monsoon oscillation is reflected at these stations. The above thermodynamic parameters increase during active monsoon situations and decrease during weak monsoon situations. The relation between specific humidity with virtual potential temperature and equivalent potential temperature are linear in all the levels but the slope of the linear trend varies with altitude for all the stations.

Another interesting result noticed on the intra seasonal oscillation is the high frequency and low frequency harmonics found in the lower troposphere. These variabilities are physical manifestation of the active and weak phases of southwest monsoon. The oscillations in the ABL are important because the transport mechanism from the surface to the upper atmosphere is governed by the ABL characteristics. The study was carried out using wind and temperature data observed at surface, 925 hPa and 850 hPa levels. The different frequencies embedded in the boundary layer parameters are identified by employing wavelet technique. Surface boundary layer characteristics over the monsoon region are closely linked to the upper layer monsoon features. It is found that the wind and temperature at different levels show oscillations in Quasi Biweekly Mode (QBM) and Intra Seasonal Oscillation (ISO) bands as observed in a typical monsoon system. Amplitude of the oscillation varies with height. The amplitude of the QBM periodicity is more in the surface

levels but in the upper levels the amplitude of the ISO periodicity is more than that of the QBM. From this it is obvious that the controlling mechanism of QBM band is surface parameters such as surface friction and that for ISO band is associated with large scale monsoon features such as northward propagation of organized convective cloud band.

This thesis also describes well about the dynamic characteristics of the marine atmospheric boundary layer (MABL) using high resolution satellite derived QuikSCAT data set with a spatial resolution of 0.25 X 0.25 latitude longitude grid. This study is used to enhance our knowledge on MABL and can be used as the estimated values of the boundary layer parameters over the marine atmosphere because the data sets available over the oceanic regions are sparse and only through some cruise tracks. This study is benefitted to know the values and variabilities of the ABL parameters such as surface wind, surface friction, drag coefficient, wind stress and wind stress curl. A detailed study on the MABL characteristics is made using high-resolution surface wind data measured by QuikSCAT satellite. Spatial variation of surface wind, frictional velocity (u_*), roughness parameter (z_0) and drag coefficient (C_D) for different seasons are studied. Surface wind pattern shows more strength during the southwest monsoon season due to modulation by the Low Level Jetstream. C_D is more during southwest monsoon season due to the strong wind and less during winter. The spatial variation of u_* over the seas is small during the post-monsoon season (0.2 ms^{-1}). Maximum spatial variation of u_* is during the southwest season due to the high surface wind due to the LLJ found over the south Arabian Sea (from 0.3 ms^{-1} to 0.5 ms^{-1}) followed by the pre-monsoon season over the Bay of Bengal (from 0.1 ms^{-1} to 0.25 ms^{-1}). The mean characteristic features of the wind stress curl during winter season is positive over the equatorial region with a maximum value of $1.5 \times 10^{-7} \text{ Nm}^{-3}$ but on either side of the equatorial belt negative wind stress curl is dominated. Area weighted average of u_* and C_D are found over $65^\circ \text{ E} - 70^\circ \text{ E}$ & $15^\circ \text{ N} - 20^\circ \text{ N}$ representing Arabian Sea and $87^\circ \text{ E} - 92^\circ \text{ E}$ & $15^\circ \text{ N} - 20^\circ \text{ N}$ representing Bay of Bengal. It is found that the average value of u_* in both the Arabian Sea and Bay of Bengal is found to be around 0.2 ms^{-1} from January to first week of May. In the Arabian Sea the value increases from first week of May to end of July (reaches to maximum of 0.4 ms^{-1}) and then decreases almost constantly till

the end of September. The variation is caused by the presence of LLJ associated with the monsoon surge. It is found that the u_* over the Bay of Bengal during southwest monsoon season is maximum by the middle of June with variability similar to intra seasonal oscillation. The C_D and u_* are more during southwest monsoon season compared to other seasons. The interrelationship between u_* and surface wind speed in both Arabian Sea and Bay of Bengal are found to be exponential. But C_D increases with the increase of wind speed and also C_D increases as the decrease of the wind speed and the value of wind speed in which the C_D is minimum is around 4ms^{-1} . The variabilities of the frictional velocity and drag coefficient is also examined over representative areas of the Arabian Sea and Bay of Bengal using the wavelet technique and from the analysis it is revealed that the variabilities in 30 to 60 day mode is prominent over the entire period over the Bay of Bengal and the variability of this mode is 95 per cent confident during monsoon seasons but over the Arabian Sea the variabilities of the above mode are prominent and 95 % confidence level during the southwest monsoon period only and this kind of variabilities are more or less absent in other seasons.

To know the inland boundary layer characteristics, high resolution wind data for clear sky days of the monsoon period is used from the UHF radar - Lower Atmosphere Wind Profiler over Gadanki (13.47°N , 79.18°E). The high-resolution UHF wind observations over Gadanki reveal that the winds are strong and are westerly in direction during southwest monsoon period. The strong LLJ features are most prominently and consistently observed in the months of June through August and are much stronger in July and August. During active monsoon period the zonal wind is stronger and westerly whereas during weak, wind is getting weakened as expected during weak monsoon period. LLJ feature is persisting continuously during day and night with varying core height and intensity. Moreover, the LLJ maximum wind core varies more than 2 km between night and day. The mean wind speed is around 20ms^{-1} . Diurnal features are well noticed on the zonal wind pattern especially in the LLJ core region. The intensity at LLJ core is maximum in the early morning hours. It is found that the intensity at LLJ core decreases during the daytime due to the high convective and other frictional activities. As the day progresses, the core of the LLJ gets shifted to high altitude. During morning hours the core height is found to be around 1.5 km but during noon hours the wind core is shifted to high altitude

region due to the convective and turbulent activities of the surface boundary layer and the mean core height is around 2.5 km. CBL forces are responsible for modifying strong monsoon LLJ in the lower layer and perhaps strong CBL mixing can completely dilute the jet structure. The inversion height is observed to be around the jet core height as found in the wind structure. Moreover, the convective activity is high during the lower part of the LLJ core and it can be seen from the vertical wind structure. The probability of CAT is moderate and it is noticed just below the core of the LLJ in the maximum shear zone. These strong shears are likely to be the main source for clear air turbulence and the information regarding this is very important in navigation fields.

6.1 Scope for future studies :

1. The onset and cessation time of sea breeze circulation can be simulated using mesoscale model. This study will help industries to dispose effluents to the atmosphere with minimum pollution during high land breeze period since they travel to the oceanic region so that effect of pollution is minimum over the densely populated residential area.
2. The surface boundary layer properties such as the surface fluxes of momentum, sensible heat and latent heat can be computed using fast response data set employing the eddy correlation method and compared with the present study. In this thesis, the analysis was carried out using slow response data set and profile method based on the similarity relation is used for estimating the fluxes.
3. It is also very important to study variation of fluxes and other surface boundary layer parameters during different seasons especially investigation during the various epochs of the monsoon such as onset, active and weak and to explore the role played by the boundary layer for the various epochs because exact reason behind this is still unexplored.
4. It is found from the analysis of the LAWP data set that the activity of the LLJ during the southwest monsoon is high during morning hours and weakened as the development of the convective boundary layer. It is construed that the weakening of LLJ during the evening hours as revealed by the LAWP analysis may be by the influence of upper layer easterly. This is to be investigated using MST Radar wind data at the upper layer.
5. Also, it is important to study the linkage of the TEJ (using MST data set) with LLJ (using LAWP data set) and to unravel the possibility to predict the monsoon activity by the proper understanding of the TEJ-LLJ combined activity.

REFERNCES

- Al-Jiboori, M. H., Xu Yumao, and Qian Yongfu, 2001: 'Turbulence characteristics over complex terrain in west China', *Bound.-Layer Meteor.*, **101**, 109–126.
- Anandan, V.K., Balmuralidhar, P., Rao, P.B. and Jain, A.R., 1996: 'A method for adaptive moments estimation technique applied to MST radar echoes', Progress in electromagnetic research symposium, Telecommunication research center, City university of Hong Kong.
- Anandan, V.K., Balmuralidhar, P., Rao, P.B., Jain, A.R and Pan, C.J., 2004: 'A method for adaptive moments estimation technique applied to MST radar echoes'. *J. Atmos. Oceanic Technol.*, 2004
- Andre, J.-C., Ph. Bougeault, and Goutorbe, J.-P., 1990: 'Regional estimates of heat and evaporation fluxes over non-homogeneous terrain, Examples from the HAPEX-MOBILHY programme', *Boundary-Layer Meteorol.*, **50** 77-108.
- Angevine, W., 1999: 'Entrainment results including advection and case studies from the Flatland boundary layer experiments', *J. Geophys. Res.* **104**(D24): doi: 10.1029/1999JD900930. issn: 0148-0227.
- Angevine, W., Grimsdell, A., McKeen, S. and Warnock, J.M., 1998: 'Entrainment results from the Flatland boundary layer experiments', *J. Geophys. Res.*, **103**(D12): doi: 10.1029/98JD01150. issn: 0148-0227.
- Anonymous, : 1966, *Climatological Tables of Observatories in India (1931 – 1960)*, India Meteorological Department, 1-470.
- Arakawa, H. and Utsugi, M., 1937: ' Theoretical investigation on land and sea breezes', *Geophys. Mag. Tokyo*, **11**, 97-104.
- Arya, S. P., 1988: '*Introduction to micrometeorology*', Accad Press, Inc., Harcourt Brace Jovanovich Publishers, Sandego, California, 307pp.
- Atkins, N. T and Wakimoto, R. M. : 1997, 'Influence of the synoptic scale flow on sea breezes observed during CaPE', *Mon. Wea. Rev.*, **125**, 2112-2130.
- Augstein, E., Riehl, H. and Ostapoff, F., 1973: 'Mass and energy transports in an undisturbed Atlantic trade wind flow', *Mon. Wea. Rev.*, **101**, 101-111.

- Badgley, F. I., Paulson, C. A., and Miyake, M., 1972: 'Profile of wind speed, temperature and humidity over the Arabian Sea', *Meteorol. Monogr.*, **6**, 66.
- Bala Subramanyam, D and Radhika Ramachandran, 2003: 'Structural characteristics of marine atmospheric boundary layer and its associated dynamics over the central Arabian Sea during INDOEX, IFP campaign', *Current Sci.*, **85**, 1334-1340.
- Bala Subramanyam, D, 2003: '*Observational and modeling studies of the marine atmospheric boundary layer over the tropical Indian Ocean during INDOEX*', Ph.D Thesis, University of Kerala, India
- Balsley, B.B. and Gage, K.S., 1982: 'On the use of radars for operational profiling', *Bull. Amer. Meteorol. Soc.*, **63**, 1009–1018.
- Barker, E. M. and Baxter, T. L.: 1975, 'A note on the computation of the atmospheric surface layer fluxes for use in numerical modelling', *J. Appl. Meteorol.* **14**, 620-622.
- Batchvarova, E. and S. Gryning, 1994: 'An applied model for the height of the daytime mixed layer and the entrainment zone', *Boundary-layer Meteorol.*, **71**, 311-323.
- Bechtold, P., J. P. Pinty and P. Mascart, 1991: ' a numerical investigation of the influence of the large scale winds on sea breeze and inland breeze type circulations', *J. Appl. Meteorol.*, **30**, 1268-1279.
- Beljaars, A. C. M. and Betts, A. K., 1993: 'Validation of the boundary layer representation in the ECMWF model. *Proc. Seminar on Validation of Models over Europe*, ECMWF, 159–196.
- Beljaars, A. C. M. and Holtslag, A. A. M., 1991: 'Flux parameterization over land surfaces for atmospheric models', *J. Appl. Meteor.*, **30**, 327–341.
- Bentamy, A., Y. Quilfen, and P. Flament, 2002: 'Scatterometer wind fields : A new release over the decade 1991 – 2001', *Can. J. Remote Sensing*, **28**, 431-449.
- Betts, A K., 1973: 'Non precipitating cumulus convection and its parameterization', *Q. J. R. Meteorol. Soc.*, **99**, 178-196.
- Betts, A. K and Albrecht, B. A., 1987: 'Conserved variable analysis of the convective boundary layer thermodynamic structure over the tropical oceans', *J. Atmos.*

- Sci.*, **44**, 83-99.
- Betts, A. K. and Miller, R. D., 1975: 'VIMMHEX-1972 Rawin sode data', *Department Atmospheric Science*, Colorado State University, Fort Collin, 150pp
- Betts, A. K., Desjardins, R. L., and MacPherson, J. I.: 1992, 'Budget Analysis of the Boundary Layer Grid Flights during FIFE 1987', *J. Geophys. Res.* **97**, 18533–18546.
- Bhat, G. S. and co-authors., 2001: 'Bay of Bengal Monsoon Experiment (BOBMEX)', *Bull. Amer. Meteorol. Soc.*, **82**, 2217-2243.
- Bolle, H.-J., J.-C. André, J.L. Arrue et al., 1993: 'EFEDA: European field experiment in a desertification-threatened area', *Ann. Geophysicae*, **11**, 173-189.
- Bolton, D., 1980: 'The computation of equivalent potential temperature', *Mon. Wea. Rev.*, **108**, 1046-1053.
- Brutsaert, W.: 1999, 'Aspects of Bulk Atmospheric Boundary Layer Similarity under Free-. Convective Conditions', *Rev. Geophys.* **37**, 439–451.
- Bunker, A. F., 1965: 'Interaction of the summer monsoon air with the Arabian Sea', *Proc. Symp. On Mer. Results*, IIOE, Bombay, 3-6.
- Businger, J. A., Wingard, J. C., Izumi, Y. and Bradley, E. E. : 1971, 'Flux profile relationships in the atmospheric surface layer', *J. Atmos. Sci.*, **28**, 181-189.
- Carter, D.A., K.S. Gage, W.L. Ecklund, W.M. Angevine, P.E. Johnston, A.C. Riddle, J. Wilson, and C.R. Williams, 1995: 'Developments in UHF lower tropospheric wind profiling at NOAA's Aeronomy Laboratory. *Radio Science*, **30**, 977-1001
- Charnock, H., 1955: 'Wind stress on a water surface'. *Quart. J. Roy. Meteor. Soc.*, **81**, 639–640.
- Chen, T.-C. and Chen, J.-M. 1993: The 10-20 day mode of the 1979 Indian monsoon: Its relation with time variation of monsoon rainfall. *Mon. Weather Rev.*, **121**, 2465-2482
- Clark, R. H., A. J. Dyer, R. R. Brook, D. G. Reid, and A. J. Troup., 1971: 'The Wangara experiment: Boundary layer data'. *Tech. paper 19, Division Meteor. Phys. CSIRO*, Australia.

- Colon, J. A., 1964: 'On interactions between the Southwest Monsoon current and the sea surface over the Arabian Sea'. *Indian J. Meteor and Geophys.*, **15**, 183-200.
- Coulter, R. L, 1990: 'A Case Study of Turbulence in the Stable Nocturnal Boundary Layer', *Boundary-Layer Meteorol.* **53**, 75-91.
- Dalu, G.A. and R.A. Pielke, 1989: 'An analytical study of the sea breeze', *J. Atmos. Sci.*, **46**, 1815-1825.
- Davidson, K. L., 1974: 'Observational results on the influence of stability and wind wave coupling on the momentum transfer and turbulent fluctuations over ocean waves', *Bound.-Layer Meteor.*, **6**, 305-331.
- Davis, K. J., D. H. Lenschow, S. P. Oncley, C. Kiemle, G. Ehret, A. Giez, and J. Mann, 1997: 'Role of entrainment in surface-atmosphere interactions over the boreal forest'. *J. Geophys. Res.*, **102**,(D24) 29219-29230.
- Deardorff, J. W. and Willis, G. E., 1985: Further results from a laboratory model of the convective boundary layer. *Bound.-Layer Meteor.*, **32**, 205-236.
- Deardorff, J. W., 1972: Numerical investigations of neutral and unstable planetary boundary layers. *J. Atmos. Sci.*, **29**, 91-115.
- Deardorff, J. W., 1974: 'Three-dimensional numerical study of the height and mean structure of a heated planetary boundary layer', *Boundary-Layer Meteor.* **7**, 81-106.
- Deardorff, J. W., 1976: 'On the entrainment rate of a stratocumulus-topped mixed layer', *Quart. J. Roy. Meteor. Soc.* **102**, 563-582.
- Deardorff, j. W., 1980: 'Cloudtop entrainment instability', *J. Atmos. Sci.* **37**, 131-147.
- DeCosmo, J., Kastaros, K. V., Smith, S. D., Anderson, R. J., Oost, W. J., Bumke, K. and Chadwich, H., 1996: 'Air sea exchange of water vapor and the sensible heat: The humidity exchange over the Sea (HEXOS) results', *J. Geophys. Res.* **101**, 12001-12016.
- Dekate, M. V., 1968: 'Climatology of Sea and land breeze over Bombay', *Ind. J. Meteorol. Geophys.*, **19**, 497-504.
- Derbyshire, S. H.: 1999, 'Stable Boundary-Layer Modelling: Established Approaches and Beyond', *Boundary-Layer Meteorol.* **90**, 423-446.

- Desai, B.N., Rangachari, N. and Subramanian, S.K., 1976: 'Structure of low-level jet stream over the Arabian Sea and the Peninsula as revealed by observations in June and July during the monsoon experiment (MONEX) 1973 and its probable origin', *Indian J. Meteorol. Hydrol. Geophys.*, **27**, 263–274.
- Dias, N. L., Brutsaert, W., and Wesely, M. L.: 1995, 'Z-Less Stratification under Stable Conditions', *Boundary-Layer Meteorol.* **75**, 175–187.
- Dobson, F., and B. Toulany, 1991: 'On the Wind-Wave Coupling Problem, in *Directional Ocean Wave Spectra*', Edited by Robert C. Beal, pp. 22-29, The John Hopkins University Press, Baltimore.
- Driedonks, A. G. M, and Duynkerke, P. G., 1989: 'Current problems in the stratocumulus-topped atmospheric boundary layer', *Bound.-Layer Meteor.*, **46**, 275–303.
- Driedonks, A. G. M, and Tennekes, H., 1984: 'Entrainment effects in the well-mixed atmospheric boundary layer', *Bound.-Layer Meteor.*, **30**, 75–105.
- Dunkel, M., Hesse, L., Krugermeyer, L., Schriever, D. and Wuchnitz, J., 1974: 'Turbulent fluxes of momentum, heat and moisture in the atmospheric surface layer at sea during ATEX: Atlantic Trade Winds Experiment', *Bound.-Layer Meteor.*, **6**, 81-106.
- Dyer, A. J. and Bradley, E. F., 1982: 'Alternative analysis of flux-gradient relationships at the 1976 ITCE', *Bound.-Layer Meteor.*, **22**, 3–19.
- Dyer, A. J., and Hicks, B. B., 1982: 'Kolmogorov constants at the 1976 ITCE', *Bound.-Layer Meteor.*, **22**, 137–151.
- Dyer, A. J., Hicks, B. B., 1970: 'Flux-gradient relationships in the constant flux layer', *Quart. J. Roy. Met. Soc.*, **96**: 715-721.
- Ecklund, W. L., Carter, D. A., Balsley, B. B., 1988: 'A UHF wind profiler for the boundary layer: Brief description and initial results', *J. Atmos. Oceanic Technol.* **5**, 432-441.
- Enriquez, A. G. and Friehe, C. A., 1994: 'Summer and Winter Coastal Air-sea Interaction Study over the Northern California Shelf Using Bulk Aerodynamic Formulations', *Eos Trans, AGU*, Vol. 75, No. 3, 1994 Ocean Sciences Meeting, Jan. 18, 1994, page 52.

- Estoque, M. A., 1961: 'The Sea Breeze as a Function of the Prevailing Synoptic Situation', Scientific Report 1, Contract AF 19(604)-7484, 26 pp.
- Estoque, M. A., 1962: 'The sea breeze as a function of the prevailing synoptic situation', *J. Atmos. Sci.*, **19** 244–250.
- Findlater, J. 1966: Cross equatorial jet streams at low levels over Kenya, *Meteor. Mag*, **95**, 353-364.
- Findlater, J., 1967: 'Some further evidence of cross-equatorial jet streams at low level over Kenya', *Meteorological Magazine*, **96**, 216–219.
- Findlater, J., 1969: 'A major low level air current near the Indian Ocean during northern summer'. *Quart. J. Roy. Meteorol. Soc.*, **95**, 362 – 380
- Fisher, E. L.: 1960, 'An observational study of the Sea Breeze', *J. Meteorol.* **17**, 645-660.
- Francey, R. J. and Garratt, J. R. 1981: 'Interpretation of flux profile observations at ITCE 1976', *J. Appl. Meteorol.*, **20**, 603-618.
- Gadgil S, Joseph PV. 2003. On breaks of the Indian monsoon. *Proc. Ind. Acad. Sci (Earth. Plan. Sci.)* **112**, 4, 529-558.
- Gadgil, S., and Mohanty, U. C., 2000: BOBMEX-Preface, *Earth Planet. Sci.*, **109**, 205.
- Gage, K.S. and Balsley, B.B., 1978: 'Doppler radar probing of clear atmosphere', *Bull. Amer. Meteorol. Soc.*, **59**, 1074–1093.
- Gage, K.S., 1990: 'Radar observations of the free atmosphere: structure and dynamics', in *Atlas, D. (Ed.), Radar in Meteorology*. American Meteorol. Soc., Boston, pp. 534– 565.
- Gage, K.S., Williams, C.R. and Ecklund, W.L., 1994: 'UHF wind profilers: a new tool for diagnosing tropical convective cloud systems', *Bull. Amer. Meteorol. Soc.*, **75**, 2289– 2294.
- Garratt, J. R., 1992: 'The Atmospheric Boundary Layer', *Cambridge University Press, Cambridge*, 316pp.
- Geernaert, G. L., Katsaros, K. B. and Richter, K., 1986: 'Variation of drag coefficient and its dependence on sea state', *J. Geophys. Res.* **96**, 3391-3400.

- Gill, A. E., 1982: '*Atmosphere-Ocean Dynamics*', Academic Press, New York.
- Godfrey, J. S. and Lindstorm, E. J., 1989: On the heat budget of the equatorial west pacific Surface mixed layer, *J. Geophys. Res.*, **94**, 8007-8017
- Godfrey, J. S., and A. C. M. Beljaars, 1991: 'On the turbulent fluxes of buoyancy, heat and moisture at the air-sea interface at low wind speeds', *J. Geophys. Res.*, **96**, 22043 - 22048.
- Goel, M. and Srivastava, H. N., 1990: 'Monsoon Trough Boundary Layer Experiment (MONTBLEX)', *Bull. Am. Meteor. Soc.* **71** 1594–1600.
- Gossard, E.E., Wolfe, D.E., Moran, K.P., Paulus, R.A. anderson, K.D. and Rogers, L.T., 1998: 'Measurements of clear-air gradients and turbulence properties with radar wind profilers', *J. Atmos. and Oceanic Technol.*, **15**, 321–342, 1998.
- Goswami, B. N. and Ajaya Mohan, R. S., 2001: 'Intraseasonal oscillations and interannual variability of the Indian summer monsoon', *J. Climate*, **14**, 1180-1198.
- Goswami, B. N. and Rajagopal, E. N., 2004: Indian Ocean surface winds from NCMRWF analysis as compared to QuikSCAT and moored buoy winds, *Proc. Indian Acad. Sci. (Earth Planet. Sci.)*, **112**, 61-77.
- Goswami, B. N., Ajayamohan, R. S., Xavier, P. K. and Sengupta, D., 2003: 'Clustering of Low Pressure Systems During the Indian Summer Monsoon by Intraseasonal Oscillations', *Geophys. Res. Lett.*, **30**, doi:10.1029/2002GL016734.
- Goswami, B. N., Sengupta, D. and Suresh Kumar, R., 1998: 'Intraseasonal oscillations and interannual variability of surface winds over the Indian monsoon region', *Proc. Ind. Acad. Sci. (Earth and Planetary Sci.)*, **107**, 45-64.
- Graham, N. E., and Barnett, T. P., 1987: 'Sea surface temperature, surface wind divergence and convection over tropical oceans, *Science*, **238**, 657-659.
- Gruber, A and Krueger, A. F., 1984: 'The status of the NOAA outgoing Longwave radiation data set, *Bull. Am. Meteorol. Soc.*, **65**, 958-976
- Harriss, R. C., M. Garstang, S. C. Wofsy, S. M. Beck, R. J. Bendura, J. Coelho, J. Drewry, J. Hoell, P. Matson, R. McNeal, L. Molion, R. Navarro, V. Rabine,

- and R. Snell., 1990: 'The Amazon Boundary Layer Experiment: Wet Season 1987 (ABLE 2B)', *J. Geophys. Res.*, **95**: 16721-16736.
- Hastenrath S and Lamb, P. J., 1979: 'Climatic atlas of the Indian Ocean, Part I: Surface climate and atmospheric circulation'. University of Wisconsin Press, Madison, USA.
- Hatcher, R. W. and Sawyer, J. S., 1947: 'Sea breeze structure with particular referenc to temperature and water vapour gradient and associated radio ducts', *Quart. J. Roy. Meteorol. Soc.*, **73**, 391-406.
- Haugen, D. A., 1973: *Workshop on Micrometeorology*. Amer. Meteor. Soc., 392 pp.
- Haugen, D. A., Kaimal, J. C. and Bradley, E. F., 1971: 'An experimental study of Reynolds stress and heat flux in the atmospheric surface layer', *Quart. J. Royal. Meteorol. Soc.*, 168-180.
- Hellerman, S. and Rosenstein, M., 1983: 'Normal monthly mean wind stress over the world ocean with error estimates', *J. Phys. Oceanogr.*, **4**, 145-167.
- Hicks, B. B., 1976: 'Wind profile relationships from the "Wangara" experiments.' *Quart. J. Roy. Meteor. Soc.*, **102**, 535-551
- Hicks, B. B., 1981: 'An examination of turbulence statitics in the surface boundary layer', *Boundary-Layer Meteorol*, **21**, 389-402.
- Hildebrand, P. H., and R. S. Sekhon, 1974: 'Objective determination of the noise level in Doppler spectra', *J. Appl. Meteor.*, **13**, 808-811.
- Hinze, J. O., 1959: 'Turbulence: An Introduction to its Mechanism and Theory', McGraw-Hill, 586 pp.
- Hogstorm, U., 1988: Non dimensional wind and temperature profinles in the atopspheric surface layer : A revaluation, *Boundary Layer Meteorol.*, **42**, 55-78.
- Hogstrom, U., 1985: 'Von Karman's constant in atmospheric boundary layer now revevaluated', *J. Atmos. Sci.*, **42** , 263 - 270 .5
- Högström, U., 1996: 'Review of some basic characteristics of the atmospheric surface layer', *Boundary-Layer Meteorology*, **78**: 215-246.

- Holloway, C. L., R.J. Doviak, R.J. Latatits, S.A. Cohn, and J. Van Baelen., 1995: 'Techniques to analyze signals from spaced antenna wind profilers', *27th Conference on Radar Meteorology*, Vail, Colorado, October 1995, 323-325.
- Holstag, A. A. M. and Moeng, C. H., 1991: 'Eddy diffusivity and countergradient transport in the convective atmospheric boundary layer', *J. Atmos. Sci.*, **48**, 1690-1698.
- Holt, S.E., Koseff, J.R., and Ferziger, J.H., 1992: 'A numerical study of the evolution and structure of homogeneous stably stratified sheared turbulence'. *J. Fluid Mech.*, **237**, 499-539.
- Holt, T and ~~Raman, S~~^{Sethuraman, T}, 1987: The study of mean boundary layer structures over the arbean sea and te Bay of Bengal durin active and break monsoon periods, *Boundary-Layer Meteorol.*, **38**, 73-94.
- Holt, T. and Sethuraman, T., 1987: 'A comparison of the significant features of the marine boundary layer over the east centrak Aranian Sea and north central Bay of Bengal during MONEX-79', *Mausam*, **38**, 171-176.
- Hsu, S. A., 1988 : Coastal Meteorology. *Academic Press*, pp260.
- Hunt, J. C. R., Kaimal, J. C., and Gaynor, J. E.: 1985, 'Some Observations of Turbulence Structure in Stable Layers', *Quart. J. Roy. Meteorol. Soc.* **111**, 793-815.
- Izumi, Y., and JS Caughey, 1976: 'Minnesota 1973 atmospheric boundary layer experiment data report'. AFCRL-TR-76-0038, 28 pp.
- Izumi, Y.: 1971: 'Kansas 1968 Field Program Data Report', Environmental Research Papers No. 369, AFCRL-72 0041, Air Force Cambridge Research Lab., Bedford, Mass.
- Jambunathan, R., and Ramamurty, K., 1975: ' *Indian J. Met. Geophys.*, **25**, 377-410.
- Jamima, P. and J. Lakshminarasimhan.: 2004, 'Numerical simulation of sea breeze characteristics observed at tropical coastal site, Kalpakkam', *Proc. Indian Acad. Sci. (Earth Planet. Sci.)*, **113**, 197-209.
- Joseph P.V. and Raman, P. L., 1966: 'Existence of low level westerly jet- stream over peninsular India during July'. *Indian J. Meteorol. Geophys.*, **17**, 407-410

- Joseph, P.V. and Sijikumar, S., 2004: 'Intra-seasonal variability of the Low-Level Jet stream of the Asian summer monsoon'. *J. Climate*, **17**, 1449–1458.
- Kadar, B. A. and Yaglom, A. M., 1990: 'Mean fields and fluctuation moments in unstably stratified turbulent boundary layers', *J. Fluid Mech.*, **212**, 637-662.
- Kagan, B. A., 1995: '*Ocean-Atmosphere Interaction and Climate Modelling*'. Cambridge University Press, 377 pp.
- Kaimal, J. C., 1973: 'Turbulent spectra, length scale and structure parameters in the stable surface layer', *Boundary-Layer Meteorol*, **4**, 289-309
- Kaimal, J. C., Wyngaard J. C., Izumi, Y. and Cote, A. R., 1972: 'Spectral characteristics of surface layer turbulence', *Q. J. R. Meteorol. Soc.*, **98**, 563-689.
- Kaimal, J. C., Wyngaard, J. C., Haughen, D. A., Coté, O. R., Izumi, Y., Caughey, S. J. and Readings, C. J., 1976: 'Turbulence Structure in the Convective Boundary Layer', *J. Atmos. Sci.*, **33**, 2152-2168.
- Kalnay, E., Kanamitsu, M., Kirtler, R., Collins, W., Deaven, D., Gandin, L., Iredell, M., Saha, S., White, G., Woollen, J., Zhu, Y., Chelliah, M., Ebisuzaki, W., Higgins, W., Janowiak, J., Mo, K. C., Ropelewski, C., Wang, J., Leetma, A., Reynolds, R., Jenne, R. and Joseph, D., The NCEP/NCAR 40-year reanalysis project. *Bull. Am. Meteorol. Soc.*, **77**, 437-471, 1996.
- Kaltenbach, H. - J., Gerz, T., and Schumann, U. 1994: 'Large-Eddy Simulation of Homogeneous Turbulence and Diffusion in Stably Stratified Shear Flow', *J. Fluid Mech.*, **280**, 1-40.
- Keen, C. S. and Lyons, W. A., 1978: 'Lake/land breeze circulations on the western shore of lake Michigan', *J. Appl. Meteorol.*, **17**, 1843-1855.
- Kiladis, G. N. and Wheeler, M. 1995: Horizontal and vertical structure of observed tropospheric equatorial Rossby waves *J. Geophys. Res.*, **100(D)**, 22981-22997
- Kimura, F.: 1983, 'A numerical simulation of local winds and photochemical air pollution (I): Two-dimensional land and sea breeze', *J. Meteor. Soc. Japan*, **61**, 862-878.

- Kitada, T.: 1987, 'Turbulence Structure of Sea Breeze Front and Its Implication in Air Pollution Transport- Application of k- Λ Turbulence Model', *Bound. Layer Meteor.* **41**, 217-239.
- Krishnamurti, T. N. and Ardunuy, P., 1980: 'The 10 - 20-day westward propagating mode and 'Breaks in the monsoons'', *Tellus*, **32**, 15-26, 1980.
- Krishnamurti, T. N. and Subramaniam, D. 1982: 'The 30-50 day mode at 850 mb during MONEX', *J. Atmos. Sci.*, **39**, 2088-2095
- Krishnamurti, T. N., Kanamitsu, M., Cesulski, B. and Mathui, M. B., 1973: Florida stae university tropical prediction model, *Tellus*, **6**, 523-535.
- Krishnamurty, T. N., Oosterhof, D. K., and Mehta, A. V., 1988: 'Air sea interaction on the time scale of 30-50 days', *J. Atmos. Sci.*, **45**, 1304-1322.
- Kuettner, JP, and DE Parker, 1976: 'GATE: report of the field phase', *Bull. Amer. Met. Soc.*, **57**, 11-27
- Kunhikrishnan, P. K., Senguptha, K. Ramachandran, R., Prakash, J. W. J. and Nair, K. N., 1993: 'Structure of the thermal internal boundary layer over Thumba, India', *Ann. Geophys.*, **11**, 52-60.
- Kusaka H., F. Kimura, H. Hirakuchi and M. Mizutori.: 2000, 'The Effects of Land-Use Alteration on the Sea Breeze and Daytime Heat Island in the Tokyo Metropolitan Area', *J. Meteorol. Soc. Japan.* **78**, 405-420.
- Kusuma, G. R., Raman, S., Prabhu, A. and Narasimha, R.: 1995, 'Turbulent heat flux variation over the monsoon trough region during MONTBLEX-90', *Atmos. Environ.* **29**, 2113-2129.
- Kusuma, G. R., Sethuraman, T. and Prabhu, A., 1991: 'Boundary layer heights over the monsoon trough region during active and break phases', *Boundary-Layer Meteorol.*, **57**, 129-138.
- LeMone, M. A., R. L. Grossman, R. L. Coulter, M. L. Wesley, G. E. Klazura, W. B. G. S. Poulos, J. K. Lundquist, R. H. Cuenca, S. F. Kelly, E. A. Bandes, S. P. Oncley, R. T. McMillan, and B. B. Hicks, 2000: 'Land-atmosphere interaction research, early results, and oppur tunities in the walnut river watershed in southeast kansas'. *Bull. Amer. Met. Soc.*, **81**, 757-780.

- LeMone, M. A., R. L. Grossman, R. T. McMillan, K.-N. Liou, S. Ou, S. McKeen, W. Angevine, K. Ikeda, and F. Chen, 2002: 'CASES-97: Late morning warming and moistening of the convective boundary layer over the Walnut River watershed'. *Bound.-layer Meteorol.*, **104**, 1–52.
- Lenschow, D. H. , 1973: 'Two examples of planetary boundary layer modification over the Great Lakes'. *J. Atmos. Sci.*, **30**, 568–581.
- Lenschow, D. H., 1986: 'Aircraft Measurements in the Boundary Layer. A chapter in Probing the Atmospheric Boundary Layer', edited by D. H. Lenschow, American Meteorological Society, Boston, MA, 39–55.
- Leopold, I. B., 1949: 'the interaction of trade wind and Sea breeze, Hawaii', *J. Meteorol.*, **6**, 312-320.
- Lettau, H. H. and Davidson, B.: 1957, 'Exploring the Atmosphere's First Mile', Pergamon Press, U.K. 578 pp.
- Li, F., W. Large, W. Shaw, E. J. Walsh, and K. Davidson, 1989: 'Ocean radar backscatter relationship with near-surface winds: A case study during FASINEX', *J. Phys. Oceanogr.*, **19**, 342–353.
- Lienhard V and Van Atta, C. W., 1990: 'The decay of turbulence in thermally stratified flow', *J. Fluid Mech.* **210**, 57.
- Lilly, D. K.: 1968, 'Models of Cloud-Topped Mixed Layer under a Strong Inversion', *Quart. J. Roy. Meteorol. Soc.* **94**, 292–309.
- Lumely, J. L. and Panofsky, H. A., 1964: '*The structure of the atmospheric turbulence*', Interscience, Newyork.
- Madhu C. R., 2004: '*Radar studies on the atmospheric boundary layer and precipitation over a tropical station Gadanki*', Ph.D Thesis, Sri Venkateswara University, India.
- Mahrt, L. 1999: 'Stratified atmospheric boundary layers', *Boundary-Layer Meteorol.*, **90**, 375-396.
- Mahrt, L. and M. Ek., 1993: 'Spatial variability of turbulent fluxes and roughness lengths in HAPEX-MOBILHY', *Bound.-Layer Meteor.*, **65**, 381-400

- Mahrt, L., R. C. Heald, D. H. Lenschow, B. Stankov, and I. Troen, 1979: 'An observational study of the nocturnal boundary layer'. *Boundary-Layer Meteor.*, **17**, 247-264.
- Manabe, S., Hahn, D. G. and Holloway, J., 1974: The seasonal variation of the tropical circulation as estimated by a global model of the atmosphere, *J. Atmos. Sci.*, **32**, 48-83.
- Maorwal, S and Seetharamayya, P., 2003: 'Thermodynamic structure of the marine atmosphere over the region 80-87°E along 13°N during August (Phase II) BOBMEX-99', *Proc. Indian Acad. Sci. (Earth Planet. Sci.)*, **112**, 295-312.
- McPherson, R. D.: 1970, 'A Numerical Study of the Effect of a Coastal Irregularity on' the Sea Breeze', *J. Appl. Meteorol.* **9**, 767-777.
- Mitra, A. P., 1999: 'INDOEX (India) Introductory note', *Curr. Sci.*, **76**, 886-889.
- Mitra, A. P., 2001: 'Introductory note', *Curr. Sci.*, **80**, 3-6.
- Mitra, A. P., Jayaraman, A., Krishnamurthy, B. V., Mohanty, U. C., Viswanathan, G., 2001: 'INDOEX – India program synthesis report', INDOEX-TR-02-2K, National steering committee, NPL, CSIR, Govt. of India, Dr. K S Krishnan Marg, New Delhi-110012, 52pp.
- Mitsumoto, S., H. Ueda, and H. Ozoe, 1983: 'A laboratory experiment on the dynamics of the land and sea breeze'. *J. Atmos. Sci.*, **40**, 1228-1240.
- Moeng, C.-H. , 1984. A large-eddy simulation model for the study of planetary boundary-layer turbulence. *J. Atmos. Sci.*, **41**:2052-2062.
- Moeng, C.-H. and JC Wyngaard 1989: Evaluation of turbulent transport and dissipation closures in second-order modeling. *J. Atmos. Sci.*, **46**, 2311-2330.
- Moeng, C.-H., 1986, Large-eddy simulation of a stratus-topped boundary Part I: Structure and budgets. *J. Atmos. Sci.*, **43**, 2886-2900.
- Moeng, C.-H., 1987: Large-eddy simulation of a stratus-topped boundary layer. Part II: Implications for mixed-layer modeling. *J. Atmos. Sci.*, **44**, 1605-1614.
- Moeng, C.-H., and M. A. LeMone, 1995: 'Atmospheric planetary boundary layer research in the U.S.: 1991-1994', *U.S. National Report to the IUGG 1991-1994, Reviews of Geophysics, Supplement*, 923-931.

- Mohanty, U. C. and Das, S., 1986: 'On the structure of the atmosphere during suppressed and active periods of convection over the Bay of Bengal', *Proc. Indian Acad. Sci. (Earth Planet. Sci.)*, **52** 625–640.
- Mohanty, U. C. and Mohan Kumar, 1990: 'A study of surface marine boundary layer fluxes over the Indian seas during different epochs of Asian Summer Monsoon', *Atmos. Environ.*, **24A**, 823-828.
- Monin, A. S. and Obukhov, A. M., 1954: 'Basic laws of turbulent mixing in the atmosphere near the ground', *Tr. Akad. Nauk SSSR Geoph. Inst.*, No.24(151), 1963-1987.
- Monin, A. S. and Yaglom, A. M., 1971: '*Statistical hydrodynamics*', (Translation Ed Lumby, J. L.) MIT press Cambridge.
- Nagar, S. G., Tyagi, A., Seetaramayya, P. and Singh, S. S., 2001: *Boundary-Layer Meteorol.*, **98**, 297–314.
- Nakane, N., and Y. Sasano.: 1986, 'Structure of a sea breeze front revealed by scanning lidar observations', *J. Meteorol. Soc. Japan*. **64**, 787-792.
- Narasimha R, Sikka DR, Prabhu A. 1997. *The Monsoon Trough Boundary Layer*. Bangalore, India: Indian Acad. Sci. 422 pp.
- Narayanan, V.: 1967, 'An observational study of the Sea Breeze at an equatorial coastal station', *Ind. J. Meteorol. And Geophys.* **18**, 497-504.
- NASA Quick Scatterometer, QuikSCAT Science Data Product, *User's Manual, Overview & Geophysical Data Products*, Version 2.0-Draft, Jet Propulsion Laboratory, California Institute of Technology, Doc. D-18053, May 2000
- Neelin J D, Held I M and Crook K H., 1987: 'Evaporation wind feedback and low frequency variability in the tropical atmospheres', *J. Atmos. Sci.* **44** 2341–2345.
- Nicholls, S., 1984: 'The dynamics of stratocumulus: aircraft observations and comparisons with a mixed layer model', *Quart. J. Roy. Meteor. Soc.*, **110**, 783–820.
- Nicholls, S., 1985: 'Air craft observations of the Ekman layer during the joint air sea interaction experiment', *Quart. J. Roy. Meteorol. Soc.* **111**, 391-426.

- Niewstadt, F. T. M, 1984: 'Turbulent structure of the stable nocturnal boundary layer', *J. Atmos. Sci.*, **41**, 2202-2216.
- Numaguti, A. 1995: Characteristics of 4- to 20-day period disturbances observed in the equatorial Pacific during the TOGA COARE IOP. *J. Meteorol. Soc. Japan*, **73**, 353-377
- Ohashi, Y. and Hideji Kida.: 2001, 'Observational Results of the Sea Breeze with a Weak Wind Region over the Northern Osaka Urban Area', *J. Meteorol. Soc. Japan*. **79**, 949-955.
- Oke, T. R.: 1978: '*Boundary Layer Climates*', Methuen and Co., London, United Kingdom, 372 pp.
- Ozoe, H., Shibata, T., sayama, H. and Uyeda, H., 1983: 'Characteristics of the air pollution in the presents of land and sea breeze – A numerical experiment', *Atmos. Environ.*, **17**, 35-42.
- Panofsky, H. A. and Dotton, J. A., 1984: '*Atmospheric turbulence*', Wiley, New York.
- Pant, M. C., 1978: 'Vertical structure of the planetary boundary layer over the western Indian ocean during the Indian summer monsoon as revealed by ISMEX data', *Indian J. Met. Hydrol. And Geophys.*, **29**, 88-98.
- Parasnis S.S., 1991: 'Convective boundary layer during active and weak conditions of the summer monsoon', *J. Atmos. Sc*, **48**, 7, 999-1002.
- Parasnis, S. S. and Morwal, S. B., 1991: 'Convective boundary layer over the Deccan Plateu, India during summer monsoon', *Boundary-Layer Meteorol.*, **54**, 59-68.
- Parasnis, S. S., 1991: 'Convective boundary layer during Active and break conditions of the summer monsoon', *J. Atmos. Sci.*, **48**, 999-1002.
- Parasnis, S. S., Morwal, S. B. and Vernekar, K. G., 1991: 'Convective boundary layer in the region of monsoon trough – A case study', *Adv. Atmos. Sci.*, **8**, 505-509.
- Paulsen, C. A.: 1970, 'The mathematical representation of wind and temperature profiles in the unstable atmospheric surface layer', *J. Appl. Meteorol.* **9**. 857-861.
- Pearson, R. A.: 1973, 'Properties of the Sea Breeze front as shown by a numerical model', *J. Atmos. Sci.* **30**, 809-830.

- Pielke, R.A., 1974: A three-dimensional numerical model of the sea breezes over south Florida. *Mon. Wea. Rev.*, **102**, 115-139.
- Pillai, J.S., Sexana, S. and Vernekar, K.G., 1998: 'Diurnal variability of meteorological parameters in the land surface interface', *Boundary-Layer Meteorol.*, **89**, 197-209.
- Prakash, J. W. J., 1993: '*Atmospheric boundary layer studies at Thumba*', Ph.D Thesis, University of Kerala, India
- Prakash, J. W. J., Radhika, R., Narayanan Nair, K., Senguptha, K. and Kunhikrishnan, P. K., 1992: 'On the structure of the sea breeze fronts observed neat the coasline of Thumba', *Bound.-Layer Meteor.*, **59**, 111-124.
- Prakash, J. W. J., Ramachandran, R., Nair, K. N., Senguptha, K. and Kunhikrishnan, P. K., 1993: 'On the spectral behavior of Atmospheric bopoundary layer parameters at Thumba, India' *Quart. J. Roy. Meteorol. Soc.*, **119**, 187-192.
- Prandtl, L., 1949: 'Report on investigation of developed turbulence, NACA TM-1231.
- Praveena, K. and Kunhikrishnan, P.K., 2004: 'Temporal variations of ventilation coefficient at a tropical Indian station using UHF wind profiler', *Current Sci.*, **86**(3), 447-451.
- Praveena, K., Kunhikrishnan, P.K. Nair, S.M., Sudha, R., Jain, A.R. and Kozu, T., 2003: 'Atmospheric boundary layer observations over Gadanki using lower atmospheric wind profiler: Preliminary results'. *Current Sci.*, **85**(1), 75-79.
- Praveena, K., P. K. Kunhikrishnan and S. Muraleedharan Nair., 2005: 'Time height evolution of intra seasonal oscillation in the tropical lower atmosphere: Multi level wind observations using UHF radar', *Geophys. Res. Lett.* **32**, doi: 10.1029/2004GL022019, 2005.
- Quilfen, Y., Chapron, B. & Vandemark, D., 2001: 'The ERS scatterometers wind measurement accuracy: evidence of seasonal and regional biases', *J. Atmos. Oceanic Technol.*, **18**, pp. 1684-1697.
- Radhika, R., 1994: '*Atmospheric boundary layer studies at Thumba*', Ph.D thesis, Unversity of Kerala, India.

- Raghukumar, A., Purnachandra Rao, M. and Sreeramamurthy, J., 1986: 'The effect of sea breezes on atmospheric stability as observed with acoustic sounders', *Boundary Layer Meteorol.*, **35**, 303-308.
- Ramadoss, L. A., 1931: 'The Sea breeze at Karachi', in *scientific note*, vol. V., India Meteorology Department, Delhi, India.
- Ramage, C. S., 1971: '*Monsoon Meteorology*', Academic Press, New York, pp 296.
- Ramakrishnan, K. P. and Jambunathan, R., 1958: 'Sea breeze and maximum temperature in Madras', *Ind. J. Meteorol. Geophys.*, **9**, 349-358.
- Ramana, 2001: '*Studies on marine, coastal and inland boundary layer*', Ph.D Thesis, Kerala University, India.
- Ramana, M. V., Krishnan, P. and P. K. Kunhikrishnan.: 2004, 'Surface boundary layer characteristics over a tropical inland station: Seasonal features', *Boundary-Layer Meteorol.* **111**, 153-175.
- Ramanathan, H. R., 1937: 'The structure of Sea breeze at Pune, In Calcutta, *India Meteorology Department*, scientific notes, vol. III.
- Ramanathan, R. and Subbaramayya, I., 1965: 'Sea breeze at Vishakhapatanam', *Ind. J. Meteorol. Geophys.*, **16**, 241-248.
- Ramanathan, V., Crutzen, P. J., Coakley, J., Dickerson, R., Heymsfield, A., Kiehl, J., Kley, D., Krishnamurty, T. N., Kuettner, J., Lelieveld, J., Mitra, A. P., Prospero, J., Sadourny, R., Valero, F. P. J., and Woodfridge, E. L., 1995: 'Indian Ocean Experiment (INDOEX) white paper, C, *Scripps Institution of Oceanography*, UCSD, La Jolla, California.
- Ramanathan, V., et al, 1996: 'Indian Ocean Experiment (INDOEX); A multi agency proposal for field experiment in the Indian Ocean', (*C⁴ Publication No. 162, Scripps institution of Oceanography, La Jolla, CA*).
- Ramanathan, V., et al., 2001: 'The Indian Ocean Experiment: wide spread haze from south and southeast Asia and its climate forcing, *J. Geophys. Res.*, **106**, 28371-28398.
- Ramanathan, Y., 1978: 'A study of the atmospheric boundary layer over the Arabian Sea', *Indian J. Met. Hydrol. & Geophys.*, **29**, 643-654.

- Rao, K. G, 1988: Diagnosis of dominant forcing factors for large scale vertical velocities during active and break phases of monsoon, *Pure Appli. Geophys.*, **127**, 669-693.
- Rao, Y.P. 1976: 'Southwest Monsoon, Meteorological Monograph', Synoptic Meteorology No. 1/1976, India Meteorological Department, Pune-411005, India.
- Reddy, K.K., Kozu, T., Ohno, Y., Nakamura, K., Srinivasula, P., Anandan, V.K., Jain, A.R., Rao, P.B., Ranga Rao, R., Viswanthan, G. and Rao, D.N., 2001: 'Lower atmospheric wind profiler at Gadanki, Tropical India: initial result'. *Meteorol. Z.*, **10**, 457-466.
- Rogers, R.R., Ecklund, W.L., Carter, D.A., Gage, K.S. and Ethier, S.A., 1993a: 'Research Applications of a boundary-layer wind profiler'. *Bull. Amer. Meteorol. Soc.*, **74**, 567- 580,
- Rotunno, R.: 1983, 'On the linear theory of the Land and Sea Breeze', *J. Atmos. Sci.* **40**, 1999-2009.
- Roy, A. K., 1941: 'The sea breeze at Madras', in *scientific notes*, vol. **VIII**, India Meteorology Department, Delhi, India.
- Sadani L.K. and Kulkarni J.R., 2001: 'Study of coherent structures in the atmospheric surface layer over short and tall grass', *Boundary-Layer Meteorol.*, **99**, 317-334.
- Sam, N V., Mohanty, U. C. and Satyanarayan, A. N. V., 2003: Simulation of marine boundary layer characteristics using a 1-D PBL model over the Bay of Bengal during BOBMEX-99, *Proc. Indian Acad. Sci. (Earth Planet. Sci.)*, **112**, 185-204.
- Sato, T., 1989: 'Radar principles', in Fukao, S., (Ed.), *MAP handbook*, SCOSTEP Secr., Urbana,III., **30**, 19-53, 1989.
- Satyanarayana A N V, Mohanty U C, Sam N V, Basu S and Lykossov V N., 2000 'Numerical simulation of the marine boundary characteristics over the Bay of Bengal as revealed by BOBMEX-98 Pilot Experiment', *Proc. Indian Acad. Sci. (Earth Planet. Sci.)* **109** 293-303.

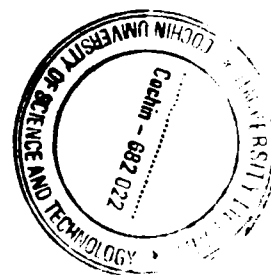
- Schumann, U. and Gerz, T.: 1995, 'Turbulent Mixing in Stably Stratified Shear Flows', *J. Appl. Meteorol.* **34**, 33–48.
- Segal, M., J. H. Cramer, R. A. Pielke, J. R. Garratt, and P. Hildebrand, 1991: 'Observational evaluation of the snow breeze'. *Mon. Wea. Rev.*, **119**, 412–424.
- Sellers, P.J., F.G. Hall, G. Asrar, D.E. Strebel, and R.E. Murphy., 1988: 'The first ISLSCP field experiment (FIFE)', *Bull. Amer. Meteorol. Soc.*, **69**, 22-27.
- Sengupta, D., Senan, R. and Goswami, B. N., 2001: 'Origin of intraseasonal variability of circulation in the tropical central Indian Ocean'. *Geophys. Res. Lett.* **28**, 1267-1270.
- Sha, W., T. Kawamura, and H. Ueda.: 1991, 'A numerical study on sea-land breezes as a gravity current: Kelvin-Helmholtz billows and inland penetration of the sea-breeze front' *J. Atmos. Sci.* **48**, 1649-1665.
- Shaw, W. J. and Businger, J. A., 1985: 'Intermittency and organisation of turbulence in the near neutral marine atmospheric boundary layer', *J. Atmos. Sci.* **42**, 2563-2584.
- Shinoda, T., Hendon, H. H. and Glick, J. G., 1998: Intra seasonal sea surface temperature variability in the tropical [pacific and Indian ocean, *J. Climate*, **11**, 1685-1702.
- Shukla, J., Strauss, D., Randall, D., Sud, Y. and Marx, L. 1981: Winter and summer simulations with the GLA climate model, NASA technical memo. 83866, p282.
- Sikka, D. R. and Gadgil, S. 1980: On the maximum cloud zone and the ITCZ over Indian longitudes during southwest monsoon. *Mon. Weather Rev.*, **108**, 1840-1853
- Sikka, D. R. and P. Sanjeeva Rao, 2000: Bay of Bengal Monsoon Experiment (BOBMEX)—A component of the Indian Climate Research Programme (ICRP). *Proc. Indian Acad. Sci. (Earth Planet. Sci.)*, **109**, 207–209.
- Sikka, S. D. and Mathur, M. B., 1965: 'Proc Symp. Meteorol. Results of IIOE, IITM, Pune, 55-67.
- Sikka, S. D. and Narasimha, R. K., 1995: 'Genesis of the monsoon trough boundary layer experiment

- Simpson, J E 1994: '*Sea Breeze and local wind* (Cambridge University Press).
- Sivaramakrishnan, S., Saxena, S. and Vernekar, K. G.: 1992, 'Characteristics of turbulent fluxes of sensible heat and momentum in the surface boundary layer during the Indian summer monsoon', *Boundary-Layer Meteorol.* **60**, 95-108.
- Sivaramakrishnan, T. R. and Rao, P. S., 1989: 'Sea breeze features over Sriharikota', *Meteorol. Magazine*, **118**, 64-67.
- Smith S. D., 1988: 'Coefficients for sea surface wind stress, heat flux and wind profiles as a function of wind speed and temperature'. *J. Geophys. Res.*, **93**, 15467-15472.
- Smith, S. D. and Coauthors, 1990: 'GAPEX: A ground-based atmospheric profiling experiment'. *Bull. Amer. Meteor. Soc.*, **71**, 3.
- Smith, S. D., Anderson, R. J., Oost, W. A., Kraan, C., Maat, N., DeCosmo, J., Katsaros, K. B., Davidson, K. L., Bumke, K., Hasse, L. and chadwick, H. M., 1992: 'Sea surface wind stress and drag coefficients: The HEXOS results', *Boundary-Layer Meteorol.*, **60**, 109-142.
- Smith, S. D., Fairall, C. W., Feernaert, G. L. and Hasse, L., 1996b: 'Air sea fluxes: 25 years of progress. *Bound.-Layer Meteor.*, **78**, 247-290.
- Stage, S., and J. Businger, 1981: 'A model for entrainment into a cloud-topped marine boundary layer. Part I: Model description and application to a cold-air outbreak episode'. *J. Atmos. Sci.*, **38**, 2213-2229.
- Stillinger, D. C., Helland, K. N., and Van Atta, C. W.: 1983, 'Experiments on the Transition of Homogeneous Turbulence to Internal Waves in a Stratified Fluid', *J. Fluid Mech.* **131**, 91-122.
- Stull, R. B. 1997: An introduction to boundary layer meteorology, *Kluwer Academic Pub.*, 664pp.
- Stull, R. B., 1988: 'An introduction to boundary layer meteorology', *Kluwer Academic Publishers*, The Netherlands, 666pp.
- Stull, R. B., 1993: 'An introduction to Boundary layer meteorology', *Kluwer Acad. Pub.*, The Netherlands, 666pp.
- Stull, R.B., and E.W. Eloranta., 1984: 'Boundary Layer Experiment - 1983', *Bulletin of the American Meteorological Society*, **65**, 450-456, 1984.

- Sumabai, K. C., 1997: '*Dynamics of atmospheric boundary layer*', Ph.D thesis, University of Kerala, India.
- Sunil, T., 1997: '*Study of coastal atmospheric boundary layer*', Ph.D thesis, University of Kerala, India.
- Torrence, C., and G. P. Compo, 1998: 'A practical guide to wavelet analysis', *Bull. Am. Meteorol. Soc.*, **79**, 61–78.
- Troen, I. B. and Mahrt, L., 1986: 'A simple model of the Atmospheric boundary layer: sensitivity to surface evaporation', *Bound.-Layer Meteorol.*, **37**, 129-148.
- Tsvang, L.R. et al., 1985: 'International turbulence comparison experiment (ITCE-81)', *Boundary-Layer Meteorol.*, **31**: 325-348.
- Van Baelen, J., C.L. Holloway, and S.B. Copeland, 1995: 'Atmospheric boundary layer investigations with a UHF Doppler/interferometric wind profiler', in Proc. 1994 International Geoscience and Remote Sensing Symposium (IGARSS), Pasadena, CA, Aug. 1994, 2248-2450.
- Vogelezang, D. H. P. and A. A. M. Holtslag, 1996: 'Evaluation and Model Impacts of Alternative Boundary-Layer Height Formulations', *Boundary-Layer Meteorol.*, **81**, 245-269.
- Volkov, Y. A., Augstein, E. and Hinzpeter, H., 1982: 'The structure of Atmospheric boundary layer under different conditions', *The GARP Atlantic tropical Experiment (GATE) monograph*, GARP Publ. Ser., **25**, 345-387.
- Wakimoto, R. M., and N. T. Atkins.: 1994, 'Observations of the sea-breeze front during CaPE. Part I: Single Doppler, satellite, and cloud photogrammetry analysis', *Mon. Wea. Rev.* **122**, 1092-1113.
- Webb, E.K., 1970: 'Profile relationships: the log-linear range and extension to strong stability', *Q.J. R. Met. Soc.* **96** 67-90.
- Weber, A. H., and R. J. Kurzeja, 1991: Nocturnal planetary boundary layer structure and turbulence episodes during the project STABLE field program. *J. Appl. Meteorol.*, **30**, 1117–1133.
- Webster, P. J. and Lukas, R. 1992: TOGA COARE: The coupled ocean atmosphere response experiment, *Bull. Amer. Meteor. Soc.*, **73**, 1377-1416.

- Webster, P. J., E. F. Bradley, C. W. Fairall, J. S. Godfrey, P. Hacker, R. A. Hopuze jr., R. Lukas, Y. Serra, J. M. Hummon, T. D. M. Lawrence, C. A. Russel, M. N. Ryan, K. sahami, P. Zuidema, 2002: 'The Joint Air-Sea Monsoon Interaction Experiment (JASMINE) Pilot Study', *Bull. Amer. Met. Soc.*, **83**, 1603-1630.
- Webster, P. J., V. O. Magana, T. N. Palmer, J. Shukla, R. T. Tomas, M. Yanai, and T. Yasunari., 1998: 'Monsoons: Processes, predictability and the prospects of prediction', *J. Geophys. Res.*, **103**, 14451–14510.
- White, A.B. and Fairall, C.W., 1991: 'Convective boundary layer structure during ROSE-I using the NOAA 915 MHz radar wind profiler', Tech. Memo. ERL-WPL-205, Natl. Oceanic and Atmos. Admin., Silver Spring, Md., 1991.
- Wieringa, J., 1980: 'A revaluation on the Kansas mast influence on measurements of stress and cup anemometer over speeding', *Boundary-Layer Meteorol*, **18**, 411-430.
- Wilczak, J. M., E. E. Gossard, W. D. Neff, and W. L. Eberhard, 1996: 'Ground-based remote sensing of the atmospheric boundary layer: 25 years of progress'. *Boundary-Layer Meteorol.*, **78**, 321–349.
- Willis, G. E., and J. W. Deardorff, 1974: 'A laboratory model of the unstable planetary boundary layer'. *J. Atmos. Sci.*, **31**, 1297–1307.
- Wyngaard, J. C. and Cote, O. R., 1971: 'The budget of turbulent kinetic energy and temperature variance in the atmospheric surface layer', *Q. J. R. Meteorol. Soc.*, **28**, 190-201.
- Wyngaard, J. C. and Cote, O. R., 1972: 'Cospectral similarity in the atmospheric surface layer', *Q. J. R. Meteorol. Soc.*, **98**, 590-603.
- Wyngaard, J. C., and M. A. LeMone, 1980: 'Behavior of the refractive index structure parameter in the entraining convective boundary layer', *J. Atmos. Sci.*, **37**, 1573-1585.
- Wyngaard, J. C., Bauman, J. T. & Lynch, R. A., 1974: 'Cup anemometer dynamics', in 'Proc. Flow, Its Measurements and Control in Science and Industry', Vol. 1, Instrument Society of America, Pittsburg, PA, 701–708.

- Wyngaard, J. C., Cote, O. R. and Izumi, Y., 1971: 'Local free convection, similarity and budgets of shear stress and heat flux', *J. Atmos. Sci.*, **28**, 1171-1182.
- Wyngaard, J.C., 1986: Measurement physics. Probing the Atmospheric Boundary Layer, D. Lenschow, Ed., American Meteorological Society, 5-18.
- Wyrski K (1973): An equatorial jet in the Indian Ocean, *Science*, **181**, 262-264
- Yamada, T., 1976: 'On the similarity functions A, B and C of the boundary layer', *J. Atmos. Sci.*, **33**, 881-793.
- Yano, J.-I., and K. A. Emanuel, 1991: 'An improved model of the equatorial troposphere and its coupling with the atmosphere'. *J. Atmos. Sci.*, **48**, 377-389.
- Yasunari, T. 1979: Cloudiness fluctuations associated with the northern hemisphere summer monsoon. *J. Meteorol. Soc. Japan*, **57**, 227-242
- Yasunari, T. 1981: Structure of an Indian summer monsoon system with around 40-day period. *J. Meteorol. Soc. Japan*, **59**, 336-354
- Yoshikado, H.: 1990, 'Vertical structure of the sea breeze penetrating through a large urban complex', *J. Appl. Meteorol.* **29**, 878-891.
- Young, J. A. 1987: 'Boundary Layer Dynamics of Tropical and Monsoonal Flows', Chapter 14 in *Monsoon Meteorology*, C. P. Chang and T. N. Krishnamurti; editors, Oxford University Press, 461-500.
- Zemba, J., and CA Friehe, 1987: The marine atmospheric boundary-layer jet in the coastal ocean dynamics experiment. *J. Geophys. Res.*, **92**, 1489-1496
- Zhang Hongsheng, Chen Jiayi, and Soon-Ung Park, 2001: 'Turbulence structure in unstable conditions over various surfaces'. *Boundary.-Layer Meteor.*, **100**, 243-261.



G9001